UNIMORE
UNIVERSITÀ DEGLI STUDI DI
MODENA E REGGIO EMILIA

UNIVERSITÀ DEGLI STUDI
DI MODENA E REGGIO EMILIA

Dottorato di ricerca in
"Molecular and Regenerative Medicine"

Ciclo XXXVIII

Evaluating the role of Phosphoinositide-specific Phospholipases C PLC in 143B human osteosarcoma cells' adhesion and mechanotransduction

Candidato: Matteo Corradini

Tutor: Prof. Carla Palumbo

Correlatore (Co-Tutor): Prof. Vincenza Rita LoVasco

Coordinatore del Corso di Dottorato: Prof. Michele De Luca

Summary

Abstract

Osteosarcoma (OS) is the most common primary malignant bone tumor in children and young adults and is characterized by high metastatic potential and poor prognosis in advanced stages. Despite multimodal treatment strategies, lung metastasis remains the leading cause of mortality, highlighting the need to better understand the molecular mechanisms regulating tumor cell plasticity and dissemination. Among signaling pathways implicated in cancer progression and cytoskeletal dynamics, the phosphoinositide–phospholipase C (PI–PLC) axis has gained increasing interest in recent years. However, the isoform-specific functions of PLC enzymes in OS remain poorly defined.

In this study, we initially adopted a broad pharmacological approach using the PLC inhibitor U73122 and its inactive analogue (U73343) to evaluate the global contribution of PLC signaling to osteosarcoma cell behavior. While PLC inhibition significantly affected cell growth and cytoskeletal organization, the broad and complex nature of the response did not allow discrimination of isoform-specific functions. We therefore refined our strategy through isozyme-specific siRNA silencing, focusing on PLCβ1, PLCβ2, and PLCγ2, selected based on preliminary data and available literature suggesting their involvement in cytoskeletal regulation and tumor progression. Subsequent analyses were performed through integrated transcriptomic profiling, protein-level characterization, and functional assays in 143B osteosarcoma cells, a well-established model characterized by high migratory and invasive potential.

Our results indicate that distinct PLC isoforms exert non-redundant functions. In particular, *PLCB2* and *PLCG2* silencing did not significantly impair proliferative capacity but induced marked cytoskeletal remodeling, focal adhesion reorganization, activation of EMT-like transcriptional programs, and enhanced invasive behavior. These alterations were associated with YAP pathway activation and changes in nuclear architecture, suggesting engagement of adhesion-dependent mechanotransductive signaling. Notably, *PLCB2* and *PLCG2* exhibited reciprocal regulatory interactions, indicating the existence of a coordinated PLC signaling module rather than independent isoform activity. This cross-isoform interconnection, not previously described in osteosarcoma, was further supported by *in-silico* analyses of patient-

derived transcriptomic datasets, which revealed coordinated downregulation patterns consistent with our experimental findings. The convergence of *in-vitro* and patient data strengthens the hypothesis that PLCβ2/PLCγ2 signaling contributes to mechanoadaptive and invasive programs in the clinical setting.

In contrast, *PLCB1* silencing resulted in a complex phenotype characterized by partial cell-cycle deceleration without significant induction of apoptosis. Although proliferative markers such as Ki67 remained largely unchanged, increased p21 levels suggested a slowing of cell-cycle progression. Concurrently, *PLCB1* depletion was associated with upregulation of ROCK2, SPARC, and MMP2 and alterations in cytoskeletal components, including β-tubulin, indicating changes in cytoskeletal tension and matrix remodeling. However, the partial reduction of N-cadherin together with a slight reappearance of E-cadherin argues against a complete mesenchymal transition. Instead, PLCβ1 depletion appears to induce a condition of structural imbalance and adaptive plasticity, potentially facilitating matrix interaction without driving a coordinated migratory program. Given the central role of invasion and metastatic dissemination in osteosarcoma prognosis, even such partial remodeling states may remain biologically relevant within the tumor microenvironment.

Collectively, these findings refine the concept of PLC signaling in osteosarcoma by identifying isoform-specific and interconnected regulatory functions that influence mechanical adaptation and invasive potential. From a translational perspective, selective modulation of PLCβ2/PLCγ2-dependent pathways may represent a strategy to target tumor dissemination without directly affecting proliferative control, and these isozymes may serve as candidate biomarkers of invasive propensity for patient stratification in osteosarcoma.

1.0 Introduction

1.1 Bone biology and physiology.

Bone is a calcified connective tissue with high mechanical resistance and modest flexibility. Bone has a crucial structural function, acting as a scaffold for organs and systems, and also has an equally important metabolic function, contributing to calcium-phosphate homeostasis. The skeleton is the main support of the muscular tissue and allows the activity of the locomotor system, in which the bones represent the passive element.

Bone acts as a reserve of minerals, but also as a deposit of growth factors and other molecules associated with the tissue. Bone has the ability to regenerate, as this tissue harbors bone marrow mesenchymal stem cells (BM-MSCs), which are capable of differentiating into cells of the bone stroma. Hematopoietic stem cells (hSCs) are initially present in all the bones of the skeleton, but after the organism development, their niche is reduced only into the flat bones and in the epiphyses of the long bones. The hematopoietic bone marrow undergoes into a fatty degeneration in the other bones. Bone also has endocrine functions, as it is involved in the control of glucose homeostasis, thanks to osteocalcin, and in cross talk with skeletal muscle, thanks to a series of osteokines. Pre-Osteoblast (Pre-Ob) differentiates from BM-MSCs, they are highly proliferating progenitors that further differentiate to mature osteoblasts under certain biochemical and mechanical stimuli. Bone Morphogenetic Protein 2 (BMP2) plays an essential role in stimulation of BM-MSCs' osteoblastic differentiation process; though Small Mother Against Decapentaplegic (Smad) and Mitogen-Activated Protein Kinase (Mapk) pathways an enhancement of Runt-related transcription factor 2 (RUNX2) activity is observed. The morphogen Wnt, through the canonical beta-catenin-mediated pathway, determines the nuclear translocation of Tcf/Lef transcription factors. They act on the *RUNX2* promoter, and on the promoters of other genes such as *OSX* and *DLX5*, determining a fundamental stimulus to the osteoblastic differentiation.

The mature osteoblast, which is characterized by the expression of several markers such as RUNX2, osterix (OSX), osteopontin (OPN), bone sialoprotein and osteocalcin. Osteoblast produce and mineralize the bone matrix, which is principally made, in terms of organic part, by type I collagen. The terminal stage of differentiation of the osteoblast

cells (hOb) is the osteocyte, a fully embedded cell in the mineralized matrix. From there, osteocytes act as “orchestrators” of bone processes. Through pathways such as the Sclerostin–Wnt axis, they can modulate the mechanisms that regulate bone deposition and resorption. Osteosarcoma cells have many of the characteristics of immature osteoblasts. Bone re-absorption is carried out by osteoclast cells, a highly specialized monocyte lineage which can resorb the bone matrix through a phagocytic-like mechanism.

1.2 Brief clinical overview.

Osteosarcoma (OS) is a primary malignant bone tumor characterized by osteoid production by malignant cells. OS is rare, with an incidence of 3–5 cases per million males and 2–4 cases per million females ≤24 years old worldwide [1]. Its epidemiology shows a bimodal distribution, affecting primarily adolescents and individuals over 60 years of age. Despite its rarity, OS is the third most common cancer in adolescence, and the overall survival rate is relatively low (65–70%). The presence of metastases at diagnosis reduces long-term survival to 20% or less [2].

Clinical presentation typically includes localized pain and swelling, often in long bones such as the distal femur, proximal tibia, and proximal humerus. Pain is initially activity-related, which may delay diagnosis until after an injury or fracture. Over time, pain occurs at rest and during the night. The median interval from symptom onset to diagnosis is approximately four months. Biomarkers are generally of limited diagnostic utility, except for alkaline phosphatase (ALP) and lactate dehydrogenase (LDH), elevated in 40% and 30% of OS patients, respectively [2].

According to the World Health Organization classification, conventional OS is the most common type, representing approximately 80% of cases [3]. Conventional OS is further classified into osteoblastic, chondroblastic, and fibroblastic subtypes based on the predominant neoplastic cell type, although these subtypes do not differ significantly in clinical outcome. Unconventional OS subtypes were described: parosteal OS (4–6%), a surface tumor originating from the periosteum; telangiectatic OS (4%)m a metaphyseal tumor with extensive bone destruction and a wide transition zone; small cell OS (1–2%), histologically similar to Ewing’s Sarcoma, but differentiated by osteoid production; periosteal OS, which develops between the cortex and the cambium layer of the periosteum; high-grade surface OS (<1%), a surface tumor with high-grade histological features [3].

Accurate diagnosis and staging are critical for treatment planning. Imaging is fundamental: X-rays reveal bone lesions, including osteoblastic and osteolytic areas, as well as soft tissue masses. MRI evaluates tumor invasion of soft tissue, vascular structures, and bone marrow involvement. PET scans can detect primary and metastatic lesions in bone and lung. Definitive diagnosis requires biopsy.

OS staging follows the American Joint Committee on Cancer (AJCC) system, based on histological grade, local extension, and metastases. Low-grade lesions (stage I) are well differentiated, with low mitotic activity and low metastatic risk. High-grade lesions (stage II) are poorly differentiated, highly proliferative, and matrix-poor. Stages I and II are further divided into A (tumor confined to bone) and B (tumor extending beyond bone). Stage III represents tumors with local and distant metastases [4].

1.3 Treatments for OS.

OS treatment involves surgery, usually limb-salvage procedures, which generally yield better outcomes than amputation. Neoadjuvant and adjuvant chemotherapy are essential. Multidrug regimens typically include methotrexate (MTX), which inhibits folate metabolism, blocking nucleic acid synthesis; doxorubicin (DOX), DNA-intercalating antibiotic that inhibits topoisomerase II, blocking replication; cisplatin, DNA intercalator that interferes with replication, preferentially killing rapidly dividing cells; ifosfamide, an alkylating agent belonging to the mustard compound class. Neoadjuvant chemotherapy is administered for ~10 weeks before surgery, followed by adjuvant therapy for ~29 weeks. Localized OS patients receiving surgery plus multidrug chemotherapy achieve ~70% recovery, whereas metastatic patients have <20% five-year survival [2, 5]. Recent advances in therapy have been guided by improved understanding of OS pathophysiology.

1.4 Chemoresistance in OS.

Chemoresistance in OS has prompted extensive research into its mechanisms and potential biomarkers or targeted therapies [6]. OS heterogeneity complicates biomarker identification, understanding recurrence, and defining the tumor-driving cell populations [7]. Resistance mechanisms include altered drug transport, enhanced DNA repair, changes in apoptosis and cell cycle regulation, signaling pathway activation, tumor microenvironment interactions, angiogenesis, autophagy, microRNA regulation, and acquisition of stem cell-like traits [8].

1.4.1 Impaired Intracellular Drug Accumulation.

OS cells may reduce intracellular drug accumulation via impaired membrane transport, increased efflux, or target enzyme alterations [8]. For example, MTX requires the reduced folate carrier (RFC) for uptake and polyglutamylation. MTX inhibits dihydrofolate reductase (DHFR), blocking DNA synthesis. MTX-resistant cells show decreased RFC, correlating with poor histological response [9]. RFC-independent drugs like trimetrexate have been tested with limited success (response rate 8%) [10]. Combination therapies with MTX are under investigation (NCT00119301).

1.4.2 Drug Efflux and Multidrug Resistance (MDR).

Enhanced drug efflux, particularly against DOX, is a major mechanism of OS chemoresistance. MDR is mainly mediated by ATP-binding cassette (ABC) transporters, especially P-glycoprotein (P-gp/ABCB1) [8]. Overexpression reduces intracellular DOX and correlates with poor outcomes [11]. Genetic ABCB1 knockout restores DOX sensitivity, and pharmacologic inhibitors like trabectedin show promise by downregulating MDR1 transcription [12].

1.4.3 Alterations in Drug targets.

Resistance can result from altered drug target enzymes. MTX-resistant cells overexpress DHFR, while DOX-resistant cells often show reduced topoisomerase II (TOP2B) levels [13] [14]. Genomic studies reveal frequent TOP2B deletions (40.5%) and TOP2A amplifications (21%) or deletions (25%) [15], highlighting these enzymes as potential predictive biomarkers.

1.4.4 DNA repair and resistance.

Enhanced DNA repair undermines chemotherapy. Cisplatin resistance is mediated by nucleotide excision repair (NER), involving ERCC proteins; polymorphisms in ERCC1/2 affect response [8, 16]. Base excision repair (BER) also contributes; elevated APE-1 correlates with poor survival [17].

Double-strand breaks are repaired by homologous recombination (HR) or nonhomologous end-joining (NHEJ). Mutations in HR genes (PALB2, CHEK2, PTEN, ATM) create a BRCA-like phenotype, sensitizing cells to PARP inhibitors. Preclinical studies show talazoparib (with SN-38) and olaparib reduce OS cell viability and enhance DOX sensitivity [19].

In summary, alterations in NER, BER, and HR pathways significantly contribute to OS chemoresistance. Preclinical evidence supports PARP inhibition, but clinical validation is ongoing.

1.4.5 Alteration of cell cycle regulation and apoptosis.

In osteosarcoma (OS), alterations in cell cycle regulation and apoptosis are critical contributors to chemoresistance. Chemotherapy primarily induces DNA damage, which should trigger cell death; however, tumor cells can evade apoptosis by arresting the cell cycle, allowing time for DNA repair and survival [20]. A central mechanism involves amplification of MDM2, a well-known inhibitor of p53. Overexpression of MDM2 suppresses p53-mediated apoptosis, enabling tumor cells to survive DNA-damaging treatments. This alteration, observed in approximately 20% of OS cases, is associated with chemoresistance and disease progression [21].

Another key regulator is cyclin-dependent kinase 4 (CDK4), responsible for phosphorylating the retinoblastoma protein during the G1–S transition. CDK4 is amplified in ~20% of OS, often as part of recurrent gains at chromosome 12q14.1. These alterations are more frequent in poor responders to chemotherapy and correlate with metastasis and unfavorable prognosis [22, 23]. Functionally, CDK4 amplification confers resistance to cisplatin, but pharmacological inhibition with CDK4/6 inhibitors such as palbociclib or abemaciclib restores chemosensitivity. In preclinical models, palbociclib reduced viability of cisplatin-resistant OS cells and enhanced apoptosis, particularly when combined with sorafenib, leading to tumor regression in xenografts [24]. Currently, both palbociclib and abemaciclib are being evaluated in pediatric and adult OS cohorts (NCT03526250; NCT04040205).

Myeloid cell leukemia-1 (MCL-1), a pro-survival member of the BCL-2 family, is another contributor to chemoresistance. MCL-1 is upregulated in OS following chemotherapy, and its elevated expression correlates with poor survival, increased recurrence, and reduced sensitivity to MTX [25]. Beyond tumor cell survival, MCL-1 is critical for endothelial cell function and angiogenesis, linking it to disease aggressiveness [26]. These findings suggest that MCL-1 inhibitors may resensitize tumors to chemotherapy, counteract anti-angiogenic resistance, or be used in combination regimens. Clinical trials investigating MCL-1 inhibitors in solid tumors, including sarcomas, are ongoing (NCT04837677).

Together, alterations in MDM2, CDK4, and MCL-1 represent interconnected mechanisms through which OS cells evade chemotherapy-induced apoptosis.

Targeted therapies against these molecules, particularly CDK4/6 and MCL-1 inhibitors, offer new therapeutic perspectives, especially in combination with conventional chemotherapy or other targeted agents, potentially overcoming intrinsic and acquired resistance in OS patients.

1.5 Osteosarcoma etiology.

Osteosarcoma (OS) is a multifactorial disease with risk factors broadly classified as biological, genetic/genomic, heritable syndromes, and environmental.

Biological risk factors include bone turnover, height, age, and sex. Rapid bone turnover and growth during puberty, as well as taller stature, are associated with increased OS risk. Incidence is higher in boys, likely reflecting sex-specific differences in bone growth and development.

Heritable syndromes can predispose individuals to OS. Li-Fraumeni syndrome (LFS) is germline dominant mutations disrupt TP53, increasing OS risk (12% of LFS patients). p53 normally suppresses angiogenesis and proliferation in OS via inhibition of the PI3K/AKT/mTOR pathway [27].

Retinoblastoma (RB) syndrome is a germline RB1 mutations increase OS incidence. pRB regulates the cell cycle and osteoblast differentiation; loss of RB1 enhances proliferation and contributes to tumorigenesis. Rothmund–Thomson Syndrome (RTS) and RAPADILINO syndrome (RAPA) are autosomal recessive disorders caused by mutations in RecQ DNA helicases, including RECQL4. These proteins participate in DNA repair (NER, BER, NHEJ). RTS carries the highest OS risk, with up to 32% of affected individuals developing the disease.

Bone disease conditions such as Paget's disease, characterized by abnormal bone remodeling, increase OS risk due to weak and structurally compromised bone.

Environmental risk factors primarily include ionizing radiation, often as a consequence of radiotherapy for other primary tumors. Radiation-induced OS is dose-dependent and may appear decades after treatment, sometimes up to 30 years later [28].

1.6 Osteosarcoma: Molecular biology and cell signaling alterations.

Conventional OS is characterized by marked genomic instability, including DNA rearrangements, chromosomal deletions, and translocations [29]. Genomic alterations may juxtapose oncogenes with active promoters or position tumor suppressors in

heterochromatin, leading to silencing. DNA breaks can delete tumor suppressors, while translocations may generate chimeric oncogenes.

Whole-genome sequencing (WGS) of pediatric OS samples shows higher rates of structural variations (SVs) and copy-number alterations (CNAs) than single nucleotide variants (SNVs), with frequent loss of heterozygosity (LOH) [30]. SNVs often cluster in hypermutated regions, a phenomenon called *kataegis*. OS exhibits the highest SV rate among pediatric cancers, with SVs and SNVs frequently inactivating TP53 (present in 95% of patients) [29]. The most recurrent genes that undergo on rearrangements critical for their own normal expression in OS patients are *TP53*, *RB1*, *MDM2*, and *CDKN2A*. Other recurrently altered genes include *RB1*, *MDM2*, and *CDKN2A*. Specific gene fusions in OS include *PMP22–ELOVL5*, affecting BM-MSC osteogenic differentiation (loss of PMP22 exon 5); *LRP1–SNRNP25* and *KCNMB4–CCND3*, associated with OS cell motility; *TP53–KPNA3*, linked to chemotherapy resistance and metastasis [31] [29]. Alternative lengthening of telomeres (ALT), a homologous recombination mechanism preventing telomere shortening, is observed in ~85% of OS and correlates with poor outcomes. Epigenetic modifications, including hypomethylation and hypermethylation, are also common in OS [30].

1.6.1 Hedgehog, Notch and WNT pathways.

Wnt signaling. Wnt proteins are cysteine-rich glycoproteins involved in numerous developmental processes and tissue homeostasis. They typically act over short distances from the cells that secrete them. Wnt signaling regulates cell fate specification, tissue differentiation, proliferation, and mitogenic stimulation.

In bone development, the canonical Wnt/β-catenin pathway is essential for osteoblast differentiation. Upon Wnt ligand binding to the Frizzled (FZD) receptor, the cytoplasmic β-catenin destruction complex is disrupted. Axin, a scaffold protein of the destruction complex, is recruited to the cell membrane via the co-receptor LRP5/6, while polymerization of Dishevelled (DVL) proteins promotes formation of the membrane complex (LRP5/6, Axin, FZD, and DVL). The kinases GSK3 and CKI are also recruited to the membrane by Axin, inhibiting β-catenin phosphorylation and subsequent ubiquitination. Stabilized β-catenin goes into the nucleus, associates with TCF/LEF transcription factors, and, together with transcriptional coactivators and chromatin remodelers, regulates genes involved in cell-cycle control. In bone, this complex promotes expression of osteoblast master regulators such as RUNX2 and OSX.

Activation of canonical Wnt signaling also inhibits alternative mesenchymal lineages, e.g., adipogenesis, by repressing transcription factors C/EBP and PPARγ [32].

Two main non-canonical Wnt pathways are the Planar Cell Polarity (PCP) pathway and the Wnt/Ca^{2+} pathway. Both are initiated by Wnt/FZD signaling but are independent of β-catenin transcriptional activity. In PCP, membrane-associated DVL activates Rho and Rac GTPases via Daam1. Rho activates ROCK, regulating actin cytoskeleton assembly, while Rac activates JNK and MAPK pathways, contributing to cell adhesion and cytoskeletal organization. Wnt/Ca^{2+} signaling, triggered by Wnt5a, involves heterotrimeric G proteins (Gq/Go) and DVL activation of IP3 via PLCs, increasing intracellular Ca^{2+} and activating calcium-sensitive enzymes such as Calcineurin (CaN), PKC, and CaMKII. PKC activates Cdc42, regulating cytoskeletal dynamics, while CaN dephosphorylates NFAT, which enters the nucleus and controls genes involved in proliferation and differentiation. In osteosarcoma, Wnt pathways are often overactive. Wnt inhibitors, such as Dickkopf 3 (DKK3) and Wnt inhibitory factor 1 (WIF1), are downregulated. Reconstitution of DKK3 or WIF1 suppresses OS growth *in-vitro* and *in-vivo* [32-34]. WIF1 is frequently epigenetically silenced, leading to β-catenin accumulation, hyperactivation of canonical Wnt signaling, and enhanced cell proliferation and tumor progression [34] [35]. Wnt3a and Wnt10b promote metastasis in murine OS models, while Wnt5a increases aggressiveness in U2OS cell lines [36] [37]. Secreted Frizzled-related protein 2 (sFRP2) negatively correlates with patient survival, promoting tumor angiogenesis and dedifferentiation of OS precursor cells [38]. β-Catenin expression is tightly linked to OS metastasis and represents a potential biomarker for patient stratification [39].

Hedgehog signaling. In vertebrates, Hedgehog signaling is closely associated with the cytoskeleton, particularly microtubules and the primary cilium, a cellular sensory organelle enriched in receptors. Most tumors lose primary cilia, correlating with increased malignancy. The primary cilium consists of a 9-microtubule axoneme anchored to a basal centriole, separated from the plasma membrane by a transition zone, and enriched in signaling proteins and lipids [40]. Hh ligands bind the Patched (PTCH) receptor on the primary cilium, relieving inhibition of Smoothened (Smo). Smo activates Gαi proteins, reducing cAMP levels and inhibiting Protein Kinase A (PKA). Consequently, Gli transcription factors are not phosphorylated or degraded. Gli1 acts as a transcriptional activator, Gli3 as a repressor, and Gli2 as both. Gli factor expression is interdependent. In OS, IHH, PTCH1, and Gli1 are highly expressed,

while Gli2 expression correlates with poor prognosis. Gli2 silencing increases chemotherapy sensitivity in OS cell lines [41, 42].

Notch signaling. The Notch pathway, comprising Notch receptors (Notch1–4) and ligands Delta (DLL1, DLL3, DLL4) and Jagged (Jagged1, Jagged2), mediates communication between adjacent cells. Non-classical ligands (secreted, GPI-anchored, or integral membrane proteins) can also activate the pathway. Ligand binding exposes metalloprotease cleavage sites on Notch, and sequential proteolysis by γ secretase releases the Notch intracellular domain (NICD). NICD translocate to the nucleus, forming a transcriptional complex with Mastermind (MAM), CSL, and chromatin remodelers (e.g., HATs, p300), displacing repressors from target genes. Main targets include HES1 and HEY1. Notch can function as a tumor suppressor or oncogene; abnormal activation promotes tumor progression, proliferation, invasion, and metastasis [43]. In PDX models, γ secretase inhibitors consistently reduce OS growth [44].

Despite extensive preclinical research on Wnt, Hedgehog, and Notch signaling in OS, clinical applications remain limited due to the essential roles of these pathways in skeletal development, especially in children and young adults.

1.6.2 Tyrosine kinase receptors.

Tyrosine kinase receptors (TKRs) constitute a large family of cell-surface receptors, encompassing more than 50 distinct receptors grouped into approximately 20 subfamilies. Their structure is highly conserved and consists of an extracellular ligand-binding domain, a single transmembrane region, and a cytoplasmic C-terminal domain with intrinsic tyrosine kinase activity.

Signal transduction downstream of TKRs is complex and involves multiple intermediate proteins. Relay proteins contain Src Homology 2 (SH2) domains, which bind phosphotyrosine residues on activated TKRs. These proteins often exhibit enzymatic activities, including tyrosine kinase, tyrosine phosphatase, phospholipase C, or Ras-GAP activity. Adapter proteins, such as Grb2, mediate signal transduction without intrinsic enzymatic activity. Grb2 contains an SH2 domain that binds phosphotyrosines on TKRs and an SH3 domain that interacts with guanine nucleotide exchange factors (GEFs) like SOS, the principal activator of the RAS-MAPK pathway. Grb2 activation is facilitated by Grb2-associated binding protein 1 (GAB1), a structural protein containing a Pleckstrin Homology (PH) domain that anchors Grb2 to the plasma membrane.

TKRs play central roles in cell growth, differentiation, and survival, and dysregulation of these pathways is frequently linked to oncogenesis. The most common oncogenic alterations include constitutive activation due to receptor overexpression and dimerization, or mutations and chromosomal translocations in the extracellular or kinase domains that result in ligand-independent receptor activation.

In osteosarcoma, several growth factors and their corresponding TKRs are frequently upregulated, including Vascular Endothelial Growth Factor (VEGF), Insulin-like Growth Factor 1 (IGF1), Platelet-Derived Growth Factor (PDGF), Human Epidermal Growth Factor Receptor 2 (HER2), and Hepatocyte Growth Factor Receptor (MET) [28]. Therapeutic targeting of TKRs in OS has been explored using multikinase inhibitors. Sorafenib, approved for renal, hepatic, and thyroid cancers, inhibits multiple kinases and effectively reduces OS cell proliferation and metastasis *in-vitro* and *in-vivo*. A phase II trial combining sorafenib with an mTOR inhibitor demonstrated activity in patients with relapsed or inoperable high-grade OS. Notably, patients with concurrent overexpression of P-ERK1/2 and P-RPS6 derived the greatest benefit. However, this combination did not significantly improve outcomes in patients with advanced-stage disease [45].

Pazopanib, an oral multikinase inhibitor targeting VEGFR1-3, PDGFR-α/β, and c-KIT, has shown partial efficacy in preclinical and phase II studies. In recurrent metastatic OS, pazopanib achieved disease stabilization and substantial tumor growth reduction in roughly half of the treated cohort [46]. Although HER2 overexpression has been observed in OS by immunohistochemistry [47], phase II trials using trastuzumab for metastatic patients showed limited efficacy, with outcomes not correlating with HER2 expression levels [48].

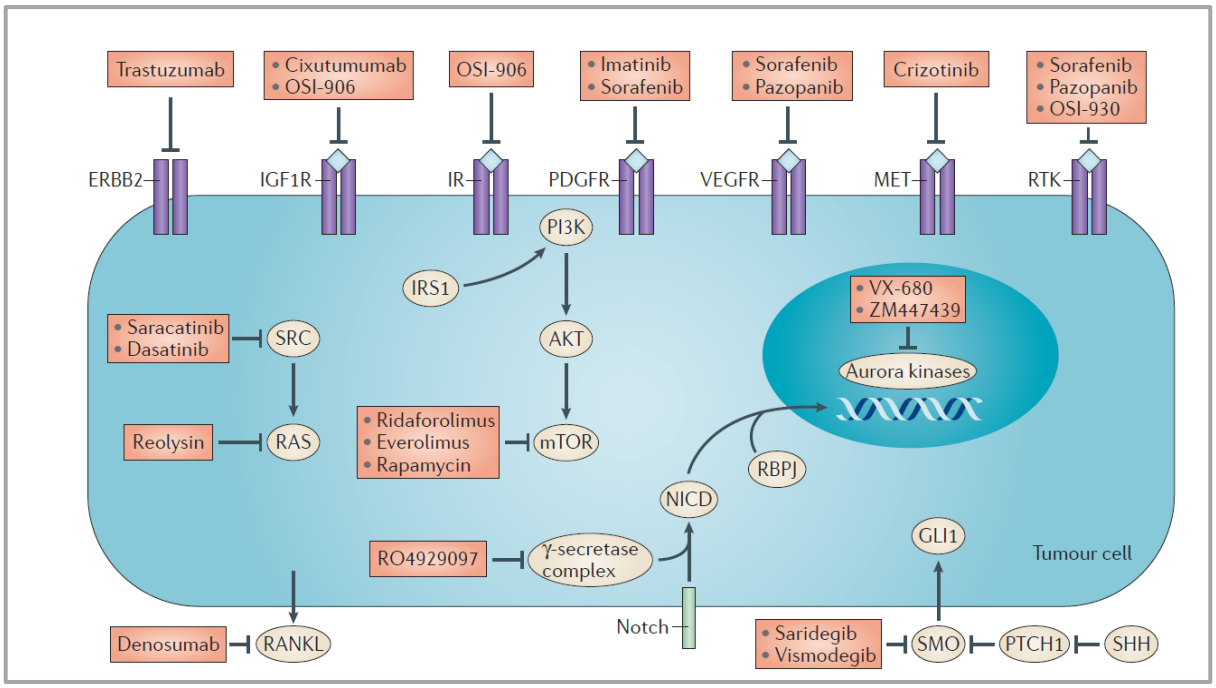

Figure 1. Principal signaling pathways involved in OS and therapeutical strategies (M. Kansara et al 2014)

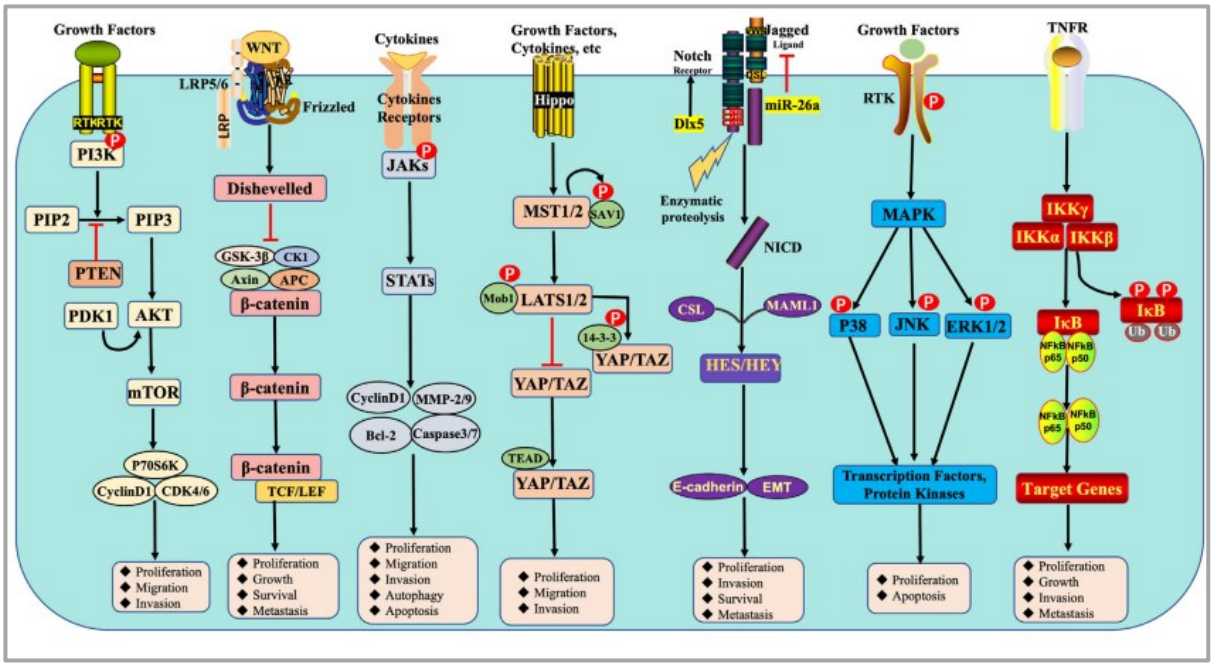

Figure 2. Principal signaling pathways involved in OS and therapeutical strategies (Ziyu Ji et al)

1.6.3 Akt-mTOR signaling pathway.

mTOR (mechanistic target of rapamycin) is a serine/threonine kinase whose activity is regulated by growth factor signaling pathways, such as PDGF and IGF, through recruitment of PI3K [49]. PI3K (phosphatidylinositol 3-kinase) is an intracellular kinase with both lipid kinase and serine/threonine kinase activities. The PI3K-Akt-mTOR signaling pathway is essential for multiple cellular functions, including survival, growth, proliferation, migration, and angiogenesis.

Upon activation of a tyrosine kinase receptor (TKR), PI3K is recruited to the plasma membrane via binding of its p85 regulatory subunit (which contains two SH2 domains) to phosphotyrosine residues on the receptor [50]. This interaction allosterically activates the p110 catalytic subunit of PI3K, leading to the conversion of phosphatidylinositol-4,5-bisphosphate (PI-4,5-P_2) into the second messenger phosphatidylinositol-3,4,5-trisphosphate (PI-3,4,5-P_3). PI-3,4,5-P_3 serves as a critical docking site for proteins containing Pleckstrin Homology (PH) domains, including Akt (also known as Protein Kinase B, PKB), facilitating their recruitment to the plasma membrane. Once localized to the membrane, Akt is phosphorylated and activated. Activated Akt regulates numerous processes involved in cell survival and cell cycle progression, including the inactivation of pro-apoptotic factors such as Bad and procaspase-9, as well as the inhibition of the Forkhead (FOXO) family of transcription factors, which are responsible for inducing the expression of pro-apoptotic genes, including Fas ligand (FasL).

Through these mechanisms, the PI3K-Akt-mTOR axis promotes cell survival, proliferation, and resistance to apoptotic stimuli, and its dysregulation is frequently observed in osteosarcoma and other cancers, contributing to tumor growth, chemoresistance, and metastatic potential.

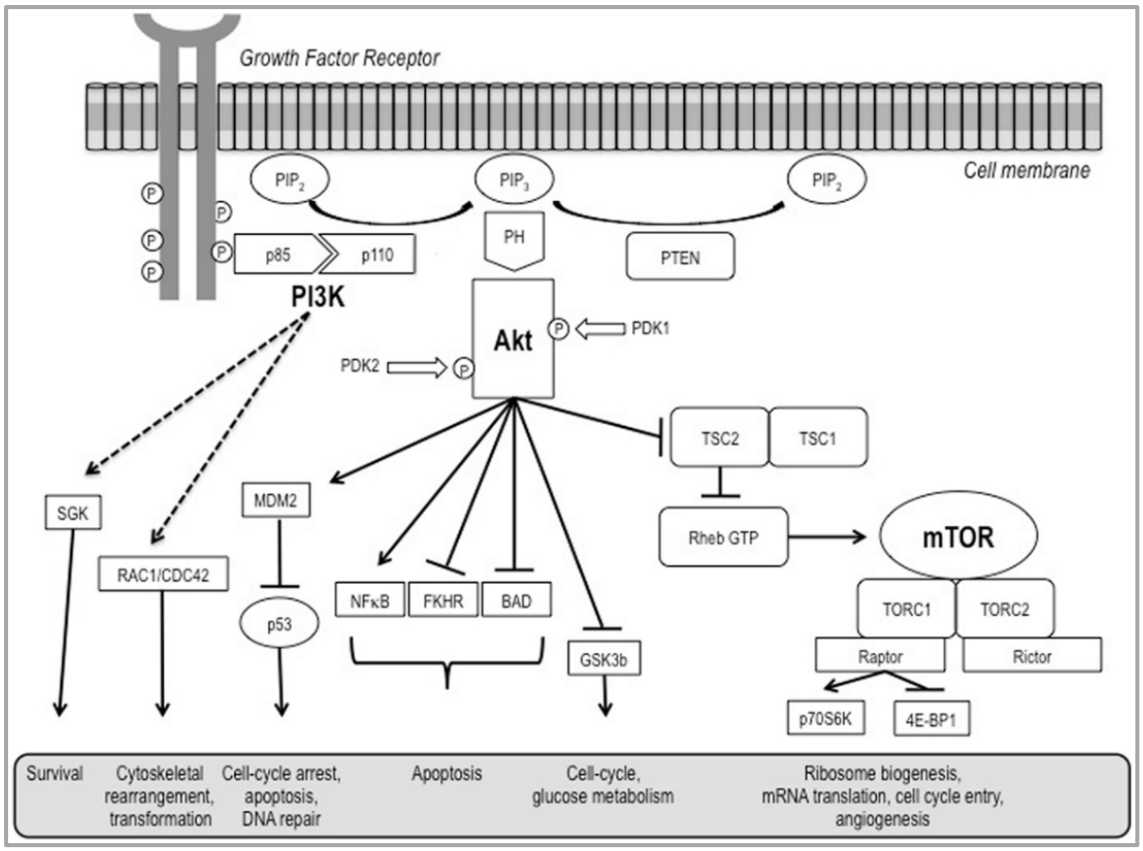

Figure 1. A schematic representation of PI3K/AKT/mTOR pathway (Camillo Porta et al 2014)

Akt/Protein Kinase B (PKB) is a central regulator of cell survival, proliferation, metabolism, and apoptosis. In addition to previously described mechanisms, Akt activates IκB kinase (IKK), a positive regulator of the survival factor NFκB, thereby promoting transcription of anti-apoptotic genes. Akt also regulates cellular metabolism, including protein synthesis, glycogen metabolism, and cell cycle progression, by targeting several molecules such as mTOR, GSK3, IRS-1, cyclin-dependent kinase inhibitors (p21^CIP1/WAF1 and p27^KIP1), and potentially Raf-1 from the MAPK pathway.

Akt recruitment to the plasma membrane via its PH domain facilitates phosphorylation by PDK1, which phosphorylates Akt at Thr308 and Ser473. Once phosphorylated, Akt is fully activated, promoting cell cycle progression via regulation of GSK3β and cyclins [51]. In normal cells, mTOR activity is tightly controlled by positive and negative upstream regulators. Positive regulators include growth factors and their receptors (e.g., IGF-1/IGFR, HER family, VEGF) that activate the GF-Akt pathway. Negative regulators include PTEN, which inhibits PI3K-Akt signaling, TSC1–TSC2 complex (with TSC2 inhibited by Akt-mediated phosphorylation), and AMPK, a nutrient-sensitive energy sensor. Nutrient deprivation inhibits AMPK, indirectly activating mTOR.

mTOR exists in two complexes: mTORC1 and mTORC2. mTORC1 consists of mTOR, Raptor, mLST8/GβL, PRAS40, and Deptor. It is particularly sensitive to rapamycin. Nutrient deprivation can activate mTORC1 indirectly via AMPK inactivation. Downstream effectors include S6K1, 4E-BP1, CDKs, and HIF1α, promoting protein synthesis, glycolytic gene expression, and cell proliferation. In nutrient-rich conditions, mTORC1 promotes protein synthesis, cell growth, and inhibits autophagy.

mTORC2 is composed of mTOR, Rictor, mLST8/GβL, PRR5/Protor-1, Sin1, and Deptor. PI3K is the principal activator of mTORC2, which in turn can phosphorylate and activate Akt, creating a positive feedback loop that enhances mTORC1 signaling[52]. mTORC2 is also involved in insulin signaling and cytoskeletal reorganization [53].

Activation of the PI3K/Akt/mTOR pathway drives synthesis of proteins implicated in tumorigenesis, including cyclin D1, a positive regulator of the cell cycle, and HIF1α, which promotes transcription of pro-angiogenic factors like VEGF [50]. Dysregulation of this pathway is frequent in osteosarcoma (OS), contributing to cell proliferation, invasion, metastasis, and chemoresistance [54]. Mutations or gain-of-function alterations in PI3K, particularly the catalytic subunit p110α (PIK3CA), are key mechanisms in OS aggressiveness. Hotspot mutations in the kinase domain (exon 20) or helix domain (exon 9) enhance PI3K activity, leading to constitutive Akt activation [55]. Phospho-Akt levels correlate with OS progression, metastasis, and poor prognosis [56]. Conversely, PTEN, an antagonist of PI3K/Akt signaling, can downregulate p-Akt and p-PI3K. In OS, miR-524 targets PTEN mRNA, reducing PTEN expression and indirectly activating the PI3K/Akt pathway, promoting tumor cell proliferation [57]. Targeted inhibition of mTOR has been explored therapeutically. Ridaforolimus, a selective mTOR inhibitor, showed modest benefits in Phase II/III trials in advanced sarcomas, including OS. While it improved progression-free survival (PFS), objective responses were rare, reflecting the limitations of mTOR monotherapy due to compensatory pathways [58, 59]. Combined therapies, such as sorafenib plus everolimus, effectively blocked mTOR signaling in preclinical OS models, suppressing tumor growth, and are under clinical investigation. To overcome this limitation, combined approaches targeting mTOR together with other kinases involved in osteosarcoma progression are being explored. Preclinical studies in mice demonstrated that the combination of sorafenib (a multi-kinase inhibitor) with everolimus (a rapamycin analogue) completely blocked mTOR signaling and impaired

tumor growth [60]. A Phase II clinical trial is currently investigating this combination in relapsed and metastatic osteosarcoma. Other kinase targets, such as Aurora kinases (A, B, C), involved in mitosis and cell cycle regulation, are overexpressed in OS and represent potential therapeutic targets [61].

PI3K and Akt inhibitors are still in early clinical development. The first-generation compounds (like Wortmannin, LY294002) functioned as broad pan-PI3K inhibitors but were limited by poor pharmacokinetics and thus never progressed as therapeutic agents. The second generation introduced compounds with improved pharmacological properties and greater isoform selectivity, several of which are currently under clinical evaluation. A third generation, consisting of dual PI3K/mTOR inhibitors, was developed in light of the structural similarity between the catalytic domains of PI3K and mTOR. These agents simultaneously inhibit all class I PI3K isoforms as well as both mTORC1 and mTORC2, potentially offering a more complete blockade of the PI3K/Akt/mTOR axis [62, 63].

Akt inhibitors, though fewer in clinical testing, have also progressed, with compounds such as Miltefosine evaluated in Phase III trials. Despite encouraging advances, resistance remains a major challenge for drugs targeting this pathway. Resistance can be intrinsic or acquired and involves diverse mechanisms, such as secondary mutations in the target, activation of alternative signaling cascades, or amplification of downstream effectors [64]. For example, feedback loops triggered by mTORC1 inhibition may activate receptor tyrosine kinases or the PI3K–Ras–MAPK pathway [65], ultimately reactivating Akt and undermining therapeutic efficacy. Additionally, MYC activation and overexpression of SGK1 have both been implicated in limiting the effectiveness of PI3K/Akt/mTOR inhibitors [66]. Another important resistance mechanism involves autophagy, which has been shown to protect malignant cells from Akt/mTOR inhibition. In lymphoma models, pharmacological or genetic suppression of autophagy effectively restored sensitivity to Akt/mTOR inhibitors by promoting activation of mitochondrial apoptosis [67]. Since autophagy also contributes to resistance against chemotherapy and radiotherapy, strategies combining autophagy inhibition with PI3K/Akt/mTOR targeting may represent a promising approach to enhance therapeutic efficacy.

1.7 Inflammation and immune system in osteosarcoma.

Immunotherapy has recently attracted significant attention in oncology [68], with promising outcomes in adoptive cellular therapies, cancer vaccines such as sipuleucel-T for prostate cancer (currently the only FDA-approved cancer vaccine), and peptide vaccines combined with cytokines in melanoma. These strategies harness both the innate and adaptive immune system to suppress tumor growth. In osteosarcoma (OS), immunomodulatory agents such as mifamurtide have also shown encouraging preclinical and clinical activity.

Osteosarcoma represents a particularly complex case for immunotherapy due to the close interplay between the skeletal and immune systems, a field now known as osteoimmunology. Signaling pathways such as RANK–RANKL and cytokines including IL-1, IL-6, IL-17, and TGF-β are key regulators of both bone remodeling and immune function. The implications of this crosstalk in OS pathogenesis are only partially understood. The interaction between the immune system and osteosarcoma can be conceptualized in three phases: elimination, equilibrium, and escape. In the elimination phase, both innate and adaptive immune cells—including $CD4^+$ T helper cells, $CD8^+$ cytotoxic T cells, γδ T cells, NK and NKT cells, macrophages, and dendritic cells—work to recognize and destroy tumor cells. When tumors persist, they may enter an equilibrium phase, during which immune pressure contains but does not eradicate malignant cells. Ultimately, tumors may progress to the escape phase, characterized by immune evasion and tolerance mediated by regulatory T cells, myeloid-derived suppressor cells, TH17 cells, and M2 macrophages. To counteract this process, several immune modulators are being investigated as therapeutic targets in osteosarcoma. The tumor microenvironment (TME) plays a critical role in OS progression. Histological analyses show that OS tissue is heavily infiltrated by immune cells, creating a complex microenvironment that paradoxically supports tumor survival rather than antitumor activity [73]. Key immunosuppressive mediators include indoleamine 2,3-dioxygenase (IDO), programmed cell death protein 1 (PD-1), IL-10, TGF-β, VEGF, and STAT3, which exert their effects primarily through TAMs and Tregs [74]. These observations highlight the urgent need for a deeper characterization of the OS immune microenvironment.

Understanding the cellular and molecular landscape of immune infiltration will be critical for identifying reliable biomarkers and designing advanced immunotherapeutic

strategies capable of overcoming the immunosuppressive barriers that currently limit clinical efficacy.

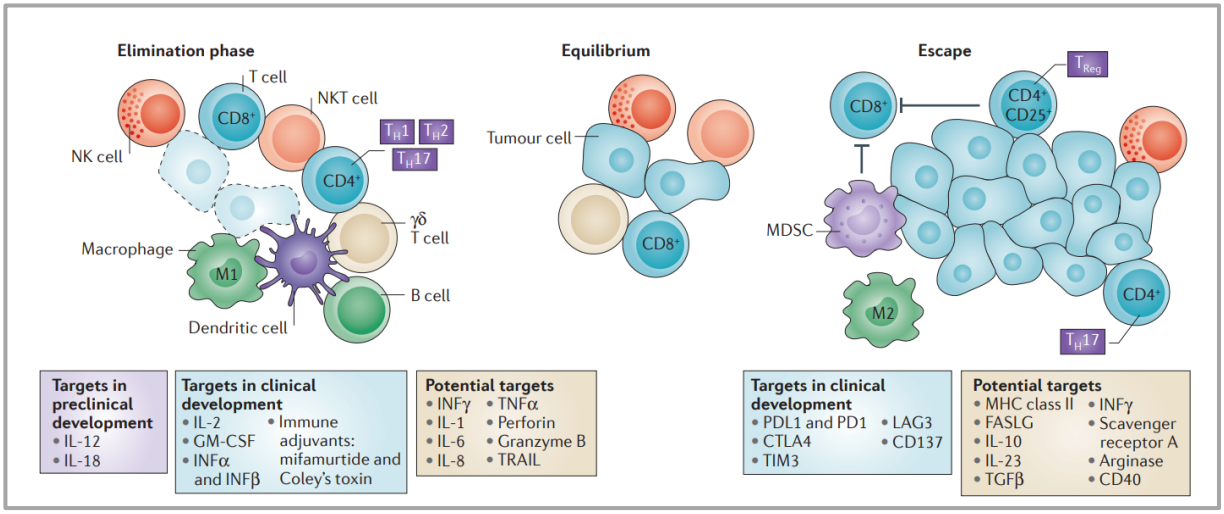

Figure 2. Osteosarcoma and immune system – elimination, equilibrium and escape (Maya Kansara et al 2014)

1.7.1 Dendritic Cells.

Dendritic cells are key antigen-presenting cells (APCs), with conventional myeloid DC1 (cDC1s) displaying strong antigen presentation and T cell priming abilities [69]. In osteosarcoma, DC-SIGN/CD11c+ DCs are particularly enriched in conventional high-grade tumors [70], and their infiltration has been linked to autophagy-related gene signatures such as RUSC1-AS1 [71]. Tumor progression can generate DC-tolerant variants, reducing their activation and contributing to immune escape. Additionally, DCs may promote OS pathogenesis via glutamate metabotropic receptor 4 (GMR-4), suggesting IL-23 blockade or GMR-4 targeting as potential therapeutic strategies [72]. DCs are also implicated in pulmonary metastasis, with CCR7 promoting their migration and CD1c+ DCs being more abundant in lung metastases [73].

Clinically, their role remains debated: while PD-L1 expression correlates with DC and T cell infiltration [74], survival analyses show contrasting results, with some evidence suggesting that patients with longer survival harbor fewer DCs relative to cytotoxic T cells and NK cells [75].

1.7.2 T Lymphocytes.

T lymphocytes are highly heterogeneous immune cells that can be classified as naïve, effector, or memory depending on activation status. Functionally, they include cytotoxic T lymphocytes (CTLs), helper T cells (Th), and regulatory T cells (Tregs), and can also be divided by TCR type (αβT or γδT). In osteosarcoma, tumor-infiltrating lymphocytes (TILs) cluster around HLA class I–rich regions, with effector T cells accumulating at the tumor–normal tissue interface and particularly within pulmonary metastases, where their numbers exceed those in primary or recurrent lesions [76, 77].

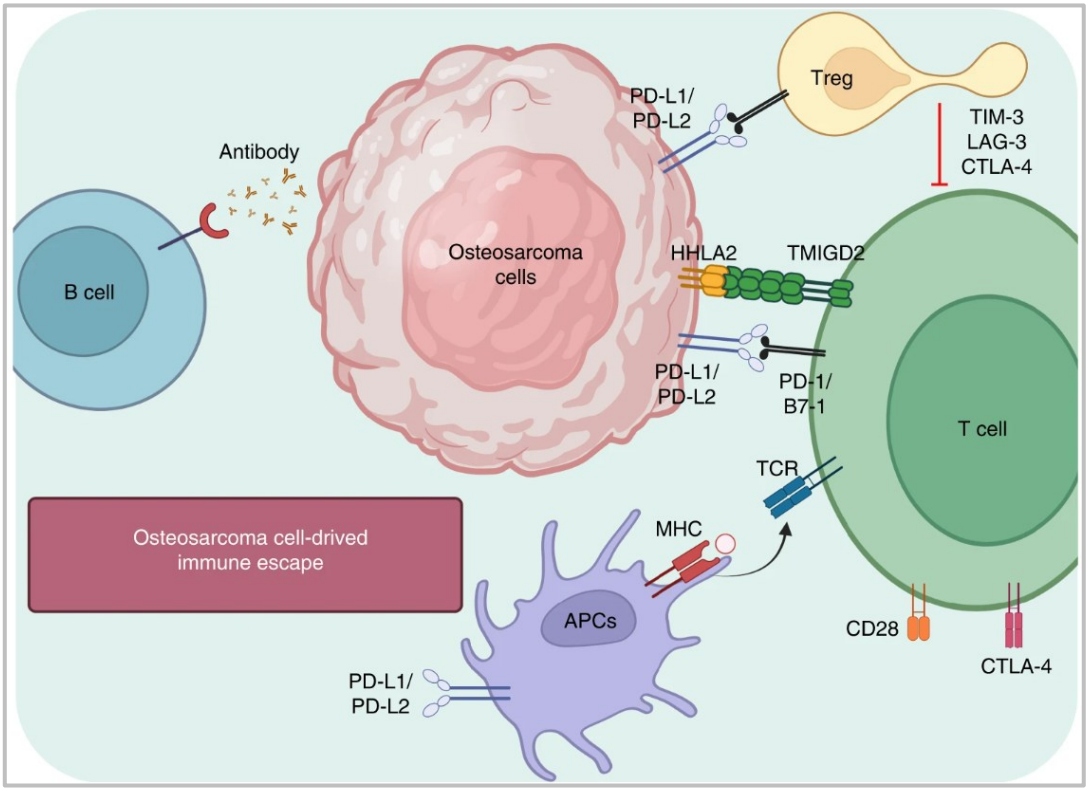

Figure 3. Osteosarcoma cell-derived immune escape (Hailong Tian et al 2023)

However, metastatic lesions exhibit elevated expression of checkpoint and immunomodulatory molecules, including PD-1, IDO, IFN-γ, and TIM-3 [78]. The enrichment of TIM-3^{+} T cells in tumor tissue versus circulation may indicate a strong local immunosuppressive microenvironment [79]. Crosstalk with other immune cells further contributes to immune suppression; M2-type TAMs inhibit T cell activity, while depletion of CD163^{+} TAMs restores T cell proliferation and promotes M1 macrophage–driven proinflammatory responses [80]. Collectively, these findings highlight the spatial and functional diversity of T lymphocyte infiltration in OS and their dual role in antitumor immunity.

1.7.3 Natural killer (NK) cells.

Natural killer (NK) cells are innate cytotoxic lymphocytes capable of eliminating malignant or infected cells without prior sensitization. Their activity depends on the balance between inhibitory receptors (e.g., KIRs, NKG2A, HLA-A/B/C recognition) and activating receptors (e.g., NKG2D, natural cytotoxicity receptors, DNAM-1) [81] [82]. NK-mediated cytotoxicity occurs when activating signals outweigh inhibitory ones and involves perforin/granzyme release and cytokine secretion (e.g., IFN-γ, TNF-α) [83].

Preclinical studies demonstrate that NK cells can efficiently lyse OS cells, achieving ~45–50% cytotoxicity *in-vitro* [84], largely dependent on NKG2D and DNAM-1 signaling [85]. KIR-ligand mismatch enhances NK cytotoxicity, especially when HLA class I molecules are downregulated on OS cells [86].

Therapeutically, combining IL-2 with intratumoral infusion of activated NK cells suppresses osteosarcoma growth, mitigates bone destruction, reduces lung metastases, and prolongs survival in murine models—underscoring NK cells' potential as immunotherapeutic agents in osteosarcoma.

1.7.4 Tumor associated macrophages (TAMs).

TAMs, primarily derived from circulating monocytes, are the predominant immune population in osteosarcoma, comprising up to 50% of the tumor mass [87]. They play critical roles in extracellular matrix remodeling, inflammation, and angiogenesis. TAMs exhibit phenotypic plasticity, adopting either M1-like (antitumor) or M2-like (protumor) phenotypes depending on microenvironmental signals [88]. M1 TAMs promote inflammatory cytokine release and cancer cell phagocytosis [89]. M2 TAMs enhance angiogenesis, tissue invasion, and immune evasion via VEGF, FGF, and MMP-9 secretion. In OS, $CD14^{+}CD68^{+}$ and $CD209^{+}$ M2-like TAMs are predominant and correlate negatively with patient survival [90]. TAM abundance also correlates with tumor vascular density, supporting angiogenesis [91]. Functionally, TAMs suppress cytotoxic T lymphocytes via PD-1 and CTLA-4 signaling, promote Treg maintenance, and contribute to premetastatic niches in bone, lung, and liver [92, 93].

Recent findings suggest that TAMs also influence local inflammation and chemotherapy resistance by interacting with other immune cells within the osteosarcoma microenvironment [94]. Targeting $CD163^{+}$ immunosuppressive TAMs, rather than broad macrophage depletion, enhances T cell–mediated antitumor responses [95]. A deeper understanding of TAM heterogeneity and signaling will be crucial for developing macrophage-targeted therapies in osteosarcoma.

1.7.5 Tumor associated Neutrophiles (TANs).

Neutrophils, constituting 50–70% of circulating leukocytes, are first responders to infection and tissue injury. In OS, an elevated neutrophil-to-lymphocyte ratio prior to treatment or surgery correlates with poor prognosis. Within the tumor microenvironment, TANs display functional plasticity and phenotypic heterogeneity similar to TAMs [96].

TANs show prolonged survival under proinflammatory stimuli such as IFN-γ [97]. They contribute to immune evasion via neutrophil extracellular traps (NETs), promoting tumor invasion and metastasis. TANs adopt N1-like (antitumor) or N2-like (protumor) phenotypes, influenced by local cytokines: TGF-β drives N2 polarization, while IFN-γ and TNF-α can revert TANs toward N1 with tumoricidal activity [98]. Due to the lack of specific markers distinguishing TAN subpopulations, their precise roles remain poorly defined. Further mechanistic and translational studies are needed to harness TANs as therapeutic targets in OS.

1.7.6 Circulating Tumor Cells (CTCs).

Circulating tumor cells (CTCs) are osteosarcoma cells that detach from the primary tumor and enter the bloodstream, enabling them to evade local therapies—including surgery, radiotherapy, and phototherapy—and contribute to metastatic dissemination and disease recurrence [99]. Increasing evidence indicates that CTCs actively interact with the osteosarcoma immune microenvironment, influencing tumor progression [100]. Pro-inflammatory cytokines appear to be key regulators of CTC behavior. For example, IL-6 inhibition significantly reduces CTC numbers and enhances therapeutic efficacy in osteosarcoma models [101]. Mechanistically, IL-6 activates both the JAK/STAT3 and MEK/ERK pathways, promoting proliferation, whereas only STAT3 drives migration, linking its activity directly to CTC dissemination. Similarly, IL-8 contributes to CTC-mediated disease progression by recruiting and activating multiple immune cell types—including T and B lymphocytes, neutrophils, basophils, and eosinophils. CTC-derived IL-8 has been shown to enhance osteosarcoma cell proliferation and lung metastasis in ex vivo models [102]. Although the interaction between CTCs and immune components remains incompletely understood, CTCs are increasingly recognized as prognostic biomarkers and therapeutic targets. Their selective elimination could provide a comprehensive antitumor strategy, particularly to prevent metastasis and recurrence.

1.7.7 Current status of immunotherapy in OS.

Immunotherapy in osteosarcoma dates back to William Coley's pioneering use of bacterial toxins in sarcoma patients over a century ago. Subsequent studies suggested potential benefit; for example, BCG treatment and tumor-cell vaccines improved survival in subsets of patients [103]. Both bacterial therapies and postoperative infections were associated with increased pro-inflammatory cytokine release and enhanced immune-mediated tumor control. Conventional chemotherapies, including doxorubicin and cisplatin, also exert indirect immunomodulatory effects by depleting immunosuppressive populations, facilitating antitumor immunity.

Interest in immunotherapy has grown based on successes in other cancers. In osteosarcoma, conventional chemotherapy not only kills tumor cells but also enhances immune responses by reducing Tregs and myeloid-derived suppressor cells; pediatric patients with faster post-chemotherapy immune recovery show improved prognosis [104, 105]. Clinical trials have demonstrated that adding immunomodulatory strategies to chemotherapy can improve overall survival in localized osteosarcoma, although results are mixed and approval remains limited to Europe. Other approaches include type I interferons, which demonstrated preclinical efficacy but modest clinical benefit in early studies. Larger trials, such as EURAMOS (NCT00134030), reported limited effects due to poor tolerance. More recently, immune checkpoint inhibitors (e.g., anti–CTLA-4, PD-1, PD-L1 antibodies) have shown promise preclinically; blocking PD-1/PD-L1 or combining checkpoint inhibitors with T cell agonists improved survival in murine OS models. However, clinical translation has been limited: trials such as PEMBROSARC indicate PD-1 inhibition has limited activity, suggesting combination strategies targeting the microenvironment may be necessary [106]. Another study evaluating anti–PD-L1 antibody ZKAB001 as maintenance therapy in localized high-grade OS reported 3-year event-free survival benefits in PD-L1-positive or MSI-H subpopulations [107]. Identifying osteosarcoma-specific antigens remains challenging due to the low immunogenicity of mesenchymal tumors. Nevertheless, potential targets include HER2, GD2, FOLR1, and CD146. Notably, GD2, associated with aggressive disease, is targeted in neuroblastoma with favorable outcomes, prompting early-phase OS trials. Additional strategies—such as dendritic cell vaccines and cytokine-based therapies (IL-2, IL-12, GM-CSF)—have shown preclinical activity but limited clinical benefit to date [108].

Overall, while immunotherapy in osteosarcoma has a long history and continues to generate interest, most approaches remain early in clinical development. Progress will depend on collaborative trials and the identification of reliable tumor-specific targets.

1.8 Targeting mechanotransduction in osteosarcoma.

The mechanical sensitivity of the skeleton appears to influence OS onset. Epidemiological studies have shown that a one standard deviation increase in height (1.7 cm in adults, 0.5 cm in adolescents) correlates with a 10% increased OS risk, with incidence peaking during adolescence when bone growth is most rapid and declining as growth stabilizes [109]. This susceptibility is likely linked to enhanced mechanosensitivity of osteocytes during accelerated skeletal growth, as elongation increases mechanical loading and activates pro-proliferative pathways mediated by YAP/TAZ in OS cells. Furthermore, high birth weight has been identified as an independent risk factor [110], and genetic studies have associated the CILP2 locus (rs8103992), involved in skeletal growth, with OS susceptibility, further implicating mechanotransduction in tumor initiation [109].

In healthy bone, osteoblasts act as mechanosensors, transmitting signals either through gap junction proteins such as Connexin 43 or indirectly via calcium ions and cytokines, thereby maintaining bone homeostasis [111, 112]. In OS, however, mechanical stress drives aberrant release of pro-tumorigenic mediators such as RANKL and TGF-β, enhancing proliferation and invasion [112]. Similarly, while YAP/TAZ signaling mediates physiological bone remodeling in normal osteocytes, OS cells exposed to cyclic hydrostatic pressure exhibit aberrant YAP/TAZ-driven proliferation [113]. Moreover, the extracellular matrix (ECM) of OS is abnormally stiff, which activates integrin β1–FAK signaling, promoting metastatic behavior [114]. Altogether, these findings suggest that dysregulated mechanotransduction links skeletal growth dynamics and tumor microenvironment mechanics to OS progression. However, critical gaps remain in understanding how mechanical cues are converted into oncogenic signals. Existing models rarely connect biomechanical signals with epigenetic regulation, even though both are crucial for understanding osteosarcoma. Mechanosensitive proteins, together with pathways such as Hippo, RANK/RANKL, and Wnt/β-catenin, drive changes in gene expression that promote tumor growth, invasion, and therapy resistance. Increased substrate stiffness has been shown to enhance tumor cell migration [115], while fluid shear stress regulates osteosarcoma (OS) cell behavior [116]. Similarly, cyclic tensile strain and compressive stress contribute to angiogenesis and colonization of the osteolytic niche, respectively [117]. Collectively, these mechanical stimuli influence OS cell proliferation, migration, invasion, and drug resistance, thereby promoting disease progression.

Under physiological conditions, osteocytes inhibit tumor development through sclerostin-mediated suppression of Wnt signaling [118]. However, evidence suggests that mechanically stressed osteocytes may instead foster OS progression. For example, fluid shear stress stimulates osteocytes to release RANKL, promoting osteoclastogenesis and establishing a pro-metastatic niche [112]. In contrast, osteocyte-derived Dickkopf-1 (DKK1) has been reported to suppress OS proliferation by blocking Wnt/β-catenin signaling [119]. These conflicting findings may be explained by differences in the type of mechanical stimulus (static vs. dynamic) and the surrounding microenvironmental context.

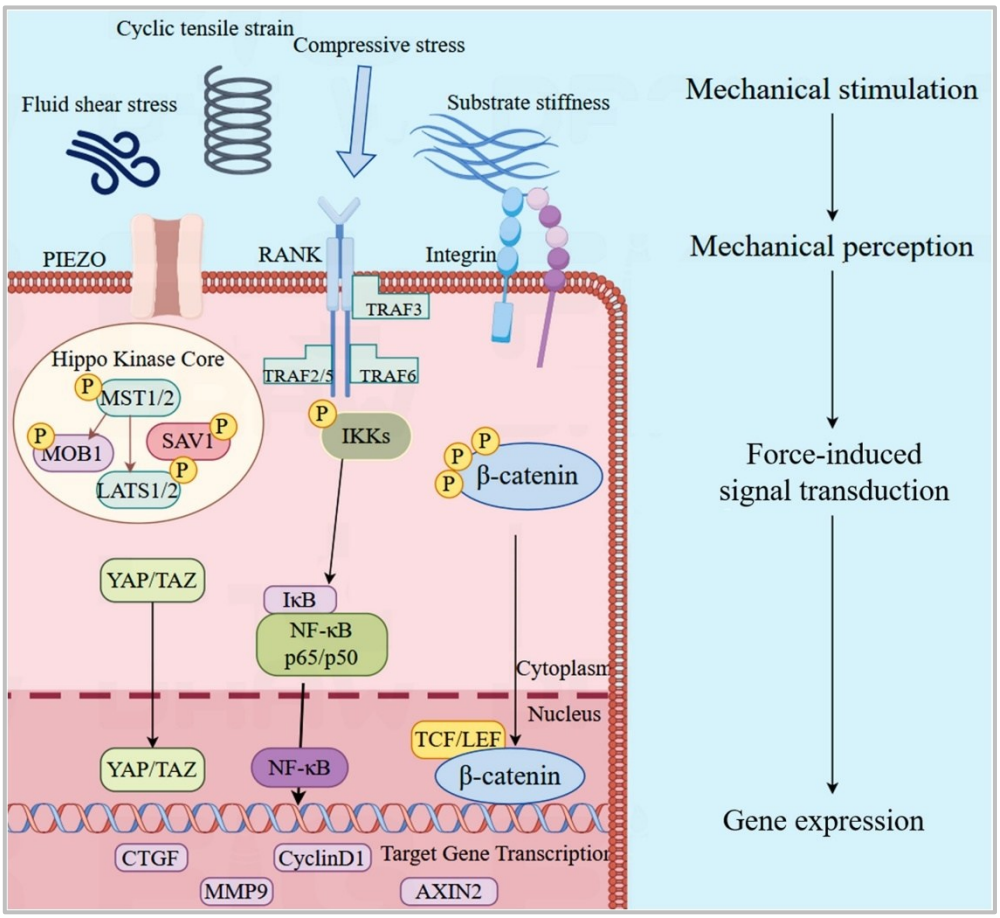

Figure 4. Types of mechanical stress and associated mechanisms for their transmission to cell nucleus (Ruoyun He et al 2025)

1.8.1 Molecular pathway of mechanotransduction.

OS cells detect mechanical cues through mechanosensory proteins [120], initiating mechanotransduction processes that involve integrins and mechanosensitive ion channels. These regulate key signaling cascades, including Hippo, Wnt, and RANK/RANKL pathways. Central mediators such as YAP/TAZ, β-catenin, and RANKL function as molecular hubs, controlling gene expression and shaping cell phenotypes. Through phosphorylation, nuclear translocation, and transcriptional regulation, they influence proliferation, differentiation (osteoclastogenesis and osteoblastogenesis), and migration [112, 121, 122]. This section reviews in detail the mechanotransduction pathways in OS and their roles in directing cellular behavior.

1.8.2 Integrins-FAK pathway.

Integrins are heterodimeric transmembrane receptors composed of 18 α and 8 β subunits that assemble into 25 distinct heterodimers. Structurally, they form a binding pocket through the association of α and β chains, enabling interaction with extracellular matrix (ECM) ligands (Collagen, Fibronectin, Laminin). Binding typically requires Ca^{2+} ions and recognition of short consensus motifs such as RGD (arginine–glycine–aspartate) sequences, although flanking amino acid residues are often critical in determining specificity and binding strength.

Integrins function as bidirectional signaling molecules. In the inactive state, they adopt a bent conformation with low affinity for ligands, whereas activation depends on intracellular adaptor proteins such as Talin, which bind to the β-subunit cytoplasmic tail and induce a high-affinity extended conformation. This process, known as inside-out signaling, modulates both the affinity and avidity of integrins for ECM ligands by dynamically linking integrins to the cytoskeleton. Once clustered at adhesion sites, integrins initiate outside-in signaling, whereby ligand binding triggers the recruitment of multiprotein complexes—including proteases, scaffolding proteins, and adaptors—that reorganize the cytoskeleton and remodel cell architecture. Through these mechanisms, integrins not only anchor cells to the ECM but also coordinate downstream pathways that regulate cell adhesion, migration, and survival. Cytoskeletal components are critical for these processes. Talin provides the physical bridge between integrins and actin filaments, while focal adhesion kinase (FAK), an associated cytoplasmatic tyrosine kinase, orchestrates intracellular signaling cascades and transcriptional reprogramming.

Furthermore, at the transmembrane level, integrins are often accompanied by cell-surface proteoglycans such as syndecans and dystroglycans, which act as co-receptors for growth factors. These proteoglycans cooperate with integrins to amplify signal transduction, further integrating ECM cues with growth factor signaling and cytoskeletal regulation. FAK plays a dual role by phosphorylating intracellular substrates and regulating gene expression, including genes encoding collagen, growth factors, adhesion molecules, and matrix metalloproteinases (MMPs). Through these mechanisms, FAK signaling influences both cell growth rates and cell motility, ultimately enhancing tumor invasiveness [123]. FAK undergoes autophosphorylation at Tyr397, creating a docking site for Src family kinases. Src subsequently phosphorylates Tyr925, enabling the recruitment of Grb2 and SOS to the FAK complex and activating, among others, Ras-dependent pathways [124]. Through this mechanism, Tyr397 phosphorylation orchestrates cell adhesion, migration, invasion, survival, and growth factor–driven proliferation [125].

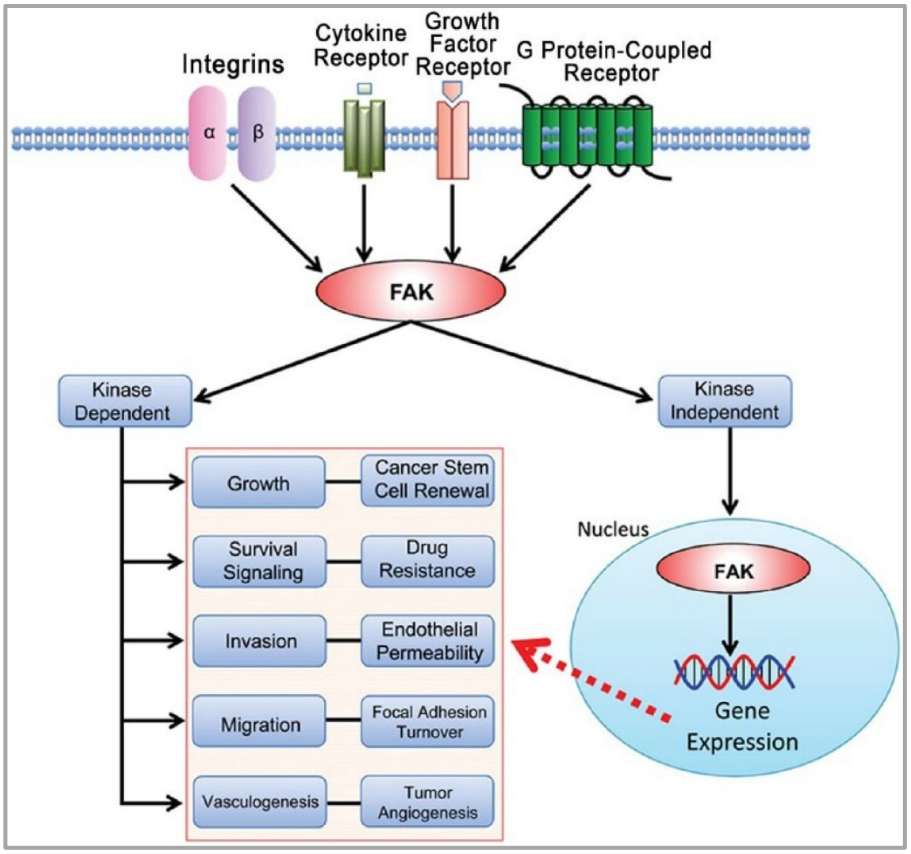

Figure 5. FAK mediated signaling (H. Yoon et al 2015)

Elevated FAK expression has been consistently associated with tumor progression. Studies suggest that FAK upregulation occurs early during the transition from in situ carcinoma to invasive cancer and serves as an independent prognostic factor in several malignancies, including ovarian, esophageal, and colon cancer [126]. Although fewer studies have focused on osteosarcoma, available evidence indicates that FAK expression and phosphorylation status may correlate with an increased metastatic progression. It is noteworthy that in normal osteoblasts, the FAK pathway primarily regulates extracellular matrix (ECM) adhesion during bone repair. By sensing ECM mechanical properties, integrins activate FAK and downstream MAPK signaling, thereby promoting tumor cell proliferation, migration, and invasion. Specifically, binding of integrin αvβ3 to the ECM has been shown to stimulate the RhoA/ROCK pathway, which remodels the cytoskeleton via the LIMK/cofilin axis, ultimately enhancing OS cell motility [127]. Furthermore, integrin signaling is tightly interconnected with the YAP/TAZ pathway. In OS cells, ECM stiffness triggers integrin–FAK-mediated nuclear translocation of YAP, leading to the activation of pro-oncogenic gene expression [128].

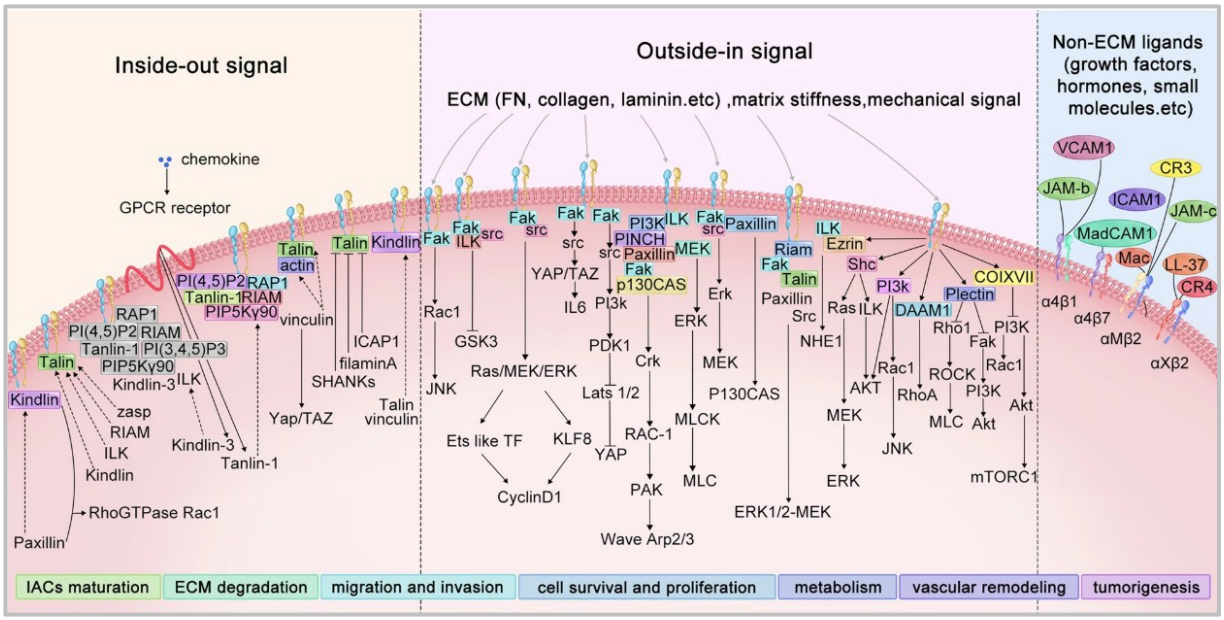

Figure 6. Schematic representation of a series of interaction mechanism between OS cell and ECM components (Ke Ren et al 2015)

1.8.3 Mechanosensitive ion channels.

Mechanosensitive ion channels such as PIEZO1 and TRPV4 are key mediators of mechanical signal transduction in OS. Upon sensing mechanical stress, PIEZO1 induces calcium influx and activates the calcium-dependent protease Calpain, which cleaves Talin and releases focal adhesion signals that promote cell migration [129]. PIEZO1 and TRPV4 also function cooperatively, regulating the formation of the Ca^{2+}/calmodulin complex and enhancing the expression of MMP-2/9 via the NF-κB pathway, thereby accelerating ECM degradation [130]. Moreover, in the OS tumor microenvironment (TME), increased matrix stiffness sustains tumor stemness through a PIEZO1–YAP positive feedback loop. Blockade of integrins with RGD peptides has been shown to significantly inhibit this mechanotransductive signaling axis [127].

1.8.4 Hippo pathway.

The Hippo signaling pathway regulates OS progression by controlling the subcellular localization and activity of the transcriptional co-activators YAP and TAZ. This evolutionarily conserved pathway plays a critical role in regulating cell proliferation, survival, and organ size, primarily by restraining YAP/TAZ activity, which otherwise drive tumor growth and progression [131]. The canonical Hippo cascade involves the core kinases MST1/2, SAV1, MOB1, and LATS1/2. Upon activation by upstream stimuli such as cell density, cytoskeletal tension, and mechanical stress, MST1/2 in complex with SAV1 phosphorylate and activate LATS1/2 kinases with the assistance of MOB1. Activated LATS1/2 subsequently phosphorylate YAP/TAZ, leading to their cytoplasmic retention and/or proteasomal degradation. This prevents their nuclear translocation and inhibits TEAD-dependent transcription of pro-proliferative, pro-migration and anti-apoptotic genes [132].

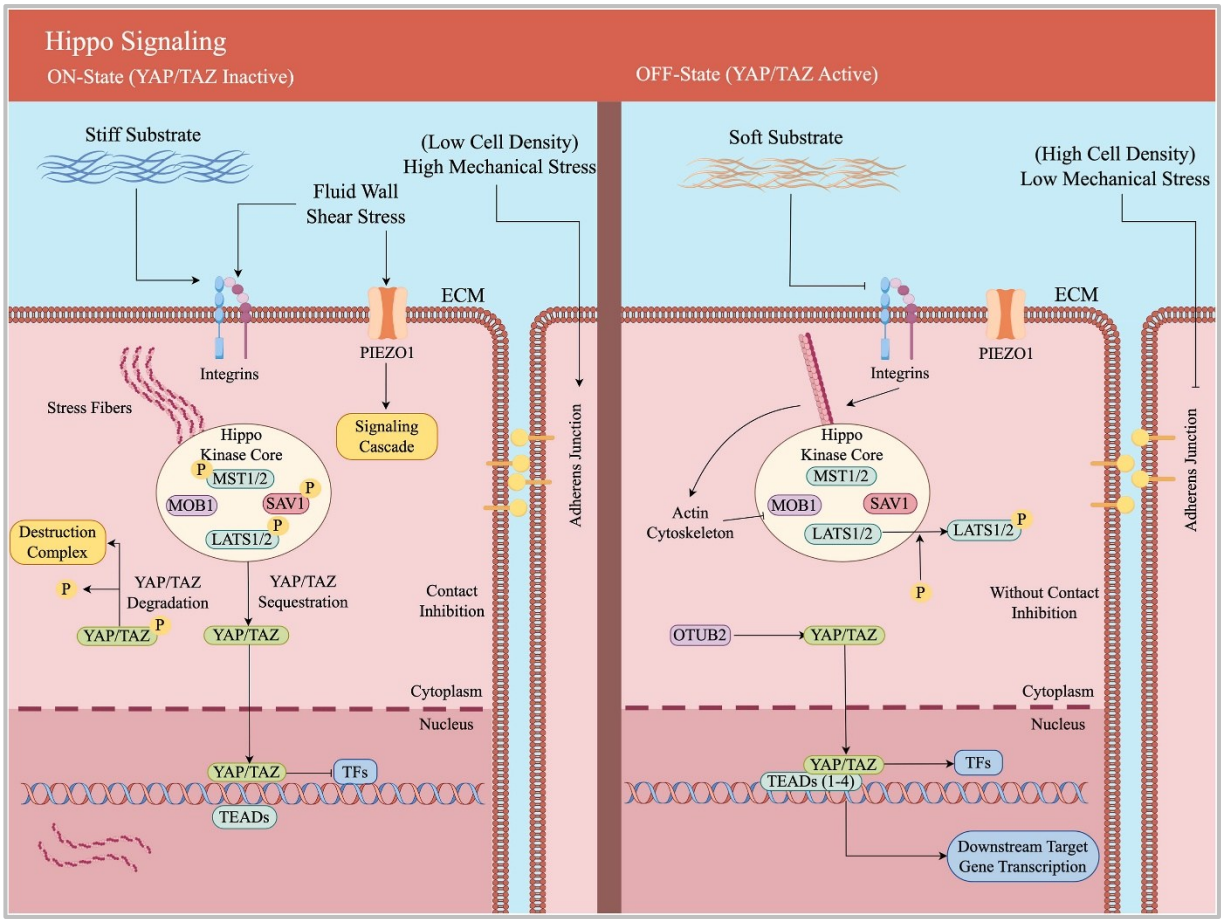

Figure 7. Hippo pathway involved in mechanosensing in OS (Ruoyun He et al 2025)

External mechanical stimuli can further modulate Hippo pathway activity. For example, PIEZO1-mediated calcium influx has been reported to suppress LATS1 activity, leading to TAZ dephosphorylation and nuclear translocation, thereby promoting OS cell migration [133]. Similarly, cyclic mechanical stretching enhances YAP nuclear localization through the integrin αVβ3–actin cytoskeleton axis, facilitating early osteogenic processes [134]. Substrate stiffness is a major regulator of YAP activity: a rigid ECM promotes YAP nuclear translocation through cooperative PIEZO1–integrin signaling, driving osteogenic differentiation partly via epigenetic regulation, whereas a soft ECM favors adipogenic differentiation.

Other stimuli, including high cell density and fluid shear stress, also influence YAP/TAZ signaling, contributing to OS progression [135, 136]. Importantly, YAP/TAZ activity can bypass canonical Hippo regulation. For instance, OTUB2-mediated stabilization of YAP/TAZ enhances metastatic behavior independently of the Hippo core kinase cascade [137].

1.8.5 RANK/RANKL pathway.

The RANK/RANKL signaling pathway is a central regulator of osteoclastogenesis and bone remodeling. RANK, expressed on osteoclast precursors and mature osteoclasts, binds to its ligand RANKL, which is primarily produced by osteoblasts, osteocytes, and activated T lymphocytes [138]. In the presence of macrophage colony-stimulating factor (M-CSF), RANK activation triggers downstream signaling cascades, including NF-κB, MAPK (ERK, JNK, p38), and PI3K/AKT pathways. These pathways collectively promote osteoclast precursor survival, fusion, differentiation, and activation, thereby enhancing osteoclast-mediated bone resorption.

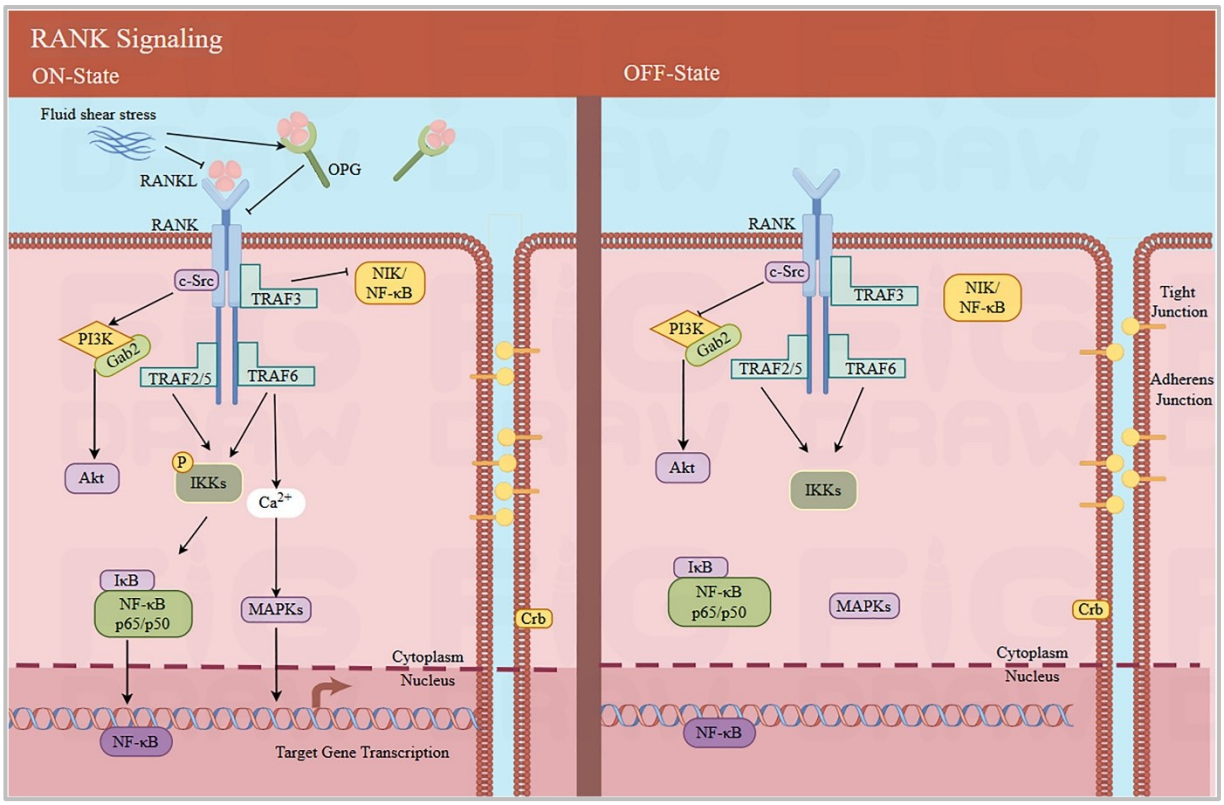

Figure 8. RANK-RANKL signaling involved in mechanosensing in OS (Ruoyun He et al 2025)

In OS, the RANK/RANKL axis is closely interconnected with mechanotransduction. Mechanical stimuli, such as fluid shear stress, can induce RANKL expression and activate downstream signaling mediators including c-Src, PI3K, TRAF family proteins (particularly TRAF6), Akt, and IKK complexes. This cascade culminates in NF-κB nuclear translocation and transcription of genes involved in osteoclastogenesis, inflammation, and tumor progression.

Mechanical regulation of RANKL is accompanied by alterations in the RANKL/osteoprotegerin (OPG) ratio, disrupting the physiological balance between osteoclastogenesis and osteoblastogenesis—typically favoring osteoclast activation

and bone resorption [139]. In OS, this imbalance contributes to a pro-tumorigenic bone microenvironment that facilitates tumor growth, local bone destruction, and metastatic dissemination. Mechanistic studies suggest that this pathway may represent a therapeutic target. For example, modulation of the RANKL/OPG balance in a YAP-driven mechanical model of orthodontic tooth movement demonstrated its regulatory potential and highlighted the functional interplay between mechanotransduction and bone remodeling pathways [140].

1.8.6 Wnt pathway.

The Wnt/β-catenin pathway is a key regulator of bone development and tumor progression. Upon binding of Wnt ligands to Frizzled receptors and co-receptors LRP5/6, LRP becomes phosphorylated and recruits AXIN to the membrane. This event disrupts the β-catenin destruction complex—composed of AXIN, APC, GSK-3β, and CK1—thereby preventing β-catenin phosphorylation and proteasomal degradation. As a result, stabilized β-catenin accumulates in the cytoplasm and translocates to the nucleus, where it interacts with TCF/LEF transcription factors to regulate the expression of downstream target genes involved in proliferation, differentiation, and survival.

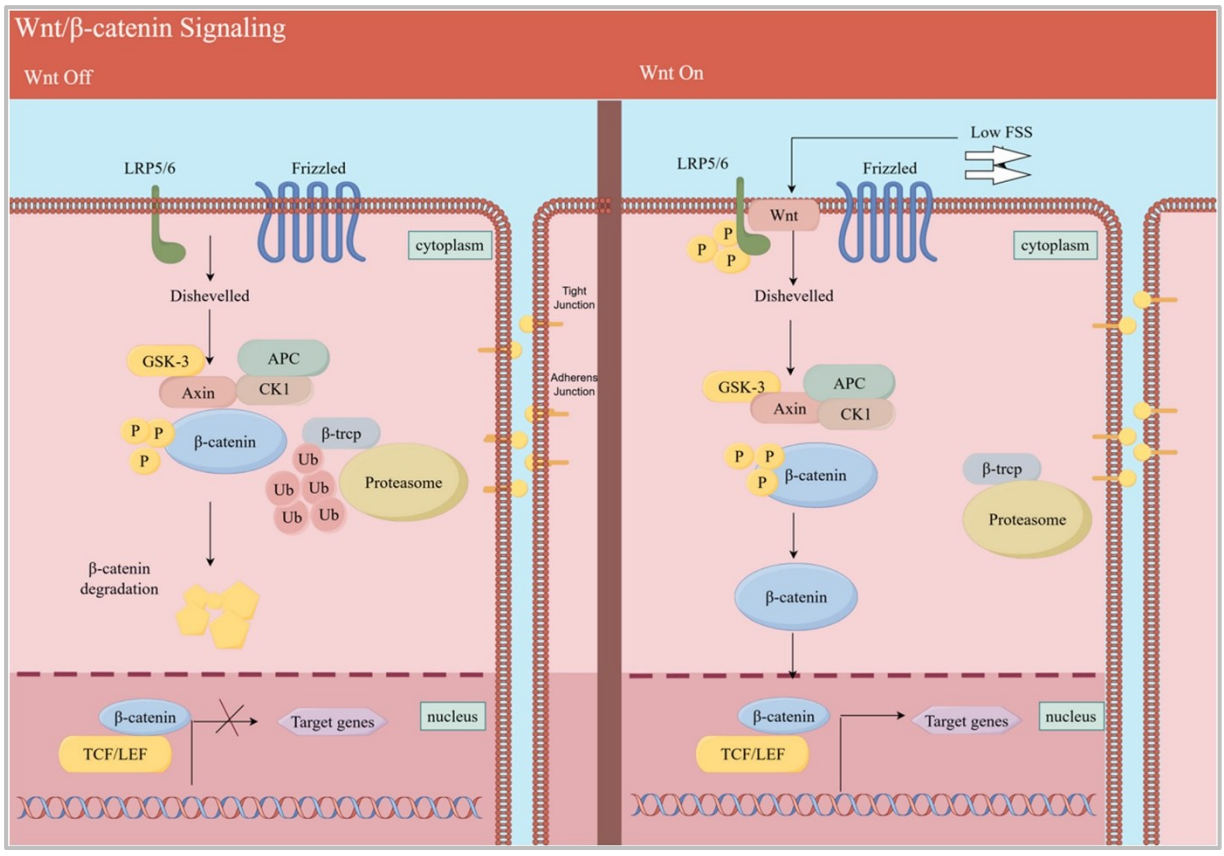

Figure 9. Wnt signaling involved in mechanosensing in OS (Ruoyun He et al 2025)

In the OS microenvironment, mechanical stimulation plays a critical role in orchestrating Wnt/β-catenin signaling, thereby contributing to malignant progression. For example, mechanical loading aligned with the gravitational axis has been shown to enhance MLO-Y4 osteocyte proliferation and reduce apoptosis through the ECM–integrin–cytoskeleton axis and activation of Wnt signaling [119]. In OS cells, increased cell density and spatial organization have been associated with enhanced cadherin–β-catenin interactions, supporting TCF/LEF-dependent transcriptional activity [141]. Higher ECM stiffness promotes β-catenin stabilization and nuclear localization, inducing cell proliferation and survival. Additionally, wall shear stress (WSS) activates β-catenin through PIEZO1-dependent mechanisms, sustaining pro-tumorigenic signaling [142].

1.8.7 Targeting of mechanotransduction: current state of the art for mechanotransduction based therapy in OS.

Targeting the ECM stiffness. Recent advances in mechanotransduction-based strategies have highlighted the therapeutic potential of bioengineered scaffolds for OS. Progress in 3D printing technologies has enabled the development of scaffolds that mimic native bone mechanical properties while modulating tumor-associated mechanobiological signals. Functional coatings and hybrid scaffold designs can fine-tune strain distribution, influence YAP/TAZ activity, and interfere with integrin-mediated signaling, thereby limiting OS progression. For example, hydrogel-based scaffolds capable of reducing interfacial shear stress have been engineered for controlled release of RGD peptides, disrupting integrin–FAK/PI3K–YAP signaling [143]. Beyond stiffness-oriented approaches, innovative piezoelectric scaffolds activated by ultrasound can generate reactive oxygen species (ROS), inducing PANoptosis—a regulated cell death program integrating pyroptosis, apoptosis, and necroptosis. This strategy selectively eliminates OS cells while promoting bone regeneration. Moreover, it enhances antitumor immunity, for instance by stimulating dendritic cell maturation [144]. Collectively, these approaches demonstrate how mechanical cues can be therapeutically harnessed for both tumor suppression and bone repair.

Targeting mechanosensitive signaling pathways. Mechanotransduction-based therapies are primarily designed to counteract abnormal mechanical stress within the tumor microenvironment. These strategies frequently focus on the YAP/TAZ signaling

pathway [145], a central regulator of OS growth, stemness, and metastasis. Small-molecule inhibitors such as Verteporfin, which disrupts the YAP–TEAD interaction, are currently under preclinical evaluation [145]. Similarly, Ciclopirox olamine (CA3) has been shown to inhibit YAP/TAZ nuclear translocation and transcriptional activity, inducing apoptosis in OS cells [146].

Targeting the RANK/RANKL pathway represents a complementary approach, as RANKL overexpression in OS contributes to osteolysis and metastatic dissemination. The monoclonal antibody Denosumab, which binds RANKL with high affinity, has demonstrated anti-tumor and anti-osteolytic effects in preclinical OS models [147] and showed encouraging results in a Phase II clinical trial (NCT02470091).

Overall, modulation of mechanotransduction—particularly through inhibition of YAP/TAZ signaling and integrin-mediated mechanosensing—represents a promising therapeutic avenue, although clinical validation in OS remains limited.

1.9 Regulation of Cancer Cell Invasion.

Malignant cell migration and invasion are central hallmarks of tumor biology and represent critical steps in metastasis, the leading cause of cancer-related mortality [148]. To disseminate, tumor cells must detach from the primary tumor mass, traverse the extracellular matrix (ECM), and intravasate into the circulation. While epithelial-to-mesenchymal transition (EMT) has traditionally been considered essential for invasion, increasing evidence indicates that tumor cells exploit multiple migration strategies [149]. Dissemination may occur through mesenchymal or amoeboid migration. Mesenchymal migration is characterized by elongated cell morphology, integrin-dependent ECM adhesion, and proteolytic remodeling of the surrounding matrix [150]. Protease-mediated ECM degradation—often involving matrix metalloproteinases—is typically required to generate migration paths. EMT and hybrid EMT states enable epithelial tumor cells to acquire mesenchymal traits and invasive capabilities.

In contrast, amoeboid migration involves rounded cells that squeeze through pre-existing ECM pores via actomyosin contractility, without extensive proteolysis. This mode of migration is characterized by bleb-like protrusions driven by cortical actomyosin tension and relatively weak, dynamic adhesion to the ECM [151]. Beyond single-cell motility, tumors may exhibit collective migration, in which groups of cancer cells maintain cell–cell junctions and migrate cooperatively while preserving partial epithelial characteristics [152]. Although these migration modes may appear distinct and tissue-specific, tumor cells can dynamically switch between them in response to ECM mechanics, biochemical signals, or therapeutic pressure. This phenomenon, known as migration plasticity, enhances metastatic potential and may undermine the efficacy of anti-invasive therapies [153].

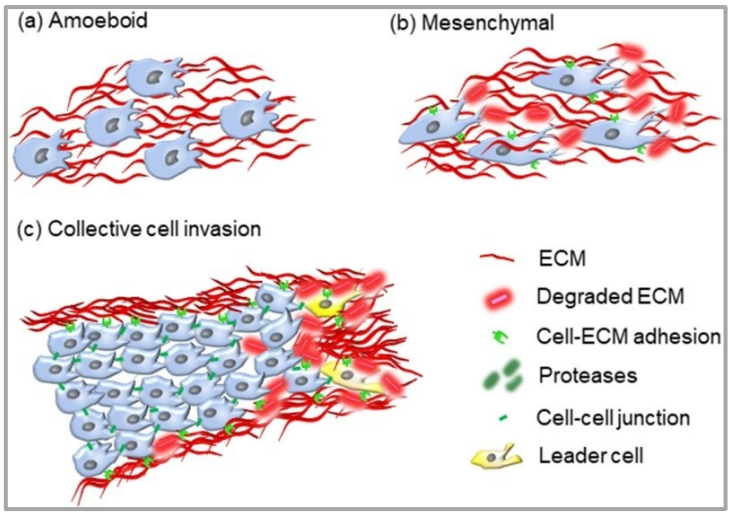

Figure 10. Mechanisms of cancer cells invasion (Jia-Shun Wu et al 2021)

Amoeboid migration is characterized by the rapid deformability of tumor cells, enabling them to squeeze through narrow gaps in the extracellular matrix (ECM) [154]. This flexibility is driven by dynamic reorganization of the cortical actin cytoskeleton, allowing cells to undergo rapid cycles of expansion and contraction and resulting in high-speed displacement [155]. The nucleus, although one of the stiffest cellular organelles, can also deform to traverse pores smaller than the cell diameter, reaching a maximally compressed state during migration [155, 156]. Another hallmark of amoeboid motility is the formation of bleb-like protrusions, which facilitate movement through confined spaces and contribute to environmental sensing via mechanotransduction mechanisms [156]. These protrusions, together with cortical actin remodeling, are predominantly regulated by RhoA and its effector ROCK [157]. Unlike mesenchymal migration, amoeboid movement does not rely on proteolytic degradation of the ECM [158] and occurs largely independently of strong integrin-mediated adhesion, as integrin inhibition does not abolish this migration mode [159]. Instead, amoeboid cells migrate at relatively high velocities (approximately 2–30 μm/min) by forming transient, weak interactions with the substrate in a crawling-like manner [160].

Mesenchymal migration is commonly observed in tumors of connective tissue, bone marrow origin, and poorly differentiated epithelial cancers [160]. It is frequently associated with epithelial-to-mesenchymal transition (EMT), a process in which epithelial cells lose intercellular junctions and epithelial markers while acquiring mesenchymal characteristics that confer motility and invasiveness [161]. Histologically,

mesenchymal tumor cells exhibit an elongated, spindle-shaped morphology with pseudopodia and filopodia. This migration mode is driven by cytoskeletal contractility, integrin-mediated adhesion to the ECM, and proteolytic matrix remodelling [150]. Focal adhesion kinase (FAK) and Src kinases regulate actin dynamics, while coordinated cycles of RhoA-driven contractility and Rac-mediated protrusion formation enable forward movement [162, 163]. Due to the relatively slow turnover of focal adhesions, mesenchymal migration generally occurs at lower velocities than amoeboid movement [160]. Integrins play a central role in substrate recognition and directional migration by transmitting both outside-in and inside-out signals that maintain cell polarity and generate traction forces [164]. Inhibition of integrins disrupts the elongated morphology and reduces migration efficiency. Unlike amoeboid motility, mesenchymal migration requires protease-dependent ECM remodeling, particularly through matrix metalloproteinases (MMPs), which degrade ECM components to create migration tracks [165]. Blocking integrins or proteases can impair mesenchymal movement and may induce a switch toward an amoeboid phenotype.

When tumor cells retain cell–cell junctions and migrate coordinately as a multicellular unit, the process is referred to as **collective cell migration**. In this mode, cells maintain front–rear polarity and cooperate in a hierarchical manner [166]. Intercellular connections are preserved through cadherins (E-, N-, and P-cadherin), members of the immunoglobulin superfamily, and gap junctions. Collective movement depends on actin cytoskeleton dynamics and integrin-mediated adhesion to the ECM, and is accompanied by coordinated, localized proteolytic remodeling of the ECM [167].

Migrating tumor cell clusters are typically heterogeneous and polarized into leading and trailing regions [168]. Leader cells, located at the invasive front, exhibit distinct morphology and gene expression profiles, along with enhanced proliferative and invasive capacity compared with follower cells. They guide collective migration through Rac-driven protrusions, integrin-mediated adhesion, and ECM remodeling [169]. Similar to single-cell migration, collective invasion requires actomyosin contractility, cell–ECM adhesion, and proteolysis, with MMP-14 and cathepsin B playing key roles in degrading tissue barriers and generating migration paths [170].

Importantly, stromal cells can also assume leader functions. Fibroblasts remodel the ECM through protease activity and mechanical forces, facilitating collective invasion in carcinoma models, such as squamous cell carcinoma [171]. At tumor margins and metastatic sites, fibroblasts release chemotactic factors, including CCL8, which

promote tumor cell invasion and dissemination [171]. Similarly, tumor-associated macrophages, recruited via CCR2 signaling, can escort cancer cells toward blood vessels by engaging the CXCL12–CXCR4 axis, thereby facilitating intravasation [172].

Cancer cells exhibit remarkable migration plasticity, allowing dynamic transitions between different motility modes in response to microenvironmental constraints. Single-cell transitions, such as mesenchymal–amoeboid transition (MAT) and amoeboid–mesenchymal transition (AMT), are regulated by protease activity, cell–matrix interactions, and Rho/Rac-dependent actomyosin dynamics. In addition, collective–individual transitions can occur in multiple directions (e.g., collective-to-amoeboid, collective-to-mesenchymal, amoeboid-to-collective, and mesenchymal-to-collective). These shifts are facilitated by EMT, partial EMT states, or mesenchymal-to-epithelial transition (MET), and involve coordinated changes in cell–cell adhesion, cytoskeletal organization, ECM interactions, and pericellular proteolysis [173].

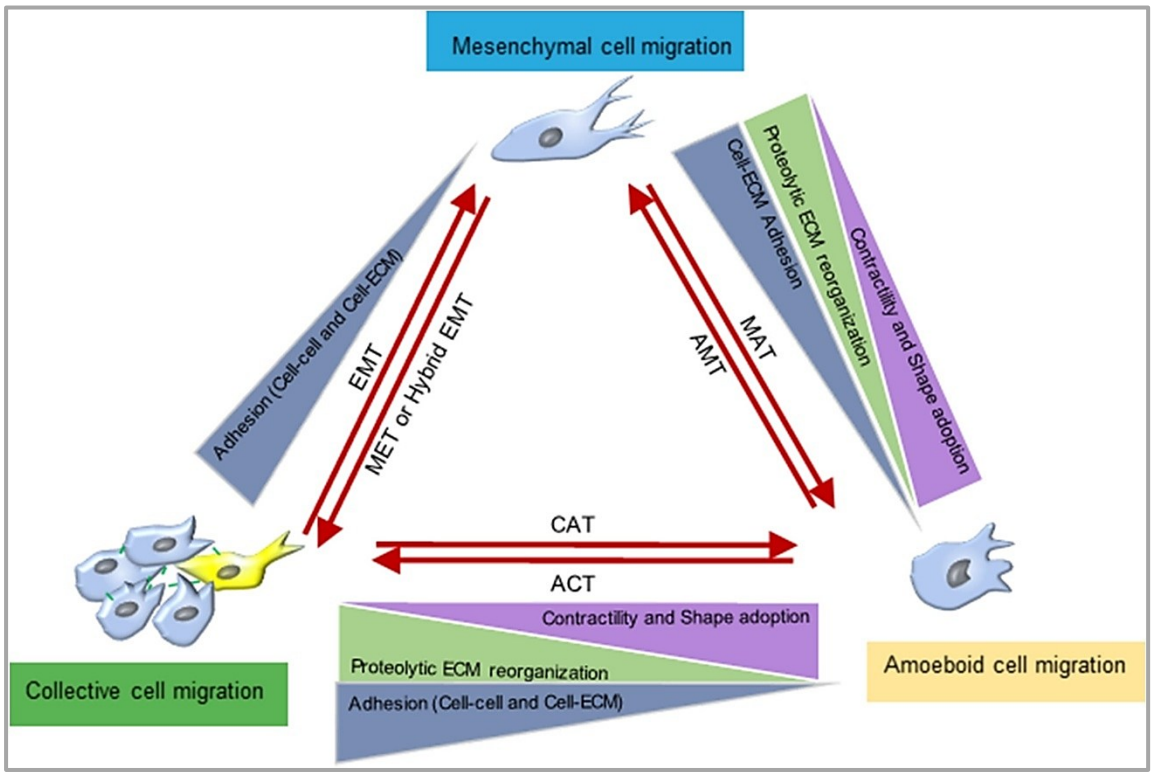

Figure 11. Migration plasticity (Jia-Shun Wu et al 2021)

1.9.1 Rho and ROCK signaling pathways.

The Rho/ROCK signaling axis plays a central role in regulating cytoskeletal dynamics during cancer cell migration. Rac1 promotes lamellipodia formation, whereas RhoA–ROCK signaling induces stress fiber assembly and actomyosin contractility [157]. This pathway is pivotal for migration plasticity: Rac activity favors amoeboid-to-mesenchymal transition (AMT), whereas Rho kinase (ROCK) activity promotes mesenchymal-to-amoeboid transition (MAT) by inhibiting Rac [174]. Pharmacological modulation of Rac1 or RhoA can alter these transitions in a context- and cancer-dependent manner. Notably, this plasticity is more pronounced in 3D culture systems than in 2D models, as demonstrated for glioblastoma cells [175].

ROCK isoforms exhibit distinct functional roles: loss of ROCK1 stabilizes the actin cytoskeleton, whereas loss of ROCK2 increases peripheral membrane folding through cofilin regulation [176]. Several molecules modulate cancer cell migration via the Rho/ROCK axis. For example, TRIM59 regulates contractility and adhesion by suppressing ROCK1 signaling [177]; Smurf1 inhibition induces MAT through RhoA/ROCK and myosin light chain phosphorylation [177]. Similarly, EphA2 expression in melanoma or CD99 overexpression in glioma cells promotes mesenchymal-to-amoeboid transitions by enhancing Rho activity while reducing Rac signaling, independently of Akt, ERK, or JNK pathways [178]. Collectively, these studies highlight the centrality of Rho/ROCK signaling in governing migration modes and invasion strategies in cancer

1.9.2 Protease function in invasion.

Unlike mesenchymal migration, amoeboid motility does not depend on protease-mediated ECM remodeling or integrin-mediated adhesion turnover. Inhibition of MMP activity can induce a mesenchymal-to-amoeboid transition (MAT), characterized by reduced integrin adhesion and impaired FAK autophosphorylation [157]. This adaptive mechanism enables tumor cells to maintain invasive potential even under protease-targeted therapies.

1.9.3 Tumor microenvironment and invasion.

The tumor microenvironment (TME) strongly shapes cancer cell invasion by modulating the balance between mesenchymal and amoeboid migration. ECM stiffness is a key determinant: low-resistance matrices favor amoeboid migration, while stiffer environments promote *invadopodia* formation and mesenchymal invasion [179].

Stromal components further influence migration plasticity. Cancer-associated fibroblasts (CAFs) can induce EMT while simultaneously enhancing amoeboid traits, partly through the recruitment of endothelial progenitor cells [180]. Elevated levels of plasminogen activator inhibitor-1 (PAI-1) in the TME promote MAT via RhoA/ROCK1/myosin light chain phosphorylation [181]. Additionally, bone marrow–derived mesenchymal stem cells (BM-MSCs) co-cultured with osteosarcoma cells can differentiate into CAFs, secreting cytokines and chemokines (e.g., MCP-1, GRO-α, IL-6, IL-8) that stimulate MAT through RhoA activation [182].

1.9.4 EMT is generally hybrid EMT in cancer.

Epithelial-to-mesenchymal transition (EMT) is a major driver of mesenchymal migration but also contributes to collective cell migration, in which tumor cells retain intercellular junctions. Loss of epithelial markers and activation of EMT transcription factors such as Snail can promote collective invasion by stabilizing junctions and modulating pathways including claudin-11 induction, Src activation, and RhoA inhibition. EMT programs are also implicated in galectin-1- and AKT-mediated collective migration through activation of Cdc42, Rac, Snail, and Slug.

Rather than being a binary process, EMT and its reverse, MET, occur along a continuum of hybrid or partial states, in which cells simultaneously express epithelial and mesenchymal features [183]. These intermediate phenotypes are critical for collective motility, as they maintain adhesion while enabling migration. Partial EMT is characterized by retention of E-cadherin along with mesenchymal markers such as N-cadherin and vimentin or by incomplete shifts in gene expression patterns [161].

1.10 Osteosarcoma dissemination and metastases.

Osteosarcoma (OS) exhibits a strong propensity for dissemination and metastasis, the primary determinant of poor patient prognosis. While OS can metastasize to multiple organs, the lungs are the most frequent site, followed by bone and lymph nodes [184]. Metastasis involves a multistep process in which tumor cells adapt to new microenvironments, undergoing profound alterations in cell cycle regulation, differentiation, karyotype, metabolism, and gene expression [185]. Understanding the mechanisms underlying OS metastasis—including contributions from the tumor microenvironment, osteoclast activity, angiogenesis, metabolism, immune interactions, and noncoding RNAs—offers opportunities for therapeutic intervention [186].

The metastatic spread of cancer cells involves a multistep cascade, during which disseminated cells acquire features distinct from the primary tumor. In osteosarcoma, pulmonary metastasis proceeds through three major stages: (i) **escape from the primary tumor**, (ii) **survival and transit through the circulation**, and (iii) colonization of the lung to **establish secondary lesions**. Despite the large number of tumor cells capable of entering this cascade, only a small fraction succeed, reflecting the inefficient and selective nature of the metastatic process [187].

i. **Local dissemination**: OS cells induce osteoclast-mediated bone resorption via RANK/RANKL signaling. Elevated MMPs and cathepsins, coupled with reduced TIMPs, drive ECM degradation. Tumor-derived SDF-1 recruits mesenchymal stem cells, which secrete CCL5 to support tumor progression. Primed dendritic cells exert anti-tumoral effects, while natural killer (NK) cells kill tumor cells via NKG2D–NKG2DL interactions.

ii. **Intravasation and circulation**: Tumor cells enter the bloodstream through pathways including urokinase-type plasminogen activator receptor (uPAR) and formyl peptide receptor type 1 (FPR1). The RUNX2/OPN axis mediates adhesion to lung endothelium, while FASN and ID1 confer resistance to *anoikis* through ERK1/2, Bcl-xL, and PI3K/AKT activation. OS cells' mechanosensitivity allows adaptation to physical stimuli, altering behavior and therapy response [188].

iii. **Lung colonization**. The lung microenvironment imposes unique challenges—including hypoxia, nutrient limitation, and immune surveillance—that influence tumor cell fate, resulting in apoptosis, dormancy, or proliferation into micrometastases. Micrometastases may remain dormant, regress, or progress

into vascularized macrometastases. OS cells exploit endoplasmic reticulum (ER) stress responses, with highly metastatic cells showing elevated HSPA5/GRP78; inhibition reduces lung colonization [189, 190]. ER stress also contributes to chemoresistance through ATF6 and NF-κB signaling. Lung tropism is influenced by mechanical entrapment of circulating cells and tumor-derived extracellular vesicles, including exosomes that precondition the metastatic niche [191] [192].

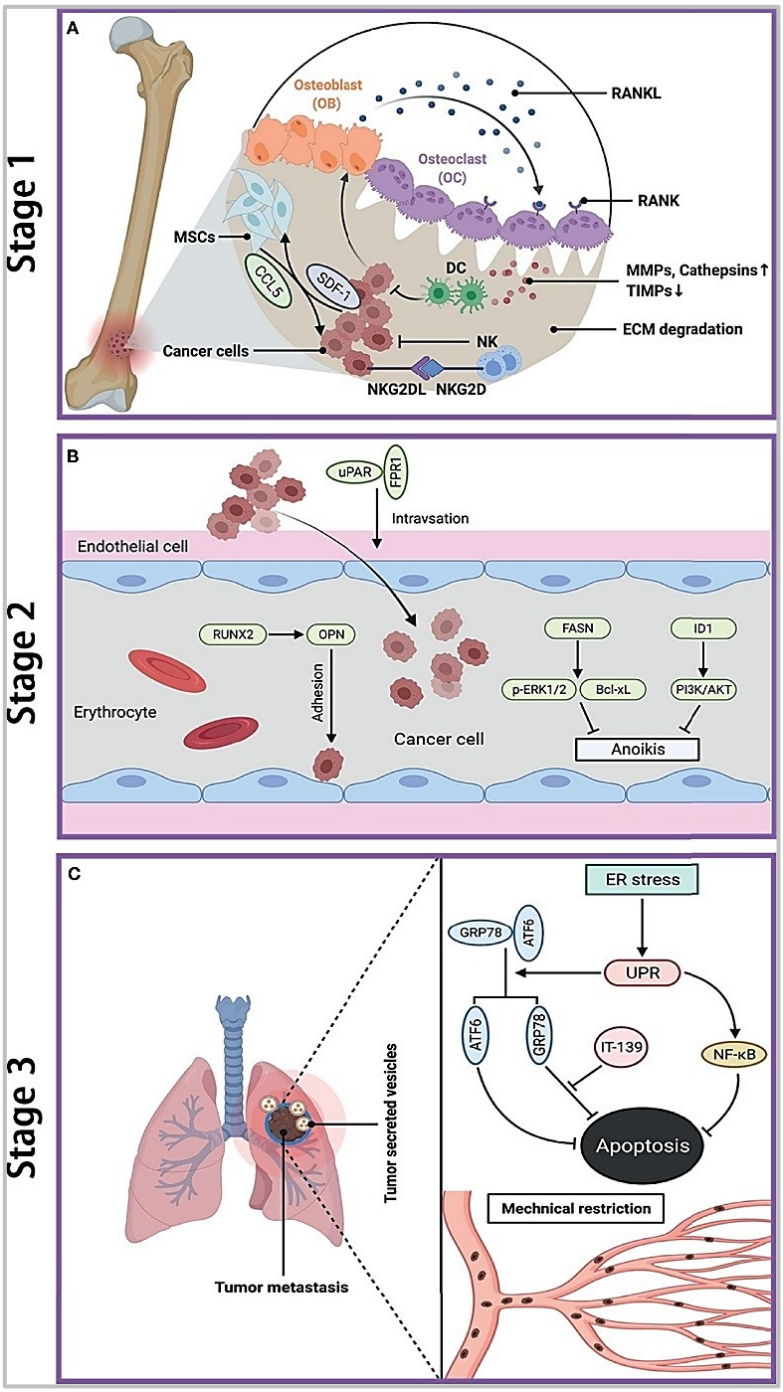

Figure 12. OS canonical metastatic spread (G. Sheng et al 2021)

1.10.1 The role of microenvironment and metastasis.

Bone is a complex connective tissue composed of multiple cell types, soluble factors, and an intricate extracellular matrix (ECM). These components interact dynamically to maintain homeostasis under physiological conditions. The balance between bone formation and resorption ensures proper bone structure. Osteosarcoma (OS) initiation and metastatic progression occur within this multifaceted bone environment. Additionally, metastatic OS cells interact with the surrounding microenvironment at each stage of dissemination, particularly in the lungs. Studying these interactions is crucial to expanding our understanding of OS biology.

Multiple molecular and microenvironmental mechanisms contribute to pulmonary metastasis of OS. The splice variant ΔNTP63 (lacking the N-terminal domain of TP63, a member of the p53 tumor suppressor family) promotes pro-metastatic signaling by enhancing IL-6 and IL-8 secretion and activating STAT3 phosphorylation. STAT3 overexpression stabilizes HIF1-α and induces VEGF secretion, thereby supporting angiogenesis and metastasis [193, 194]. Inhibition of IL-6 and IL-8 reduces metastatic burden in mouse models, highlighting the therapeutic potential of targeting these cytokine pathways [195]. ΔNTP63α also cooperates with TGFβ signaling in a Smad4/TβRII-dependent manner. Moreover, TGFβ-rich extracellular vesicles (EVs) from OS cells stimulate IL-6 secretion from mesenchymal stem cells (MSCs), further enhancing STAT3 activation and metastatic growth [193]. In parallel, fibrotic reprogramming driven by FGF signaling and fibronectin deposition supports lung colonization, a process disrupted by nintedanib targeting the FGFR–FN axis [196].

At the metastatic site, selective pressure from the Fas/FasL system in the lung parenchyma eliminates Fas^+ tumor cells, favoring survival of Fas-deficient clones. Therapeutic strategies that restore Fas expression can induce regression of lung metastases, but only in $FasL^+$ environments, emphasizing the importance of microenvironmental context [197].

Extracellular vesicles play a central role in OS metastasis. OS-derived exosomes carry metastasis-related proteins, including PD-L1 and N-cadherin, which promote immune evasion and pulmonary colonization [198, 199]. Proteomic and transcriptomic analyses reveal distinct EV signatures between low- and high-metastatic OS, and highly metastatic EVs can transfer pro-metastatic traits to otherwise indolent cells via horizontal phenotypic transfer [200]. EVs derived from stromal cells, such as MSCs and tumor-associated macrophages, also modulate OS aggressiveness [201].

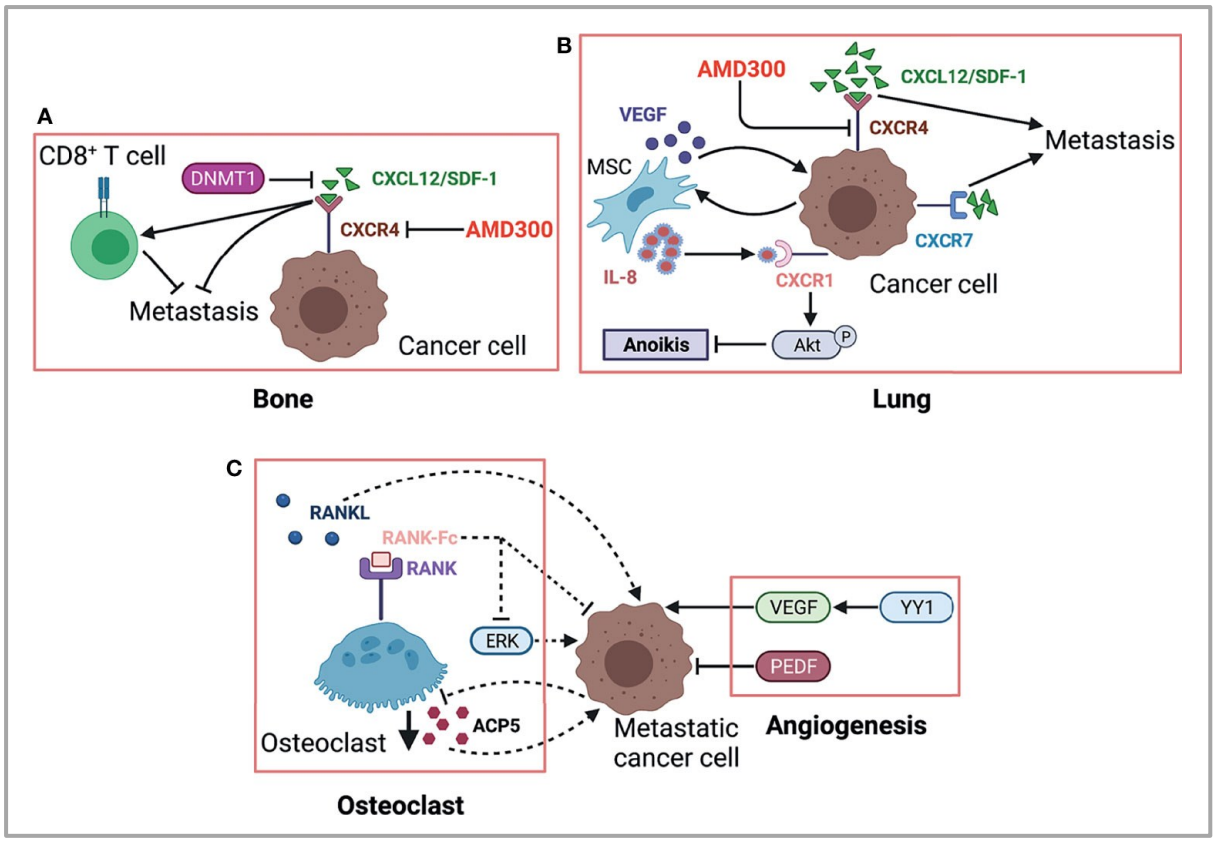

Figure 13. The role of microenvironment in invasion and spreading (Gaohong Sheng et al 2021)

The CXCL/CXCR chemokine axis orchestrates organotropism and invasion. OS cells exploit the CXCL12/CXCR4-CXCR7 network, with lung-derived CXCL12 gradients directing tumor cell migration [202, 203]. This axis promotes angiogenesis, *anoikis* resistance, and immune evasion, and is further regulated by lung-MSCs: IL-8 enhances *anoikis* resistance and OS metastasis via CXCR1/Akt signaling [204]. Therapeutic targeting of CXCR4 with blocking antibodies or inhibitors such as AMD300 effectively reduces lung metastasis [205]. Collectively, these findings highlight the interplay between tumor-intrinsic pathways (ΔNTP63, TGFβ/STAT3, Fas regulation), microenvironmental factors (fibrotic remodeling, FasL expression), and extracellular mediators (EVs, CXCL/CXCR axis) in shaping the metastatic trajectory of OS, providing multiple potential targets for novel therapeutic interventions.

1.10.2 The role of osteoclasts.

Osteosarcoma (OS) progression induces osteolysis, which facilitates tumor cell dissemination and establishes a vicious cycle between osteoclast activity and metastasis [206]. Targeting this interplay represents a promising therapeutic strategy. Inhibition of the RANK/RANKL pathway using RANK-Fc (a recombinant fusion protein combining the IgG Fc region with the extracellular ligand-binding domain of RANK)

reduces metastasis by promoting *anoikis* and apoptosis in OS cells [207, 208]. Additional strategies to impede bone resorption include targeting transcription factors such as Sp7, TNFSF10, and the TGF-β/Smad signaling pathway, as well as anti-resorptive drugs like zoledronic acid, which may synergistically enhance therapeutic efficacy [209]. However, some evidence suggests that metastasis-competent OS cells can suppress osteoclastogenesis—for instance, by reducing $ACP5^+$ osteoclast numbers or via OS-derived extracellular vesicles that inhibit osteoclast differentiation while promoting metastasis [210]. Therefore, while reciprocal regulation between OS cells and osteoclasts is established, the precise role of osteoclasts in OS metastasis remains incompletely understood.

1.10.3 Angiogenesis and metastasis.

Angiogenesis is a critical driver of OS progression, supplying nutrients to the tumor and forming the primary route for tumor cells to enter the circulation and colonize distant sites [211]. Clinical and experimental evidence demonstrates the pro-metastatic role of VEGF, with higher expression correlating with advanced tumor grade and poor prognosis [212]. VEGF-mediated angiogenesis can be enhanced by factors such as angiopoietin-like protein 2 and YY1, whereas VEGF knockdown significantly limits metastasis [212]. Targeting angiogenesis through VEGFR2 blockade, for example with the tyrosine kinase inhibitor anlotinib, has shown preclinical efficacy in reducing metastasis [213]. Although these preclinical data support antiangiogenic therapy as a potential approach against OS metastasis, its safety and clinical efficacy remain unproven, warranting further investigation before clinical translation [214].

1.10.4 Cell metabolism.

Metabolic reprogramming distinguishes metastatic OS cells from their primary tumor counterparts, driven by differences in nutrient availability, oxygenation, and energy demands [215]. Metabolomic studies reveal a shift from carbohydrate and amino acid metabolism toward lipid metabolism during metastasis, with elevated lipid metabolites detected in serum and metastatic OS cells [216]. Inhibition of cholesterol synthesis reduces metastasis, highlighting the central role of lipid metabolism [217]. Additionally, supplementation with inositol hexaphosphate suppresses lung metastasis by inhibiting MAPK and PI3K signaling [218].

Hypoxia also promotes metastasis through HIF1-α, which enhances invasion via VEGF-A upregulation and activates the CXCR4 pathway, facilitating pulmonary

colonization [219]. Hypoxia-induced Cyr61/CCN1 expression contributes to angiogenesis, EMT, and poor prognosis [220, 221].

Transcriptional regulators further modulate metabolic adaptation. The tumor suppressor WWOX (WW domain–containing oxidoreductase) antagonizes the Warburg effect by inhibiting HIF1-α and c-Jun, thereby suppressing metastasis [222, 223]. The Warburg effect refers to the tendency of tumor cells to rely on glycolysis rather than mitochondrial oxidative phosphorylation for ATP production. Conversely, the AP-1 transcriptional complex (c-Jun, c-Fos, ATF, MAF) promotes metastatic traits, angiogenesis, and EMT by upregulating podoplanin, TGF-β, and FGFR1 [224, 225]

Finally, OS adaptation to the acidic tumor microenvironment reflects an epigenetically stabilized metabolic shift. While acute acidosis induces cell death, chronic exposure enhances invasiveness via activation of cIAP proteins (Cellular Inhibitor of Apoptosis) and NF-κB signaling, conferring stress resilience and metastatic potential [226].

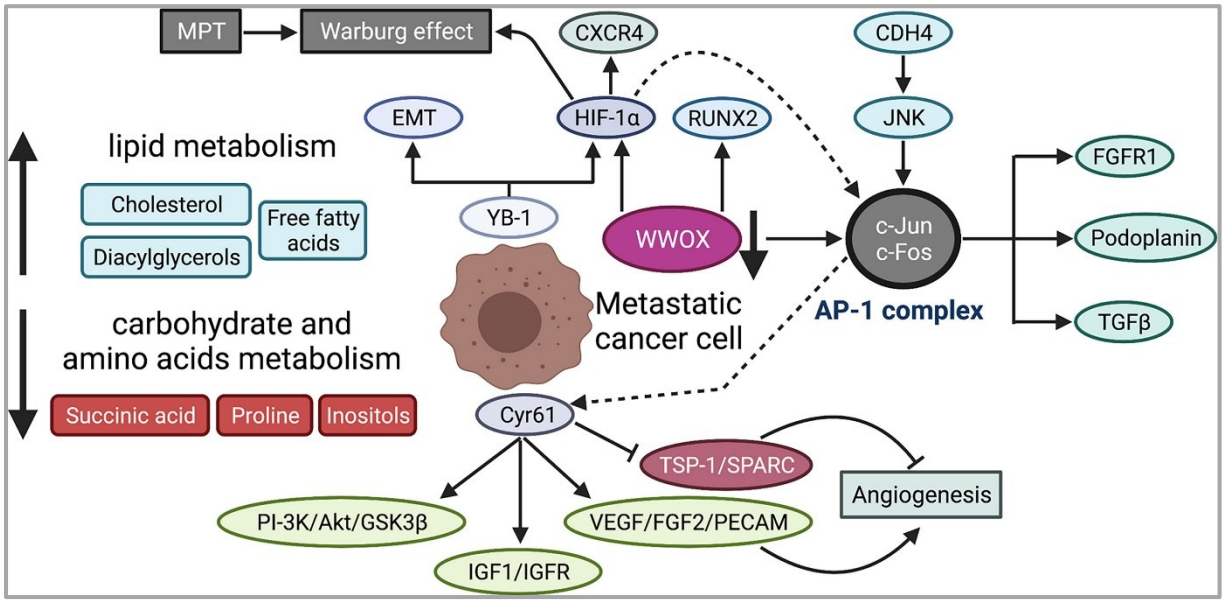

Figure 14. Microenvironment: metabolism and OS cell spreading (Gaohong Sheng et al 2021)

1.10.5 Immune system.

Both the innate and adaptive immune systems play critical roles in shaping osteosarcoma (OS) progression and metastasis. Recent studies have highlighted macrophages, dendritic cells, and T lymphocytes as central regulators of the metastatic process [79, 227]. The abundance, phenotype, and interactions of these immune cells can either promote or suppress metastasis, reflecting a highly dynamic tumor–immune interplay.

For instance, M2-polarized tumor-associated macrophages (TAMs) enhance OS stemness and metastatic potential [228]. Therapeutic strategies targeting TAMs, such as mifamurtide treatment or suppression of M2 polarization with trans-retinoic acid, have been shown to reduce tumor progression [229]. Nevertheless, conflicting findings underscore the complexity and context-dependent functions of TAMs in OS.

Tumor-infiltrating lymphocytes (TILs) also modulate metastatic behavior. Elevated levels of $CD8^+$ T cells and a higher $CD8^+/FOXP3^+$ ratio correlate with improved prognosis [230]. Interestingly, metastatic lesions often display denser TIL populations than primary tumors, forming a distinct immune niche [77]. The cytotoxic activity of T lymphocytes is, however, frequently suppressed by immune checkpoint pathways: PD-L1 expression on metastatic OS cells and PD-1 on TILs dampen cytotoxic responses, facilitating immune evasion.

Overall, the immune landscape in OS metastasis is defined by complex interactions among immune checkpoints, cell surface markers, and immune cell plasticity. Understanding these mechanisms is essential for the development of effective immunotherapeutic strategies, although current clinical applications remain limited and under investigation [231].

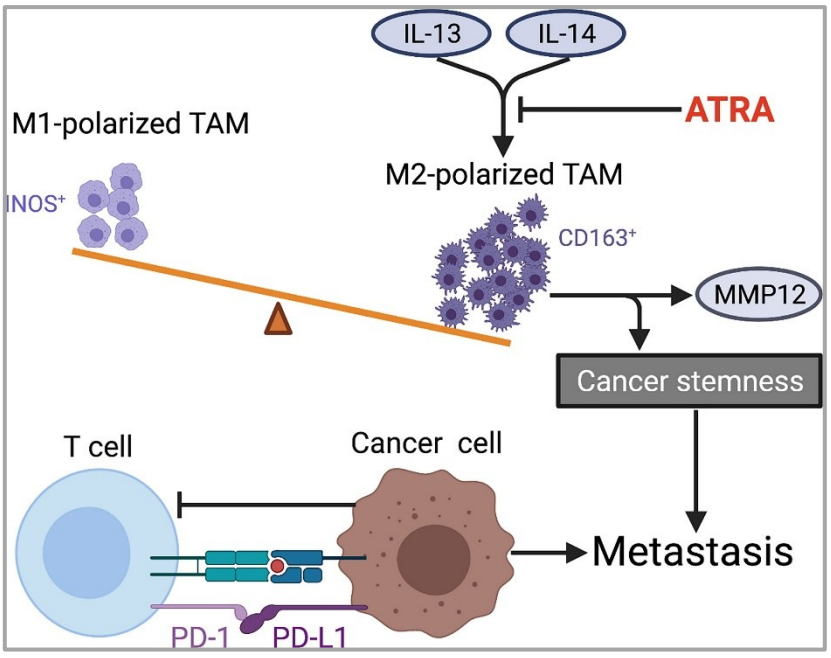

Figure 15. Immune system and OS cells spreading (Gaohong Sheng et al 2021)

1.10.6 Role of miRNAs in bone sarcoma.

MicroRNAs (miRNAs) are short non-coding RNAs (18–25 nucleotides) that regulate gene expression by binding to the 3′ untranslated region (3′UTR) of target mRNAs within the RNA-induced silencing complex (RISC), leading to translational repression or mRNA degradation [232]. Given that a single miRNA can target multiple mRNAs and, conversely, individual mRNAs can be regulated by multiple miRNAs, these molecules influence diverse biological processes, including proliferation, apoptosis, and angiogenesis. Distinct miRNA expression profiles have been identified in osteosarcoma (OS) metastasis, suggesting potential diagnostic and prognostic value. Most miRNAs studied to date act as metastasis suppressors, although some exhibit pro-metastatic activity. For example, miR-195 suppresses metastasis by targeting FASN [233], but elevated serum levels have been reported in OS patients [234], indicating possible stage-dependent or context-specific roles. Interestingly, miR-27a*, derived from the passenger strand, has been shown to target CBFA2T3 directly, promoting OS lung and bone metastasis *in-vivo* [235]. Moreover, miRNA expression is dynamically regulated by metastasis-associated genes (e.g., MYC, TP53, TGFB1) and by epigenetic modulators such as APEX1 [236]. Certain chemotherapeutics, including epirubicin and diallyltrisulfide, also reshape miRNA profiles [237, 238].

Despite extensive preclinical evidence, miRNA-based therapies remain in early stages, with delivery being a major challenge due to low efficiency, rapid degradation, and off-target accumulation. Promising approaches include hyaluronic acid-coated liposomes to improve stability and cellular uptake, as well as viral vectors encoding hairpin structures processed into mature miRNAs.

In conclusion, the mechanisms underlying OS metastasis remain incompletely understood. Key points include:

- **Angiogenesis**: OS cells can both promote endothelial proliferation and induce contact-dependent apoptosis, potentially facilitating vascular invasion.
- **Lung tropism**: The lungs are the predominant metastatic site, likely due to organ-specific premetastatic niches formed by tumor-derived exosomes, although the exact drivers remain unclear.
- **Immune niche**: The immune microenvironment in OS metastasis is distinct from other cancers, and effective immunotherapies are still limited.

- **Mechanical cues**: Beyond biochemical signals, mechanical forces such as substrate stiffness and fluid shear stress significantly influence OS invasiveness and therapy response.

1.11 Phospholipase C enzymes.

The phospholipids of cell membranes are the target of numerous enzymes, among which are the phospholipases, a molecular superfamily of proteins essential for lipid metabolism. The hydrolysis process triggered by phospholipases produces a series of hydrophobic molecules that are involved in multiple signaling pathways underlying cell development and metabolism [239].

Phospholipases are classified into four main families: phospholipase A, phospholipase B, phospholipase C, and phospholipase D; this subdivision is primarily determined by their distinct biochemical behavior. While phospholipases A and B are acyl hydrolases (they hydrolyze the bonds between the acyl groups and the glycerol hydroxyl), phospholipases C and D are phosphodiesterases (they hydrolyze the ester bonds between glycerol and phosphate or between phosphate and the substituent of the phospholipid) [240]. Members of the phospholipase superfamily also differ in molecular weight, quaternary protein structure (type and number of subunits), physiological actions, and regulatory mechanisms.

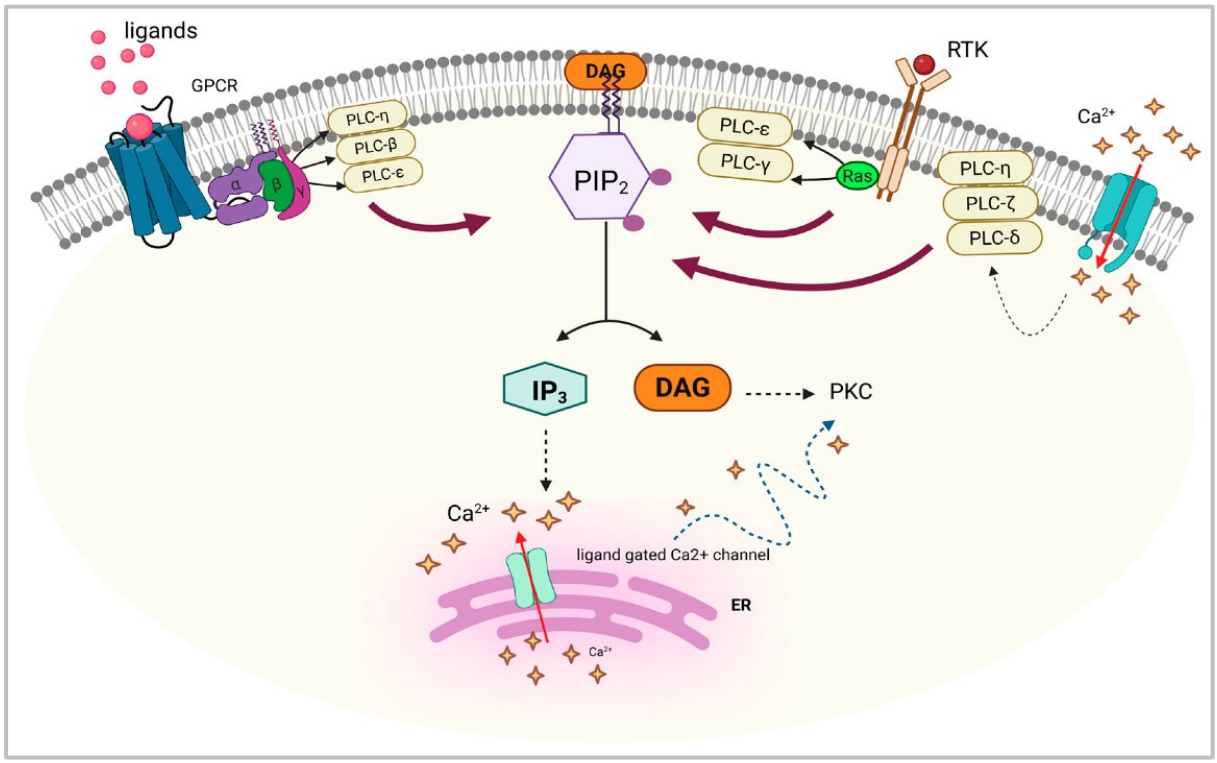

Figure 16. Phosphoinositide pathway (Hamdi M et al 2025)

Phosphoinositide-specific phospholipase C enzymes (PLCs) catalyze the hydrolysis of the phosphodiester bond between the hydrocarbon chain and the R group of

phosphatidylinositol 4,5-bisphosphate (PIP2), generating two second messengers: 1,2-diacylglycerol (DAG) and inositol-1,4,5-trisphosphate (IP3) [Figure 18]. The second messenger IP3 binds to its receptors located on the endoplasmic reticulum, leading to calcium release; DAG binds intracellular calcium and mediates the activation of protein kinase C (PKC), or it can be converted into phosphatidic acid, another signaling molecule [241]. Thirteen different PLCs are known in mammals and are classified into six isoforms: β, γ, δ, ε, ζ, and η, a classification primarily dictated by structural features. Most PLCs encoded by eukaryotic organisms contain conserved common sequences, such as a Pleckstrin Homology N-terminal (PH) domain, which enables the enzyme to bind to the plasma membrane; an EF-hand motif, which mediates calcium cation binding; two catalytic domains (X and Y); and a C-terminal C2 domain (calcium-dependent), which allows the enzyme to bind target phospholipids. In addition, some phospholipases also contain other specific sites that enable them to interact with particular molecular targets.

- **Catalytic domains X and Y**. The catalytic X and Y domains consist of highly conserved amino acid sequences with 60–70% sequence identity. They are generally located between the EF-hand motif and the C2 domain, and their secondary structure is characterized by alternating α-helices and β-sheets, which fold into a tertiary structure forming an incomplete α/β barrel known as a TIM Barrel (Triosephosphate Isomerase). For the proper functioning of the catalytic site, the presence of calcium ions bound to the enzyme is essential, as they decrease the pKa and promote a nucleophilic attack reaction on the phosphate group at position 1 of PIP2. Studies conducted on PLCδ1 have identified four fundamental amino acid residues within the active site: Lys438, Lys440, and Ser522 are involved in interactions with the phosphate groups at positions 4 or 5 of the substrate, while Arg549, through its positive charge, is directly associated with the hydrolysis event of PIP2. The aromatic ring of Tyr551 is positioned parallel to the inositol group, stabilizing it within the active site through the formation of numerous Van der Waals interactions. The active site can be described as a solvent-accessible molecular depression located at the carboxy-terminal end of the β-sheet structures. According to evidence from Essen et al. (1996), another set of hydrophobic amino acids (Leu320, Tyr358, Phe360, Leu529, and Trp555) surrounds the active site (of PLCδ1) and facilitates the insertion of the catalytic domain into the lipid bilayer. These

sequences are highly conserved across all PLC isoforms, where they maintain the same orientation and three-dimensional structure.

- **PH domain**. In PLCδ1, the PH domain binds PIP2, thereby bringing the enzyme close to the inner leaflet of the plasma membrane. In PLCβ2 and β3, the same domain specifically binds the βγ subunit of the G protein. The PH domain is also present in PLCγ1, where it mediates interaction with PIP3 and is therefore required for phospholipase translocation and activation within the PI3K-dependent pathway. PLCγ1 and PLCγ2 also possess an additional PH domain, which is separated from the first PH domain by two tandem Src Homology 2 domains and one Src Homology 3 domain.
- **C2 domain**. The C2 domain of PLCδ1 contains three to four calcium-binding sites; calcium ions enhance enzyme activity by forming ternary protein–calcium–phosphatidylserine complexes.
- **EF-hand motif**. EF-hand motifs have a helix–loop–helix structure and are capable of binding calcium cations. It has been demonstrated that depletion of EF-hand motifs in PLCδ1 results in decreased PLC activity in a calcium-independent manner. Moreover, EF motifs may play an important regulatory role, although no evidence to date supports their ability to bind other metal ions.

Sequence alignment studies of human PLC isoforms have been conducted to identify the most conserved sequences. When these alignments are represented in dendrograms [Figure 10], it becomes evident that all enzymatic activities share several analogies in the presence of specific domains—domains that are essential for the proper functioning of these enzymes: PH, EF-hands, catalytic TIM barrel, and C2 [242]. In addition to these common domains, some PLCs contain more specific and distinctive sequences: PLCγ isoforms possess **Src Homology 2** and **3** domains (SH2 and SH3) interposed between a duplicated PH domain; PLCε isoforms contain both a guanine nucleotide exchange factor (GEF) domain, which can activate Rap1 and other GTPases, and two RA sequences at the C-terminal region for binding Ras and Rap1 GTPases [243].

They also contain an N-terminal Cys-rich sequence with as yet unknown function. PLCζ is structurally the simplest enzyme, lacking the PH domain; PLCη isoforms contain a serine/proline-rich region at the C-terminal, while PLC-like enzymes are characterized by a core shared with other isoforms, but with a series of mutations in the catalytic site sequence that repress its enzymatic function [244].

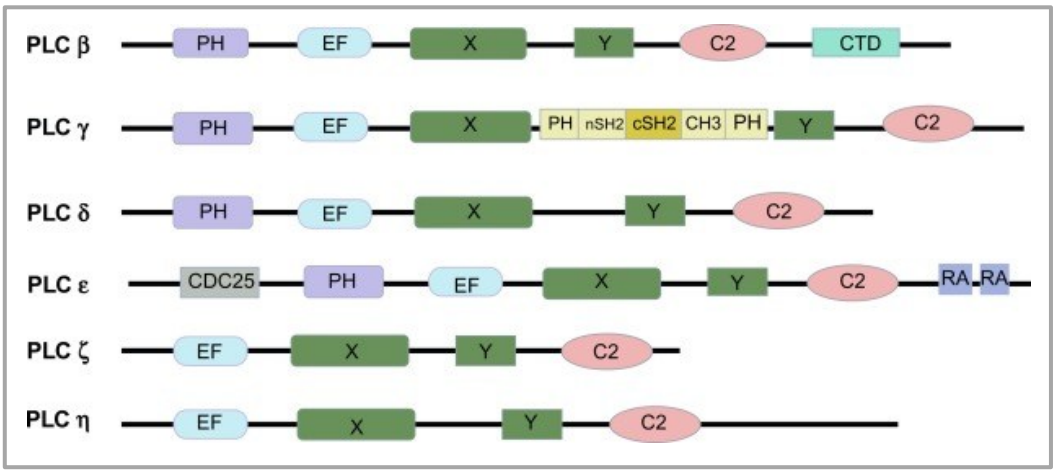

Figure 17. PLCs sequences (Abdul Wasai et al 2023)

Phospholipase C beta (PLCβ) comprises four isoforms—PLCβ1, PLCβ2, PLCβ3, and PLCβ4—and structurally contains the catalytic X and Y domains, a pleckstrin homology (PH) domain, and a C2 domain. Its activation is mediated through interactions with Gβγ, Rac, and Cdc42 (Park et al., 2022). In addition, PLCβ possesses a C-terminal domain (CTD) that plays a dual role: it is essential for plasma membrane binding and enzymatic activation, but in resting cells it functions as a self-inhibitory module by interacting with the catalytic core and blocking enzymatic activity (Park et al., 2022). Functionally, PLCβ participates in diverse physiological processes, including mast cell and hematopoietic stem cell proliferation, myeloid differentiation, neutrophil superoxide production, and apoptosis in macrophages (Garwain et al., 2018).

Phospholipase C Beta 1 (PLCβ1) is upregulated during differentiation processes in osteoblast, myoblast and adipocyte precursors [245] and has been linked to cancer progression [246]. In breast cancer, PLCβ1 promotes directional migration through lipid-dependent sequestration of the actin regulator cofilin at the plasma membrane [247].It has also been detected in podosome-like structures of endothelial cells, reinforcing its role in cytoskeletal rearrangements and migration. Importantly, PLCβ1 is activated by Rac, a member of the Rho GTPase family [248], further establishing its connection to

actin dynamics. Notably, osteosarcoma-derived extracellular vesicles (EVs) were shown to carry higher levels of PLCβ1 compared to osteoblast-derived EVs, suggesting a potential role in modulating distant target cells through EV-mediated signaling.

Phospholipase C Beta 2 (PLCβ2) has emerged as an important player in cancer biology through its ability to regulate proliferation, differentiation, and metabolism by activating protein kinase C (PKC) and downstream signaling cascades. It is activated by G-protein-coupled receptors and participates in diverse cellular processes, including platelet function, where its transcription is regulated by NF-κB [249]. In several tumor types, PLCβ2 has been linked to tumorigenesis and disease progression. For instance, in melanoma, PLCβ2 inhibits tumor cell apoptosis via activation of the RAS/RAF/MAPK pathway [250], while in breast cancer, it promotes progression through regulation of the G2/M phase and mitosis [251]. Moreover, PLCβ2 has been shown to regulate vascular endothelial growth factor (VEGF)-induced vascular permeability by controlling intracellular calcium flux [252].

Also PLCβ2 may contribute to Renal Cell Carcinoma (RCC) progression through the regulation of epithelial–mesenchymal transition (EMT), a process that underlies invasion and metastasis and is strongly associated with poor clinical outcome. Using bioinformatics and functional approaches, PLCβ2 was recently shown to be significantly upregulated in renal clear cell carcinoma (KIRC) and correlated with poor prognosis. High-throughput RNA sequencing and molecular assays revealed that PLCβ2 acts as a mediator linking Wnt and PI3K/AKT pathways, thereby orchestrating EMT and driving RCC cell proliferation, migration, and invasion. These findings indicate that PLCβ2 may represent both a prognostic biomarker and a potential therapeutic target in RCC progression [253].

There is an old study in which authors investigated which PLC isoform mediates mechanotransduction in osteosarcoma cells and primary osteoblasts. Using a 4-point-bending system, the authors compared several OS cell lines (MG-63, MMNG/HOS, OST, U-2/OS, SaOS-2) and primary osteoblasts. Functional assays focused on MG-63 (mechanosensitive) and U-2/OS (non-mechanosensitive) cells, employing inducible antisense constructs against PLCβ1 and PLCβ2. When exposed to physiological fluid shear stress MG-63

cells expressing PLCβ2-antisense showed a marked increase in detachment compared to controls, with most detachments occurring within 30s of flow increase. Notably, intracellular free calcium responses to shear flow were significantly reduced in PLCβ2-antisense MG-63 cells, while PLCβ1 knockdown had no effect. The authors claim that these findings provide the first strong evidence that PLCβ2 plays a specific and central role in mechanotransduction in OS cells, linking shear stress-induced calcium signaling to cell adhesion dynamics [254].

Phospholipase C gamma (PLCγ) consists of two isoforms, PLCγ1 and PLCγ2, and is distinguished by a multidomain insert between the catalytic X and Y domains that includes a PH domain, an SH3 domain, and both N- and C-terminal extensions (Jang et al., 2018). Through its SH2 domains, PLCγ binds phosphorylated tyrosine residues on receptor tyrosine kinases (RTKs), thereby playing a pivotal role in the activation of downstream RTK and non-RTK signaling cascades [255]. Most of its regulatory activity depends on the multidomain insert, which controls enzyme function. Physiologically, PLCγ contributes to key processes such as regulatory T-cell and hematopoietic stem cell development, lymph node organogenesis, B-cell maturation, and Fc receptor-mediated responses in immune cells including mast cells, NK cells, and neutrophils (Walliser et al., 2018).

Phospholipase C Gamma 1 (PLCγ1). PLCγ1 is a ubiquitously expressed isoform activated through binding with receptor tyrosine kinases such as EGFR, PDGFR, and VEGFR, which are frequently overexpressed in diverse cancers [256]. Its activation hydrolyzes phosphoinositides to generate diacylglycerol (DAG), thereby engaging the PKC–PKD signaling axis and downstream effectors, that can promote tumorigenesis [257]. Aberrant PLCγ1 expression, both at mRNA and protein levels, as well as somatic mutations in PLCG1, have been identified across a wide range of solid tumors and hematological malignancies. Analyses from large-scale cancer genomics resources—including TCGA, cBioPortal, and the Human Protein Atlas—demonstrate consistent overexpression of PLCγ1 in lung, breast, gastric, liver, colon, prostate, and ovarian carcinomas. Supporting this, integrative transcriptomic and proteomic studies on patient samples revealed robust PLCγ1 expression in most tumor types, further underscoring its pathogenic role in carcinogenesis

[258]. Collectively, these findings highlight PLCγ1 not only as a critical player in phosphoinositide signaling and oncogenic transformation but also as a potential therapeutic target in multiple malignancies.

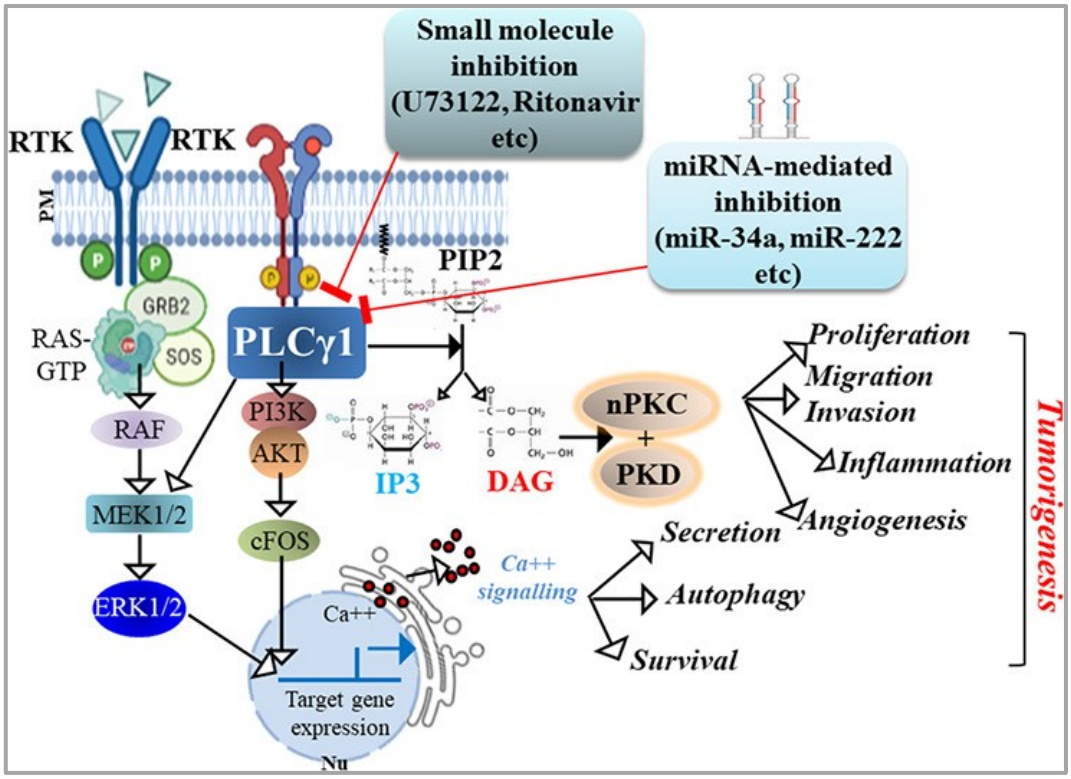

Figure 18. PLCG1 and its role as oncogene in cancers (S. Mandal et al 2021)

Its oncogenic activity is largely driven through functional crosstalk with growth factor receptors, including EGFR, PDGFR, VEGFR, NGF, and FGF, which phosphorylate PLCγ1 at specific tyrosine residues (Y771, Y783, Y1253), leading to conformational changes in its SH2 domain and full enzymatic activation [259]. Given the frequent overexpression of these receptors in breast, gastric, and colon cancers [260, 261], growth factor–mediated hyperactivation of PLCγ1 contributes to uncontrolled proliferation, a hallmark of cancer [262].

Activated PLCγ1 also regulates actin cytoskeleton dynamics and cell motility by modulating profilin–PIP2 interactions, cofilin-mediated actin polymerization [263], and Rho GTPases such as Rac1 and Cdc42 [264]. Beyond growth factor pathways, PLCγ1 cooperates with c-Met and c-Src to promote migration in head and neck carcinoma [265], while the focal adhesion protein Migfilin enhances motility through an EGFR–PLCγ1–STAT3 axis [266].

In the metastatic context, PLCγ1 supports EMT, invasion, and cytoskeletal remodeling, and activates PKC-dependent signaling that intersects with PDK1,

AKT, and RAS/RAF/ERK pathways, thereby enhancing metastatic potential in breast cancer [267]. Angiogenesis, a critical component of metastasis, can also be driven by PLCγ1. For instance, in endothelial cells like the HUVECs, TXNIP knockdown reduces VEGFR2 phosphorylation and PLCγ1 activity, indicating a TXNIP–VEGFR–PLCγ1 axis in angiogenesis [268]. Taken together, PLCγ1 acts as a multifaceted oncogenic regulator, driving proliferation, invasion, metastasis, and angiogenesis, highlighting its potential as a promising therapeutic target across multiple cancers.

Using proximity-dependent biotin labeling combined with label-free quantitative mass spectrometry, Kostas and colleagues identified PLCγ1 as a direct interactor of FGFR1, suggesting that this association may contribute to osteosarcoma development [269].

Phospholipase C Gamma 2 (PLCγ2) is an essential signaling molecule in B cell development and function, acting as a proximal component of the B cell receptor (BCR) cascade. Upon antigen engagement, PLCγ2 is phosphorylated through interactions with kinases such as Syk and Btk, leading to IP3/DAG production, calcium flux, and downstream activation of pathways including ERK. While its function in T cells is limited compared to PLCγ1, PLCγ2 contributes to TCR signaling in certain contexts. Overall, PLCγ2 is a central regulator of adaptive immunity, and its dysregulation has been linked to immune-related diseases.

PLCγ2 plays an important role in hematological malignancies, most notably in chronic lymphocytic leukemia (CLL), where activating mutations drive Ibrutinib resistance and disease relapse, making it a key biomarker and therapeutic target. It is also implicated in diffuse large B-cell lymphoma (DLBCL), Hodgkin's lymphoma, MALT lymphoma, and EBV-driven lymphomas, with context-dependent effects that may either promote oncogenesis or modulate immune responses. Beyond blood cancers, PLCγ2 dysregulation has been linked to several solid tumors, including osteosarcoma, esophageal and cervical cancers, lung cancer, and breast cancer, where it influences migration, drug resistance, and signaling pathways such as EGFR and Wnt [270].

PLCγ isoforms are essential regulators of early migration events, activating actin polymerization and cell protrusion formation [271]. PLCγ enzymes are frequently overexpressed in cancers, where they contribute to migration,

invasion, growth, and survival [272, 273]. Specifically, PLCγ2 has a well-established role in osteoclast biology, being required for adhesion, migration, and early differentiation [274]. In osteosarcoma, PLCγ2 has been identified in EV membranes, with the highest levels observed in the highly metastatic 143B cell line [245]. These findings support the hypothesis that osteosarcoma-derived EVs carrying PLCγ2 may fuse with osteoclast precursors, thereby promoting osteoclast activation and contributing to the osteolytic lesions characteristic of primary OS.

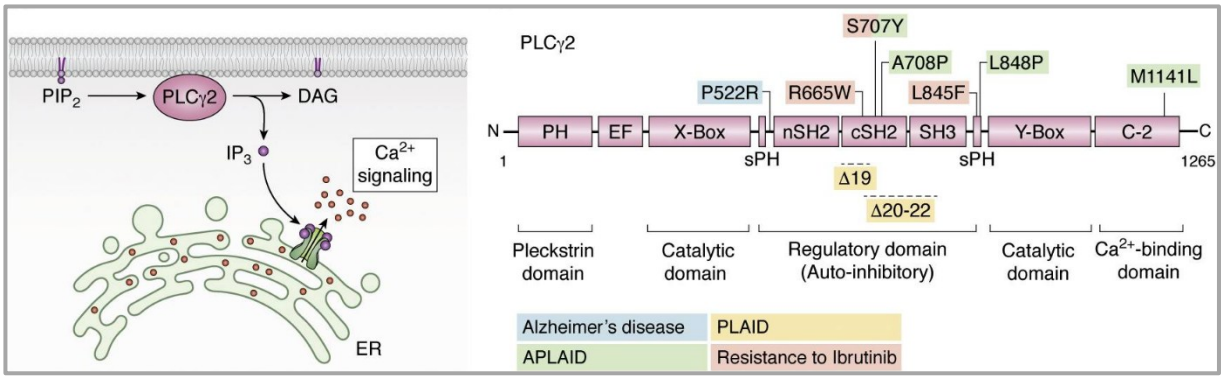

Figure 19. PLCγ2 structure, frequent mutations, involvement in disease and signaling.

In osteoclasts, PLCγ2 is essential for integrin-mediated adhesion, migration, and bone resorption. Loss of PLCγ2 disrupts integrin-dependent phosphorylation of Src and PYK2, severely reducing the interaction between Src, β3 integrin, and PYK2, and impairing Src localization to the actin ring. Both the catalytic activity and adapter domains of PLCγ2 are required for proper Src positioning. These findings indicate that PLCγ2 functions as a key signal transducer downstream of αvβ3 integrin, modulating the formation and stability of the integrin adhesion complex and ensuring correct recruitment of Src to adhesion sites. Loss of PLCγ2 disrupts integrin-dependent phosphorylation of Src and PYK2, reduces Src–β3 integrin–PYK2 interactions, and prevents proper Src recruitment to the actin ring. Although low Src levels persist at the membrane in PLCγ2$^{-/-}$ cells, actin structures formed are abnormal, indicating that PLCγ2 is specifically required for osteoclast polarization and sealing zone formation on physiological substrates. Consequently, PLCγ2-deficient cells display defective adhesion and resorptive capacity. PLCγ2 seems to act both downstream and upstream of Src. Following integrin engagement, Src phosphorylates PLCγ2 to activate its lipase function, while PLCγ2, through its

SH2/SH3 adaptor domains, stabilizes Src recruitment to adhesion complexes. Inhibition of PLCγ2 catalytic activity (e.g., with U73122) disrupts Src/PYK2/β3 interactions, highlighting the dual enzymatic and scaffolding role of PLCγ2. Furthermore, PLCγ2 is necessary for calcium-dependent PYK2 autophosphorylation at Tyr402, a key event for Src recruitment to adhesion complexes. PLCγ2 orchestrates both the formation and stability of integrin adhesion complexes and the localization/activation of Src, thereby ensuring proper osteoclast adhesion and resorption [274].

Phospholipase C epsilon (**PLCε**) exists as a single isoform and shares structural homology with both PLCβ and PLCδ, but it also contains unique domains that distinguish its function. In particular, it possesses a CDC25 homology domain and two Ras-association (RA) domains, RA1 and RA2 (Tyutyunnykova et al., 2017). The RA domains provide an autoinhibitory function (Garland-Kuntz et al., 2018), while the CDC25 domain acts as a guanine nucleotide exchange factor (GEF) for the small GTPase Rap1A (Nakamura and Fukami, 2017). RA1 and RA2 interact with muscle-specific A-kinase anchoring protein (mAKAP) at the perinuclear membrane, binding to activated Rap1A and Ras, thereby linking PLCε activity to Ras-dependent signaling. Functionally, PLCε is implicated in diverse physiological processes, including cardiac function, skin inflammation, and neuroinflammation (Wing et al., 2001).

1.11.1 Ezrin, cytoskeleton, Phospholipases C and bone sarcoma.

Ezrin, a member of the ezrin/radixin/moesin (ERM) protein family, functions as a linker between the plasma membrane and the actin cytoskeleton, thereby regulating essential cellular processes such as adhesion, motility, proliferation, and apoptosis [275, 276]. Structurally, ERM proteins consist of an N-terminal membrane-binding domain, an α-helical region, and a C-terminal actin-binding domain [277]. Ezrin activity depends on conformational changes rather than intrinsic enzymatic function. Its activation requires binding of the N-terminal domain to phosphatidylinositol 4,5-bisphosphate (PIP2) and phosphorylation of a conserved threonine (T567) within the actin-binding domain, enabling interactions with adhesion molecules such as CD43, CD44, ICAM-1, and ICAM-2 [277].

Importantly, high ezrin expression has been identified as a critical determinant of metastatic potential in osteosarcoma (OS) and correlates with poor prognosis in murine, canine, and human OS cases [278, 279]. Similar associations with adverse clinical outcomes have been reported in other metastatic cancers, including rhabdomyosarcoma and pancreatic cancer [279, 280]. Pharmacological targeting of ezrin has shown therapeutic promise: the small-molecule inhibitor NSC 668394, which blocks phosphorylation of T567, significantly impairs ezrin function, reducing OS cell migration and metastatic behavior both *in-vitro* and *in-vivo* [281].

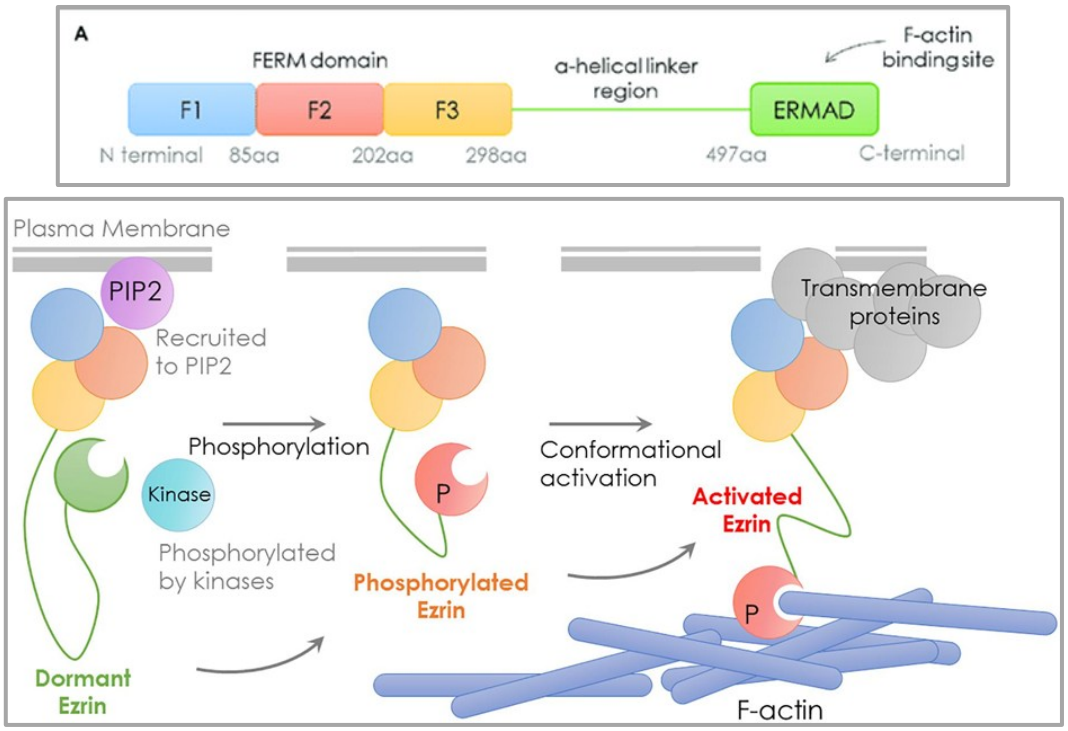

Figure 20. Ezrin structure and its role as linker between plasma membrane and cytoskeleton (Yanan Song et al 2020)

Activation of ezrin and other ERM proteins requires local accumulation of phosphatidylinositol 4,5-bisphosphate (PIP2), which guides ezrin to the plasma membrane [282, 283]. Reduction of PIP2 levels leads to ERM dissociation from the membrane [284]. PIP2 turnover is tightly regulated by phosphoinositide-specific phospholipase C (PI-PLC) enzymes, which are modular, multi-domain proteins involved in multiple regulatory interactions, including direct crosstalk with Ras GTPases [242].

Once activated, ezrin participates in a wide range of signaling networks, linking adhesion complexes and receptor tyrosine kinase signaling to Rho GTPase and Akt-mediated apoptotic pathways [285]. Its phosphorylation regulates cytoskeletal dynamics, including the morphogenesis of apical microvilli and the assembly of E-cadherin-dependent adherens junctions [286, 287]. Ezrin interacts directly with PI3K, and phosphorylation at Tyr-353 is mediated by the PI3K/Akt pathway [285] whereas phosphorylation of Thr-567 depends on p38 MAPK activity [288]. Additionally, ezrin undergoes preferential proteasome-mediated degradation and resynthesis after oxidative stress [289].

Experimental models have confirmed its oncogenic relevance: transfection of full-length *VIL2* (Ezrin) constructs in low-metastatic cell lines conferred metastatic ability, enabling the formation of macroscopic pulmonary lesions in experimental models [290]. In murine osteosarcoma models, ezrin was indispensable for metastasis, while canine tumors and pediatric OS patients showed a strong correlation between high ezrin expression and early metastatic development [278]. Functional inhibition of ezrin, shRNA-mediated knockdown, or dominant-negative mutants, markedly reduced metastatic behavior, accompanied by decreased Akt and MAPK activity [290]. Mechanistically, ezrin-driven metastasis is linked to activation of the Akt/mTOR axis [291] but the precise molecular connection remains unclear.

There exists several evidence that indicates a reciprocal regulatory relationship between ezrin and PI-PLC isoforms. Silencing of ezrin affects PLCE gene transcription, while conversely, PI-PLCε silencing alters ezrin expression [292, 293]. Ezrin localization is strongly influenced by PIP2 availability, as reduced PIP2 levels trigger its intracellular redistribution [283]. Small GTPases also modulate this process: dominant-negative Rac1 decreases ezrin at adherens junctions, while RhoA inactivation prevents ezrin relocation [294].These findings suggest that RhoA acts upstream of ezrin, either by masking its actin-binding site or via a shared downstream

effector. The current evidence supports the hypothesis that PI-PLC isoforms may function as such effectors, thereby integrating ezrin activity with phosphoinositide signaling and cytoskeletal regulation.

In osteosarcoma 143B cells, ezrin and PI-PLCε are tightly interconnected with RhoA and Rac1 signaling. Silencing ezrin increased PLCγ2, RhoA, and Rac1, while reducing PLCε, whereas *PLCE* silencing downregulated ezrin (*VIL2*), RhoA, Rac1, and PLCδ4, but upregulated PLCβ1. Notably, RhoA expression and localization correlated with PLCε activity, including its unusual nuclear translocation after ezrin silencing. Overall, the data indicate a complex regulatory network where suppression of ezrin induces compensatory upregulation of PLCβ1, while PLCε and RhoA appear to act in the same pathway. However, the role of PI-PLC isoforms in cancer remains controversial and likely context-dependent, underscoring the need for further studies to clarify their contribution to osteosarcoma metastasis [245].

1.11.2 PLCs Small molecule inhibitors: U73122 and U73343.

U73122, a clinically and translationally relevant amino-steroid (1-(6-((17β-3-methoxyestra-1,3,5(10)-trien-17-yl)amino)hexyl)-1H-pyrrole-2,5-dione), was originally described as a potent inhibitor of pharmacologically induced platelet aggregation. In this process, phospholipase C (PLC)–dependent signaling plays a central role, since IP_3-mediated calcium release is essential for platelet activation.

The structurally related analogue **U73343**, in which the reactive maleimide group is replaced by a less electrophilic succinimide group, appears enzymatically inactive and is therefore widely used as a negative control in studies on PLC inhibition [295] [296].

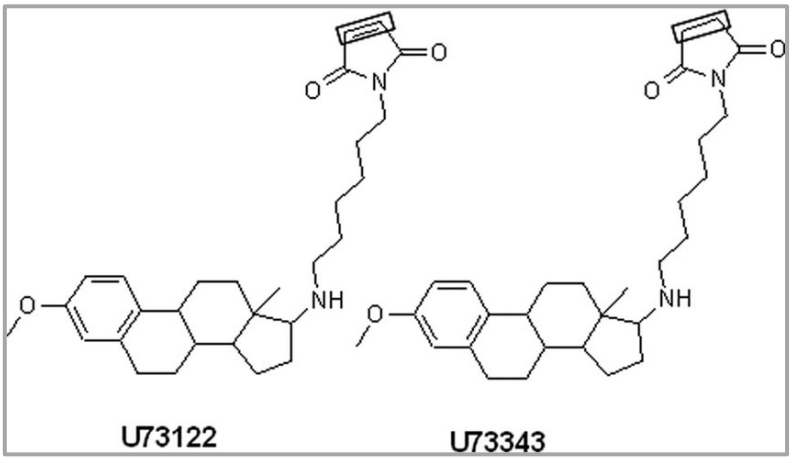

Figure 21. U73122 PLCs inhibitor and the analogue U73343 (R.R. Klein et al 2011)

Despite its broad use, the mechanism of action of U73122 remains incompletely understood. *In-vitro* studies suggest that the maleimide moiety alone is insufficient to account for PLC inhibition [295]. Current evidence indicates that U73122 may interact with PLCs through covalent modification of cysteine residues by alkylation of sulfhydryl groups, although detailed biochemical confirmation is still lacking and contradictory data exists regarding its isoform-specific inhibitory effect [296]. Importantly, additional findings emphasize the role of the steroid scaffold in modulating PLC functionality, suggesting a synergistic contribution of both chemical domains to the inhibitory activity. Alkylation events induced by U73122 may serve as an anchoring mechanism for the inhibitor on PLC enzymes, thereby allowing the steroid moiety to directly interfere with enzymatic activity [296].

Interestingly, the compound exhibits ambivalent behavior, acting either as an inhibitor or as an agonist, largely depending on the subcellular localization of the targeted PLC. Specifically, cytosolic isoforms appear more prone to activation, whereas membrane-associated PLCs are preferentially inhibited. Moreover, this dual effect is influenced by the availability of nucleophilic groups susceptible to alkylation, whether in the culture medium, within the cytosol, or at the plasma membrane [297].

1.11.3 U73122 off-target effects.

The molecular inhibition mediated by U73122 appears to be non-specific, extending beyond phospholipase C to other enzymes such as phospholipase D (PLD) and additional components of calcium-dependent signaling pathways [298]. Structurally, U73122 and its analog U73343 share strong similarity with 17β-estradiol, and both can activate nuclear estrogen receptors (ERα and ERβ) at standard treatment concentrations (1–5 μM), thereby exerting an estrogenic effect [298]. Moreover, U73122 has been shown to modulate a variety of ion channels, including G-protein–gated inwardly rectifying potassium channels (Kir3), independently of PLC activity. Within integrin-mediated signaling, a pathway central to cell adhesion, phosphorylation of the β2 subunit upon ECM binding triggers PLCγ2 activation via its SH2 domain, leading to IP3 production and intracellular calcium release. Studies in immune cells, particularly neutrophils, indicate that U73122 lacks isoform-specific selectivity for PLC enzymes [299]. At the commonly used inhibitory concentrations (3–10 μM), U73122 also irreversibly interacts with the histamine H1 receptor, nonspecifically activating H1-dependent signaling cascades. This off-target effect undermines the reliability of experimental results that employ U73122 to assess H1 receptor–PLC signaling

interactions [300]. Treatment with the PLC inhibitor U73122 has been shown to reduce the growth rate of the human osteosarcoma cell line MG-63 and to alter the expression profile of several PLC isoforms. Specifically, following drug exposure, PLCs previously linked to tumor progression were downregulated (with PLCβ3 becoming undetectable after six hours), whereas isoforms associated with differentiation, such as PLCβ1, were upregulated [301]. Similar effects were observed in murine glioma cells, where U73122 rapidly modified the expression of PLCβ3 and PLCγ2. PLCβ3 protein was absent in the hours following treatment, consistent with depletion of vesicular protein reservoirs, and only reappeared in the cytoplasm after 24 hours. In parallel, PLCγ2 localization shifted, being detected exclusively in the cytoplasm, while absent from the nucleus, in contrast with untreated controls. Notably, after 24 hours, no *PLCG2* transcript or protein could be detected [241]. Although the precise mechanisms remain unclear, these findings suggest that U73122 may influence PLC gene expression at the transcriptional level, potentially in a non-isoform-specific manner. Such effects highlight a previously underappreciated dimension of U73122 activity and open new perspectives in translational medicine, warranting further investigation into its regulatory impact on PLC signaling.

2.0 Materials and methods.

2.1 Cell culture.

143b cells, obtained from Deutsche Sammlung von Mikroorganismen und Zellkulturen GmbH (DSMZ, Braunschweig, Germany), were cultured in DMEM low glucose medium (1g/l glucose, Sigma D6046) supplemented with 10% FBS,1% Penicillin-Streptomycin antibiotics (SIAL, Sial-PEN/STREP) and 1% of l-Glutamine (Aurogene, MS02K1004). Cells were incubated at 37°C into a humid environment at 5% CO_2.

2.1.1 U73122-U73343 treatments.

Cells were seeded at concentration of 2500 cells/ cm^2 (by day 0) and cultured for five days. After two days of cell culturing, they were treated with U73122 inhibitor (Merk, 662035-5MG) and U73343 (Merk, 662041-5MG) at 10-15µM concentrations (single treatment); some of these cells were re-treated with the same inhibitors and same molecular concentrations three days after cell seeding (double treatment). Biological samples were collected by day 4 for single treatment condition and then used for RT-q-PCR technique, and by day 5 for double treatment samples and then used for RT-q-PCR, Western blot and immunofluorescence.

2.1.2 RNA interference with siRNAs.

Celle were seeded at concentration of 8000 cells/ cm^2 (10000 cells/ cm2 for wound healing assays) and cultured for five days. Cells were incubated overnight then cells were treated with the mixture of cationic lipoplexes conjugated with siRNAs according to Lipofectamine™ 3000 (Invitrogen, L3000015 1.5ml) protocol. The protocol was fine tuned in terms of siRNA concentration in order to obtain best gene expression downregulation; Optimem® and Lipofectamin volumes were chosen following manufacturer protocol. siRNA concentrations were calculated on lipoplexes final solution volume. Two separate solutions were prepared, the first one with the siRNA – Optimem® (Gibco 31985062, 100ul) solution and the second one with Lipofectamin® - Optimem® solution. Two solutions were gently mixed and incubated for 15 minutes, then cationionic lipoplexes were directly administrated following manufacturers guidelines in fresh new cell culture media. 24h after the first treatment siRNA administration was performed again in order to achieve the higher downregulation possible. Experiments always stopped between day 4 or 5, the transient

downregulation has been proven to be effective for a maximum of 72 hours after the first treatment.

2.1.3 Wound Healing Assay.

Transfected OS cells were seeded in 6well plates (10,000 cells/ cm^2) and left to grow until they reached confluence. Subsequently, a reproducible longitudinal scratch was made in the confluent monolayer using a sterile micropipette tip. The process of scratch closure was monitored up to 36 hours; photos were taken every 6 hours with OLYMPUS Provi™ CM20. ImageJ (Fiji) was used to assess morphometric analysis of cell migration by using the CSMA plugin (https://github.com/AminaSagymbayeva/CSMA_Wound Healing). The wound healing closure was determined as the normalization on the day 0 original area (= 0%).

2.1.4 Growth curve analysis.

143b cells were seeded into 12 well plate at 7500 cells/ cm^2 density and transfected by using the protocol described in chapter 2.1.2. By the day of the first transfection photos were taken every 12 hours with OLYMPUS Provi™ CM20. Prior to experimental analyses, the image-analysis workflow was optimized to ensure accurate recognition of 143B osteosarcoma cells under the specific seeding densities and culture conditions used in this study. Briefly, preliminary acquisitions were performed at different cell densities to fine-tune segmentation parameters, including cell area thresholds and contrast settings, allowing reliable discrimination of individual cells from background and debris. These parameters were then fixed and applied uniformly across all experimental conditions and timepoints. Cell confluency was calculated by the software as the percentage of the culture surface area occupied by cells. For each condition, multiple non-overlapping fields of view were acquired at each

2.1.5 Boyden chambers invasion assay.

CytoSelect Cell Invasion Assay Kit (CBA-110, Cell Biolabs) was used to study the invasion capabilities of 143b osteosarcoma cells. Kit is composed of transwells covered with 8µm pore size polycarbonate membrane which contains also a layer of Matrigel®. To be considered invasive cells must before degrade the Matrigel layer and then migrate through the pores of the membrane. Each experiment was performed in 24-well plates. For the experiment 300µl of serum-free medium was added to each transwells to rehydrate the membranes and the matrix and incubated them at 37°C for one hour. Then, the serum-free medium was removed and 500µl of 20% fetal bovine

was pipetted below the transwell. An exact number of 143b cells have been resuspended with 1% serum-free medium and seeded in 300µl for each transwell (80,000 cells/ transwell). Then the plates were incubated at 37°C, in 5% CO2 in a humidified atmosphere. After 24h of incubation (= 72h after the first treatment) the medium was removed from the transwell and the inserts have been stained with 400 µl of Cell Stain Solution and incubated for 15 minutes at room temperature. Next several washings have been performed and cotton swabs were used to remove the excess of colorant. At the end, inserts were incubated with 200µl of washing solution from the kit and the stained solution has been read using an ELISA plate reader (absorbance at 595 nm). Finally, the data obtained were reported as percentages (ratio), considering the scramble control as 100%.

2.2 Molecular biology.

2.2.1 RNA extraction and retro-transcription.

Cell pellets were mixed and incubated with TRIZOL (Invitrogen, 15596018) for 5 minutes at room temperature. Then Chloroform (Carlo Erba, 438601) was added to the samples which were mixed by inversion for 2 minutes and centrifuged for 15 minutes at 12,000xg at 4°C. Next, the aqueous phases were collected and the nucleic acids were precipitated by centrifugation with isopropanol for 10 minutes at 12,000xg at 4°C (Carlo Erba, 438901) and cold ethanol for 5 minutes at 7500xg at 4°C (Hysto-Line, R0099). Then nucleic acids were resuspended in Nuclease Free pure water (SIGMA, W4502-1L), then RNA concentration and its purity were assessed by spectrophotometric analysis (SPEX Nanosnap®).

Finally mRNAs were retro-transcribed using “High-Capacity cDNA reverse transcription kit” (ThermoFisher Scientific, 4374966); the reaction was stetted for 1µg of total RNA per 20µl of reaction volume. Master mixes were prepared according to the kit guidelines. The thermal cycler was programmed using the following conditions (always according to manufacturer guidelines): annealing at 25°C for 10 minutes, polymerization at 37°C for 120 minutes and enzymatic inactivation at 85°C for 5 minutes.

2.2.2 RT-q-PCR.

RT-q-PCR reactions were performed using “SsoAdvanced Universal SYBR Green supermix” (BioRad, 1725274); for each reaction 50ng of cDNA were added to the biochemical reaction. The optimal primers concentrations were previously assessed

by testing each primer in different experimental conditions. The PCR reaction was set to the following steps: polymerase activation at 95°C for 30s, cDNA denaturation at 95°C for 10s, annealing and extension at 5°C below the mean of primers melting temperatures. These steps were repeated for 40 cycles, then a melting reaction was performed for every PCR product (from 65°C for 5s to 95°C with a ramp rate of 0.5°C/5s). Differences in relative quantifications were assessed by using ΔΔCq methodology and then by calculating the Fold Change.

2.3 Protein analysis.

2.3.1 Protein extraction and Western Blot.

Cell pellets were lysed by adding both the Lysis buffer 6 (R&D, 895561) and the Halt protease inhibitor cocktail (ThermoFisher Scientific, 87786). Cellular membranes breakup was also promoted by sonication (10 pulses/ sample). Proteins fraction was recovered by centrifugation at 13000xg, at 4°C for 10 minutes and prepared for Sodium Dodecyl Suplphate PolyAcrylamide Gel Electrophoresis (SDS-PAGE) loading by using Leamli Sample Buffer (BioRad, #160747). Then samples were boiled for 5 minutes at 100°C, cooled down and finally loaded in to Acrylamide Gel. After the gel electrophoresis proteins were transferred to a nitrocellulose membrane using BioRad® Trans Blot Turbo instrument. Blotting membranes were blocked with a PBS-T-milk powder 5% solution (homemade solution: PBS 10X Gibco diluted to 1X, 0.01% Tween-20, no fat powder milk) for 1 hour, then the membranes were incubated at 4°C over night (ON) with primary antibodies: β-Actin as housekeeping (for *PLCB1* silencing and inhibitors treatments only) 1:1000 dilution (Origene TP303643), Cleaved Caspase 3 1:1000 dilution (Cell Signaling, 9664), p211:1000 dilution (Cell Signaling, 2947), p53 1:2000 dilution (Abclonal, A0263), Vimentin 1:2000 dilution (Abclonal, A19607).
For *PLCB2* and *PLCG2* silencing actin become much more variable since cytoskeleton has undergone great changes, so housekeeping protein was changed from Actin to Histone 3 (Cell Signaling 9715, 1:2000 dilution). Other antibodies used were: AKT 1:1000 (Cell Signaling 9272), β-Tubulin 1:1000 (Cell Signaling 2146), E-Cadherin 1:1000 (Cell Signaling 3195), ERK 1:1000 (Cell Signaling 9102), Lamnin A/C 1:800 (Cell Signaling 4777), Lamin B1 1:1000 (Cell Signaling 12586), MMP2 1:1000 (Cell Signaling 4022), N-Cadherin 1:2000 (Cell Signaling 4061), p-4E-BP1 Thr 37/46 1:1000 (Cell Signaling 9459), p-AKT Ser 437 1:2000 (Cell signaling 9271), p-ERK Thr202/Tyr204 1:2000 (Cell Signaling 9101), PLCβ2 1:250 (Santa Cruz Biotechnology,

sc-515912), PLCγ2 1:250 (Santa Cruz Biotechnology, sc-390389), p-s6RP Ser235/236 1:1000 (Cell Signaling 2211), p-YAP Ser127 1:1000 (Cell Signaling 4911), ROCK2 1:1000 (Invitrogen PA5-78290), SPARC 1:3000 (AbClonal RP00217), s6RP 1:1000 (Cell Signaling 2217), Vimentin 1:2000 (Abclonal, A19607), YAP 1:1000 (Cell Signaling 4912). Next day two secondary antibodies, conjugated with HRP were used to target primary antibodies; one against mouse epitopes at 1:5000 dilution (Thermo Fisher Scientific, 31430) and one against rabbit epitopes at 1:3000 dilution (Southern Biotech 4050-05). Proteins were visualized using ChemiDoc® imager by BioRad, the chemoluminescence reaction was triggered using Clarity Western ECL substrate (BioRad, #1705060) and Westar Supernova luminol (Cyanagen, XLS3,0100).

2.3.2 Immunofluorescence.

Cells were fixed in paraformaldehyde 4%, washed several times in PBS (homemade) and blocked for 30 minutes in a PBS-BSA 5% solution (homemade, PBS 10X Gibco 10010023, BAS powder Sigma A9418-500G), then the cells were incubated ON at 4°C in a humid chamber with primary antibodies:

- Osteogenic Differentiation:
    - Phosphatase alkaline (ALP) 1:500 dilution (Santa Cruz Biothecnology, sc-271431)
    - Osteocalcin (OCN) 1:500 dilution (Santa Cruz Biothecnology, sc-376726)
    - Osteonectin (SPARC) 1:200 dilution (Abclonal, A14494)
    - Osteopontin (OPN) 1:500 dilution (Santa Cruz Biotechnology, sc-21742)
    - Runx-2 1:500 dilution (Santa Cruz Biotechnology, sc-376726)
- Cytoskeleton:
    - Beta Actin (β-Actin) 1:1000 dilution (Origene, TA335770)
    - Phalloidin-TRITC 100µM Sigma P1951-.1MG (1:200).
    - Ezrin (EZR): 1:500 dilution (Santa Cruz Biotechnology, sc-58758)
    - Beta Tubulin (β-tubulin): 1:100 dilution (Bioss Antibodies, bsm-52290R)
    - E-Cadherin (e-cad): 1:100 dilution (Abcam, ab-1416)
    - Vimentin: 1:200 dilution (Abclonal, A19607)
- Cell proliferation, Apoptosis and Cancer related proteins:
    - Cleaved Caspase 3 (Cleav-Casp3): 1:1000 dilution (Cell Signaling, 9664)
    - P21: 1:1800 dilution (Cell Signaling, 2947)

- Ki67: 1:400 dilution (Cell Signaling, 9129)
- P53: 1:200 dilution (Abclonal, A0263)
- CD99: 1:200 dilution (Abclonal, A2028)
- CD34: 1:200 dilution (Abclonal, A13929)
- Caveolin 1 (Cav-1): 1:200 dilution (Abclonal, A22417).

- Focal Adhesion complexes and mechanotransduction:
  - Focal Adhesion Protein Antibody Sampler Kit (Cell Signaling 13430)
  - Total YAP 1:1000 (Cell Signaling 4912)

Next day primary antibodies were washed away with PBS solution ad cells were incubated with secondary antibodies for 1 hour at 4°C in the dark:

- Anti mouse:
  - FITC: 1:200 dilution (SIGMA, F2883)
  - TRITC (Cy3): 1:200 dilution (SIGMA, C2131)
- Anti rabbit:
  - FITC: 1:200 dilution (SIGMA, F1262)
  - TRITC (Cy3): 1:200 dilution (SIGMA, C2306)

Then secondary antibodies were washed away with PBS solution and coverslips were mounted using a DAPI in antifade ready to use solution (SIGMA S7113).

Phospholipase C immunofluorescence.

Cells were fixed in paraformaldehyde 4%, washed several times in PBS (homemade) and incubated ON at 4°C in a humid chamber with primary antibodies:

- Anti PLCβ1 (Santa Cruz Biotechnology, sc-5291)
- Anti PLCβ2 (Santa Cruz Biotechnology, sc-515912)
- Anti PLCβ3 (Santa Cruz Biotechnology, sc-133221)
- Anti PLCβ4 (Santa Cruz Biotechnology, sc-166131)
- Anti PLCγ1 (Santa Cruz Biotechnology, sc-7290)
- Anti PLCγ2 (Santa Cruz Biotechnology, sc-390389)
- Anti PLCδ1 (Santa Cruz Biotechnology, sc-376058)
- Anti PLCδ3 (Santa Cruz Biotechnology, sc-514912)
- Anti PLCδ4 (Santa Cruz Biotechnology, sc-373875)
- Anti PLCε1 (ThermoFisher Scientific, PA5-100856,)
- Anti PLCη1 (ThermoFisher Scientific, PA5-57558)
- Anti PLCη2 (Sigma-Aldrich Inc, HPA003346)

Next day primary antibodies were washed away with PBS solution ad cells were incubated with secondary antibodies for 1 hour at 4°C in the dark:

- Anti mouse:
    - FITC: 1:200 dilution (SIGMA, F2883)
- Anti rabbit:
    - FITC: 1:200 dilution (SIGMA, F1262)

Then secondary antibodies were washed away with PBS solution and coverslips were mounted using a DAPI in antifade ready to use solution (SIGMA S7113).

2.4 Next generation sequencing.

2.4.1 RNA extraction for NGS.

RNA was extracted from PLCs silenced cells, and from control cells, with the TRIzol Reagent (Invitrogen 15596018), cDNA-libraries were synthetized from 250 ng total RNA using the TruSeq RNA Sample Preparation Kit v2 (Illumina) according to manufactures protocol and paired-end libraries were sequenced on a NextSeq500 instrument (Illumina, San Diego, CA, USA). Quality control of all the FASTQ files was performed with FastQCR. Gene expression was quantified and normalized as count per million (CPM) from raw gene counts generated with the Python package HTseq-count. Transcripts with a count-per-million greater than one in at least three samples underwent differential gene expression analysis was performed using the edgeR R package. CPM were then used to perform a principal component analysis (PCA) using the R package prcomp. Signatures with absolute log fold change > 0.6 and $P < 0.05$ were considered as biologically relevant.

2.4.2 Enrichment analysis.

Enrichment analysis of hallmark (H), curated gene sets (C2) was performed by using Gene set enrichment analysis (GSEA) software (Broad Institute-version 2.2.0) and Molecular signatures database (MSigDB) version 5.1 (Liberzon et al., 2015; Subramanian et al., 2005). Gene expression data were loaded into GSEA as unfiltered data in a tab-delimited format. The permutation type chosen was “Gene Set” as directed in the GSEA user guide when having fewer than 7 samples per phenotype, permutation number was set at 1000 for testing significance, the minimum and maximum gene sets were set to 5 and 500 with 1000 times of permutation number. A p-value and FDR of less than 0.05 was considered significant.

2.5 Statistical analysis.

Quantitative data were described as the mean ± SD and were compared by two-tailed Student's t-test and ANOVA with Bonferroni's post-test multiple comparisons test when appropriate. Statistical analysis such as graphics generation was performed on RStudio 4.2.1. Differences with p values < 0.05 were considered statistically significant (p values: *p < 0.05, **p < 0.01; ***p < 0.001). Statistical analyses were performed with RStudio software (RStudio 2022.12.0, build 353).

2.6 ELISA.

The secretion of IL-6, IL-8, and CXCL1 in conditioned media was quantified using commercially available sandwich ELISA kits (IL-6 Mabtech 3460-1HP-1, IL-8 Mabtech 3560-1HP-1, CXCL1 FineTest EH0005), according to the manufacturer's instructions. Kits included pre-coated 96-well plates, recombinant cytokine standards, biotin-conjugated detection antibodies, streptavidin–HRP, TMB substrate, stop solution, wash buffer concentrate, and assay diluents.

All reagents were equilibrated to room temperature prior to use, with the exception of the TMB substrate, which was kept cold until use. Wash buffer was prepared by diluting the concentrate 1:20 in ultrapure water. Cell culture supernatants were collected at the indicated time points and NOT diluted 1:2 in ELISA diluent. Standard curves were generated using recombinant cytokine standards reconstituted according to the manufacturer's protocol to obtain a range of concentrations spanning from 0 to 3160 pg/mL. Standards, samples, blanks (substrate and stop solution only), and background controls (ELISA diluent only) were loaded in triplicate (100 µL/well). Absorbance was measured within 15 min using a microplate reader at 450 nm with a reference wavelength between 570–650 nm. Final absorbance values were calculated by subtracting the reference wavelength and blank readings. Cytokine concentrations were determined by interpolation from the standard curve.

3.0 Results.

3.1 PLCs modulation trough U73122 and U73343 inhibitors.

3.1.1 Cell growth and confluency.

First, we evaluate cell confluency across all experimental conditions, untreated (CTR), and single (S) or double (D) treatments with U73122 and its analogue U73343 at 10 μM and 15 μM, measured at four timepoints (from 48h to 120h from the seeding). The first administration of U73122/U73343 occurs at 72 h. Cells before treatment (at 48h after seeding) show comparable confluency. Likewise, at 72 h immediately after the first treatment no appreciable differences in growth are detectable. By 96 h (24 h post-treatment), however, the effect of U73122 becomes evident. In particular, U73122 at 15 μM significantly reduces confluency compared with U73343 at the same concentration ($p = 0.033$; $p = 0.048$).

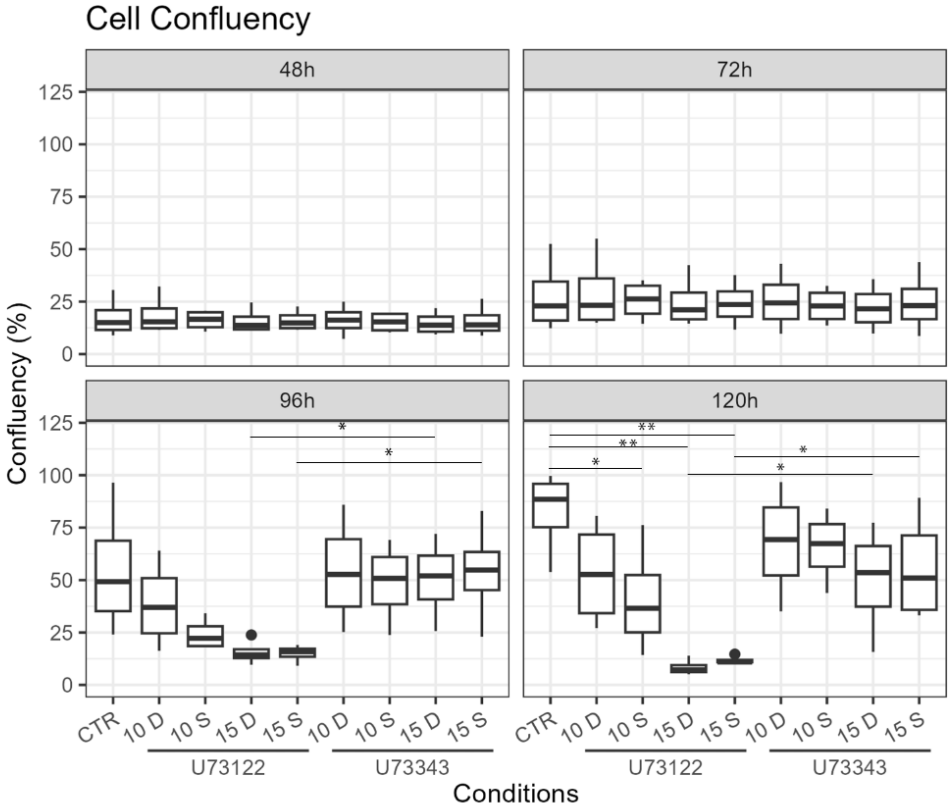

Figure 22. Cell Confluency for pharmacological treatment experiments. Cells were treated at 72h after seeding and eventually retreated at 96h after seeding (D treatment). Experiment stopped at 120h after seeding.

At this stage, the impact of the second treatment (D) is not yet observable. By 120h timepoint (48 h after the first and 24 h after the second treatment), differences between experimental conditions are pronounced. Untreated cells show significantly higher

confluency than U73122-treated cells at both concentrations (10 µM S: p = 0.05; 15 µM S: p = 0.005; 15 µM D: p = 0.006). Moreover, U73343-treated cells display significantly higher confluency than those treated with U73122 at 15 µM, for both single (p = 0.043) and double (p = 0.05) treatments. Overall, U73122 exhibits a stronger and earlier growth-inhibitory effect compared with its inactive analogue U73343 and the untreated control condition.

3.1.2 Evaluation of PLCs gene expression by RT-qPCR after inhibitors treatments.

96h timepoint.

We performed real-time qPCR to measure the relative expression (log(FC)) of PLC transcripts across all experimental conditions 24 h after the first treatment with U73122 or U73343 at 10 µM and 15 µM. In the figure, the red dotted line indicates a FC threshold of ±1.5. After treatment with U73122 at 10 µM, all PLC transcripts were downregulated, each showing at least a 1.5-fold decrease. At 15 µM, the transcriptional response was more heterogeneous: *PLCB1*, *PLCB2*, *PLCE*, *PLCG1*, *PLCG2*, *PLCH1*, and *PLCH2* were downregulated, although only *PLCH2* exceeded the -1.5 threshold,

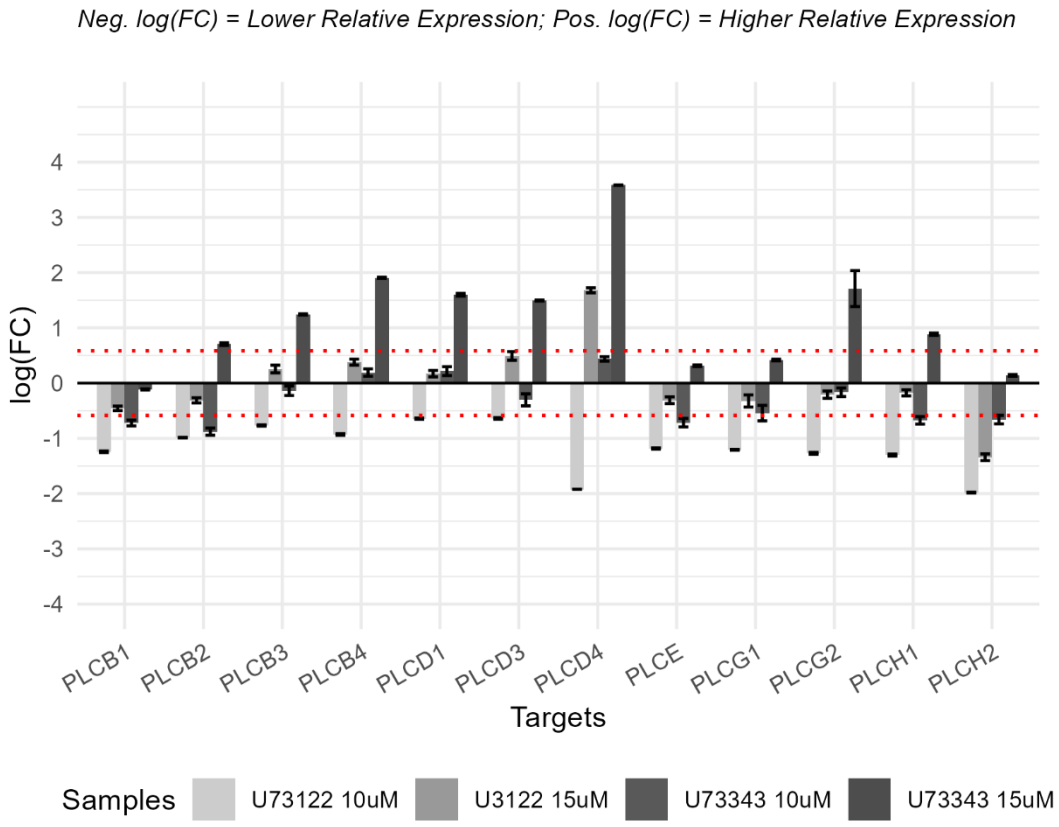

Figure 23. PLCs gene expression at 96h after seeding time point (which correspond to 24h after first treatment).

whereas *PLCB3*, *PLCB4*, *PLCD1*, *PLCD3*, and *PLCD4* were upregulated, with *PLCD4* being the only transcript above +1.5 FC. In contrast, U73343 treatment produced a markedly variable transcriptional profile without consistent or interpretable patterns of PLC gene modulation.

When aggregating PLC expression data across all transcripts and treating the PLC family as a single interconnected module, the single-treatment condition with U73122 at 10 µM produced the strongest overall downregulatory effect. This reduction was significantly greater than that observed with U73122 at 15 µM ($p = 0.00014$) and with U73343 at 10 µM ($p = 9.71 \times 10^{-5}$). Nevertheless, PLC transcript levels remained significantly lower after U73122 15 µM treatment than after U73343 15 µM exposure ($p = 0.0039$).

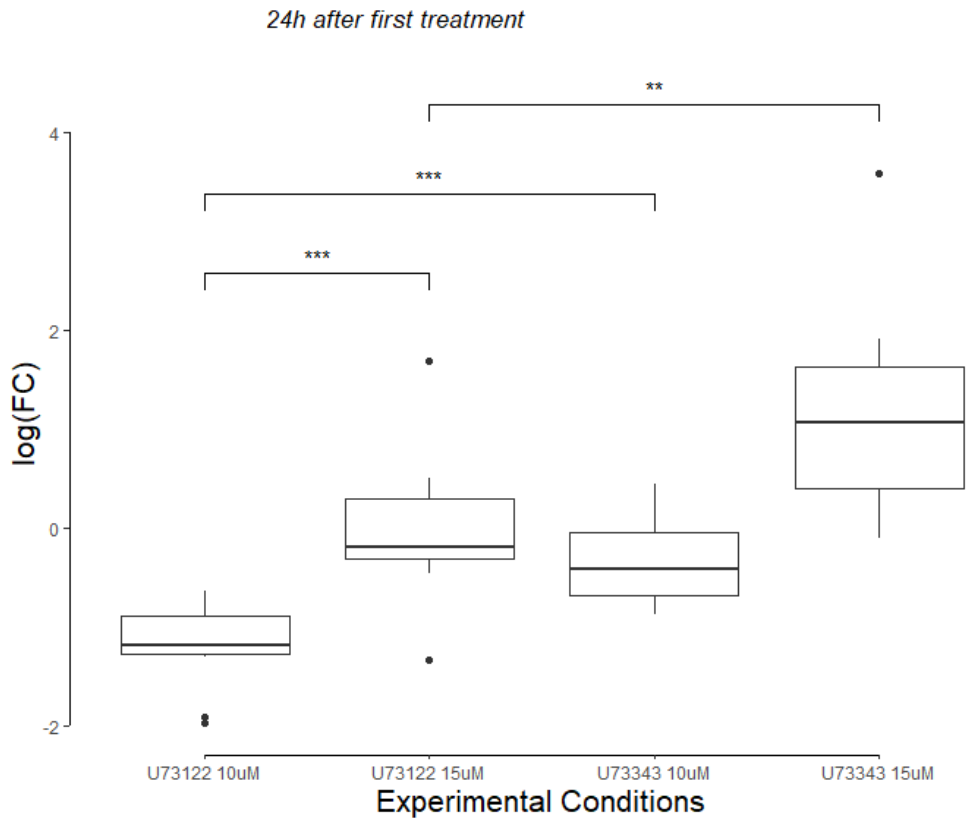

Figure 24. Aggregated gene expression data for PLC family 24h after first treatment.

120h timepoint.

At 24 h after the second treatment (120 h timepoint), PLC transcript responses were considerably more variable across conditions. Notably, U73122 at 10 µM no longer induced a coordinated downregulation of PLC genes, indicating that the off-target transcriptional suppression observed after the first treatment was no longer detectable. Overall, U73122 produced smaller changes in relative PLC expression compared with U73343, which continued to cause broader and more heterogeneous alterations in transcript levels, although without any recognizable or consistent expression pattern.

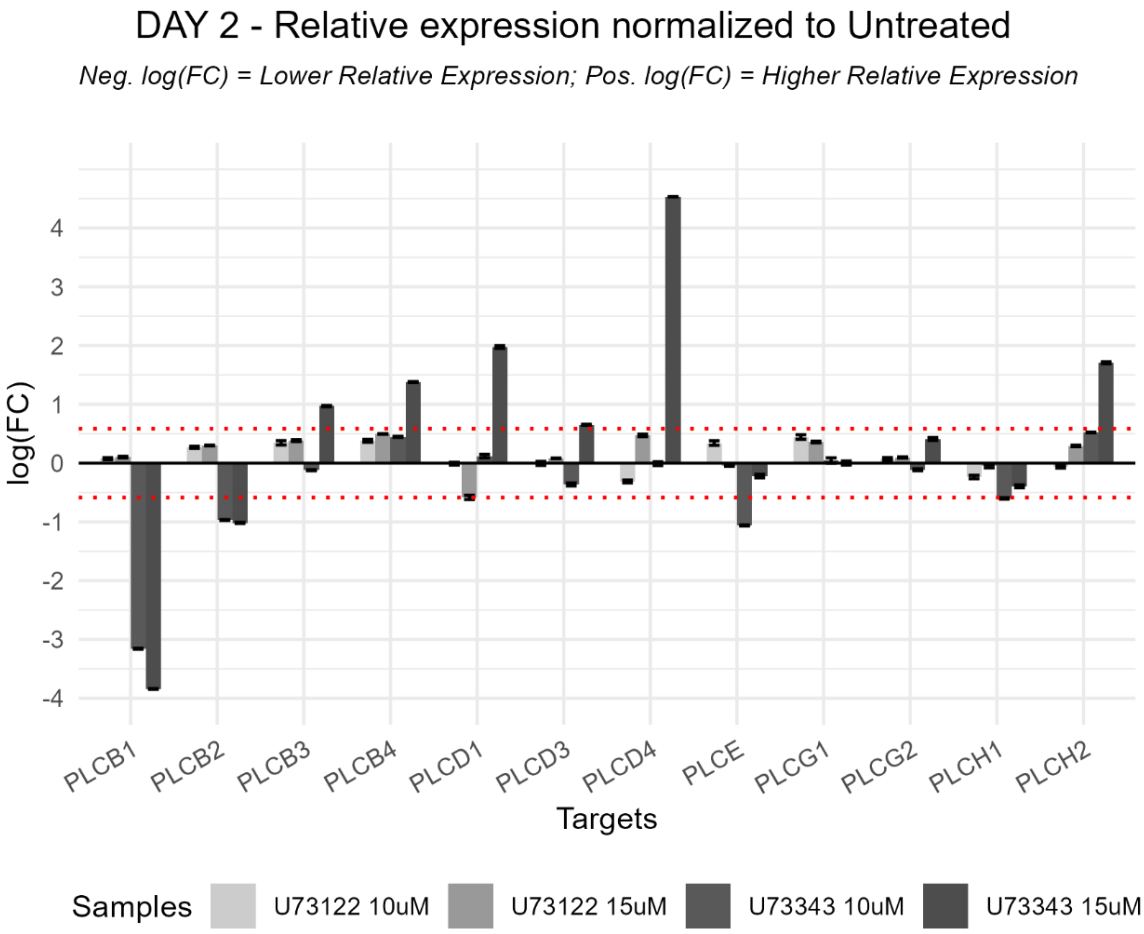

Figure 25. PLCs gene expression at 120h after seeding time point (which correspond to 48h after first treatment and 24h after second treatment).

When aggregating PLC expression across all isoforms, no significant differences in relative PLC levels were detected between treatment groups at this timepoint. These data confirm that the off-target transcriptional effects of U73122 observed after the first administration are no longer evident following the second treatment. Conversely, the distribution of values obtained from U73343-treated cells again shows the highest variability in PLC expression, consistent with the broader and more heterogeneous transcriptional response induced by the inactive analogue.

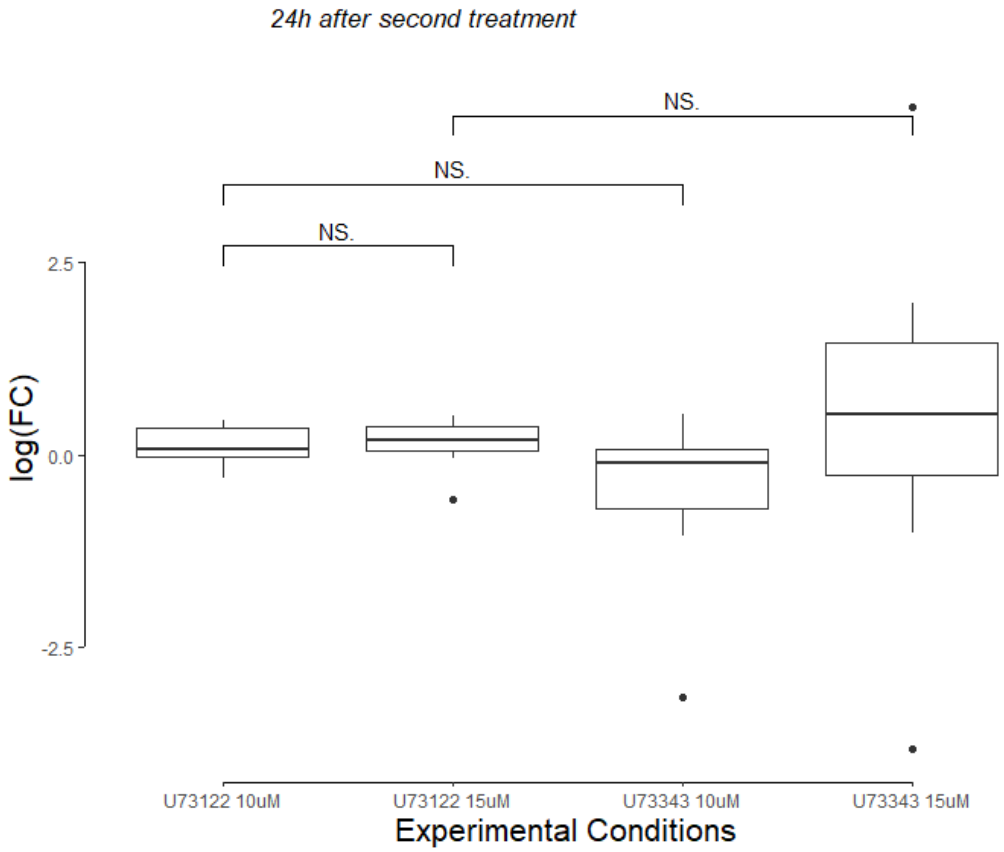

Figure 26. Aggregated gene expression data for PLC family 24h after second treatment.

3.1.3 Apoptosis an cell cycle regulation.

To investigate how U73122 and its inactive analogue U73343 influence apoptotic and proliferative programs in osteosarcoma cells, we performed an immunofluorescence analysis of key regulatory markers in 143B cells following double treatments with 10 µM and 15 µM concentrations. Cells were fixed at 120 h, ensuring that both the untreated control and treated samples were processed under identical conditions.

In untreated cells, apoptotic activation was minimal: cleaved Caspase-3 was nearly absent, Ki67 expression was low, and p21, together with its upstream regulator p53, was only weakly detectable. Despite the low marker expression, cells showed typical proliferative morphology with numerous mitotic figures.

Exposure to U73122 induced dose-dependent alterations. At 10 µM, cells retained a proliferative phenotype, accompanied by increased Ki67 and enhanced p53 localization in both the nucleus and cytoplasm. At 15 µM, however, proliferation was reduced and cell morphology became heterogeneous, with both rounded and elongated phenotypes emerging. Apoptotic activation became evident, as cleaved Caspase-3 accumulated in the cytoplasm and in vesicle-like structures. Consistent with reduced proliferation, Ki67 levels decreased, whereas p21 expression increased markedly. p53 expression was slightly lower than in the 10 µM condition. In contrast, U73343 treatment elicited a broad intensification of all marker signals. At 10 µM, cells remained proliferative but showed a strong apoptotic response, with very intense cleaved Caspase-3 staining. Ki67 and p53 signals were markedly higher than those observed in both controls and U73122-treated cells, and p21 was broadly distributed throughout the cytoplasm. Treatment with 15 µM U73343 induced pronounced morphological changes, with cells becoming more rounded and displaying reduced cytoplasmic volume. Despite a cessation of proliferation, Ki67 remained highly expressed, and p21 levels were strongly elevated. p53 expression was reduced compared to the 10 µM analogue condition and localized exclusively to the cytoplasm.

	Untreated		**U122_10µM**		**U122_15µM**		**U343_10µM**		**U343_15µM**	
	pos/ neg	*Loc.*	*pos/ neg*	*Loc.*	*pos/ neg*	*Loc.*	*pos/ neg*	*Loc.*	*pos/ neg*	*Loc.*
CLEAV. CASP. 3	+	C	- +	N, C	+	C,Vs	+ +	C	++	C, Vs
p21	+	N, C	- +	C	+	C, Vs	+ +	C	++	C, Vs
KI67	+	N (some) , C	+	N, C	- +	N (few), C	+ +	C	+	N, C
p53	+ -	N, C	+	N, C	+	N,C	++	N,C	+	C, Vs

LEGEND:		J	Junction
N	Nuclei	V	Vacuole
C	Cytoplasm	EX	Cellular extensions
CM	Cell membrane	Vs	Vesicles

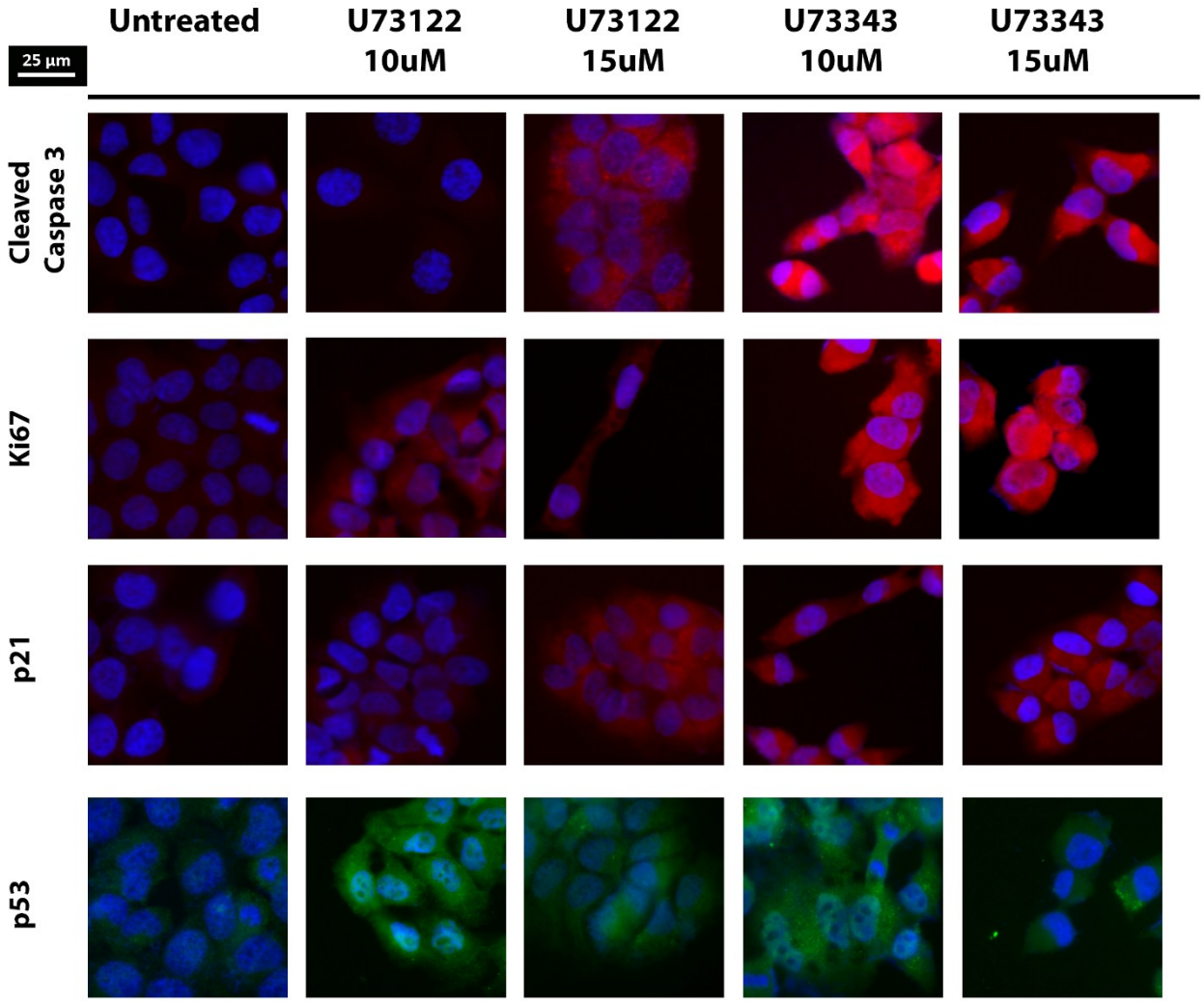

Figure 27. Immunofluorescence analysis for apoptosis, proliferation and cell cycle regulation markers after inhibitor treatments and untreated control.

3.1.4 Induction of osteogenic differentiation.

To assess whether PLC inhibition interferes with the osteoblastic phenotype of 143B cells, we evaluated the expression of key osteogenic differentiation markers under all treatment conditions. Even in the absence of an induced differentiation program, 143B cells display a molecular profile consistent with late-stage osteoblast-like cells. Alkaline phosphatase, osteonectin, osteopontin, and osteocalcin, canonical markers of mature osteoblasts, were consistently expressed across all experimental groups, indicating that neither U73122 nor U73343 disrupts this baseline osteogenic signature.

RUNX2 represented the only marker showing treatment-dependent variation. After exposure to U73122 at 10 μM, RUNX2 was undetectable, whereas in untreated cells and in the U73122 15 μM and U73343 10 μM conditions, the transcription factor localized both to the cytoplasm and nucleus. Notably, the 15 μM U73343 treatment induced a complete cytoplasmic relocalization of RUNX2, suggesting altered transcriptional regulation.

As observed for apoptosis and proliferation markers, U73343 treatment enhanced overall signal intensity for all osteogenic markers, consistent with a general increase in cellular metabolic activity induced by the inactive analogue.

	UNTREATED		**U122_10μM**		**U122_15μM**		**U343_10μM**		**U343_15μM**	
	pos/ neg	*Loc.*	*pos/ neg*	*Loc.*	*pos / neg*	*Loc.*	*pos/ neg*	*Loc.*	*pos/ neg*	*Loc.*
ALP	+	N,C	+	C	+	N, C	+ +	N, C	++	N, C, Vs
OCN	+ -	N,C	-		+	C	+ +	N, C	+	N, C, Vs
OPN	+	N,C	-		+	C,V	+	C	++	C
RUNX2	+	N,C	-		+	N, C, EX	+ +	N, C	+	C
SPARC	+	C	+	C	+	C	+	C	+	C

LEGEND:

N	Nuclei
C	Cytoplasm
CM	Cell membrane
J	Junction
V	Vacuole
EX	Cellular extensions
Vs	Vesicles

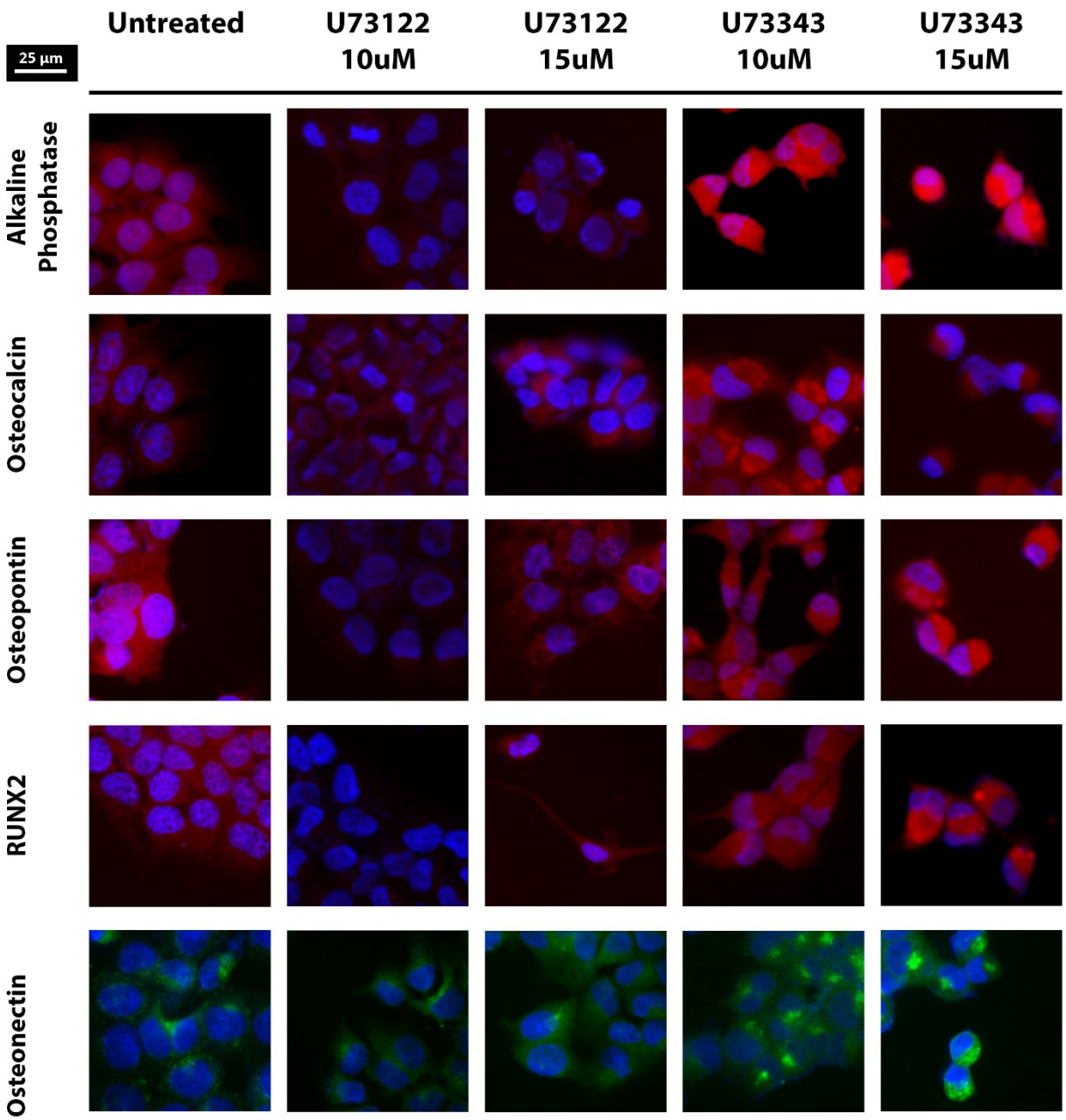

Figure 28. Immunofluorescence analysis for osteogenic differentiation markers after inhibitor treatments and untreated control.

3.1.5 Cytoskeleton and cell adhesion.

Different treatment conditions are not able to impact upon Actin overall expression in 143b cells, however the signal given by this filamentous protein of the cytoskeleton appears to be quite widespread all over the cytoplasm meaning that it could be poorly spatial organized in these cells. Ezrin levels are slightly increased by the treatment with U73122 15μM compared to untreated condition, also Ezrin is poorly organized in this cells too; the signal comes from all over the cytoplasm and only few membrane reinforcements are observed.

Beta Tubulin seems to be not affected by all treatments, the signal given by this protein is barely detectable and mainly cytoplasmatic. E-Cadherin is rarely present at cellular junction in 143b cells, the signal is diffuse from the cytoplasm. E-cadherin signal is stronger in U73343 treatment condition. Vimentin is a structural protein and the most widely distributed of all intermediate filament proteins, and it is also the main component of the cytoskeleton of mesenchymal cells and it is strictly involved in epitaxial mesenchymal transition process in cancer. This component of the cytoskeleton is the mostly affected by U73122 treatment, not only the protein expression appears strongly downregulated in both 10μM and 15μM treatments, but also this treatment impact on localization compared to the controls: after U73122 treatment the protein is mostly relegated to the extremities of the cell. Vimentin signal is very intense after U73343 treatment, but its distribution is more homogeneous in the cells.

	UNTREATED		**U122_10μM**		**U122_15μM**		**U343_10μM**		**U343_15μM**	
	pos/ neg	Loc.	pos/ neg	Loc.	pos/ neg	Loc.	pos/ neg	Loc.	pos/ neg	Loc.
ACTIN	+	C	+	C	+	C	+ +	N, C	++	C, CM
EZRIN	+	C, CM	+	C, CM	+	C,V, CM	+ +	C, CM	+	C
B-TUB.	+	C	+	C	+	N, C	+ +	C	++	C
E-CAD.	+	C, J	+	C, CM	+ -	C, EX	+ +	C, J	++	N, C, Vs
VIM.	+	C, CM, Vs	+ -	C, VS	+ -	C, CM, Vs	+ +	C, CM, Vs	+ +	C, CM, Vs

LEGEND:	
N	Nuclei
C	Cytoplasm
CM	Cell membrane
J	Junction
V	Vacuole
EX	Cellular extensions
Vs	Vesicles

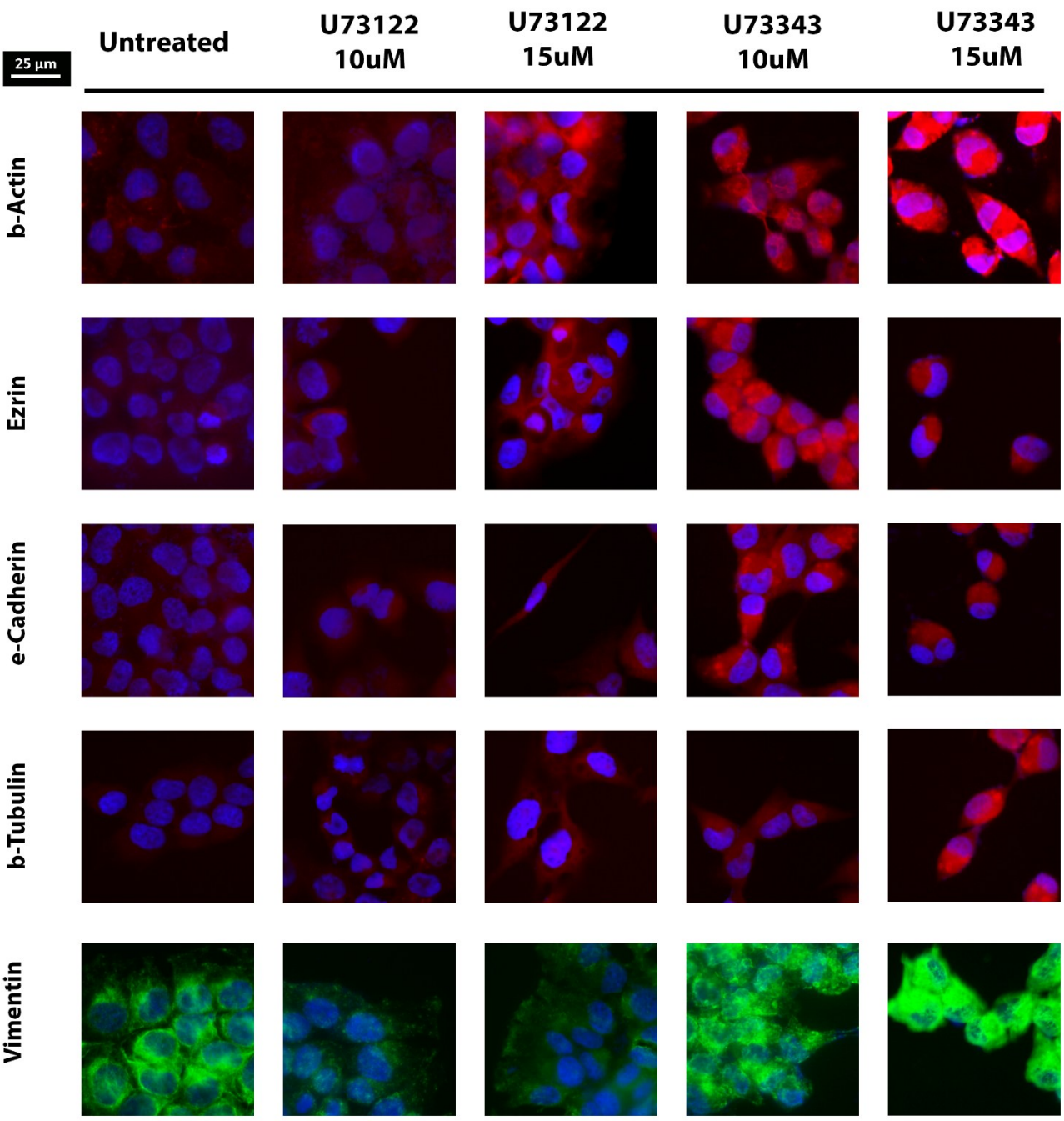

Figure 29. Immunofluorescence analysis for cytoskeleton, cell adhesion and EMT markers after inhibitor treatments and untreated control.

3.1.6 Expression of CD34, CD99, CAV-1 and Western blotting validation.

To further characterize the cellular response to PLC inhibition, we assessed the expression of CD34, CD99, and CAV-1 by immunofluorescence and validated key findings by Western blotting. CD34 levels increased in 143B cells following both U73122 and U73343 treatments compared to the untreated condition. The receptor localized to the plasma membrane but was also detectable throughout the cytoplasm, exhibiting both diffuse distribution and accumulation within vesicle-like structures. In contrast, CD99 expression remained unchanged across treatments, consistently displaying cytoplasmic localization with prominent membrane reinforcements. Similarly, CAV-1 was not affected by treatment and was distributed throughout the cytoplasm, occasionally outlining vesicular structures.

	UNTREATED		**U122_10µM**		**U122_15µM**		**U343_10µm**		**U343_15µm**	
	pos/ neg	*Loc.*	*pos/ neg*	*Loc.*	*pos/ neg*	*Loc.*	*pos/ neg*	*Loc.*	*pos/ neg*	*Loc.*
CD34	+	C	+	C, CM	+ +	C, CM	+ +	N, C, CM	+ +	C, CM
CD99	+ +	C, CM	+ +	C, CM	+ +	C, CM	+ +	C, CM	+ +	C
CAV-1	+	C, Vs	+	C, Vs	+	C, Vs	+ +	N, C	+ +	C

LEGEND:	
N	Nuclei
C	Cytoplasm
CM	Cell membrane
J	Junction
V	Vacuole
EX	Cellular extensions
Vs	Vesicles

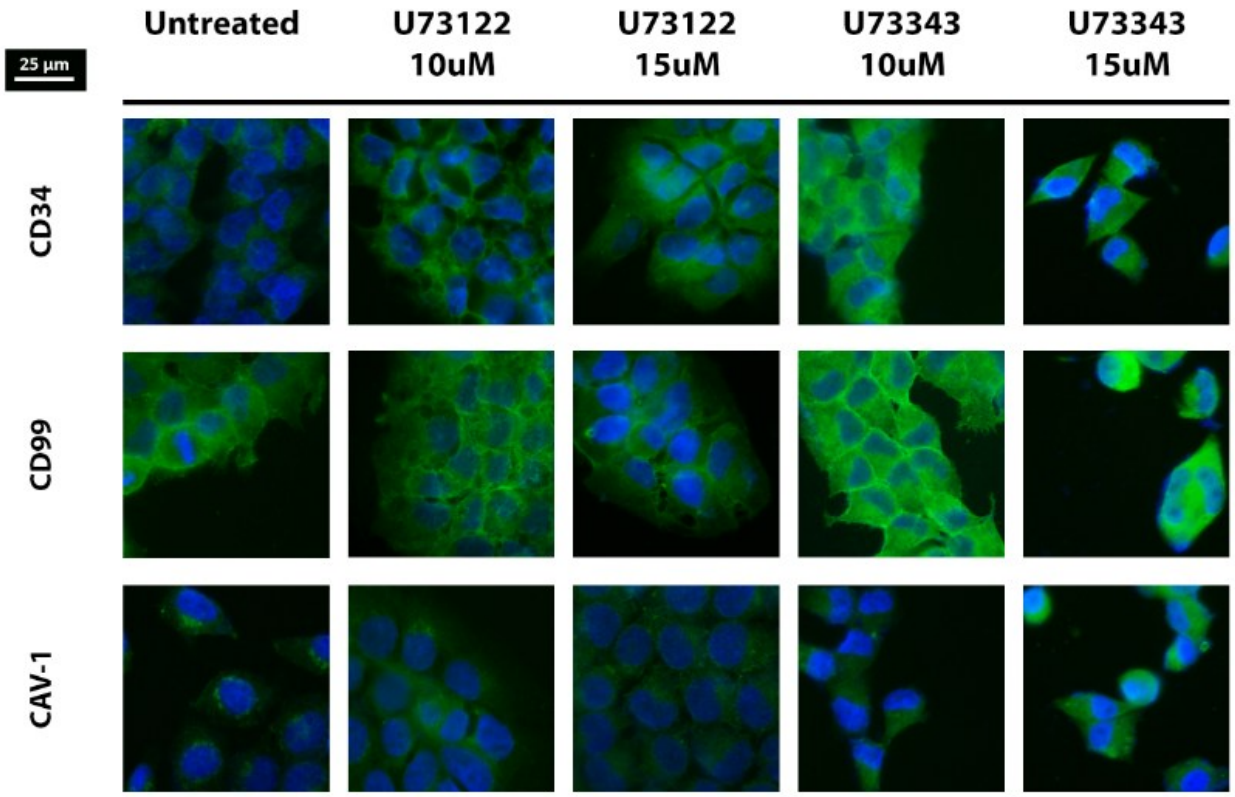

Figure 30. Immunofluorescence analysis for membrane markers after inhibitor treatments and untreated control.

Western blot analysis supported the immunofluorescence data and further clarified treatment-specific effects. Vimentin appeared abundantly expressed in 143B cells. The cell-cycle inhibitor p21 was markedly induced by U73122, with the 15 µM treatment producing approximately a twofold increase relative to control. p53 levels showed a more variable pattern: they increased following U73122 10 µM exposure but were reduced upon 15 µM treatment compared to untreated cells. Cleaved Caspase-3 showed minimal expression across all conditions, indicating limited activation of apoptotic pathways at the protein level under these experimental settings.

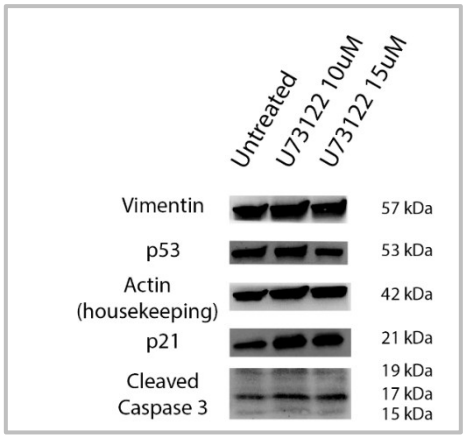

Figure 31. Western blot analysis for EMT and cell cycle markers.

3.2 PLCs modulation trough U73122 and U73343 inhibitors.

3.2.1 *PLCB1* silencing.

Silencing of *PLCB1* was effective up to 72 h after transfection, as demonstrated by both transcript and protein analyses. qPCR confirmed a marked reduction in PLCB1 mRNA levels during the first 48 h, while at 72 h transcript levels began to rise again, suggesting the onset of recovery from silencing (**figure 34 a**). Despite this partial mRNA rebound, PLCB1 protein levels remained suppressed at 72 h, as shown by Western blot (**figure 34 c**) and corroborated by immunofluorescence (**figure 34 b**). Among the tested concentrations, 0.6 µM siRNA produced the most robust and reproducible knockdown and was therefore selected for all subsequent experiments.

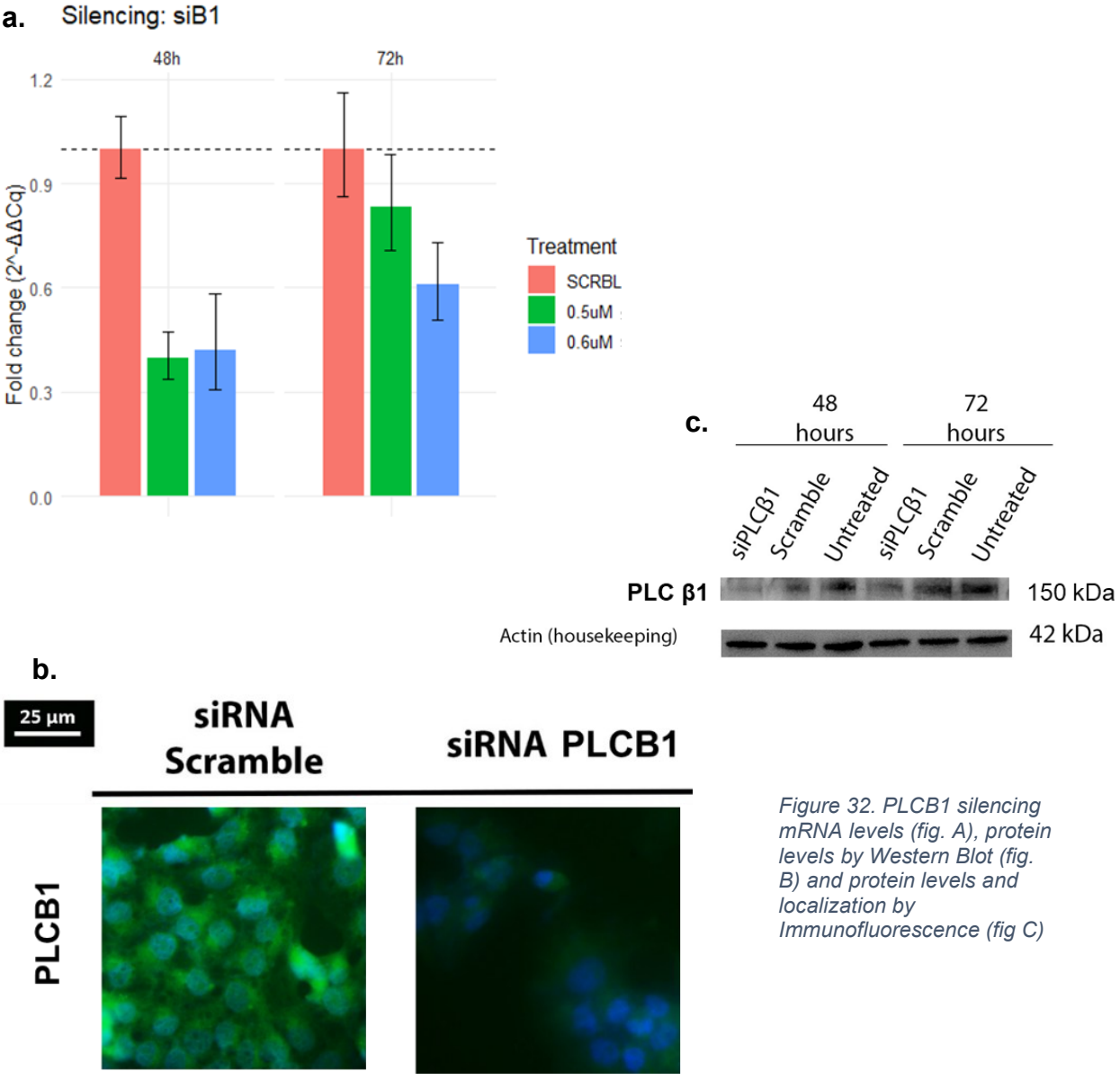

Figure 32. PLCB1 silencing mRNA levels (fig. A), protein levels by Western Blot (fig. B) and protein levels and localization by Immunofluorescence (fig C)

3.2.2 *PLCB1* silencing: biological effect.

From a biological point of view, *PLCB1* silencing did not alter the proliferative behavior of 143B cells. Cell confluency assays revealed no appreciable differences in growth relative to the untreated condition from 24 up to 72 hours after the first treatment (**figure 35 a**). In wound-healing assays (n = 3), PLCβ1-silenced cells displayed a significant but modest delay in scratch closure (**figure 35 b, c**).

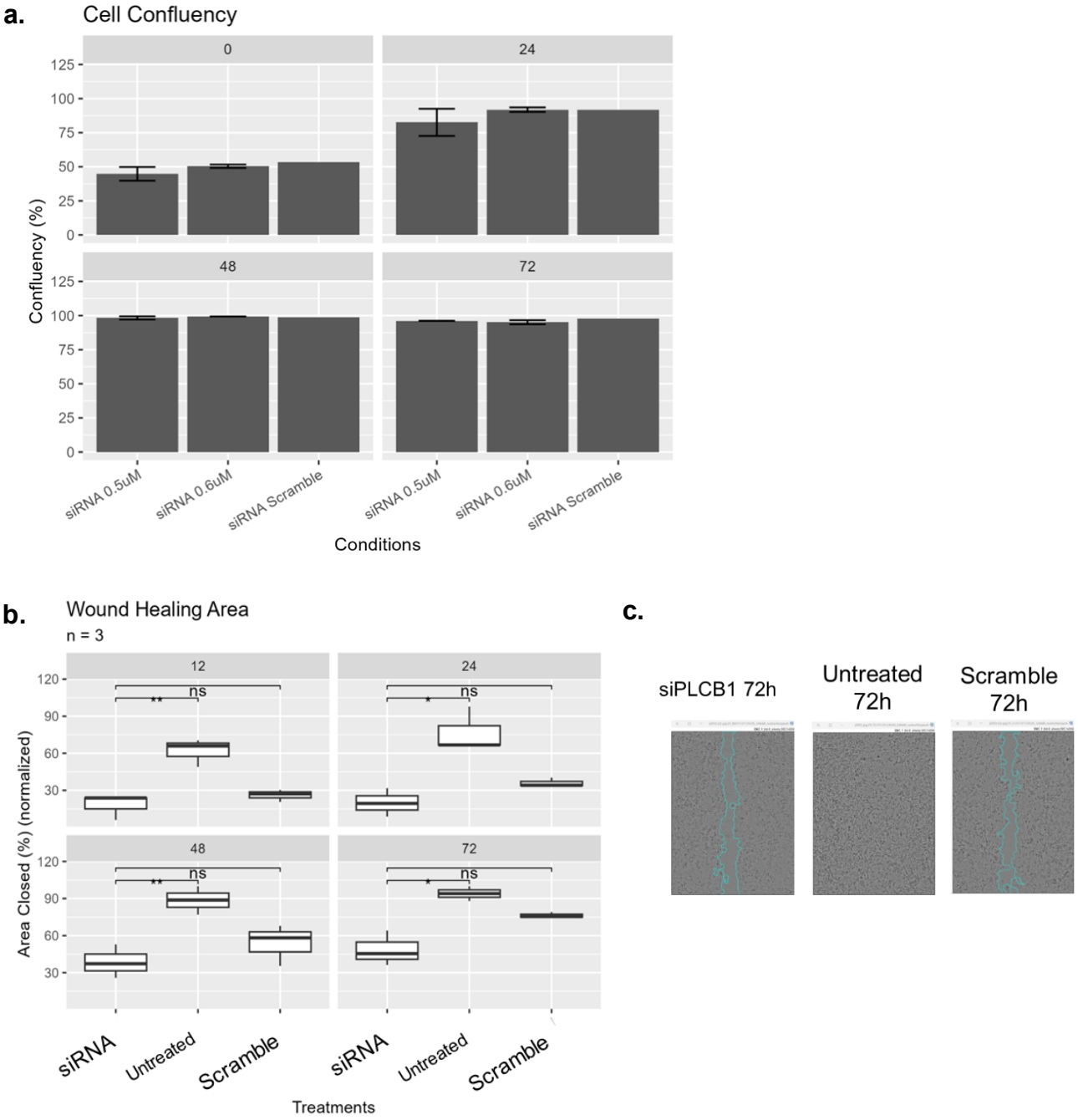

Figure 33. Cell confluency (fig a) and wound healing closed area (fig b and c) after siPLCB1 treatment.

3.2.3 *PLCB2* silencing.

PLCB2 silencing remained effective up to 72 h for both the transcript (**figure 36 a**) and protein levels. At this timepoint, *PLCB2* protein abundance was markedly reduced compared to controls, as demonstrated by immunofluorescence (**figure 36 b**) and Western blot (**figure 36 c**) analyses. Based on these results, a final siRNA concentration of 0.5 µM was selected for all subsequent *PLCB2* silencing experiments.

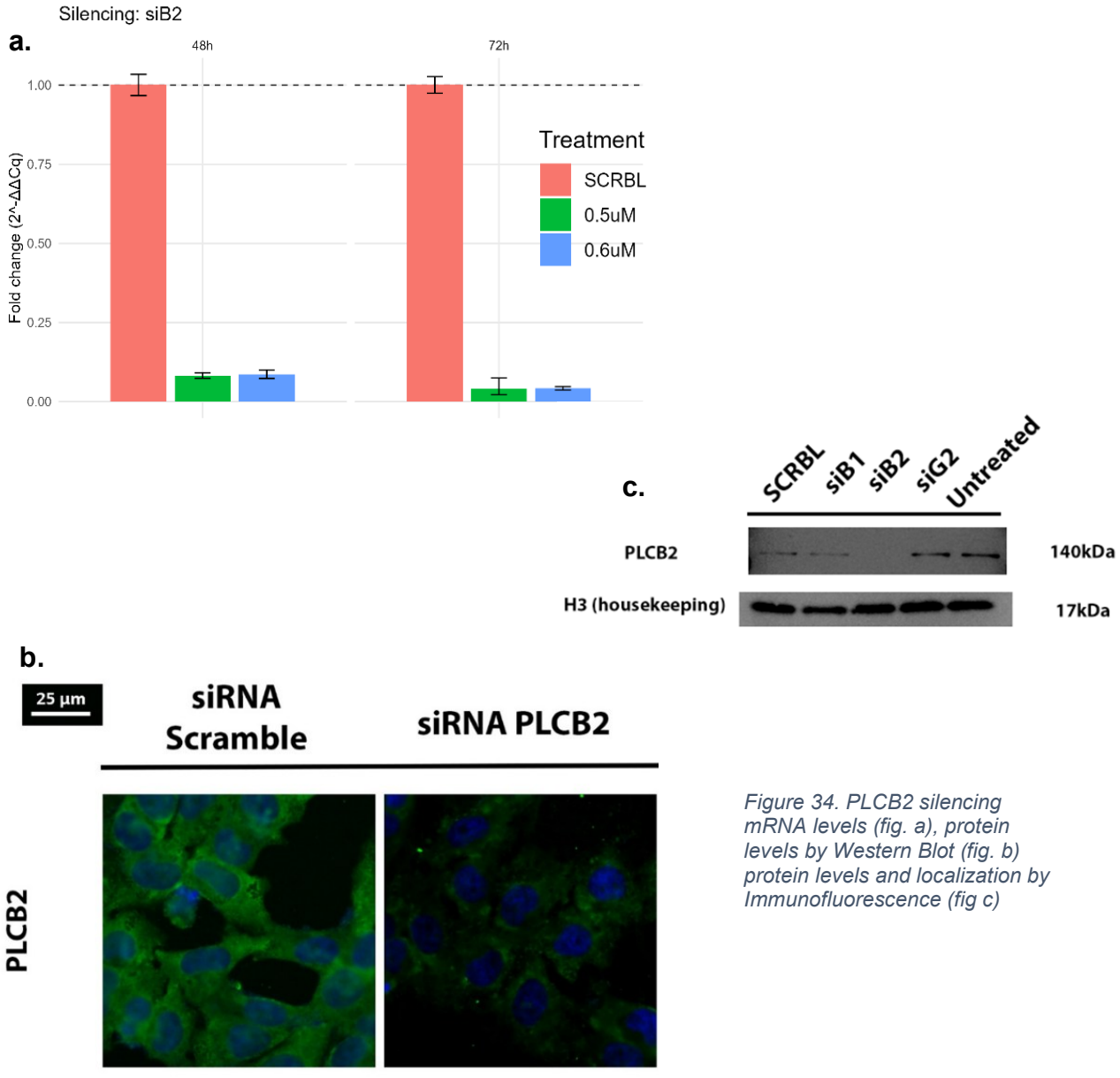

Figure 34. PLCB2 silencing mRNA levels (fig. a), protein levels by Western Blot (fig. b) protein levels and localization by Immunofluorescence (fig c)

3.2.4 *PLCB2* silencing: biological effect.

Regarding the biological consequences of *PLCB2* silencing, we observed a significant increase in **cell proliferation** compared with the scramble control. Notably, the knockdown condition appeared to counteract the mild cytotoxic effect of the transfection vehicle (Lipofectamine 3000), which was evident in scramble-treated cells. As a result, *PLCB2*-silenced cells exhibited a growth rate comparable to that of untreated cells (**figure 37 a**). Consistent with the proliferation data, the **wound-healing assay** revealed a migration pattern closely mirroring the growth phenotype.

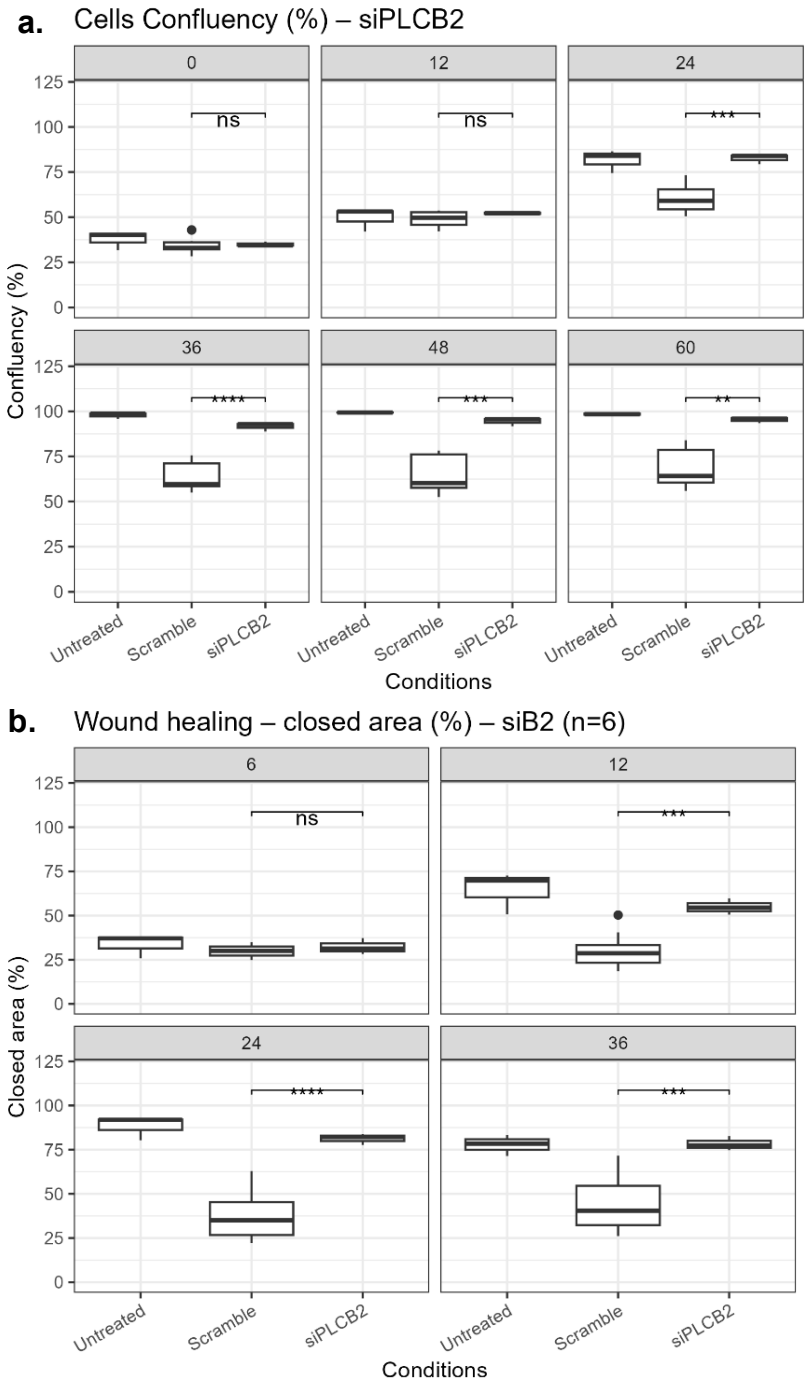

Figure 35. Cell confluency (fig a) and wound healing closed area (fig b) after siPLCB2 treatment.

The scratch area closed significantly faster in *PLCB2*-silenced cells than in scramble controls, with the most pronounced differences occurring between 12 and 36 hours after treatment. Notably, the closure rate in the siPLCB2 condition was comparable to that of untreated cells (**figure 37 b**).

At the **transcriptional level**, *PLCB2* silencing induced a broader compensatory response within the PLC family. An initial upregulation of *PLCG2*, and a minor increase of *PLCB1*, was already detectable after the first treatment (**figure 38**).

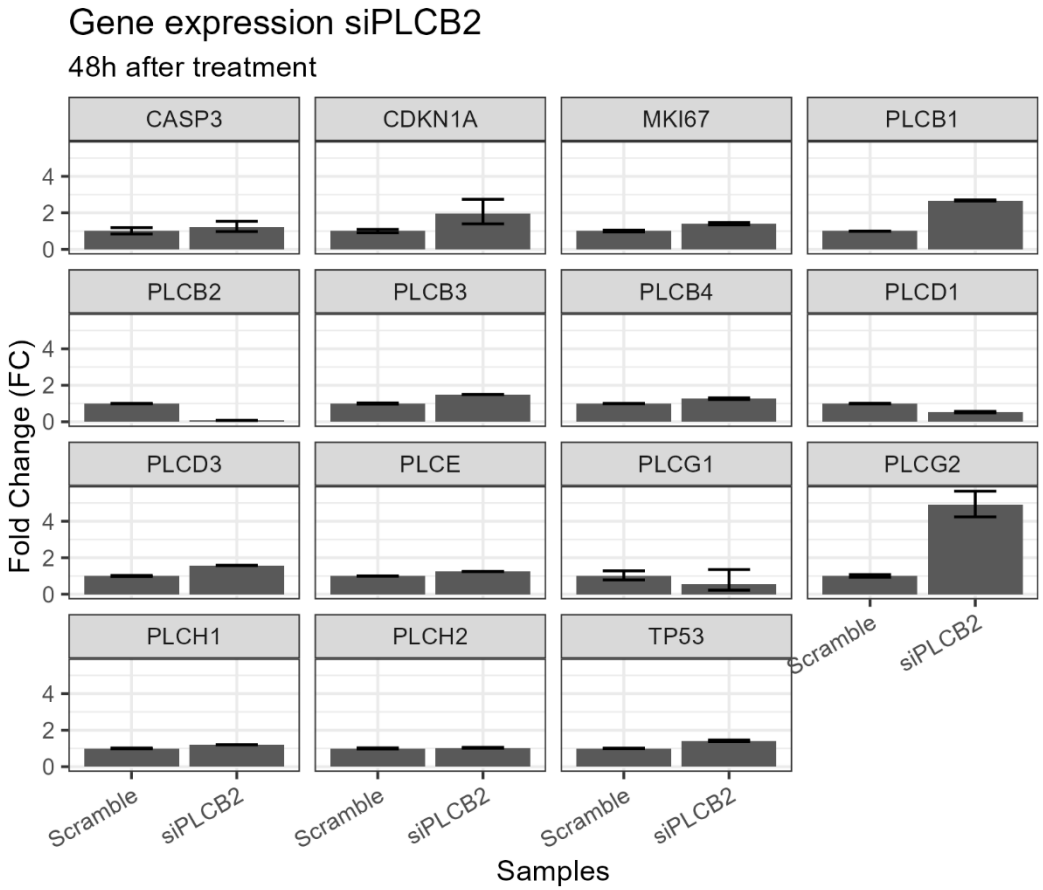

Figure 36. Gene expression (FC) 48h after PLCB2 silencing.

This effect became more pronounced at 72 hours after the first administration (which correspond also to 24 hours after the second administration), when a coordinated increase in several PLC transcripts emerged: *PLCB1*, *PLCB4*, *PLCG2*, and *PLCH2* all showed marked upregulation relative to scramble controls. Beyond PLC-related transcripts, *CDKN1A* (p21) and *TP53* were also moderately increased, whereas *MKI67* expression was reduced (**figure 39**). Together, these findings indicate that *PLCB2* knockdown triggers a structured transcriptional adaptation involving both PLC family members and key regulators of cell-cycle control.

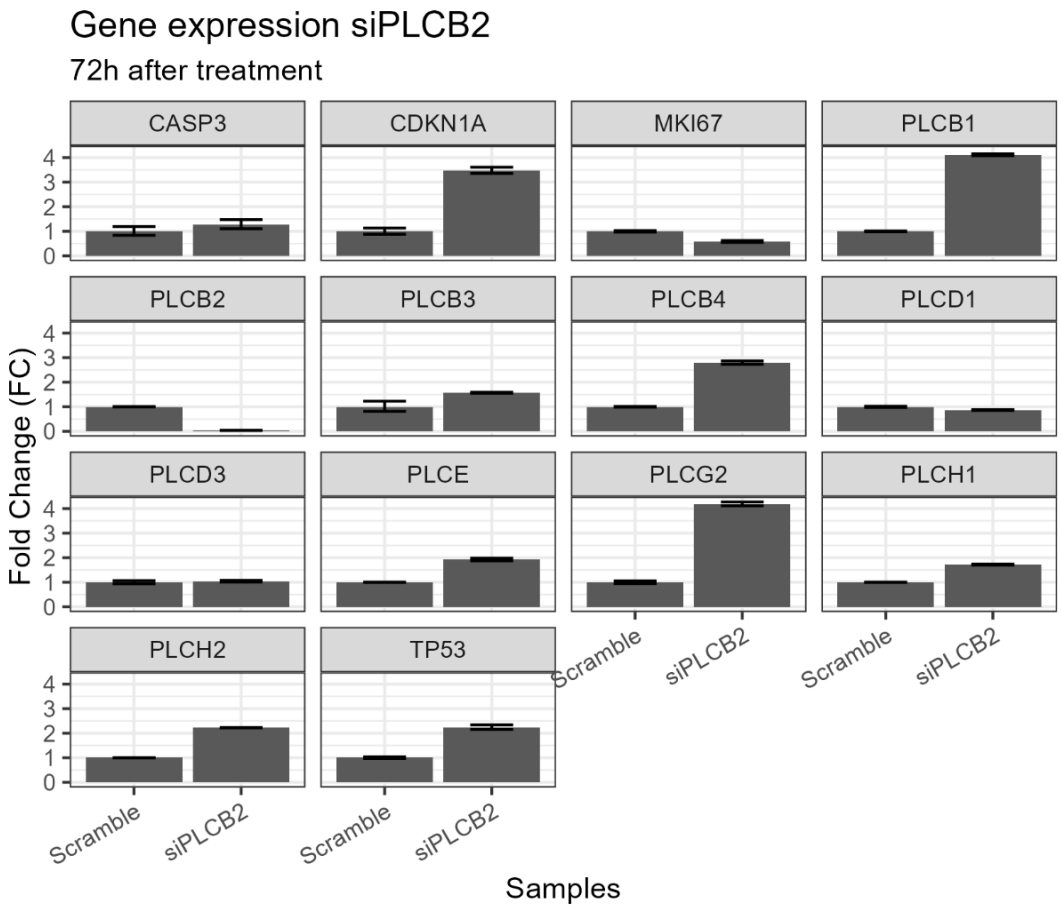

Figure 37. Gene expression (FC) 72h after PLCB2 silencing.

3.2.5 *PLCG2* silencing.

Silencing PLCG2 was technically challenging, as both its basal mRNA and protein levels are intrinsically low in 143B osteosarcoma cells, consistent with expression patterns observed across multiple public osteosarcoma datasets (see paragrapher *Bioinformatic analyses of patient-derived osteosarcoma datasets*).

Apart of this problematic, *PLCG2* silencing was achieved at the transcriptional level for up to 72 hours following the first treatment when using 0.6 µM siRNA (**figure 40 a**), the concentration subsequently adopted for all PLCG2-silencing experiments. Protein depletion mirrored the transcriptional trend: Western blot (**figure 40 c**) and immunofluorescence (**figure 40 b**) confirmed a clear reduction of PLCG2 protein up to 72 hours after treatment. Notably, PLCB2 silencing also led to a measurable decrease in PLCG2 protein

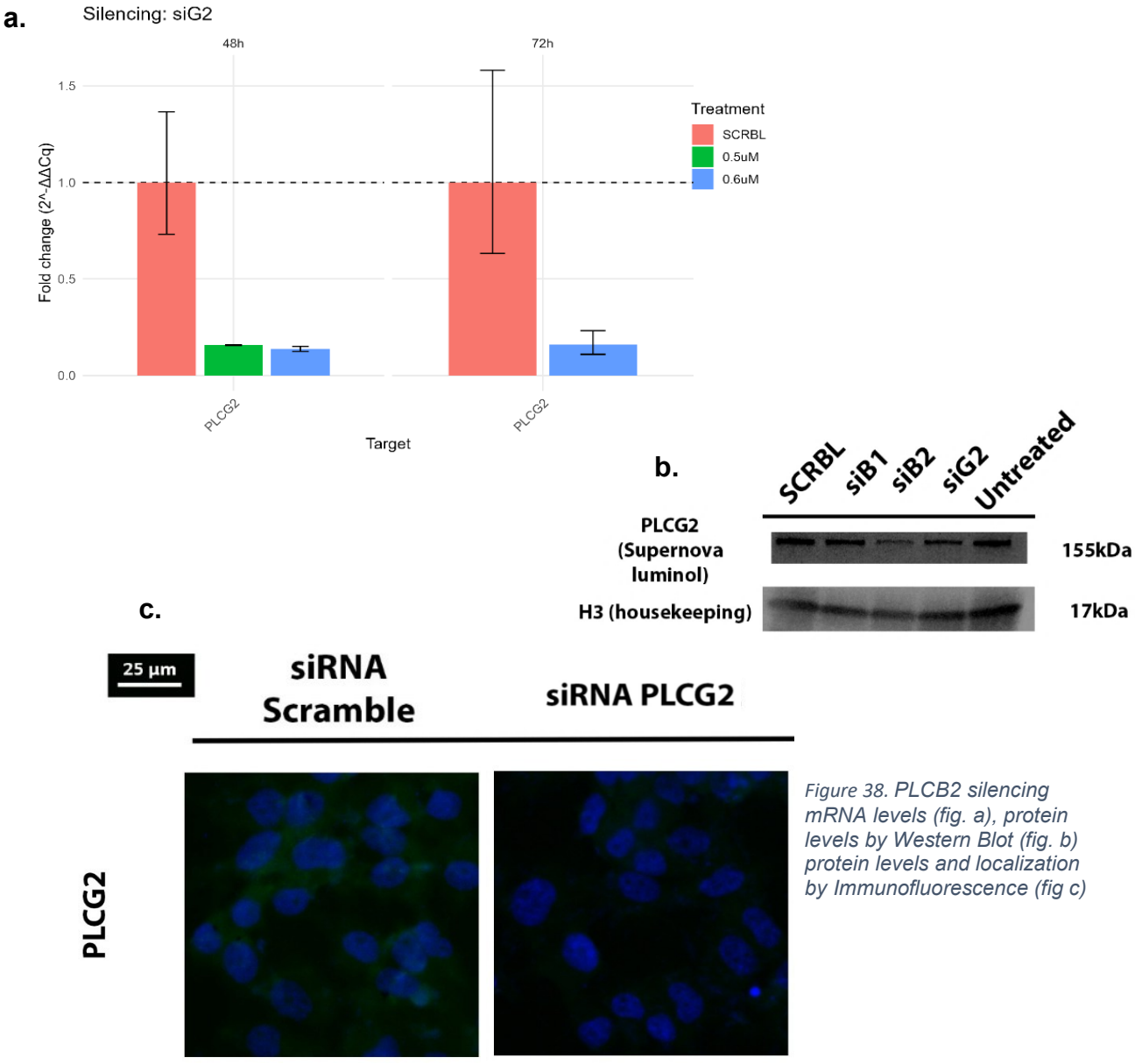

Figure 38. PLCB2 silencing mRNA levels (fig. a), protein levels by Western Blot (fig. b) protein levels and localization by Immunofluorescence (fig c)

3.2.6 *PLCG2* silencing: biological effect.

In terms of biological effect, *PLCG2* silencing led to a significant increase in **cell growth** compared with the scramble control. During the first 12 hours after treatment, *PLCG2*-depleted cells even exhibited a slightly faster growth rate than untreated cells, although this initial difference did not reach statistical significance.

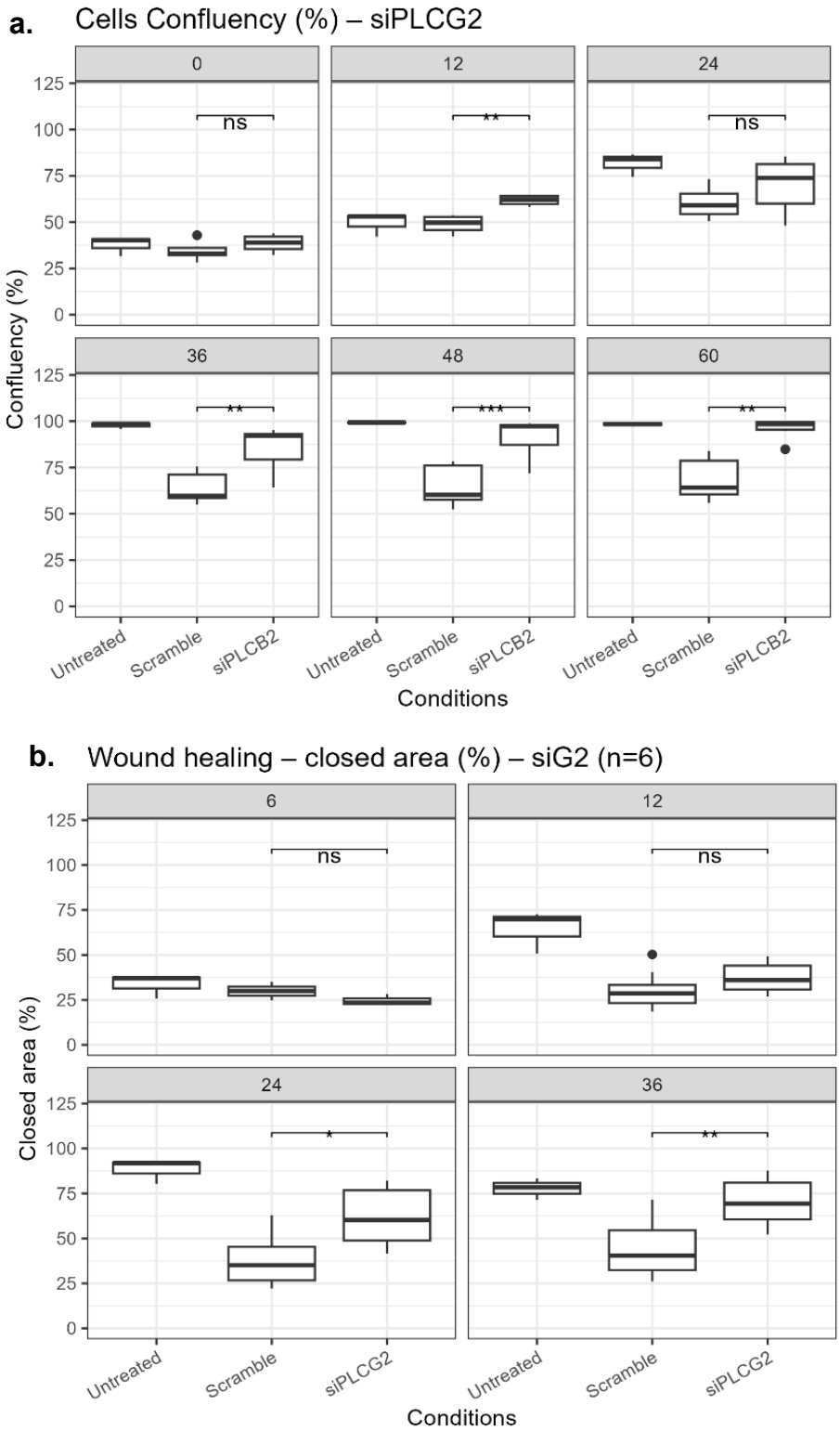

Figure 39. Cell confluency (fig a) and wound healing closed area (fig c) after siPLCG2 treatment.

From 24 hours onward, however, the growth rate of siPLCG2 cells became indistinguishable from those of the untreated condition, still the grow rate of the treated cells remains constantly higher compared to scramble condition (**figure 41 a**).

A similar trend emerged from the **wound-healing assay**, where *PLCG2*-silenced cells closed the scratch significantly earlier than the scramble control, displaying a migration rate essentially comparable to untreated cells (**figure 41 b**). Together, these results suggest that PLCγ2 reduction enhances proliferative and migratory behavior, a modest pro-proliferative effect appears to persist, and its biological relevance remains unclear. This observation will be further investigated using a dedicated invasion assay employing Boyden chambers to better characterize the impact of *PLCG2* silencing on invasive capabilities.

At the **transcriptional level**, *PLCG2* silencing produced early secondary effects on other PLC family members. At 48 hours after the first treatment, *PLCB2* was already markedly downregulated, indicating a rapid interconnected regulatory response. *PLCB1* also showed reduced expression, although to a lesser extent. In contrast, the cell-cycle inhibitor *CDKN1A* (p21) was upregulated (**figure 42**).

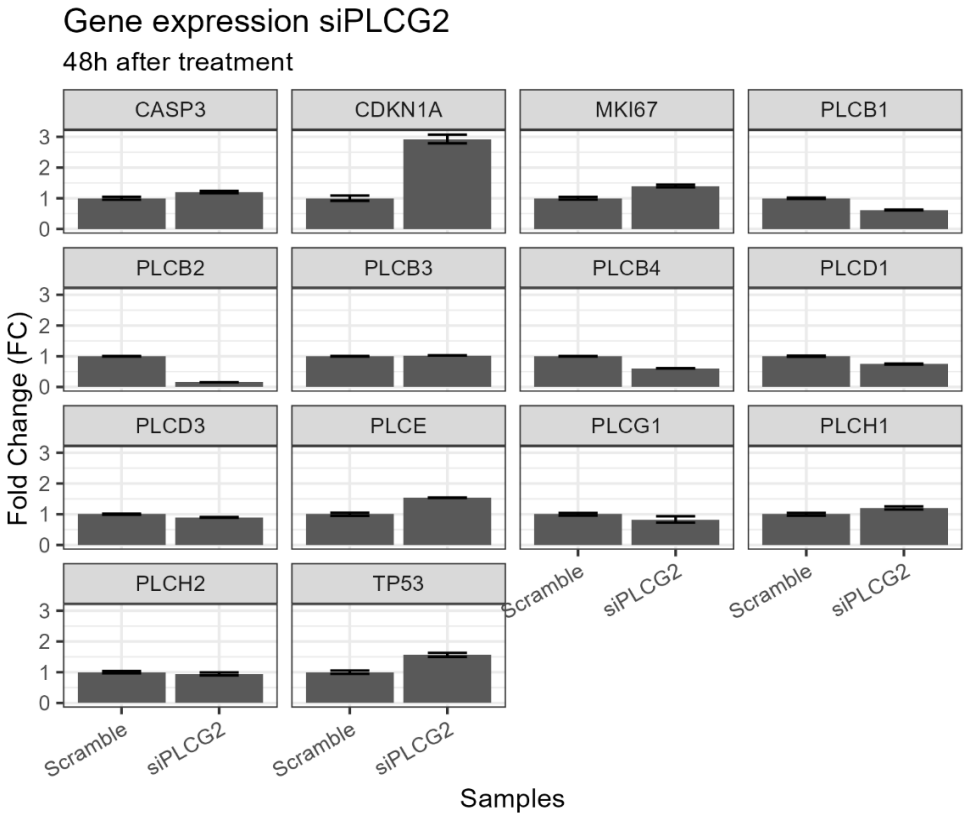

Figure 40. Gene expression (FC) 48h after PLCG2 silencing.

By 72 hours (**figure 43**), *PLCB2* remained profoundly downregulated, confirming the persistence of this effect. In parallel, the proliferation marker *MKI67* was reduced, while *CASP3* expression showed a slight downregulation. Overall, these data indicate that *PLCG2* knockdown may trigger a coordinated transcriptional shift affecting both PLC signaling components and cell-cycle regulators, with sustained suppression of PLCB2 being the most prominent effect.

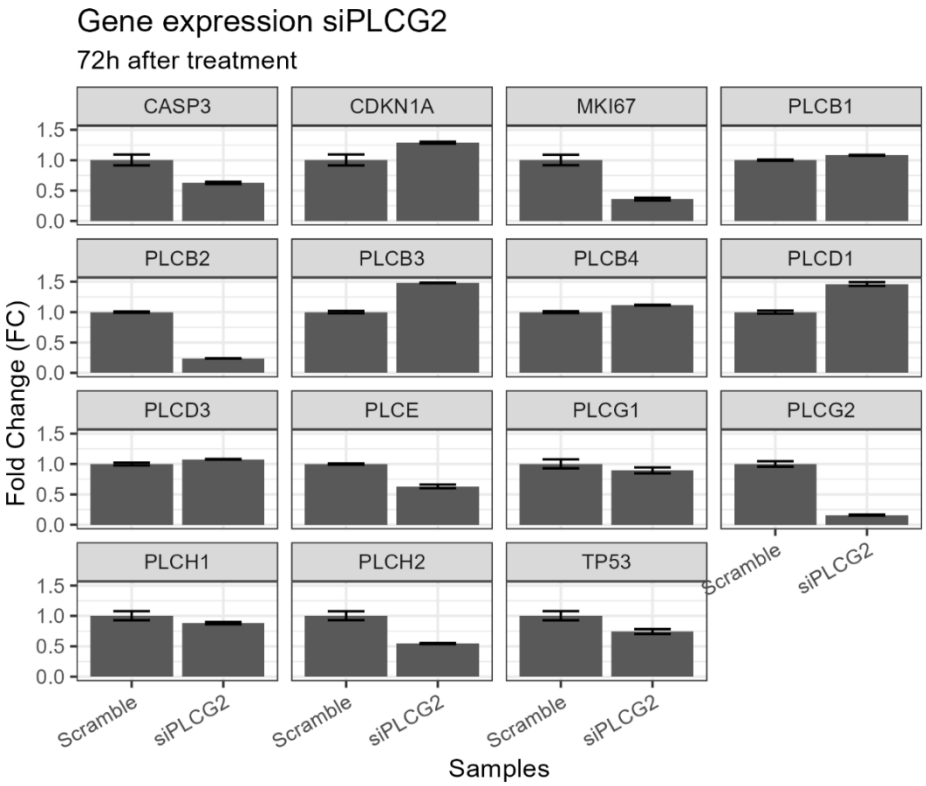

Figure 41. Gene expression (FC) 72h after PLCG2 silencing.

3.2.7 NGS Analysis.

To obtain a broader perspective on the biological consequences of *PLCB1*, *PLCB2*, and *PLCG2* silencing in 143B OS cells, we performed next-generation sequencing (NGS)-based gene expression profiling using an Illumina platform. This approach allowed us to capture global transcriptional changes induced by the individual knockdowns and to identify pathway-level alterations that may not be evident from targeted assays. By integrating these high-resolution datasets, we aimed to delineate the downstream molecular programs affected by each PLC isoform and to better understand their functional relationships in the osteosarcoma cellular context.

3.2.8 PLCB1 silencing.

Silencing of *PLCB1* was successful, as confirmed by NGS analysis. The transcriptomic profile of *PLCB1*-silenced cells clustered distinctly from the scramble control, indicating a robust and specific silencing effect**.** This separation is clearly visible in the heatmap (**figure 44 a**), where siPLCB1 samples group into an independent cluster, and in the volcano plot (**figure 44 b**), which highlights a substantial set of differentially expressed genes. Together, these data demonstrate that *PLCB1* silencing induces a marked transcriptional reprogramming in 143B cells.

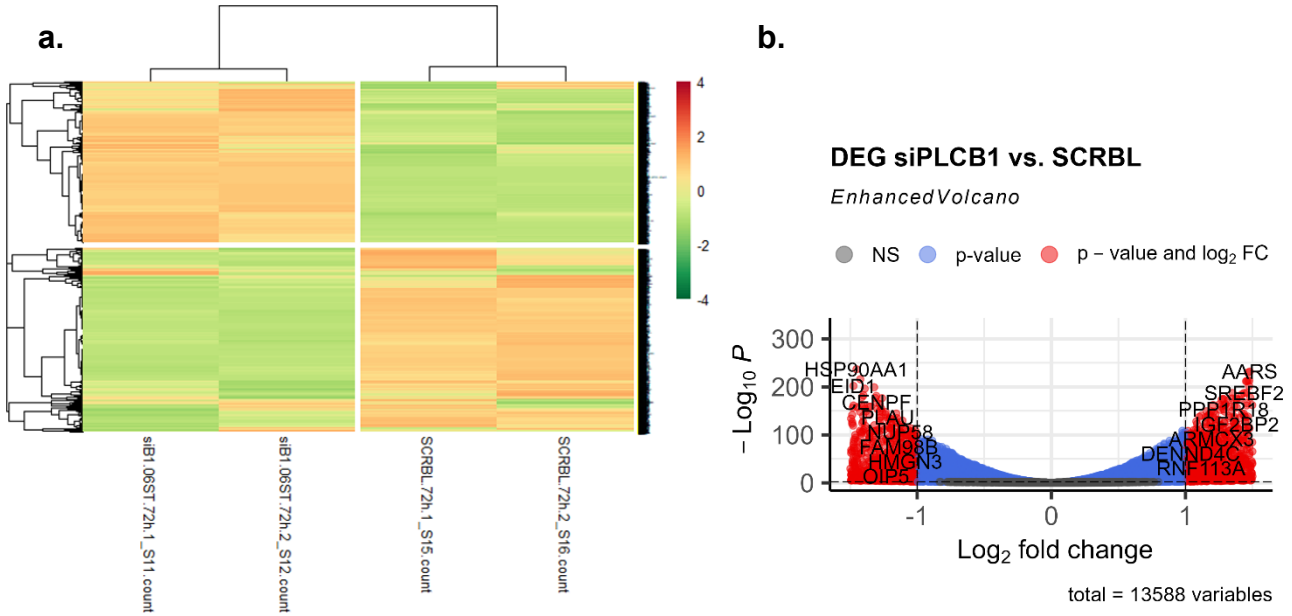

Figure 42. PLCB1 silencing NGS: heatmap-cluster analysis (fig a) and volcano plot (fig b).

Gene-expression profiles obtained by RNA sequencing were further examined through a ranked Gene Set Enrichment Analysis (GSEA) using the Hallmark 2025 collection. The resulting Normalized Enrichment Scores (NES) are displayed in the plot below (**figure 45**). In this representation, a negative NES denotes enrichment of a given gene set in the scramble control, whereas a positive NES reflects enrichment in the silenced condition. To account for differences in pathway size, NES values are reported as gene-set–size–normalized ratios, and statistical significance is indicated based on the false discovery rate (FDR). This analysis provides a compact overview of the major transcriptional programs modulated upon gene silencing.

The most notable outcome of the GSEA performed on *PLCB1*-silenced cells concerns the transcriptional programs that are significantly downregulated. In particular, both G2M checkpoint and E2F targets show strong negative enrichment, indicating a

coordinated suppression of genes involved in cell-cycle progression and mitotic entry. conversely, several pathways emerge as upregulated in the silenced condition, including unfolded protein response, IL2-STAT5 signaling, MTORC1 signaling, complement, and hypoxia.

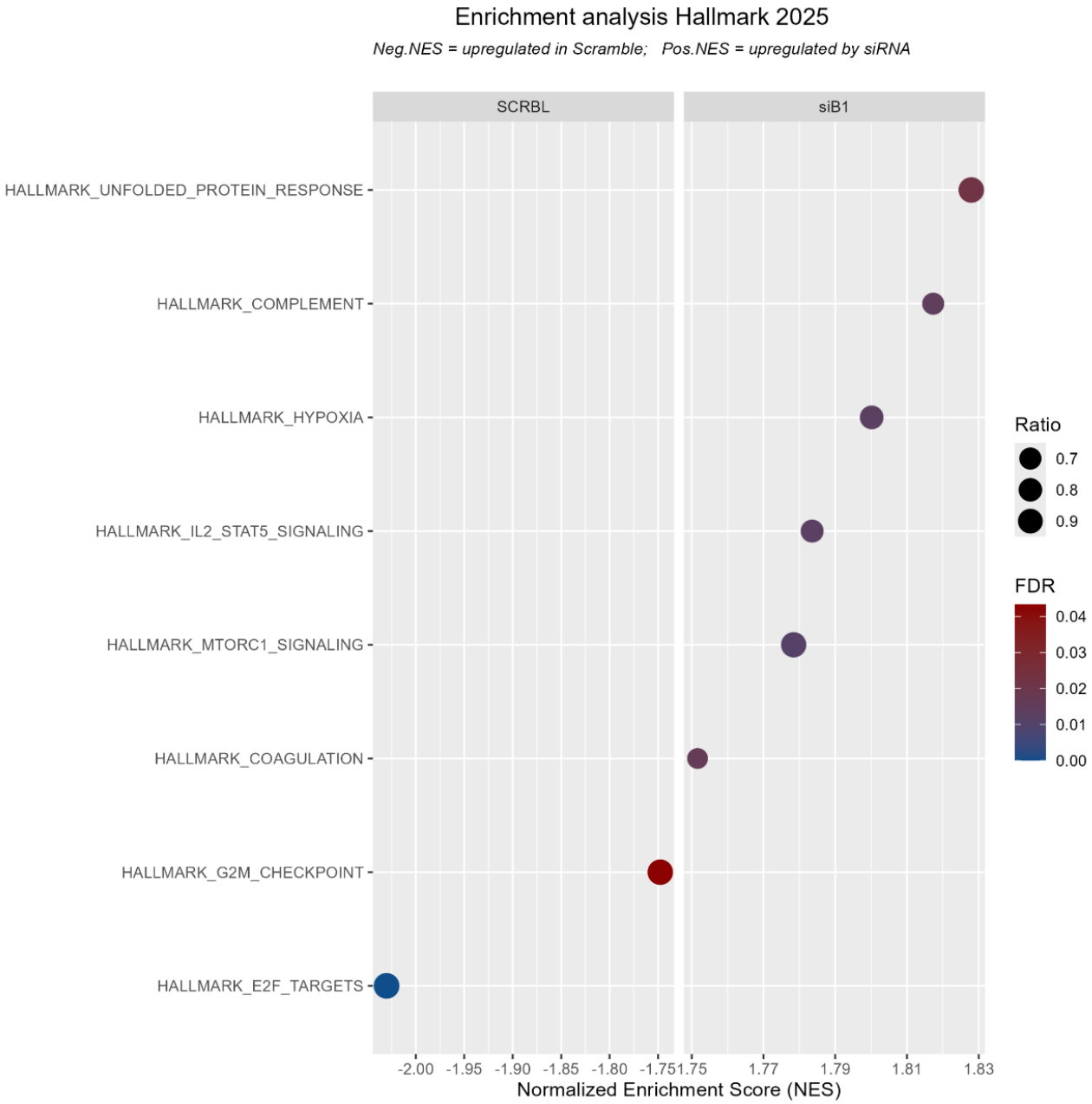

Figure 43. PLCB1 silencing enrichment analysis with GSEA (Hallmark 2025 collection)

3.2.9 PLCB2 silencing.

Silencing of *PLCB2* was successfully achieved, as confirmed by NGS-based gene-expression profiling. *PLCB2*-silenced cells form a clearly distinct transcriptional cluster compared to the scramble control, indicating a robust and specific molecular response to the downregulation. This separation is readily appreciable in both the heatmap (**figure 46 a**), where the two populations segregate into non-overlapping expression groups, and in the volcano plot (**figure 46 b**), which reveals a substantial set of differentially expressed genes distinguishing the silenced condition from the control.

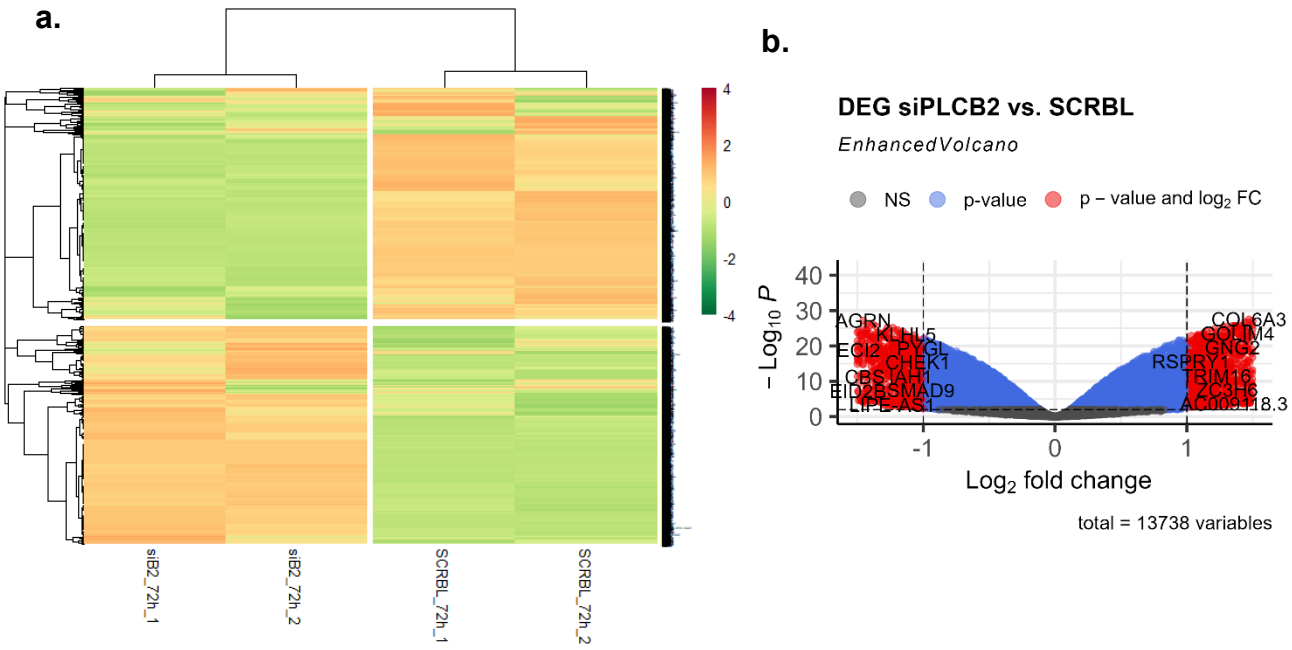

Figure 44. PLCB2 silencing NGS: heatmap-cluster analysis (fig a) and volcano plot (fig b).

The most notable effect emerging from the *PLCB2*-silencing transcriptomic analysis concerns the upregulated signaling associated gene sets (**figure 47**). the epithelial mesenchymal transition gene set displayed the strongest enrichment in *PLCB2*-depleted cells, followed closely by the gene set associated to coagulation, suggesting a shift toward a more migratory and pro-remodeling phenotype. conversely, several pathways were preferentially enriched in the scramble control, including E2F targets, oxidative phosphorylation, unfolded protein response, and MYC targets_v1, indicating that *PLCB2* silencing suppresses proliferative and metabolic pathways typically active in untreated 143b cells.

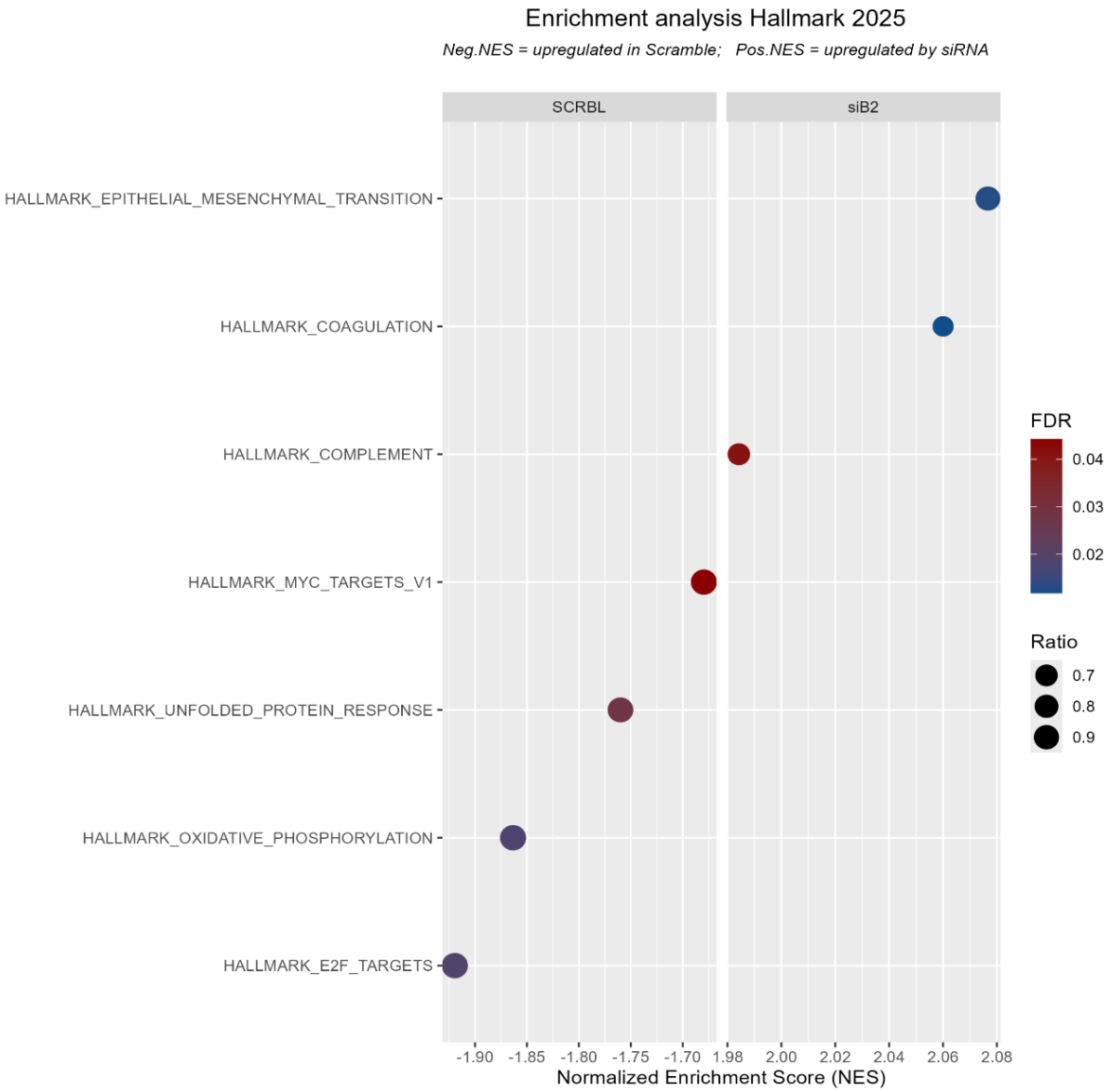

Figure 45. PLCB2 silencing enrichment analysis with GSEA (Hallmark 2025 collection)

3.2.10 *PLCG2* silencing.

PLCG2 silencing was successfully achieved, as confirmed by the NGS expression data. The *PLCG2*-silenced population clustered distinctly from the scramble control, a separation clearly evident in both the heatmap (**figure 48 a**) and the volcano plot (**figure 48 b**). These visualizations highlight a markedly divergent transcriptional profile between the two groups, indicating robust and specific gene-expression changes driven by *PLCG2* silencing. The most notable outcome of the *PLCG2*-silencing analysis concerns the pathways that become upregulated upon silencing (**figure 49**). The strongest enrichment is observed for Hypoxia, Complement, and Coagulation, indicating that *PLCG2* depletion shifts the transcriptional landscape toward stress-related, inflammatory, and pro-remodeling programs. As seen for *PLCB2* silencing, the epithelial–mesenchymal transition (EMT) gene set is also markedly enriched, further supporting the idea that perturbation of PLC signaling can promote mesenchymal features in 143B cells. Additional but more moderate enrichment is detectable for gene sets related to glycolysis, unfolded protein response, MTORC1 signaling, IL2–STAT5, KRAS, and TNFα–NF-κB, collectively suggesting that PLCγ2 loss enhances metabolic reprogramming and stress/inflammatory signaling networks.

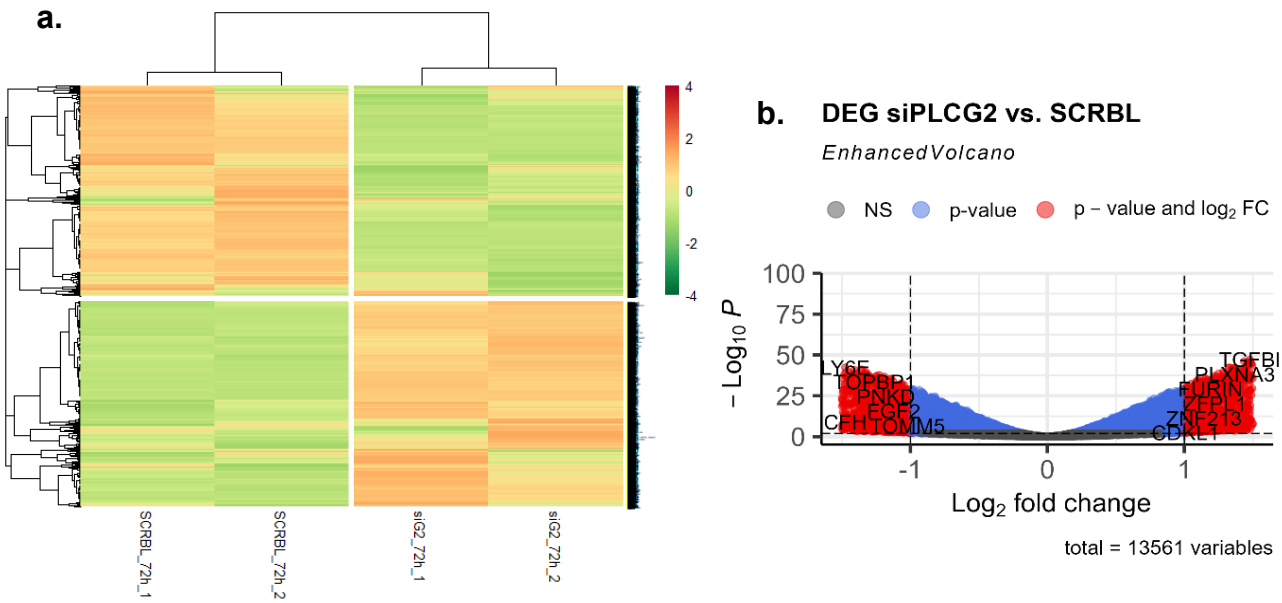

Figure 46. PLCG2 silencing NGS: heatmap-cluster analysis (fig a) and volcano plot (fig b).

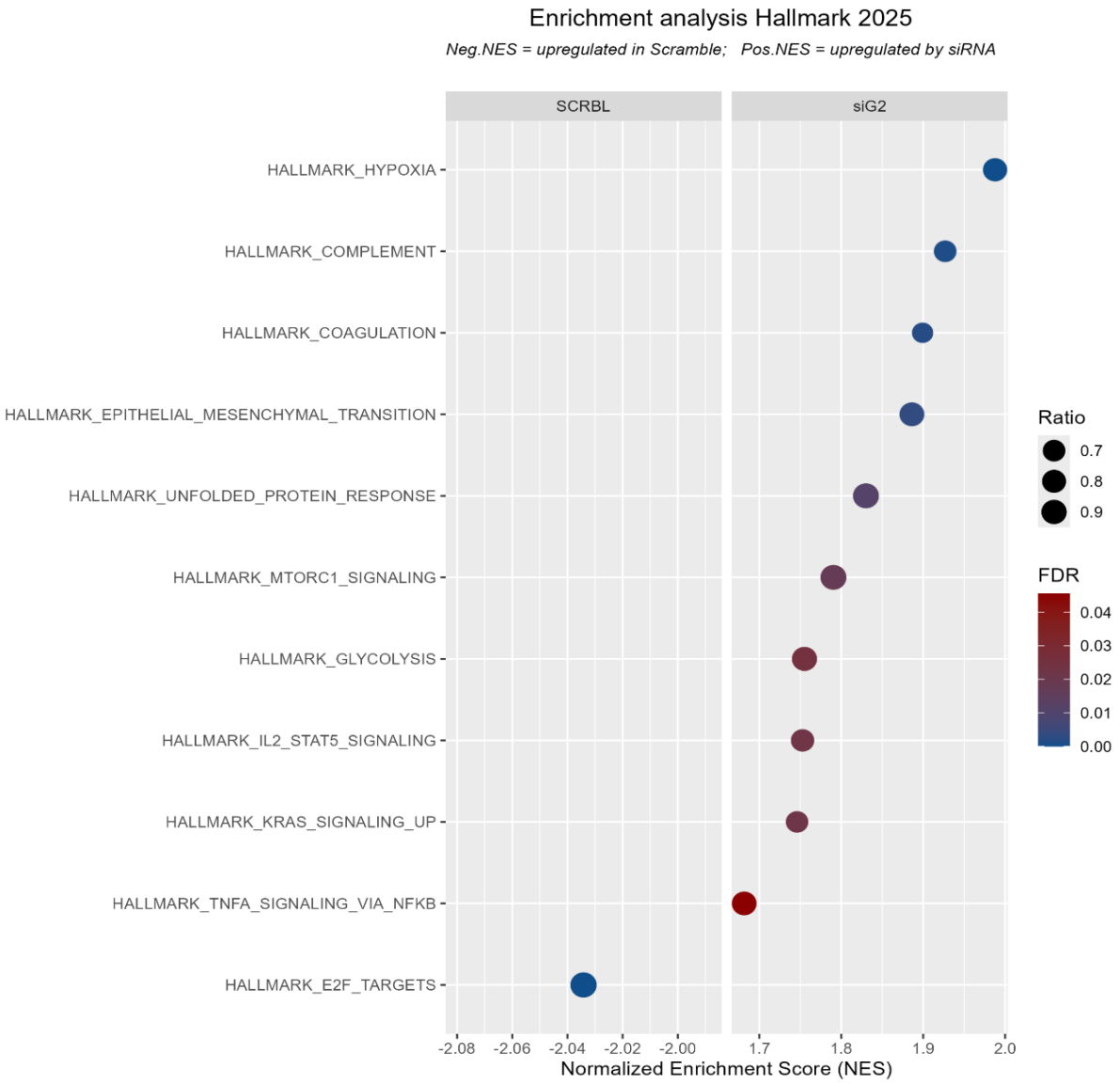

Figure 47. PLCG2 silencing enrichment analysis with GSEA (Hallmark 2025 collection)

3.2.11 *PLCB1* silencing: effect on apoptosis and cell cycle.

To investigate whether *PLCB1* silencing affects apoptotic or proliferative programs in 143B osteosarcoma cells, we assessed the expression of cleaved Caspase-3, Ki-67, p21, and p53 by immunofluorescence 72 h after transfection (**figure 50**). Overall, *PLCB1* downregulation did not induce major alterations in apoptosis or proliferation. Cleaved Caspase-3 remained barely detectable in both siPLCB1 and scramble controls, indicating that *PLCB1* depletion barley trigger or does not trigger apoptotic activation. Similarly, Ki-67 displayed comparable nuclear staining across conditions, confirming that the proliferative rate is similar to the control after *PLCB1* loss. In contrast, a modest but reproducible increase in p21 signal was observed in siPLCB1-treated cells, with staining detectable in both the nucleus and cytoplasm. p53 levels also appeared slightly elevated relative to the scramble control, although the signal remained heterogeneous across the population.

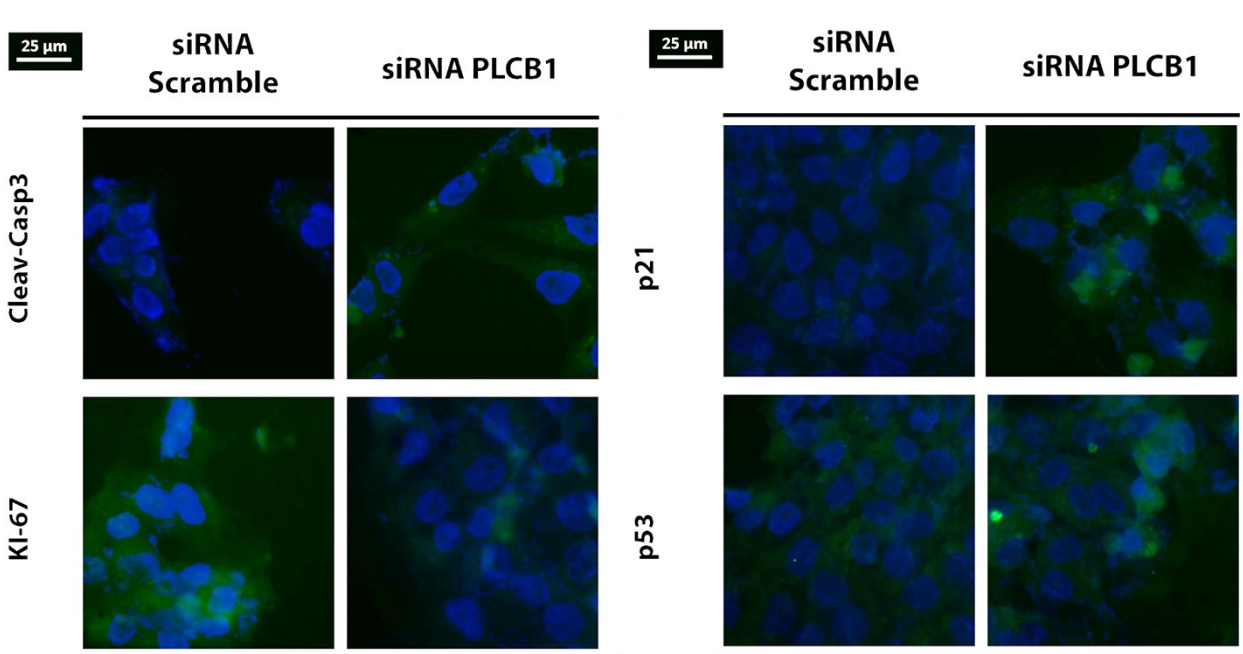

Figure 48. siPLCB1 effect on apoptosis and cell cycle markers (immunofluorescence analysis)

3.2.12 *PLCB2 – PLCG2* silencing: effect on apoptosis and cell cycle.

To evaluate the molecular consequences of *PLCB2* and *PLCG2* depletion in 143B osteosarcoma cells, we examined by immunofluorescence the expression of several PLC family members (PLCβ1, PLCγ1, and PLCε) together with the proliferation marker Ki-67 and the cell-cycle regulators p21 and p53 (**figure 51**).

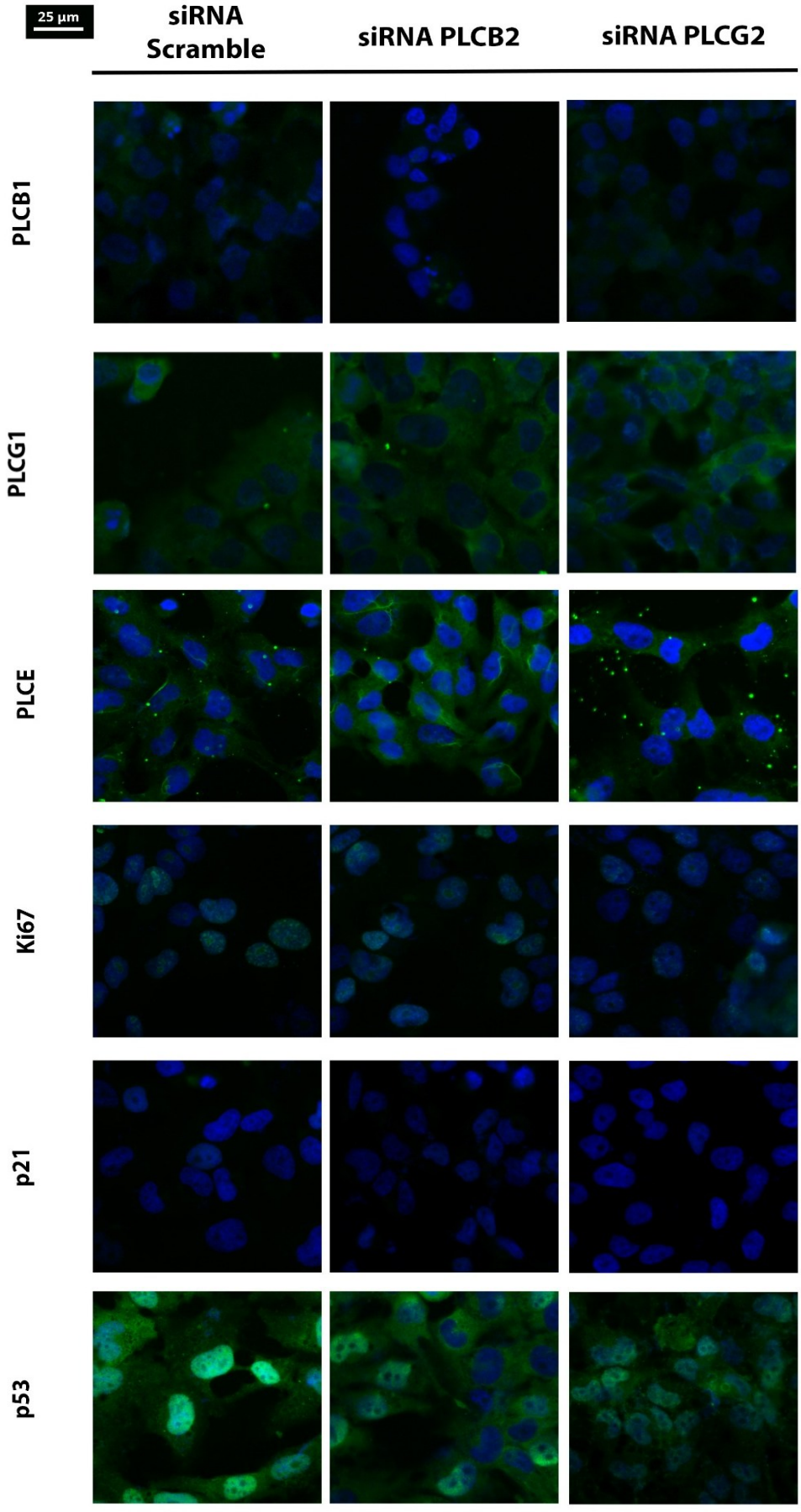

Figure 49. Proliferation- cell cycle markers and selected PLCs abundance after PLCB2 and PLCG2 silencing.

PLCB2 silencing produced a clear reduction of PLCβ1 staining intensity, which is unexpected considering the compensatory transcriptional effects observed in qPCR after the downregulation of *PLCB2*. In contrast, *PLCG2* silencing did not visibly modify PLCβ1 abundance, in line with the gene expression data of *PLCG2* silencing in 143B cells. PLCγ1 and PLCε showed broadly comparable staining abundance across all conditions. PLCγ1 is more present around the cytoplasmatic or nuclear membrane compared to the scramble condition. PLCε assumes a more filamentous pattern after *PLCB2* downregulation, while the signal seems to be slightly weaker after *PLCG2* silencing. Regarding functional markers, Ki-67 remained predominantly nuclear and comparable to the scramble control, indicating that the proliferative capacity of 143B cells is preserved upon depletion of either isozyme. p21 signal remains barley undetectable following *PLCB2* or *PLCG2* silencing. p53 signal appears similar in both treatments compared to the scramble control, but its localization seems to be more nuclear in the scramble control compared to treatments.

3.2.13 *PLCB2 – PLCG2* silencing: effect on cell adhesion proteins.

Based on the transcriptional signatures emerging from RNA-seq, which highlighted enrichment of adhesion- and EMT-related pathways, we next examined how *PLCB2* and *PLCG2* depletion affects cytoskeletal organization and focal adhesion machinery in 143B cells. Immunofluorescence staining revealed marked structural alterations compared with scramble and untreated controls.

Actin fibers displayed clear remodeling in both treatments. While controls exhibited a planar, well-organized filamentous network, *PLCB2*- and *PLCG2*-silenced cells showed a less structured cytoskeleton, with collapsed or folded actin bundles and increased accumulation of disorganized intracellular actin structures.

Ezrin expression was strongly increased following both PLCs downregulations, with a predominantly cytoplasmic distribution with a pronounced membrane reinforcement and bleb-like structures, which often tends to co-localize with membrane reinforcement of actin fibers.

FAK levels also appeared elevated in silenced cells, although the protein was primarily distributed along the cytoplasm without taking part of mature focal adhesion structure patterns; only a subset of cells displayed FAK-enriched punctiform structures.

Paxillin intensity increased for both treatments, though with distinct patterns: siPLCB2 cells exhibited mainly diffuse perinuclear cytoplasmic localization, whereas siPLCG2 cells showed prominent punctate accumulations, characteristic of focal adhesion engagement of paxilin.

Talin expression was markedly enhanced in both treatments. In contrast to controls, where talin was barely detectable, silenced cells displayed both diffuse cytoplasmic signal and distinct spot-like structures, consistent with recruitment to focal adhesion sites.

Vinculin was nearly absent in control cells but became detectable upon silencing. In siPLCB2 cells the signal was weak and diffusely cytoplasmic, whereas *PLCG2*-silenced cells showed strong vinculin accumulation with a filamentous pattern, membrane-associated reinforcements, and abundant focal adhesion-like structures.

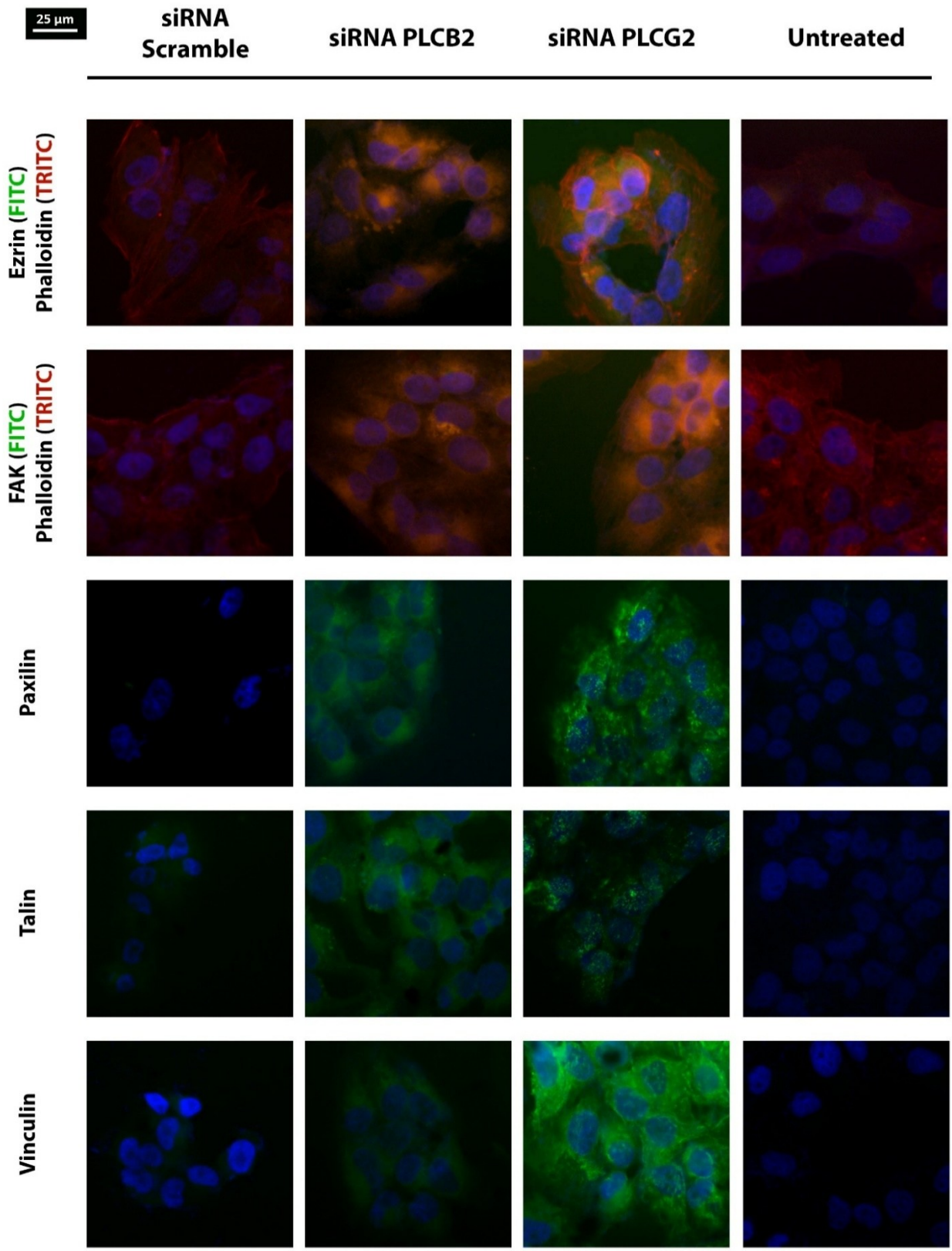

Figure 50. Cytoskeleton and FA complexes proteins analysis after PLCB2 and PLCG2 silencing.

Vimentin expression also increased following PLCs downregulations. In controls it appeared weak/ nearly absent (untreated control) or modestly filamentous (scramble), while siPLCB2 cells showed diffuse, non-filamentous cytoplasmic staining.

In contrast, siPLCG2 cells exhibited a markedly more intense and filamentous vimentin network, consistent with cytoskeletal modulation associated with an increased pro-migratory or EMT-like phenotypes.

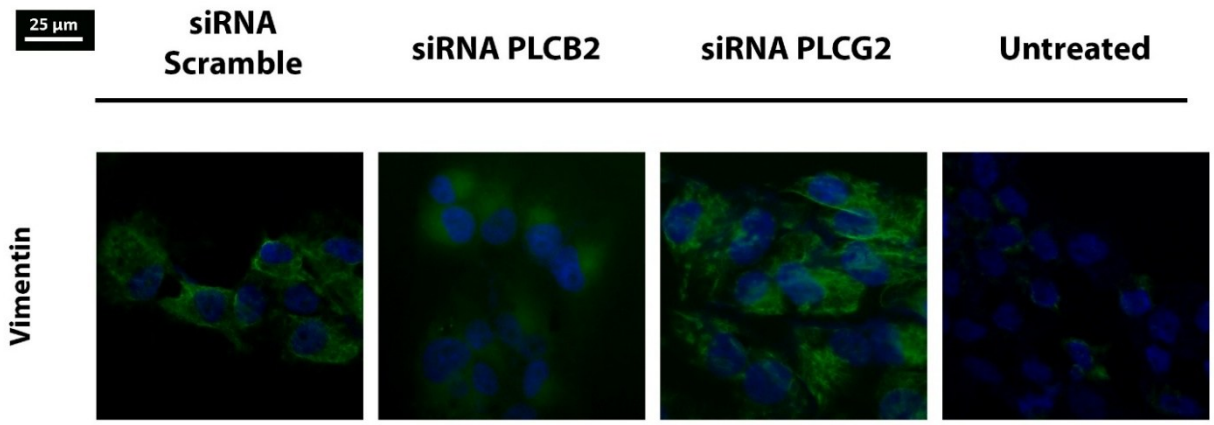

Figure 51. Vimentin protein after PLCB2 and PLCG2 silencing.

Collectively, these data reveal that PLCB2 and PLCG2 depletion induces substantial remodeling of both the actin cytoskeleton and focal adhesion complexes, with PLCG2 knockdown producing the most pronounced acquisition of focal adhesion structures and cytoskeletal reorganization.

Given the pronounced alterations in focal adhesion architecture and cytoskeletal organization observed upon *PLCB2* and *PLCG2* silencing, we next investigated downstream mechanotransduction pathways known to translate adhesion- and tension-dependent cues into transcriptional responses. As a first step, we focused on the Hippo pathway effector YAP, a central mechanosensor whose subcellular localization and activation state reflect changes in cell adhesion, cytoskeletal tension, and extracellular mechanical cues.

3.2.14 *PLCB2 – PLCG2* silencing: effect on mechanotransduction and YAP pathway.

To determine whether the alteration of focal adhesion architecture observed after *PLCB2* and *PLCG2* silencing propagated to downstream mechanotransduction pathways, we examined the Hippo effectors YAP and TAZ at protein and transcript levels. **Immunofluorescence** (**figure 54 a**) revealed that YAP abundance was consistently higher in both knockdowns compared with the scramble control. The effect was particularly pronounced in *PLCG2*-silenced cells, which displayed a strong YAP signal with a predominantly nuclear localization. Notably, YAP in the siPLCG2 condition also exhibited a distinctive punctate distribution throughout the cytoplasm and nucleus, suggesting extensive reorganization of mechanosensory complexes. **Western blot** analysis (**figure 54 b**) confirmed that total YAP was detectable across all samples; however, the phosphorylated (inactive) form YAP-Ser127 was reduced in both siPLCB2 and siPLCG2 conditions, indicating a shift toward the active state of the protein.

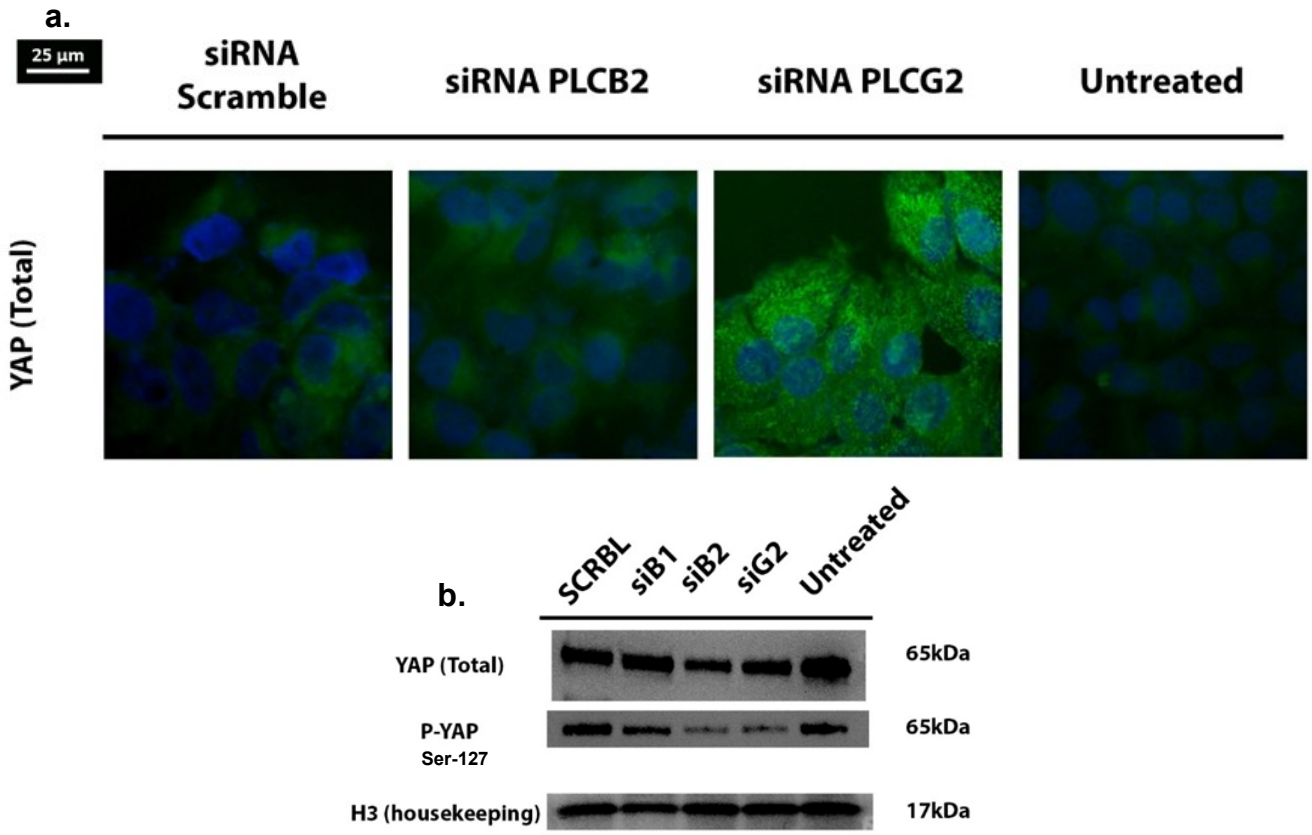

Figure 52. Yap abundance and localization by immunofluorescence (fig a) analysis and western blotting analysis (fig. b).

Consistent with these findings, qPCR analysis (**figure 55**) showed transcriptional activation of the YAP/TAZ pathway. Following *PLCB2* silencing, *TAZ* expression was already upregulated at 48 h (FC 3.57±0.79), accompanied by the expected compensatory increase in *PLCG2* (FC 4.46±0.60). At 72 h, *TAZ* expression further

increased (FC 6.22±1.02), together with strong induction of the canonical YAP/TAZ target *CTGF* (FC 3.11±0.86) and a more modest upregulation of *CYR61* (FC 1.78±0.95). *PLCG2* silencing also produced transcriptional changes in this pathway. At 48 h, *TAZ* and *CTGF* were modestly upregulated (FC 1.78±0.81), whereas at 72 h only *TAZ* remained slightly increased (FC 1.83±0.08), with downstream YAP/TAZ target genes returning to reduced expression levels (*CTGF* FC: 0.57±0.03, *CYR61* FC: 0.45±0.05).

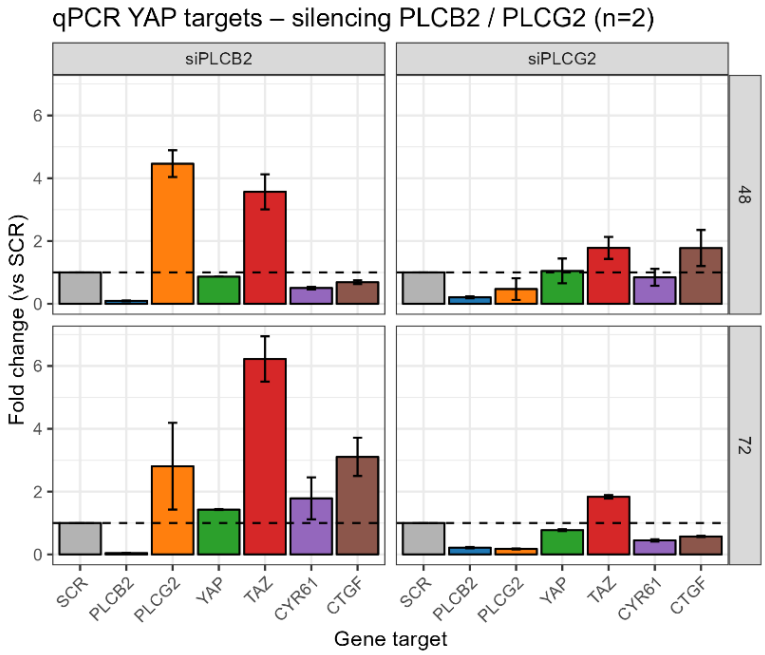

Figure 53. YAP/ TAZ and their downstream related genes relative expression (FC)

Together, these results indicate that depletion of *PLCB2* or *PLCG2* enhances YAP activation through reduced inhibitory phosphorylation and increased nuclear accumulation, with downstream transcriptional outputs being more pronounced and sustained in *PLCB2*-silenced cells.

3.2.15 Western blot analysis of cytoskeletal, mechanotransduction, and invasion-associated pathways.

To better define how *PLCB1*, *PLCB2*, and *PLCG2* depletion alters mechanotransduction and cytoskeletal signaling programs in 143B osteosarcoma cells, we performed a broad Western blot analysis covering major regulators of cytoskeletal architecture, adhesion, invasion, and downstream transduction pathways.

Cytoskeletal and invasion-related proteins. ROCK2 was barely detectable in the scramble control and in the siPLCB2 and siPLCG2 samples, while it appeared clearly upregulated upon *PLCB1* silencing. MMP2 expression was enhanced in siPLCG2 and siPLCB1 compared to the control. Vimentin abundance remained unchanged across all the treatments compared to the control, indicating that certain PLC depletion does not alter the mesenchymal baseline state of 143B cells at the level of this intermediate filament marker. β-tubulin levels showed a modest increase in siPLCB1, siPLCB2 and siPLCG2, possibly reflecting microtubule rearrangements. SPARC was nearly undetectable in scramble, siPLCB2, and siPLCG2, whereas *PLCB1* silencing resulted in a clear increase in SPARC protein levels.

Akt pathway. Total AKT levels were comparable across all samples; however, phosphorylation at Ser473 was higher in the scramble control and markedly reduced in all three treatments, and this may a broad suppression of AKT activation downstream of PLC depletion. Total S6RP remained unchanged, while phospho-S6RP (Ser235/236) was strongly reduced specifically in siPLCB1 (reduction of phospho-S6RP (Ser235/236) may indicate a downregulation of mTORC1-dependent translation). Phospho-4EBP1 (Thr37/46) was undetectable in the scramble control but clearly present in all knockdowns, with siPLCG2 showing the weakest bands (this may indicate a compensatory activation of translation-related pathways for all silenced cells).

Cadherins. E-cadherin was absent in scramble, siPLCB2, and siPLCG2, as expected for high-grade osteosarcoma cells, but became faintly detectable in siPLCB1. Conversely, N-cadherin was present in the scramble control and weakly expressed in siPLCB2 and siPLCG2, but completely absent upon *PLCB1* knockdown.

MAPK pathway. Total ERK was detectable with the characteristic double band in all samples, with siPLCB2 and siPLCG2 showing higher abundance than the scramble control. Phosphorylated ERK, however, was only faintly detectable in all conditions.

Nuclear envelope proteins. Lamin B1 was detectable in the scramble control, slightly reduced in siPLCB1, and nearly absent in siPLCB2 and siPLCG2. Lamin A/C displayed the expected doublet in all conditions. siPLCG2 was comparable to the untreated and siPLCB1 samples, whereas siPLCB2 showed a loss of the higher-molecular-weight Lamin A band while preserving the lower band Lamin C, suggesting altered nuclear mechanics selectively induced by *PLCB2* depletion.

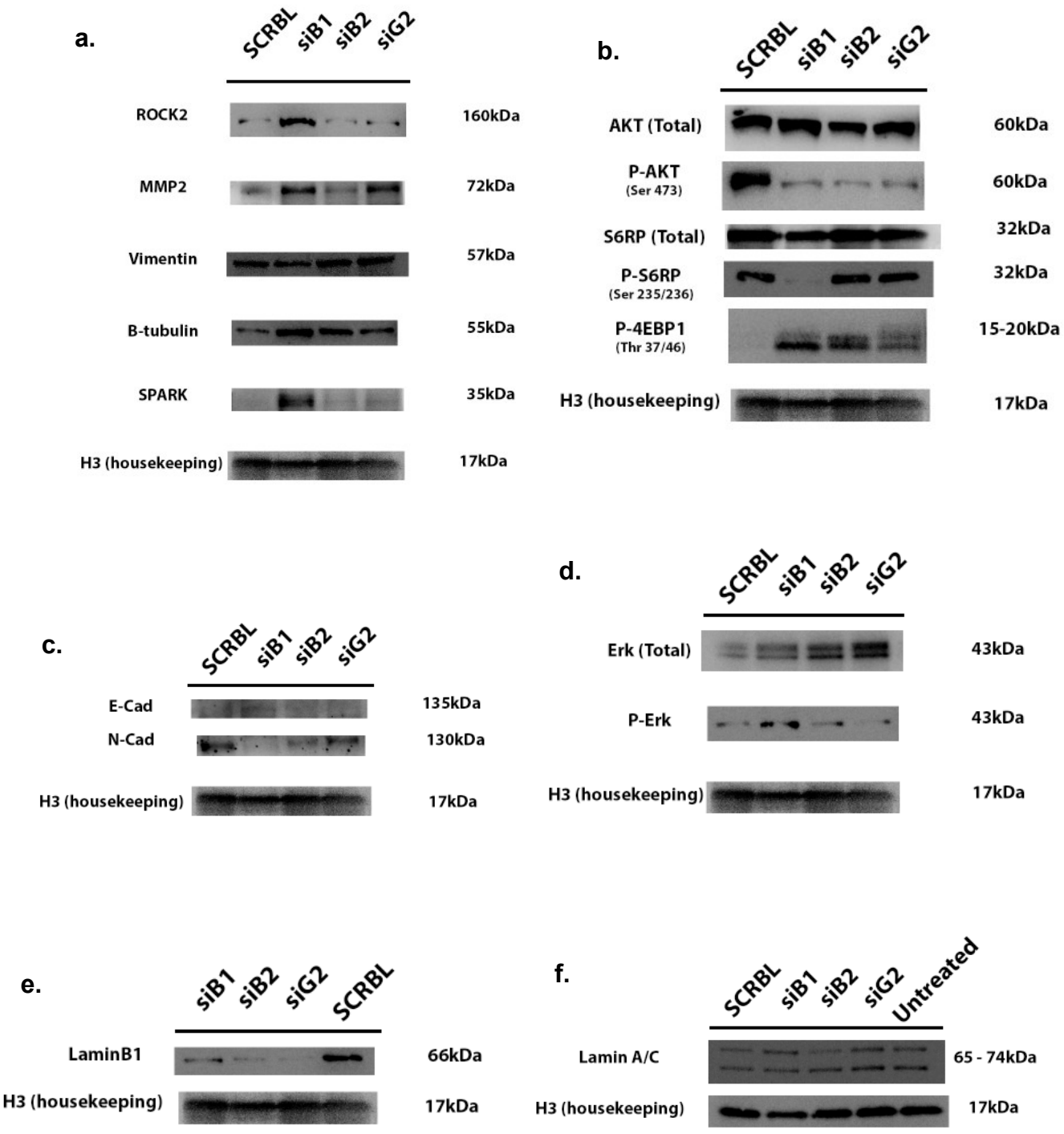

Figure 54. Western blot analysis of cytoskeletal, mechanotransduction, proliferation and invasion associated pathways. Fig a: cytoskeleton, cytoskeleton tension, invasion; fig b I: AKT pathway; fig c: cadherins; fig d: ERK total/active; fig e and f: Lamins.

3.2.16 Boyden Chamber Invasion Assay.

To directly assess the invasive capacity of 143B osteosarcoma cells following PLC silencing, we performed a Matrigel-coated Boyden chamber invasion assay (n = 3). After 24 h, invading cells were stained, lysed, and quantified by absorbance measurement; invasion was expressed as a ratio over the scramble control.

PLCG2 silencing produced the strongest pro-invasive phenotype (**figure 57 b**, **figure 57 a**), with a 53.4% increase in membrane traversal relative to the scramble control. *PLCB2* silencing also enhanced invasion (+38.1%), closely matching the non-treated condition (+37.4%). All three treatments, siPLCG2, siPLCB2, and the untreated control, showed statistically significant increases in invasion when compared to the scramble control, whereas no significant differences emerged among these three conditions themselves. Notably, siPLCG2 outperformed even the non-treated cells, indicating that *PLCG2* loss confers a measurable gain-of-function phenotype in terms of invasive capacity, consistent with the EMT- and adhesion-related alterations observed in the molecular analyses.

a.

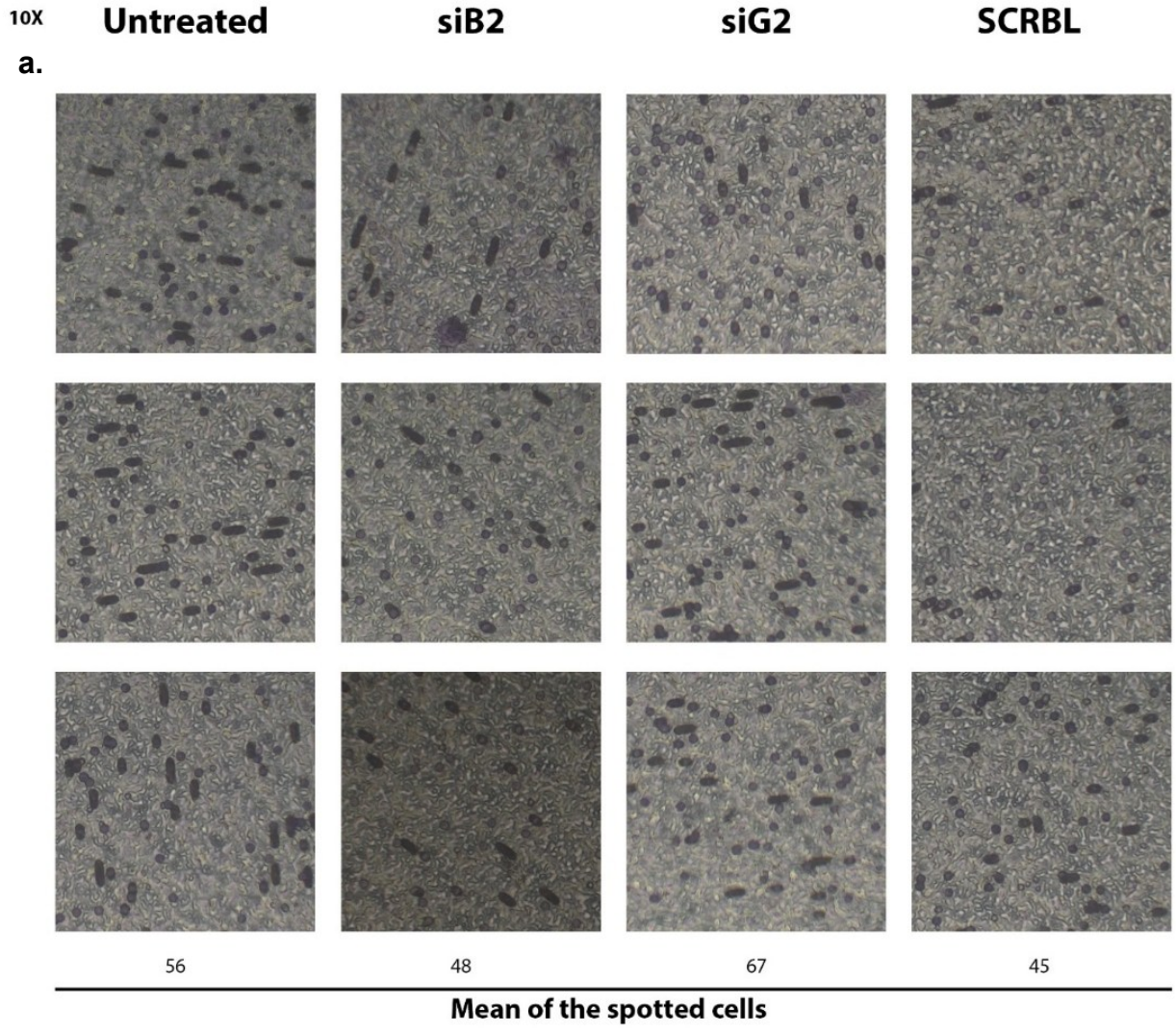

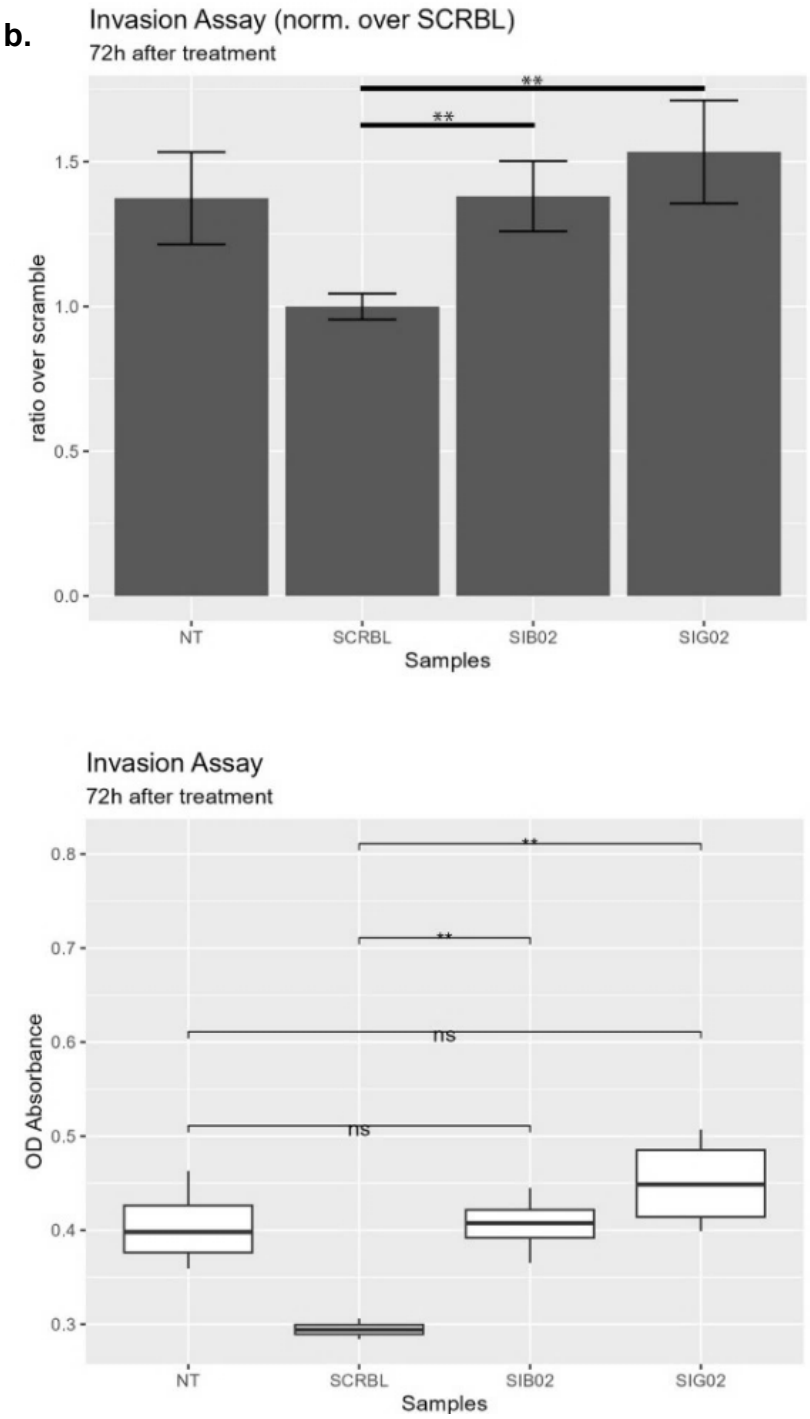

Figure 55. Invasion assay in transwell coated with Matrigel®. Fig a stained spotted cells for each condition. Fig b statistical analysis normalized over scramble control.

3.2.17 Bioinformatic analyses of patient-derived osteosarcoma datasets.

To complement and contextualize our experimental findings, we performed a series of bioinformatic analyses across multiple publicly available osteosarcoma datasets. These analyses independently corroborate several of the molecular and phenotypic trends observed in our *in-vitro* models.

Across three transcriptomic datasets (GSE36001, GSE87624, GSE16088) (**figure a**), *PLCB2* and *PLCG2* expression was consistently reduced in osteosarcoma patient samples and in commonly used osteosarcoma cell lines when compared to healthy bone tissue. This recurrent downregulation across independent cohorts supports the hypothesis that both isozymes are broadly suppressed in the osteosarcoma transcriptional landscape.

Survival analyses using the GDC TARGET-OS cohort further revealed that patients stratified by *PLCG2* expression (Q1 vs. Q4) show a statistically significant difference in overall survival (p = 0.03, Kaplan–Meier). Although the cohort size remains a limitation, a well-known issue for osteosarcoma datasets, the trend suggests that *PLCG2* levels may hold prognostic relevance.

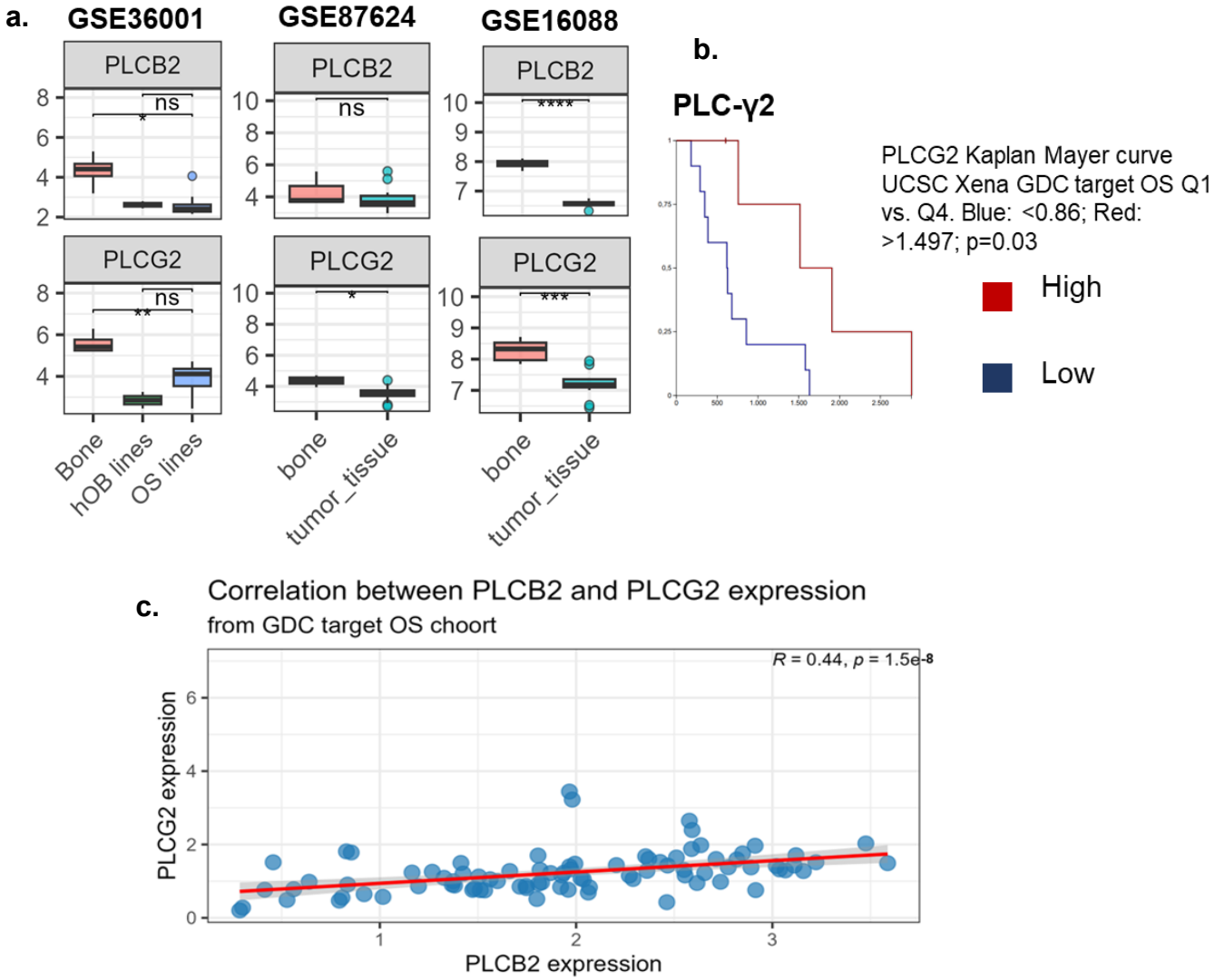

Figure 56. In-silico analyses of publicly available OS dataset. Fig a: Expression of specific isoforms in patient's dataset. Fig b: Kaplan Mayer curves (quartiles) for differential PLCG2 expression. Fig c: correlation between PLCB2 and PLCG2 expression in GDC target OS dataset.

Finally, within the same dataset, a Pearson correlation analysis demonstrated a moderate but highly significant positive association between *PLCB2* and *PLCG2* transcript levels ($R = 0.44$, $p = 1.5\times10^{-8}$), indicating that the two genes tend to co-vary in patient tumors. This observation is in line with our experimental results, where functional perturbation of one isoform often influenced the expression or activity of the other.

3.2.18 Preliminary assessment of the *in-vitro* osteosarcoma microenvironment and its role in inflammation.

Given the central role of inflammatory cues in shaping the osteosarcoma microenvironment, we quantified the secretion of IL-6, IL-8, and CXCL1 in conditioned media following PLC isozyme silencing (*PLCB1*, *PLCB2*, *PLCG1*, *PLCG2*), or pharmacological PLC inhibition with U73122 and its inactive analogue (double treatment). The ELISA assay included a kit-provided negative control and a highly enriched positive control consisting of media collected from 143B cells at the first post-thawing change, a condition known to trigger strong cytokine release.

Across all samples, **IL-6** (**figure 59 a**) secretion was low, consistent with the limited ability of 143B cells to produce this cytokine under standard culture conditions. IL-6 was clearly detectable in the positive control and in untreated cells at 48 h, but remained close to background in all remaining treatments (< 50 pg/mL), including all siRNA conditions and both U73122 concentrations.

In contrast, **IL-8** (**figure 59 b**) was abundantly secreted, reaching concentrations near the assay's upper detection limit (~3000 pg/mL) in most conditions, closely matching the positive control. PLCB2 silencing resulted in a significant reduction of IL-8 secretion (~2000 pg/mL). A similar reduction emerged upon treatment with the PLC inhibitor U73122: ~2500 pg/mL at 10 µM, and <1000 pg/mL at 15 µM, it seems that may be a dose-dependent suppression of IL-8 release. The silencing of PLCG1 or PLCG2 did not markedly alter IL-8 secretion, which remained comparable to the scramble control.

CXCL1 (**figure 59 c**) release displayed a peculiar profile, with high levels detectable in the positive control and in untreated cells at 48 h (~1000 pg/mL). At 72 h, both untreated (~625 pg/mL) and scramble (~400 pg/mL) samples exhibited a physiological decline in CXCL1, likely reflecting the combined effects of medium renewal and the natural temporal dynamics of chemokine release.

This is an interesting contrast to the more sustained IL-8 release. Among siRNA treatments, PLCG2 silencing produced a clear reduction of CXCL1 at 72 h (approaching ~250 pg/mL). Strikingly, both U73122 and U73343 treatments reduced CXCL1 to similarly low levels (<250 pg/mL) at 72 h, indicating a suppression independent of inhibitor specificity.

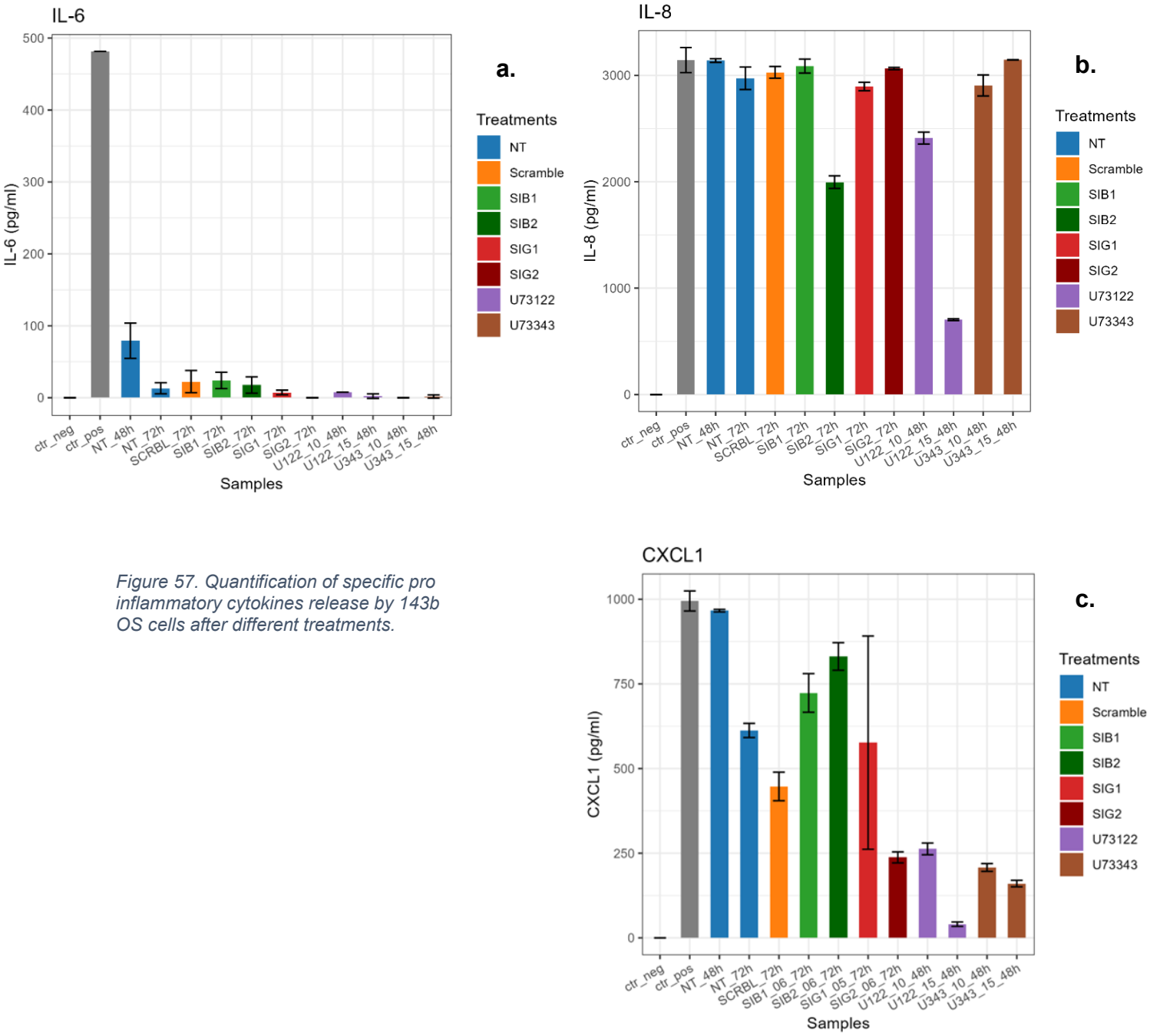

Figure 57. Quantification of specific pro inflammatory cytokines release by 143b OS cells after different treatments.

4.0 Discussion.

In this study, we investigated the functional role of specific PLC isoforms in OS cells using both inhibition and isoform-specific silencing approaches. PLC signaling is canonically associated with mitogenic and survival pathways in several tumor types, as extensively described in chapter 1.11.

4.1 Treatments with U73122 and U73343 and their biological effect on 143b cells.

Our results accord to literature data indicating that U73122 exposure induced a dose-dependent modulation of proliferation and stress-response pathways rather than a clear induction of apoptotic program [301]. With both 10 μM and 15μM U73122 treatments, cells largely retained a proliferative phenotype, as evidenced by increased Ki67 expression. In these conditions we observed also a concomitant increase and nuclear localization of p53 and p21 suggesting an activation of a stress-sensing response that remains compatible with a partial cell-cycle progression. And this increase in p21 and p53 signals reflects the increase of U73122 concentration. We hypothesize that the perturbation of PLC signaling, which is sufficient to activate adaptive responses, slow down the cell cycle (as shown from the growth curves data and from both p21 and p53 signals) but insufficient to impose a complete cell-cycle arrest and apoptosis (Ki67 stays high and the cleaved caspase 3 is barely detectable). In contrast, treatments with U73122 at 10 μM and 15μM resulted in a clear shift toward growth restraint phenotype. Reduced Ki67 expression, induction of p21, and the appearance of cleaved Caspase-3 indicate engagement of cell-cycle inhibitory mechanisms accompanied by at least a partial activation of apoptotic pathways. Together, these observations suggest that the analogue concentration amount primarily enforces a checkpoint-mediated growth arrest rather than triggering full apoptotic execution. Despite its widespread use as a negative control, U73343 also induced several off-target effects. A pronounced and dysregulated activation of both proliferative and apoptotic markers was observed. The simultaneous increase in Ki67, p21, and cleaved Caspase-3, along with marked morphological alterations, indicates a state of cellular stress rather than a coordinated cell-cycle response. These findings strongly argue against considering U73343 biologically inert in osteosarcoma cells and underscore the need for caution when interpreting data obtained using this analogue as a control. Like U73122, U73343 exhibits multiple off-target effects, which are far

less predictable. These effects induce stress in OS cells and broadly perturb cellular homeostasis, potentially confounding conclusions drawn from comparative pharmacological studies.

The analysis of **osteogenic differentiation markers** indicates that pharmacological perturbation of PLC signaling does not substantially interfere with the osteoblast-like identity of 143B osteosarcoma cells, at least when OS cells are not induced into differentiation.143B cells express alkaline phosphatase, osteonectin, osteopontin, and osteocalcin, consistent with an almost mature-osteoblast-like phenotype. The preservation of this molecular signature across all treatment conditions suggests that neither U73122 or the analogue U73343 are sufficient to reprogram lineage-associated differentiation states in this cellular context. RUNX2 was the only osteogenic marker displaying treatment-dependent variability. Its absence following double U73122 treatment at 10μM concentration may reflect transient suppression of osteogenic transcriptional activity under non-lethal stress conditions, rather than a stable loss of osteoblastic identity. Conversely, the complete cytoplasmic re-localization of RUNX2 observed after U73343 treatment at 15 μM further supports the fact that the analogue induces a broader perturbation of cellular homeostasis.

Consistent with this interpretation, the expression of major **cytoskeletal components** was largely preserved, although clear differences in spatial organization emerged. Actin levels were not altered by treatment, but its widespread cytoplasmic distribution suggests a loss of higher-order organization, particularly under PLC inhibition with U73122. Ezrin, a protein which mediate cytoskeleton membrane binding and it's involved into membrane tension, bleb formation and vesical trafficking [245], showed a modest increase following U73122 treatment at 15 μM concentration. This increase was accompanied by diffuse cytoplasmic localization and limited membrane reinforcement, pointing to altered membrane–cytoskeleton coupling. Beta-tubulin expression remained largely unaffected across conditions, indicating that microtubule abundance is not a primary target of PLC perturbation in 143B cells. Similarly, E-cadherin was weakly expressed and diffusely localized in all conditions, consistent with the mesenchymal and poorly epithelialized nature of this cell line [161]. In contrast, vimentin emerged as the cytoskeletal component most sensitive to PLC modulation. U73122 treatment induced a marked reduction in vimentin expression and a re-localization of the protein toward the cell periphery, suggesting an alteration of intermediate filament organization [161]. Given the established role of vimentin in

maintaining mesenchymal architecture, mechanical resilience, and migratory behavior, this redistribution is consistent with the broader effects of PLC inhibition on cytoskeletal dynamics and mechanotransduction. Notably, U73343 treatment produced intense but homogeneously distributed vimentin staining, again supporting the interpretation that the analogue induces a metabolically hyperactive yet poorly organized cellular state. Finally, the analysis of **membrane-associated and structural markers** further supports a model in which PLC inhibition affects cellular organization rather than identity. CD34 was upregulated following both U73122 and U73343 treatments and displayed both membrane localization and vesicular accumulation, potentially reflecting altered membrane trafficking or stress-associated remodeling. In contrast, CD99 and CAV-1 remained unchanged across conditions, indicating that not all membrane or adhesion-associated components are equally sensitive to PLC perturbation.

Taken together, these findings suggest that PLC inhibition does not alter the osteoblastic differentiation status of 143B cells but selectively impacts cytoskeletal architecture, membrane organization, and spatial distribution of key structural proteins. These effects likely represent early changes that prime cells for altered mechanosensing, adhesion, and migratory behavior, rather than terminal differentiation or identity shifts. This interpretation provides a coherent framework for the subsequent observations obtained for a more specific PLC downregulation by using siRNAs. The use of isoform-specific silencing allowed us to dissect whether modulation of individual PLC isoforms could more precisely account for the widespread and sometimes difficult-to-interpret cytoskeletal reorganization and EMT-related alterations observed after treatment with the broad PLC inhibitor U73122.

4.2 Specific isoforms downregulation.

Although inhibition with U73122 clearly indicated that PLC activity affects cell-cycle regulation, cytoskeletal organization, and migratory behavior in 143B cells, these effects could not be unequivocally attributed to a specific PLC isoform. U73122 is a broad inhibitor with well-documented off-target effects, as further supported by the heterogeneous transcriptional responses observed following treatment, particularly at the higher dosage. Together, these observations suggest that PLC signaling plays a role in regulating proliferation and cell dynamics in osteosarcoma cells, while also highlighting the need for a more refined, isoform-specific approach.

Based on literature evidence implicating PLCβ2 and PLCγ2 isoforms in mechanotransduction, adhesion, and migration [4, 7, 8], we therefore adopted targeted gene silencing strategies. This approach allowed us to dissect the contributions of individual PLC isoforms while avoiding the confounding effects inherent to pharmacological inhibition. Functional assays following isoform-specific knockdown revealed coherent but distinct phenotypes, assessed through cell growth measurements (confluency) and migratory and proliferative capacity assays (wound healing assay). *PLCB1* downregulation exerted modest effects on migration, whereas *PLCB2* and *PLCG2* silencing had a stronger impact on migratory capacities, with *PLCG2* silencing also modestly affecting cell proliferation.

To gain a comprehensive view of the molecular programs underlying these phenotypes, we subsequently performed transcriptome-wide gene expression profiling by RNA sequencing following *PLCB1*, *PLCB2*, and *PLCG2* silencing. Importantly, this analysis was hypothesis-driven rather than exploratory, aiming to validate and contextualize the phenotypic observations from the functional assays and to confirm some findings reported in the literature. The clear segregation between silenced and scramble populations, together with the enrichment of gene sets related to cell-cycle control and mechanotransduction, EMT, and metabolic stress, provided strong molecular support for the experimental data.

4.2.1 PLCβ1.

Based on the enrichment analysis results, we found that *PLCB1* downregulation not only dampens proliferative and cell-cycle–dependent programs but also activates stress-response, metabolic, and inflammatory pathways, consistent with broader cellular reprogramming following *PLCB1* silencing. We initially hypothesized that PLC-dependent PIP2/DAG signaling contributes to maintaining a basal signaling tone that buffers cytoskeletal tension and stabilizes adhesion dynamics. Disruption of this balance, through either pharmacological inhibition or isoform-specific silencing, may lead to loss of this buffering function and trigger compensatory stress-response pathways that promote cytoskeletal remodeling and mechanotransductive adaptation. From the gene expression enrichment analysis we observe that E2F target genes were downregulated in silenced cells, a finding that was corroborated by immunofluorescence assays (cell cycle and apoptosis markers), which produced results largely consistent with the enrichment analysis. Signals for the apoptosis marker cleaved Caspase-3 and the pro-proliferative marker Ki67 were comparable

between silenced and control conditions, while p21 showed a modest increase along with p53. These data suggest that *PLCB1* silencing induces a mild activation of cell-cycle stress pathways, reflected by increased p21 and p53, without significantly impairing proliferation or triggering apoptosis in 143B cells. Therefore, *PLCB1* silencing did not induce overt cytotoxicity or apoptosis in 143B osteosarcoma cells, but instead triggered profound phenotypic and signaling reprogramming, consistent with a stress-adaptive and mechanically altered cellular state, accompanied by only a modest slowdown of the cell cycle (almost undetectable from proliferation curve data). Western Blot analyses indicated that ROCK2 was strongly upregulated following *PLCB1* silencing. Given the central role of ROCK2 in actin–myosin contractility [157], this finding suggests an increase in intracellular tension and contractile forces, consistent with a shift toward a more mechanically active phenotype. This observation aligns with the concomitant increase in β-tubulin, indicating cytoskeletal reorganization rather than simple structural stabilization. Together, these changes point to a remodeling of the actin–microtubule network that may support altered cell shape dynamics and force transmission. In parallel, MMP2 upregulation and increased SPARC expression strongly suggest activation of ECM remodeling programs [165]. Both molecules are well-established mediators of invasion, matrix degradation, and tumor–stroma interaction, supporting the interpretation that *PLCB1* silencing promotes a phenotype permissive to invasion rather than uncontrolled proliferation.

Despite these pro-invasive adaptive features, *PLCB1* downregulation was associated with a marked suppression of canonical survival and growth signaling. Phosphorylated AKT (Ser473) was strongly reduced, indicating attenuation of PI3K/AKT-mediated survival pathways. Downstream of AKT, p-S6RP levels were markedly decreased, pointing to a substantial inhibition of mTOR-dependent protein synthesis. Interestingly, phosphorylated 4EBP1 became detectable, suggesting a compensatory rewiring of translational control mechanisms, potentially favoring selective translation under stress conditions [54].

PLCB1 silencing displayed ERK levels comparable to scramble, with only a minimal trend toward increased pERK, which is comparable with the absence of evidences of an increased cell growth rate after *PLCB1* downregulation.

Importantly, *PLCB1* silencing did not activate apoptotic pathways, as evidenced by the absence of cleaved Caspase-3 induction. Instead, the observed increase in p21 (*CDKN1A*) and p53 (*TP53*) at both transcriptional and protein levels the transcriptional

level supports activation of stress-responsive cell-cycle checkpoint mechanisms, potentially slowing cell-cycle progression without triggering cell death. This interpretation is consistent with growth curve analysis, which showed no statistically significant differences, and with the modest impairment observed in wound-healing assays, where migration was delayed but not abolished. These data indicate that PLCβ1 does not function as a primary regulator of proliferation or survival in 143B osteosarcoma cells, but rather as an upstream modulator of multiple signaling pathways, including cytoskeletal tension and ECM interactions. Reduced *PLCB1* expression induces a mechanically and transcriptionally reprogrammed state characterized by increased contractility and enhanced stress adaptation. The partial reduction of N-cadherin together with a slight reappearance of E-cadherin argues against a complete mesenchymal transition. This phenotype suggests that *PLCB1* downregulation may contribute to the development of a cellular state more prone to matrix remodeling and adaptation to the stresses typical of the tumor microenvironment and this is still highly relevant in OS since cells migration and invasion is one of the main causes of the low life expectancy at the moment of the diagnosis [2].

4.2.2 PLCβ2 and PLCγ2.

In the transcriptional profile of *PLCB2*-silenced cells, the most prominent signature identified by enrichment analysis was epithelial–mesenchymal transition (EMT), followed by coagulation, both of which are typically associated with extracellular matrix remodeling, enhanced migratory competence, and increased crosstalk with the surrounding microenvironment. The coordinated enrichment of these pathways suggests that PLCB2 loss shifts 143B cells toward a pro-remodeling, motility-permissive state, rather than merely altering the expression of isolated genes. Notably, these transcriptomic findings provide independent support for early hypotheses proposed in the literature regarding the involvement of PLCB2 in migration and mechanotransduction [254], which had remained largely unexplored in subsequent years. Conversely, multiple pathways were preferentially enriched in the scramble control, including E2F targets, MYC targets_v1, oxidative phosphorylation, and unfolded protein response, indicating that control cells retain a stronger proliferative and translational program. These data suggest that *PLCB2* silencing pushes cells away from a predominantly “proliferative–metabolic” program toward a more “adaptive and migratory” transcriptional configuration. Importantly, this should not be interpreted

as an obligatory reduction in proliferation at the phenotypic level. The mild downregulation of proliferation- and metabolism-related pathways can be seen as a trade-off, where cells prioritize remodeling and motility programs, slightly reducing their proliferation capacity.

Transcriptomic profiling of *PLCG2*-silenced cells revealed a similarly profound reshaping of the transcriptional landscape. The strongest enrichment was observed for Hypoxia, Complement, and Coagulation gene sets, indicating a shift toward stress-related, inflammatory, and pro-remodeling programs. Notably, and in close analogy with *PLCB2* downregulation, the EMT gene set was also markedly enriched, reinforcing the notion that perturbation of PLC-dependent signaling promotes mesenchymal features in osteosarcoma cells. Beyond EMT, *PLCG2* silencing induced a broader adaptive transcriptional response, suggesting that loss of PLCγ2 favors metabolic reprogramming and activation of stress- and inflammation-associated signaling networks, consistent with a cellular state oriented toward survival and matrix remodeling rather than proliferation.

Based on these findings, we next examined if *PLCB2* and *PLCG2* reduced expression translated into convergent phenotypic effects on cell-cycle and cell proliferation. Consistent with the transcriptomic enrichment of EMT- and stress-related pathways following PLCB2 and PLCG2 silencing, protein-level analyses confirmed that proliferative markers were largely preserved, supporting a functional shift toward adhesion and mechanotransduction programs rather than a major alteration in cell-cycle control. Ki-67 localization and abundance remained comparable to scramble controls, p21 expression was barely detectable for all the conditions, and p53 levels were largely unchanged, indicating that downregulation of either isozyme does not induce any kind of cell-cycle arrest. These observations suggest that the primary biological consequence of PLCβ2 and PLCγ2 loss is not a direct modulation of proliferative programs. Functional assays revealed a consistent and coherent phenotype too. Growth curve analyses showed that both *PLCB2*- and *PLCG2*-silenced cells proliferated significantly faster than scramble controls, counteracting the mild cytotoxic effect associated with the transfection procedure. Importantly, the growth rates of silenced cells closely matched those of untreated cells, indicating restoration of basal proliferative capacity rather than a hyperproliferative state. A similar pattern emerged in wound-healing assays, where *PLCB2*- and *PLCG2*-depleted cells closed the scratch significantly faster than scramble controls, reaching migration rates

comparable to untreated cells. This observation was confirmed by Matrigel®-based Boyden chamber assays, which demonstrated a clear increase in invasive capacity of silenced cells (in particular for *PLCG2* silenced cells). *PLCB2* silencing restored invasion to levels comparable with untreated cells, whereas *PLCG2* downregulation produced a more pronounced effect, outperforming even the invasive capacity of non-treated cells for this specific assay. Notably, all three conditions, siPLCB2, siPLCG2, and untreated, were significantly more invasive than scramble controls, once again highlighting that this specific PLC silencing targeting primarily acts upon migration and invasion rather than actively driving proliferation. Taken together, these data indicate that PLCβ2 and PLCγ2 act as modulators of migratory–invasive competence in 143B osteosarcoma cells. While *PLCB2* silencing mainly restores basal motility and invasion suppressed by experimental stress, *PLCG2* loss confers a measurable gain-of-function invasive phenotype. This functional divergence is fully consistent with the transcriptional activation of EMT and adhesion-related pathways and anticipates the extensive cytoskeletal and focal adhesion remodeling observed at the molecular and at the protein level.

Beyond their effects on migration and invasion, silencing of *PLCB2* and *PLCG2* revealed profound alterations in cytoskeletal organization, nuclear architecture, and mechanotransduction pathways, highlighting the important role that these two isoforms have in regulating cellular mechanical homeostasis. PLCB2-silenced cells exhibited enhanced migration relative to scramble controls, they did not display the invasive drive observed upon *PLCB1* loss. Instead, the most alterations involved focal adhesion organization and nuclear integrity. *PLCB2* silencing was associated with a reduction in Lamin B1 protein levels and a concomitant decrease in Lamin A/C, suggesting impaired nuclear envelope stability and altered nuclear cytoskeletal signaling coupling. These changes are consistent with an altered transmission of mechanical cues from the actin cytoskeleton to the nucleus. In fact, actin and focal adhesion proteins intensity and distribution were quite different from the untreated conditions, resulting into an increase of actin abundance and disorganization. An increase in focal adhesion protein is observed; FAK, Paxillin, Talin, Vinculin were more expressed but poorly structural organized. In line with those observations, *PLCB2* reduced expression induced a modest activation and nuclear accumulation of protein YAP. Altered mechanical cues were reflected in transcriptional responses mediated by the Hippo–YAP axis, as indicated by upregulation of *YAP/TAZ* transcripts and downstream targets such as

CYR61 and *CTGF*. Together with the observed changes in nuclear lamina proteins, these findings support the existence of a PLCβ2-dependent mechanosensitive pathway regulating cytoskeletal tension, nuclear dynamics, and transcriptional plasticity.

In contrast, *PLCG2* silencing produced a more pronounced pro-invasive phenotype. *PLCG2*-depleted cells exhibited strong upregulation of mesenchymal markers, including N-cadherin and a highly filamentous vimentin network, together with increased MMP2 expression. Unlike *PLCB2* silencing, Lamin A/C levels remained largely preserved but expressed at low levels, which is typical of pro metastatic OS cells. Lamin B1 protein was reduced, suggesting selective remodeling of nuclear mechanics. In this context, the absence of major changes in lamin A/C expression following *PLCG2* silencing is not unexpected [302], as 143B cells already display a baseline lamin A/C–low state. Instead, our data reveal a selective reduction of lamin B1, suggesting that *PLCG2* downregulation further fine-tunes nuclear mechanics through modulation of the B-type lamina. Consistent with this phenotype, *PLCG2* silencing resulted in enhanced focal adhesion remodeling with an increase of FAK, Paxillin, Talin and Vinculin intensity with a more specific cellular distribution compatible with FA complexes formation. Actin reorganization is also observed; Actin was more expressed in silenced cells but with a peculiar collapsed and folded structure. After PLCG2 downregulation a robust nuclear localization of protein YAP was observed. Although downstream YAP target genes were less strongly induced than in *PLCB2*-silenced cells. The overall transcriptional and functional outputs converged on an invasion-prone state, as directly confirmed by the Boyden chamber assay. These findings indicate that *PLCG2* plays a more direct role in restraining invasive behavior, and its loss actively promotes EMT-associated cytoskeletal and adhesion remodeling. The MAPK/ERK axis showed only modest changes for both treatments. *PLCB2* and *PLCG2* silencing was associated with a slight increase in total ERK but a concomitant reduction in phosphorylated ERK, suggesting that ERK signaling is not robustly activated under these conditions.

Notably, all PLC silencing conditions shared a reduction in AKT activation, as evidenced by decreased pAKT levels. Given the central role of PLC enzymes in controlling PIP2 availability and PIP3-dependent signaling [241], these results point to a conserved and highly sensitive PLC–PIP–AKT axis. Despite this shared signaling attenuation, cells did not undergo apoptosis, indicating that reduced AKT signaling is

buffered by compensatory mechanisms. One such common adaptive response may involve translational control, as all silencing conditions exhibited stabilization of phosphorylated 4EBP1. This suggests a coordinated shift in protein synthesis regulation, potentially representing a generalized response to cytoskeletal stress and altered mechanotransduction. Together, these data support a model in which PLCβ2 and PLCγ2 differentially regulate mechanosensing pathways that integrate cytoskeletal dynamics, nuclear mechanics, and transcriptional responses, ultimately shaping the balance between cellular plasticity and invasive competence in osteosarcoma cells.

4.3 *In-silico* analysis of public datasets.

To place our experimental findings in a broader biological and clinical context, we interrogated publicly available osteosarcoma transcriptomic datasets. Across independent patient cohorts, PLCB2 and PLCG2 were consistently expressed at lower levels in osteosarcoma compared with healthy bone tissue. This observation supports the biological relevance of our *in-vitro* model, suggesting that reduced activity of these isozymes may represent a disease-associated feature rather than a cell line–specific artifact. Importantly, these *in-silico* data strengthen the potential clinical significance of our findings, as they indicate that the mechanotransductive and pro-invasive programs observed upon PLCB2 and PLCG2 depletion may reflect molecular dynamics occurring in osteosarcoma patients. This observation is particularly relevant looking at our experimental data, where partial suppression of *PLCB2* or *PLCG2* was sufficient to reshape adhesion, mechanotransduction, and invasive behavior without directly acting upon proliferation. Notably, PLCG2 expression also showed an association with patient survival, despite the limited cohort, supporting the idea that modulation of specific isoforms of PLC-IP3 signaling axis may have biological consequences *in-vivo*. The positive correlation between *PLCB2* and *PLCG2* expression further points to a coordinated regulation of some of these isozymes in osteosarcoma, consistent with the compensatory and interconnected responses observed following isoform-specific perturbation *in-vitro*. Taken together, these analyses do not establish causality but reinforce the translational relevance of our experimental model, indicating that alterations in PLC-dependent signaling and mechanosensitive programs identified in 143B cells may reflect vulnerabilities present in patient tumors.

4.4 Early evaluation of inflammatory modulation of tumor microenvironment (TME).

In line with the molecular and functional alterations observed following PLC isozyme perturbation, we next investigated whether PLC signaling also influences the inflammatory output of 143B osteosarcoma cells. Given the well-established role of immune components within the osteosarcoma tumor microenvironment—where inflammatory mediators contribute to immune modulation and tumor progression [8]—we performed a preliminary evaluation of cytokine secretion. Using ELISA assays, we quantified the release of selected pro-inflammatory cytokines commonly implicated in OS-driven modulation of the tumor microenvironment. This exploratory analysis aimed to determine whether PLC-dependent mechanotransductive remodeling is accompanied by changes in inflammatory signaling that could further impact tumor–immune interactions.IL-6 secretion remained low across most conditions, consistent with the limited ability of 143B cells to produce this cytokine under basal culture conditions, and suggesting that PLC signaling is not a dominant regulator of IL-6 in this context. In contrast, IL-8 and CXCL1 were more selectively modulated. IL-8 release was reduced following *PLCB2* silencing and pharmacological PLC inhibition, supporting a link between PLCβ2 activity and the maintenance of a pro-inflammatory, secretory profile. CXCL1 secretion was instead markedly decreased upon *PLCG2* silencing and after treatment with both U73122 and its inactive analogue Together, these findings suggest that PLCβ2 and PLCγ2 differentially contribute to inflammatory signaling in osteosarcoma and these data are consistent with the broader phenotypic changes observed in this study and support a role for PLC signaling may influence tumor cell behavior with microenvironmental remodeling.

4.5 Conclusions.

Our results indicate that phospholipase C signaling contributes to the regulation of osteosarcoma cell plasticity. By combining pharmacological inhibition, isozyme-specific silencing, transcriptomic profiling, and functional assays, we observed that distinct PLC isoforms differentially modulate mechanotransduction, cytoskeletal organization, and invasive behavior in 143B cells. In particular, PLCβ2 and PLCγ2 depletion was consistently associated with activation of EMT-like transcriptional programs, focal adhesion remodeling, YAP pathway engagement, and increased invasive capacity.

Based on these experimental observations, we hypothesize that specific PLC isoforms may function as modulators of adhesion-dependent mechanosensitive signaling networks, influencing the balance between proliferative control and migratory competence. The convergence between *in-vitro* findings and publicly available patient transcriptomic datasets further supports the potential biological relevance of these mechanisms in the osteosarcoma context.

Collectively, these data refine the concept that PLC signaling—particularly through selected isoforms—may regulate mechanical and transcriptional adaptation in osteosarcoma cells, contributing to tumor cell aggressiveness. In particular, from our experimental data it seems possible thar rather than acting as isolated or redundant signaling enzymes, PLCβ2 and PLCγ2 exploit their function as an interconnected signaling module in 143b cells. Perturbation of either isozyme influenced the expression, activity, and downstream effects of the other, indicating the existence of a coordinated PLC network regulating mechanotransduction, adhesion dynamics, and invasive behavior (at least for PLCβ2 and PLCγ2 isoforms). This functional interconnection has not been previously described in osteosarcoma and may represent an unrecognized regulatory layer contributing to tumor plasticity and invasiveness. Importantly, this association is further supported by in silico analyses of patient-derived transcriptomic datasets, which reveal coordinated downregulation patterns consistent with our experimental findings. The convergence between *in-vitro* and patient data strengthens the hypothesis that cross-isoform PLC regulation may play a clinically relevant role in shaping osteosarcoma aggressiveness. From a translational perspective, the differential impact of PLCβ2 and PLCγ2 depletion on invasive behavior, in the absence of major effects on proliferative control, raises the possibility that selective modulation of these isoforms could represent a strategy to interfere with osteosarcoma dissemination rather than tumor growth per se. In this context, PLCβ2 and PLCγ2 may serve not only as functional regulators of mechanoadaptation but also as potential biomarkers of invasive propensity or candidate therapeutic nodes within adhesion-dependent signaling networks.

In contrast to *PLCB2* and *PLCG2*, *PLCB1* silencing did not induce a coherent mechanotransduction alteration. Instead, downregulation of *PLCB1* resulted in increased cellular stress, cell-cycle deceleration, and profound cytoskeletal reorganization. Although matrix-remodeling factors such as MMP2 and SPARC were upregulated, this was accompanied by reduced N-cadherin and a slight recovery of E-

cadherin, suggesting a failure to fully engage a migratory mesenchymal phenotype [161]. Collectively, these features point to a role for PLCB1 as a regulator of cytoskeletal and proliferative homeostasis rather than a direct driver of invasion.

4.6 Future perspectives.

Further studies are required to dissect the mechanistic axis linking PLCβ2/PLCγ2 to focal-adhesion remodeling and nuclear mechanotransduction. Our data suggest that perturbation of these isozymes reshapes the focal adhesion complexes (FAK/paxillin/talin/vinculin), reorganizes actin architecture, and promotes nuclear YAP accumulation together with alterations in nuclear envelope components, particularly Lamin B1. These findings support a model in which PLC-dependent signaling modulates cytoskeletal tension and force transmission through two interconnected routes:

- the actin–LINC–lamin axis, potentially influencing nuclear integrity, mechanosensing, transcriptional output, and migratory competence;
- the Hippo/YAP pathway, acting as a central mediator of adhesion-dependent mechanotransduction.

A key open question concerns whether these effects primarily reflect catalytic PLC activity (PIP_2 hydrolysis, DAG/IP3/Ca^{2+} signaling, PKC and RhoA–ROCK engagement) or non-catalytic/scaffolding functions at focal adhesion sites, including potential competition for membrane PIP_2 binding. Clarifying this distinction will be essential for understanding the signaling hierarchy underlying PLC-dependent mechanoadaptation.

To strengthen the translational relevance of these findings, validation in more complex biological systems is desired. In particular, *in-vivo* studies using xenograft models will be necessary to determine whether PLCβ2/PLCγ2 modulation directly impacts tumor invasion, metastatic dissemination, and colonization of secondary sites. Such approaches would clarify whether the mechanoadaptive phenotype observed *in-vitro* translates into altered metastatic behavior. From a therapeutic perspective, rather than directly targeting PLC enzymes, future work may explore pharmacological modulation of downstream effectors, such as the YAP pathway or focal adhesion components, to selectively interfere with invasive behavior while preserving proliferative balance. This strategy may offer a complementary approach aimed at limiting dissemination rather than tumor growth per se.

Additional investigations should also address the interaction between PLC-dependent mechanotransduction and the tumor microenvironment. Given the complex immune and stromal landscape of osteosarcoma, it will be important to evaluate how PLCβ2/PLCγ2 modulation influences crosstalk with stromal cells, extracellular matrix components, and immune populations within the bone niche.

Finally, temporal dynamics of cytoskeletal and transcriptional remodeling should be explored through prolonged silencing or stable knockout models, to determine whether the observed phenotypes represent transient adaptations or stable reprogramming events. Parallel analyses correlating PLCβ2 and PLCγ2 expression levels with clinical outcomes in patient cohorts may further establish their potential role as biomarkers of invasive propensity and metastatic risk.

5.0 References.

[1] L. Mirabello, R.J. Troisi, S.A. Savage, International osteosarcoma incidence patterns in children and adolescents, middle ages and elderly persons, Int J Cancer 125(1) (2009) 229-34.
[2] D.S. Geller, R. Gorlick, Osteosarcoma: a review of diagnosis, management, and treatment strategies, Clin Adv Hematol Oncol 8(10) (2010) 705-18.
[3] A. Misaghi, A. Goldin, M. Awad, A.A. Kulidjian, Osteosarcoma: a comprehensive review, SICOT J 4 (2018) 12.
[4] Z.S. Kundu, Classification, imaging, biopsy and staging of osteosarcoma, Indian J Orthop 48(3) (2014) 238-46.
[5] G. Ottaviani, N. Jaffe, The epidemiology of osteosarcoma, Cancer Treat Res 152 (2009) 3-13.
[6] J. Gill, R. Gorlick, Advancing therapy for osteosarcoma, Nat Rev Clin Oncol 18(10) (2021) 609-624.
[7] S.M. Botter, D. Neri, B. Fuchs, Recent advances in osteosarcoma, Curr Opin Pharmacol 16 (2014) 15-23.
[8] L. Marchandet, M. Lallier, C. Charrier, M. Baud'huin, B. Ory, F. Lamoureux, Mechanisms of Resistance to Conventional Therapies for Osteosarcoma, Cancers (Basel) 13(4) (2021).
[9] W.F. Flintoff, H. Sadlish, R. Gorlick, R. Yang, F.M. Williams, Functional analysis of altered reduced folate carrier sequence changes identified in osteosarcomas, Biochim Biophys Acta 1690(2) (2004) 110-7.
[10] R. Gorlick, P. Anderson, I. Andrulis, C. Arndt, G.P. Beardsley, M. Bernstein, J. Bridge, N.K. Cheung, J.S. Dome, D. Ebb, T. Gardner, M. Gebhardt, H. Grier, M. Hansen, J. Healey, L. Helman, J. Hock, J. Houghton, P. Houghton, A. Huvos, C. Khanna, M. Kieran, E. Kleinerman, M. Ladanyi, C. Lau, D. Malkin, N. Marina, P. Meltzer, P. Meyers, D. Schofield, C. Schwartz, M.A. Smith, J. Toretsky, M. Tsokos, L. Wexler, J. Wigginton, S. Withrow, M. Schoenfeldt, B. Anderson, Biology of childhood osteogenic sarcoma and potential targets for therapeutic development: meeting summary, Clin Cancer Res 9(15) (2003) 5442-53.
[11] C.M. Gomes, H. van Paassen, S. Romeo, M.M. Welling, R.I. Feitsma, A.J. Abrunhosa, M.F. Botelho, P.C. Hogendoorn, E. Pauwels, A.M. Cleton-Jansen, Multidrug resistance mediated by ABC transporters in osteosarcoma cell lines: mRNA analysis and functional radiotracer studies, Nucl Med Biol 33(7) (2006) 831-40.
[12] M. D'Incalci, N. Badri, C.M. Galmarini, P. Allavena, Trabectedin, a drug acting on both cancer cells and the tumour microenvironment, Br J Cancer 111(4) (2014) 646-50.
[13] A.J. Chou, R. Gorlick, Chemotherapy resistance in osteosarcoma: current challenges and future directions, Expert Rev Anticancer Ther 6(7) (2006) 1075-85.
[14] T. Rajkumar, M. Yamuna, Multiple pathways are involved in drug resistance to doxorubicin in an osteosarcoma cell line, Anticancer Drugs 19(3) (2008) 257-65.
[15] A. Nguyen, C. Lasthaus, E. Guerin, L. Marcellin, E. Pencreach, M.P. Gaub, D. Guenot, N. Entz-Werle, Role of Topoisomerases in Pediatric High Grade Osteosarcomas: TOP2A Gene Is One of the Unique Molecular Biomarkers of Chemoresponse, Cancers (Basel) 5(2) (2013) 662-75.
[16] M. Fanelli, E. Tavanti, M.P. Patrizio, S. Vella, A. Fernandez-Ramos, F. Magagnoli, S. Luppi, C.M. Hattinger, M. Serra, Cisplatin Resistance in Osteosarcoma: In vitro Validation of Candidate DNA Repair-Related Therapeutic Targets and Drugs for Tailored Treatments, Front Oncol 10 (2020) 331.
[17] C.M. Hattinger, M.P. Patrizio, L. Fantoni, C. Casotti, C. Riganti, M. Serra, Drug Resistance in Osteosarcoma: Emerging Biomarkers, Therapeutic Targets and Treatment Strategies, Cancers (Basel) 13(12) (2021).
[18] M. Kovac, C. Blattmann, S. Ribi, J. Smida, N.S. Mueller, F. Engert, F. Castro-Giner, J. Weischenfeldt, M. Kovacova, A. Krieg, D. Andreou, P.U. Tunn, H.R. Durr, H. Rechl, K.D. Schaser, I. Melcher, S. Burdach, A. Kulozik, K. Specht, K. Heinimann, S. Fulda, S. Bielack, G. Jundt, I. Tomlinson, J.O. Korbel, M. Nathrath, D. Baumhoer, Exome sequencing of osteosarcoma reveals mutation signatures reminiscent of BRCA deficiency, Nat Commun 6 (2015) 8940.

[19] H.J. Park, J.S. Bae, K.M. Kim, Y.J. Moon, S.H. Park, S.H. Ha, U.K. Hussein, Z. Zhang, H.S. Park, B.H. Park, W.S. Moon, J.R. Kim, K.Y. Jang, The PARP inhibitor olaparib potentiates the effect of the DNA damaging agent doxorubicin in osteosarcoma, J Exp Clin Cancer Res 37(1) (2018) 107.
[20] J. Fellenberg, M.J. Dechant, V. Ewerbeck, H. Mau, Identification of drug-regulated genes in osteosarcoma cells, Int J Cancer 105(5) (2003) 636-43.
[21] Y. Suehara, D. Alex, A. Bowman, S. Middha, A. Zehir, D. Chakravarty, L. Wang, G. Jour, K. Nafa, T. Hayashi, A.A. Jungbluth, D. Frosina, E. Slotkin, N. Shukla, P. Meyers, J.H. Healey, M. Hameed, M. Ladanyi, Clinical Genomic Sequencing of Pediatric and Adult Osteosarcoma Reveals Distinct Molecular Subsets with Potentially Targetable Alterations, Clin Cancer Res 25(21) (2019) 6346-6356.
[22] S. Iwata, Y. Tatsumi, T. Yonemoto, A. Araki, M. Itami, H. Kamoda, T. Tsukanishi, Y. Hagiwara, H. Kinoshita, T. Ishii, H. Nagase, M. Ohira, CDK4 overexpression is a predictive biomarker for resistance to conventional chemotherapy in patients with osteosarcoma, Oncol Rep 46(1) (2021).
[23] Y. Zhou, J.K. Shen, Z. Yu, F.J. Hornicek, Q. Kan, Z. Duan, Expression and therapeutic implications of cyclin-dependent kinase 4 (CDK4) in osteosarcoma, Biochim Biophys Acta Mol Basis Dis 1864(5 Pt A) (2018) 1573-1582.
[24] T. Higuchi, N. Sugisawa, K. Miyake, H. Oshiro, N. Yamamoto, K. Hayashi, H. Kimura, S. Miwa, K. Igarashi, S.P. Chawla, M. Bouvet, S.R. Singh, H. Tsuchiya, R.M. Hoffman, Sorafenib and Palbociclib Combination Regresses a Cisplatinum-resistant Osteosarcoma in a PDOX Mouse Model, Anticancer Res 39(8) (2019) 4079-4084.
[25] W. Xu, Z. Li, X. Zhu, R. Xu, Y. Xu, miR-29 Family Inhibits Resistance to Methotrexate and Promotes Cell Apoptosis by Targeting COL3A1 and MCL1 in Osteosarcoma, Med Sci Monit 24 (2018) 8812-8821.
[26] E.C. Watson, L. Whitehead, R.H. Adams, G. Dewson, L. Coultas, Endothelial cell survival during angiogenesis requires the pro-survival protein MCL1, Cell Death Differ 23(8) (2016) 1371-9.
[27] B.S. Moriarity, G.M. Otto, E.P. Rahrmann, S.K. Rathe, N.K. Wolf, M.T. Weg, L.A. Manlove, R.S. LaRue, N.A. Temiz, S.D. Molyneux, K. Choi, K.J. Holly, A.L. Sarver, M.C. Scott, C.L. Forster, J.F. Modiano, C. Khanna, S.M. Hewitt, R. Khokha, Y. Yang, R. Gorlick, M.A. Dyer, D.A. Largaespada, A Sleeping Beauty forward genetic screen identifies new genes and pathways driving osteosarcoma development and metastasis, Nat Genet 47(6) (2015) 615-24.
[28] M. Kansara, M.W. Teng, M.J. Smyth, D.M. Thomas, Translational biology of osteosarcoma, Nat Rev Cancer 14(11) (2014) 722-35.
[29] Y.H. Lin, B.E. Jewell, J. Gingold, L. Lu, R. Zhao, L.L. Wang, D.F. Lee, Osteosarcoma: Molecular Pathogenesis and iPSC Modeling, Trends Mol Med 23(8) (2017) 737-755.
[30] X. Chen, A. Bahrami, A. Pappo, J. Easton, J. Dalton, E. Hedlund, D. Ellison, S. Shurtleff, G. Wu, L. Wei, M. Parker, M. Rusch, P. Nagahawatte, J. Wu, S. Mao, K. Boggs, H. Mulder, D. Yergeau, C. Lu, L. Ding, M. Edmonson, C. Qu, J. Wang, Y. Li, F. Navid, N.C. Daw, E.R. Mardis, R.K. Wilson, J.R. Downing, J. Zhang, M.A. Dyer, P. St. Jude Children's Research Hospital-Washington University Pediatric Cancer Genome, Recurrent somatic structural variations contribute to tumorigenesis in pediatric osteosarcoma, Cell Rep 7(1) (2014) 104-12.
[31] S. Lorenz, T. Baroy, J. Sun, T. Nome, D. Vodak, J.C. Bryne, A.M. Hakelien, L. Fernandez-Cuesta, B. Mohlendick, H. Rieder, K. Szuhai, O. Zaikova, T.C. Ahlquist, G.O. Thomassen, R.I. Skotheim, R.A. Lothe, P.S. Tarpey, P. Campbell, A. Flanagan, O. Myklebost, L.A. Meza-Zepeda, Unscrambling the genomic chaos of osteosarcoma reveals extensive transcript fusion, recurrent rearrangements and frequent novel TP53 aberrations, Oncotarget 7(5) (2016) 5273-88.
[32] M.P. Yavropoulou, J.G. Yovos, The role of the Wnt signaling pathway in osteoblast commitment and differentiation, Hormones (Athens) 6(4) (2007) 279-94.
[33] C.H. Lin, Y. Guo, S. Ghaffar, P. McQueen, J. Pourmorady, A. Christ, K. Rooney, T. Ji, R. Eskander, X. Zi, B.H. Hoang, Dkk-3, a secreted wnt antagonist, suppresses tumorigenic potential and pulmonary metastasis in osteosarcoma, Sarcoma 2013 (2013) 147541.
[34] M. Kansara, M. Tsang, L. Kodjabachian, N.A. Sims, M.K. Trivett, M. Ehrich, A. Dobrovic, J. Slavin, P.F. Choong, P.J. Simmons, I.B. Dawid, D.M. Thomas, Wnt inhibitory factor 1 is epigenetically silenced

in human osteosarcoma, and targeted disruption accelerates osteosarcomagenesis in mice, J Clin Invest 119(4) (2009) 837-51.
[35] J. Yang, M. Kitami, H. Pan, M.T. Nakamura, H. Zhang, F. Liu, L. Zhu, Y. Komatsu, Y. Mishina, Augmented BMP signaling commits cranial neural crest cells to a chondrogenic fate by suppressing autophagic beta-catenin degradation, Sci Signal 14(665) (2021).
[36] H. Lin, T. Wu, L. Peng, W. Su, Y. Wang, X. Li, Q. Liu, C. Zhong, J. Huang, B. Wei, Lnc-MAP6-1:3 knockdown inhibits osteosarcoma progression by modulating Bax/Bcl-2 and Wnt/beta-catenin pathways, Int J Med Sci 17(15) (2020) 2248-2256.
[37] M. Enomoto, S. Hayakawa, S. Itsukushima, D.Y. Ren, M. Matsuo, K. Tamada, C. Oneyama, M. Okada, T. Takumi, M. Nishita, Y. Minami, Autonomous regulation of osteosarcoma cell invasiveness by Wnt5a/Ror2 signaling, Oncogene 28(36) (2009) 3197-208.
[38] K. van Loon, E.J.M. Huijbers, A.W. Griffioen, Secreted frizzled-related protein 2: a key player in noncanonical Wnt signaling and tumor angiogenesis, Cancer Metastasis Rev 40(1) (2021) 191-203.
[39] L. Li, L. Hobson, L. Perry, B. Clark, S. Heavey, A. Haider, A. Sridhar, G. Shaw, J. Kelly, A. Freeman, I. Wilson, H. Whitaker, E. Nurmemmedov, S. Oltean, S. Porazinski, M. Ladomery, Targeting the ERG oncogene with splice-switching oligonucleotides as a novel therapeutic strategy in prostate cancer, Br J Cancer 123(6) (2020) 1024-1032.
[40] E. Peixoto, S. Richard, K. Pant, A. Biswas, S.A. Gradilone, The primary cilium: Its role as a tumor suppressor organelle, Biochem Pharmacol 175 (2020) 113906.
[41] W. Yang, X. Liu, E. Choy, H. Mankin, F.J. Hornicek, Z. Duan, Targeting hedgehog-GLI-2 pathway in osteosarcoma, J Orthop Res 31(3) (2013) 502-9.
[42] F.C. Kelleher, J.E. Cain, J.M. Healy, D.N. Watkins, D.M. Thomas, Prevailing importance of the hedgehog signaling pathway and the potential for treatment advancement in sarcoma, Pharmacol Ther 136(2) (2012) 153-68.
[43] J. Reichrath, S. Reichrath, Notch Signaling in Prevention And Therapy: Fighting Cancer with a Two-Sided Sword, Adv Exp Med Biol 1287 (2021) 1-7.
[44] E.A. Kolb, R. Gorlick, S.T. Keir, J.M. Maris, R. Lock, H. Carol, R.T. Kurmasheva, C.P. Reynolds, M.H. Kang, J. Wu, P.J. Houghton, M.A. Smith, Initial testing (stage 1) by the pediatric preclinical testing program of RO4929097, a gamma-secretase inhibitor targeting notch signaling, Pediatr Blood Cancer 58(5) (2012) 815-8.
[45] G. Grignani, E. Palmerini, V. Ferraresi, L. D'Ambrosio, R. Bertulli, S.D. Asaftei, A. Tamburini, Y. Pignochino, D. Sangiolo, E. Marchesi, F. Capozzi, R. Biagini, M. Gambarotti, F. Fagioli, P.G. Casali, P. Picci, S. Ferrari, M. Aglietta, G. Italian Sarcoma, Sorafenib and everolimus for patients with unresectable high-grade osteosarcoma progressing after standard treatment: a non-randomised phase 2 clinical trial, Lancet Oncol 16(1) (2015) 98-107.
[46] P. Frankel, C. Ruel, A. Uche, E. Choy, S. Okuno, N. Somiah, W.A. Chow, Pazopanib in Patients with Osteosarcoma Metastatic to the Lung: Phase 2 Study Results and the Lessons for Tumor Measurement, J Oncol 2022 (2022) 3691025.
[47] Y. Liu, Y.H. Ma, Z.Z. Sun, Y.J. Rui, Q.D. Yin, S. Song, X.M. Wei, J. Liu, X.G. Liu, K.J. Hu, Effect of c-erbB2 overexpression on prognosis in osteosarcoma: evidence from eight studies, Tumour Biol 35(9) (2014) 8939-43.
[48] D. Ebb, P. Meyers, H. Grier, M. Bernstein, R. Gorlick, S.E. Lipshultz, M. Krailo, M. Devidas, D.A. Barkauskas, G.P. Siegal, W.S. Ferguson, G.D. Letson, K. Marcus, A. Goorin, P. Beardsley, N. Marina, Phase II trial of trastuzumab in combination with cytotoxic chemotherapy for treatment of metastatic osteosarcoma with human epidermal growth factor receptor 2 overexpression: a report from the children's oncology group, J Clin Oncol 30(20) (2012) 2545-51.
[49] N. Hay, N. Sonenberg, Upstream and downstream of mTOR, Genes Dev 18(16) (2004) 1926-45.
[50] C. Porta, C. Paglino, A. Mosca, Targeting PI3K/Akt/mTOR Signaling in Cancer, Front Oncol 4 (2014) 64.
[51] Z. Ji, J. Shen, Y. Lan, Q. Yi, H. Liu, Targeting signaling pathways in osteosarcoma: Mechanisms and clinical studies, MedComm (2020) 4(4) (2023) e308.

[52] L. Ding, L. Congwei, Q. Bei, Y. Tao, W. Ruiguo, Y. Heze, D. Bo, L. Zhihong, mTOR: An attractive therapeutic target for osteosarcoma?, Oncotarget 7(31) (2016) 50805-50813.
[53] L. Liu, C.A. Parent, Review series: TOR kinase complexes and cell migration, J Cell Biol 194(6) (2011) 815-24.
[54] D. Tewari, P. Patni, A. Bishayee, A.N. Sah, A. Bishayee, Natural products targeting the PI3K-Akt-mTOR signaling pathway in cancer: A novel therapeutic strategy, Semin Cancer Biol 80 (2022) 1-17.
[55] W. Yu, P.B. Chen, F.C. Chen, S.L. Ding, X.Y. Pan, MicroRNA-744 promotes proliferation of osteosarcoma cells by targeting PTEN, Mol Med Rep 21(5) (2020) 2276-2282.
[56] Y. Sukawa, H. Yamamoto, K. Nosho, H. Kunimoto, H. Suzuki, Y. Adachi, M. Nakazawa, T. Nobuoka, M. Kawayama, M. Mikami, T. Matsuno, T. Hasegawa, K. Hirata, K. Imai, Y. Shinomura, Alterations in the human epidermal growth factor receptor 2-phosphatidylinositol 3-kinase-v-Akt pathway in gastric cancer, World J Gastroenterol 18(45) (2012) 6577-86.
[57] M. Zhuang, X. Qiu, D. Cheng, C. Zhu, L. Chen, MicroRNA-524 promotes cell proliferation by down-regulating PTEN expression in osteosarcoma, Cancer Cell Int 18 (2018) 114.
[58] G.D. Demetri, S.P. Chawla, I. Ray-Coquard, A. Le Cesne, A.P. Staddon, M.M. Milhem, N. Penel, R.F. Riedel, B. Bui-Nguyen, L.D. Cranmer, P. Reichardt, E. Bompas, T. Alcindor, D. Rushing, Y. Song, R.M. Lee, S. Ebbinghaus, J.E. Eid, J.W. Loewy, F.G. Haluska, P.F. Dodion, J.Y. Blay, Results of an international randomized phase III trial of the mammalian target of rapamycin inhibitor ridaforolimus versus placebo to control metastatic sarcomas in patients after benefit from prior chemotherapy, J Clin Oncol 31(19) (2013) 2485-92.
[59] S.P. Chawla, A.P. Staddon, L.H. Baker, S.M. Schuetze, A.W. Tolcher, G.Z. D'Amato, J.Y. Blay, M.M. Mita, K.K. Sankhala, L. Berk, V.M. Rivera, T. Clackson, J.W. Loewy, F.G. Haluska, G.D. Demetri, Phase II study of the mammalian target of rapamycin inhibitor ridaforolimus in patients with advanced bone and soft tissue sarcomas, J Clin Oncol 30(1) (2012) 78-84.
[60] Y. Pignochino, C. Dell'Aglio, M. Basirico, F. Capozzi, M. Soster, S. Marchio, S. Bruno, L. Gammaitoni, D. Sangiolo, E. Torchiaro, L. D'Ambrosio, F. Fagioli, S. Ferrari, M. Alberghini, P. Picci, M. Aglietta, G. Grignani, The Combination of Sorafenib and Everolimus Abrogates mTORC1 and mTORC2 upregulation in osteosarcoma preclinical models, Clin Cancer Res 19(8) (2013) 2117-31.
[61] T. Saeki, M. Ouchi, T. Ouchi, Physiological and oncogenic Aurora-A pathway, Int J Biol Sci 5(7) (2009) 758-62.
[62] M. Martini, E. Ciraolo, F. Gulluni, E. Hirsch, Targeting PI3K in Cancer: Any Good News?, Front Oncol 3 (2013) 108.
[63] A.M. Martelli, F. Chiarini, C. Evangelisti, A. Cappellini, F. Buontempo, D. Bressanin, M. Fini, J.A. McCubrey, Two hits are better than one: targeting both phosphatidylinositol 3-kinase and mammalian target of rapamycin as a therapeutic strategy for acute leukemia treatment, Oncotarget 3(4) (2012) 371-94.
[64] K.E. O'Reilly, F. Rojo, Q.B. She, D. Solit, G.B. Mills, D. Smith, H. Lane, F. Hofmann, D.J. Hicklin, D.L. Ludwig, J. Baselga, N. Rosen, mTOR inhibition induces upstream receptor tyrosine kinase signaling and activates Akt, Cancer Res 66(3) (2006) 1500-8.
[65] A. Carracedo, L. Ma, J. Teruya-Feldstein, F. Rojo, L. Salmena, A. Alimonti, A. Egia, A.T. Sasaki, G. Thomas, S.C. Kozma, A. Papa, C. Nardella, L.C. Cantley, J. Baselga, P.P. Pandolfi, Inhibition of mTORC1 leads to MAPK pathway activation through a PI3K-dependent feedback loop in human cancer, J Clin Invest 118(9) (2008) 3065-74.
[66] E.M. Sommer, H. Dry, D. Cross, S. Guichard, B.R. Davies, D.R. Alessi, Elevated SGK1 predicts resistance of breast cancer cells to Akt inhibitors, Biochem J 452(3) (2013) 499-508.
[67] L. Rosich, D. Colomer, G. Roue, Autophagy controls everolimus (RAD001) activity in mantle cell lymphoma, Autophagy 9(1) (2013) 115-7.
[68] Y. Zhou, Y. Wei, X. Tian, X. Wei, Cancer vaccines: current status and future directions, J Hematol Oncol 18(1) (2025) 18.
[69] Y. Zhou, N. Slone, T.T. Chrisikos, O. Kyrysyuk, R.L. Babcock, Y.B. Medik, H.S. Li, E.S. Kleinerman, S.S. Watowich, Vaccine efficacy against primary and metastatic cancer with in vitro-generated CD103(+) conventional dendritic cells, J Immunother Cancer 8(1) (2020).

[70] Y. Inagaki, E. Hookway, K.A. Williams, A.B. Hassan, U. Oppermann, Y. Tanaka, E. Soilleux, N.A. Athanasou, Dendritic and mast cell involvement in the inflammatory response to primary malignant bone tumours, Clin Sarcoma Res 6 (2016) 13.
[71] G.Z. Zhang, Z.L. Wu, C.Y. Li, E.H. Ren, W.H. Yuan, Y.J. Deng, Q.Q. Xie, Development of a Machine Learning-Based Autophagy-Related lncRNA Signature to Improve Prognosis Prediction in Osteosarcoma Patients, Front Mol Biosci 8 (2021) 615084.
[72] M. Kansara, K. Thomson, P. Pang, A. Dutour, L. Mirabello, F. Acher, J.P. Pin, E.G. Demicco, J. Yan, M.W.L. Teng, M.J. Smyth, D.M. Thomas, Infiltrating Myeloid Cells Drive Osteosarcoma Progression via GRM4 Regulation of IL23, Cancer Discov 9(11) (2019) 1511-1519.
[73] M. Kawano, I. Itonaga, T. Iwasaki, H. Tsumura, Enhancement of antitumor immunity by combining anti-cytotoxic T lymphocyte antigen-4 antibodies and cryotreated tumor lysate-pulsed dendritic cells in murine osteosarcoma, Oncol Rep 29(3) (2013) 1001-6.
[74] P. Koirala, M.E. Roth, J. Gill, S. Piperdi, J.M. Chinai, D.S. Geller, B.H. Hoang, A. Park, M.A. Fremed, X. Zang, R. Gorlick, Immune infiltration and PD-L1 expression in the tumor microenvironment are prognostic in osteosarcoma, Sci Rep 6 (2016) 30093.
[75] T. Le, S. Su, L. Shahriyari, Immune classification of osteosarcoma, Math Biosci Eng 18(2) (2021) 1879-1897.
[76] H. Yabe, T. Tsukahara, S. Kawaguchi, T. Wada, T. Torigoe, N. Sato, C. Terai, M. Aoki, S. Hirose, H. Morioka, H. Yabe, Prognostic significance of HLA class I expression in Ewing's sarcoma family of tumors, J Surg Oncol 103(5) (2011) 380-5.
[77] Y.T. Sundara, M. Kostine, A.H. Cleven, J.V. Bovee, M.W. Schilham, A.M. Cleton-Jansen, Increased PD-L1 and T-cell infiltration in the presence of HLA class I expression in metastatic high-grade osteosarcoma: a rationale for T-cell-based immunotherapy, Cancer Immunol Immunother 66(1) (2017) 119-128.
[78] J.A. Ligon, W. Choi, G. Cojocaru, W. Fu, E.H. Hsiue, T.F. Oke, N. Siegel, M.H. Fong, B. Ladle, C.A. Pratilas, C.D. Morris, A. Levin, D.S. Rhee, C.F. Meyer, A.J. Tam, R. Blosser, E.D. Thompson, A. Suru, D. McConkey, F. Housseau, R. Anders, D.M. Pardoll, N. Llosa, Pathways of immune exclusion in metastatic osteosarcoma are associated with inferior patient outcomes, J Immunother Cancer 9(5) (2021).
[79] Q. Han, H. Shi, F. Liu, CD163(+) M2-type tumor-associated macrophage support the suppression of tumor-infiltrating T cells in osteosarcoma, Int Immunopharmacol 34 (2016) 101-106.
[80] T. Matsuo, S. Shimose, T. Kubo, Y. Mikami, K. Arihiro, Y. Yasunaga, M. Ochi, Extraskeletal osteosarcoma with partial spontaneous regression, Anticancer Res 29(12) (2009) 5197-201.
[81] D. Pende, M. Falco, M. Vitale, C. Cantoni, C. Vitale, E. Munari, A. Bertaina, F. Moretta, G. Del Zotto, G. Pietra, M.C. Mingari, F. Locatelli, L. Moretta, Killer Ig-Like Receptors (KIRs): Their Role in NK Cell Modulation and Developments Leading to Their Clinical Exploitation, Front Immunol 10 (2019) 1179.
[82] A.D. Barrow, C.J. Martin, M. Colonna, The Natural Cytotoxicity Receptors in Health and Disease, Front Immunol 10 (2019) 909.
[83] F. Souza-Fonseca-Guimaraes, J. Cursons, N.D. Huntington, The Emergence of Natural Killer Cells as a Major Target in Cancer Immunotherapy, Trends Immunol 40(2) (2019) 142-158.
[84] H.J. Baek, J.S. Kim, M. Yoon, J.J. Lee, M.G. Shin, D.W. Ryang, H. Kook, S.K. Kim, D. Cho, Ex vivo expansion of natural killer cells using cryopreserved irradiated feeder cells, Anticancer Res 33(5) (2013) 2011-9.
[85] L. Fernandez, J. Valentin, M. Zalacain, W. Leung, A. Patino-Garcia, A. Perez-Martinez, Activated and expanded natural killer cells target osteosarcoma tumor initiating cells in an NKG2D-NKG2DL dependent manner, Cancer Lett 368(1) (2015) 54-63.
[86] F. Otegbeye, M.A.F. Vina, T. Wang, Y.T. Bolon, A. Lazaryan, A. Beitinjaneh, V.R. Bhatt, P. Castillo, S.G.E. Marsh, G.C. Hildebrandt, A. Assal, V.I. Brown, J. Hsu, S. Spellman, M. de Lima, S.J. Lee, Natural Killer Cell Alloreactivity Predicted By Killer Cell Immunoglobulin-Like Receptor Ligand Mismatch Does Not Impact Engraftment in Umbilical Cord Blood and Haploidentical Stem Cell Transplantation, Transplant Cell Ther 28(8) (2022) 483 e1-483 e7.

[87] Q. Huang, X. Liang, T. Ren, Y. Huang, H. Zhang, Y. Yu, C. Chen, W. Wang, J. Niu, J. Lou, W. Guo, The role of tumor-associated macrophages in osteosarcoma progression - therapeutic implications, Cell Oncol (Dordr) 44(3) (2021) 525-539.
[88] K. Kielbassa, S. Vegna, C. Ramirez, L. Akkari, Understanding the Origin and Diversity of Macrophages to Tailor Their Targeting in Solid Cancers, Front Immunol 10 (2019) 2215.
[89] S.O. Dudzinski, J.E. Bader, K.E. Beckermann, K.L. Young, R. Hongo, M.Z. Madden, A. Abraham, B.I. Reinfeld, X. Ye, N.J. MacIver, T.D. Giorgio, J.C. Rathmell, Leptin Augments Antitumor Immunity in Obesity by Repolarizing Tumor-Associated Macrophages, J Immunol 207(12) (2021) 3122-3130.
[90] C. Deng, Y. Xu, J. Fu, X. Zhu, H. Chen, H. Xu, G. Wang, Y. Song, G. Song, J. Lu, R. Liu, Q. Tang, W. Huang, J. Wang, Reprograming the tumor immunologic microenvironment using neoadjuvant chemotherapy in osteosarcoma, Cancer Sci 111(6) (2020) 1899-1909.
[91] L. Cassetta, J.W. Pollard, Targeting macrophages: therapeutic approaches in cancer, Nat Rev Drug Discov 17(12) (2018) 887-904.
[92] B.Z. Qian, J.W. Pollard, Macrophage diversity enhances tumor progression and metastasis, Cell 141(1) (2010) 39-51.
[93] P. Zhang, Y.F. Jin, Q. Zhang, Y.M. Wu, W.D. Wu, W. Yao, Y.J. Wu, Z.T. Li, Y. Zhao, Y. Liu, F.F. Feng, Macrophages promote coal tar pitch extract-induced tumorigenesis of BEAS-2B cells and tumor metastasis in nude mice mediated by AP-1, Asian Pac J Cancer Prev 15(12) (2014) 4871-6.
[94] Y. Han, W. Guo, T. Ren, Y. Huang, S. Wang, K. Liu, B. Zheng, K. Yang, H. Zhang, X. Liang, Tumor-associated macrophages promote lung metastasis and induce epithelial-mesenchymal transition in osteosarcoma by activating the COX-2/STAT3 axis, Cancer Lett 440-441 (2019) 116-125.
[95] A. Etzerodt, K. Tsalkitzi, M. Maniecki, W. Damsky, M. Delfini, E. Baudoin, M. Moulin, M. Bosenberg, J.H. Graversen, N. Auphan-Anezin, S.K. Moestrup, T. Lawrence, Specific targeting of CD163(+) TAMs mobilizes inflammatory monocytes and promotes T cell-mediated tumor regression, J Exp Med 216(10) (2019) 2394-2411.
[96] L. Wu, S. Saxena, M. Awaji, R.K. Singh, Tumor-Associated Neutrophils in Cancer: Going Pro, Cancers (Basel) 11(4) (2019).
[97] J. Pillay, I. den Braber, N. Vrisekoop, L.M. Kwast, R.J. de Boer, J.A. Borghans, K. Tesselaar, L. Koenderman, In vivo labeling with 2H2O reveals a human neutrophil lifespan of 5.4 days, Blood 116(4) (2010) 625-7.
[98] Z.G. Fridlender, J. Sun, S. Kim, V. Kapoor, G. Cheng, L. Ling, G.S. Worthen, S.M. Albelda, Polarization of tumor-associated neutrophil phenotype by TGF-beta: "N1" versus "N2" TAN, Cancer Cell 16(3) (2009) 183-94.
[99] Z.J. Wu, J.C. Tan, X. Qin, B. Liu, Z.C. Yuan, Significance of circulating tumor cells in osteosarcoma patients treated by neoadjuvant chemotherapy and surgery, Cancer Manag Res 10 (2018) 3333-3339.
[100] M. Cortini, A. Armirotti, M. Columbaro, D.L. Longo, G. Di Pompo, E. Cannas, A. Maresca, C. Errani, A. Longhi, A. Righi, V. Carelli, N. Baldini, S. Avnet, Exploring Metabolic Adaptations to the Acidic Microenvironment of Osteosarcoma Cells Unveils Sphingosine 1-Phosphate as a Valuable Therapeutic Target, Cancers (Basel) 13(2) (2021).
[101] Y. Zhang, Q. Ma, T. Liu, G. Guan, K. Zhang, J. Chen, N. Jia, S. Yan, G. Chen, S. Liu, K. Jiang, Y. Lu, Y. Wen, H. Zhao, Y. Zhou, Q. Fan, X. Qiu, Interleukin-6 suppression reduces tumour self-seeding by circulating tumour cells in a human osteosarcoma nude mouse model, Oncotarget 7(1) (2016) 446-58.
[102] T. Liu, Q. Ma, Y. Zhang, X. Wang, K. Xu, K. Yan, W. Dong, Q. Fan, Y. Zhang, X. Qiu, Self-seeding circulating tumor cells promote the proliferation and metastasis of human osteosarcoma by upregulating interleukin-8, Cell Death Dis 10(8) (2019) 575.
[103] J. Karbach, A. Neumann, K. Brand, C. Wahle, E. Siegel, M. Maeurer, E. Ritter, T. Tsuji, S. Gnjatic, L.J. Old, G. Ritter, E. Jager, Phase I clinical trial of mixed bacterial vaccine (Coley's toxins) in patients with NY-ESO-1 expressing cancers: immunological effects and clinical activity, Clin Cancer Res 18(19) (2012) 5449-59.
[104] C. Moore, D. Eslin, A. Levy, J. Roberson, V. Giusti, R. Sutphin, Prognostic significance of early lymphocyte recovery in pediatric osteosarcoma, Pediatr Blood Cancer 55(6) (2010) 1096-102.

[105] L.M. Jeys, R.J. Grimer, S.R. Carter, R.M. Tillman, A. Abudu, Post operative infection and increased survival in osteosarcoma patients: are they associated?, Ann Surg Oncol 14(10) (2007) 2887-95.
[106] A. Le Cesne, P. Marec-Berard, J.Y. Blay, N. Gaspar, F. Bertucci, N. Penel, E. Bompas, S. Cousin, M. Toulmonde, A. Bessede, W.H. Fridman, C. Sautes-Fridman, M. Kind, F. Le Loarer, M. Pulido, A. Italiano, Programmed cell death 1 (PD-1) targeting in patients with advanced osteosarcomas: results from the PEMBROSARC study, Eur J Cancer 119 (2019) 151-157.
[107] Y. Zhou, Q. Yang, Y. Dong, T. Ji, B. Zhang, C. Yang, S. Zheng, L. Tang, C. Zhou, G. Qian, Y. Huang, W. Yu, H. Li, Y. Wang, A. He, Z. Shen, Q. Bao, Y. Hua, H. Bai, J. Zhao, X. Li, X. Dai, J. Zhang, H. Hu, Y. Yao, First-in-Maintenance Therapy for Localized High-Grade Osteosarcoma: An Open-Label Phase I/II Trial of the Anti-PD-L1 Antibody ZKAB001, Clin Cancer Res 29(4) (2023) 764-774.
[108] N. Himoudi, R. Wallace, K.L. Parsley, K. Gilmour, A.U. Barrie, K. Howe, R. Dong, N.J. Sebire, A. Michalski, A.J. Thrasher, J. Anderson, Lack of T-cell responses following autologous tumour lysate pulsed dendritic cell vaccination, in patients with relapsed osteosarcoma, Clin Transl Oncol 14(4) (2012) 271-9.
[109] C. Zhang, L.M. Morimoto, A.J. de Smith, H.M. Hansen, J. Gonzalez-Maya, A.A. Endicott, I.V. Smirnov, C. Metayer, Q. Wei, W.C. Eward, J.L. Wiemels, K.M. Walsh, Genetic determinants of childhood and adult height associated with osteosarcoma risk, Cancer 124(18) (2018) 3742-3752.
[110] S. Chen, L. Yang, F. Pu, H. Lin, B. Wang, J. Liu, Z. Shao, High Birth Weight Increases the Risk for Bone Tumor: A Systematic Review and Meta-Analysis, Int J Environ Res Public Health 12(9) (2015) 11178-95.
[111] A.K. Luu, A.M. Viloria-Petit, Targeting Mechanotransduction in Osteosarcoma: A Comparative Oncology Perspective, Int J Mol Sci 21(20) (2020).
[112] R. Ayyasamy, S. Fan, P. Czernik, B. Lecka-Czernik, S. Chattopadhyay, R. Chakravarti, 14-3-3zeta suppresses RANKL signaling by destabilizing TRAF6, J Biol Chem 300(7) (2024) 107487.
[113] C.Y. Lin, A. Sassi, Y. Wu, K. Seaman, W. Tang, X. Song, R. Bienenstock, H. Yokota, Y. Sun, F. Geng, L. Wang, L. You, Mechanotransduction pathways regulating YAP nuclear translocation under Yoda1 and vibration in osteocytes, Bone 190 (2025) 117283.
[114] S. Lu, T. Lu, J. Zhang, L. Gan, X. Wu, D. Han, K. Zhang, C. Xu, S. Liu, W. Qin, F. Yang, W. Wen, CD248 promotes migration and metastasis of osteosarcoma through ITGB1-mediated FAK-paxillin pathway activation, BMC Cancer 23(1) (2023) 290.
[115] M. Cortini, F. Macchi, F. Reggiani, E. Vitale, M.V. Lipreri, F. Perut, A. Ciarrocchi, N. Baldini, S. Avnet, Endogenous Extracellular Matrix Regulates the Response of Osteosarcoma 3D Spheroids to Doxorubicin, Cancers (Basel) 15(4) (2023).
[116] W.D. Rindt, M. Krug, S. Yamada, F. Sennefelder, L. Belz, W.H. Cheng, M. Azeem, M. Kuric, M. Evers, E. Leich, T.N. Hartmann, A.R. Pereira, M. Hermann, J. Hansmann, C. Mussoni, P. Stahlhut, T. Ahmad, M.A. Yassin, K. Mustafa, R. Ebert, F. Jundt, A 3D bioreactor model to study osteocyte differentiation and mechanobiology under perfusion and compressive mechanical loading, Acta Biomater 184 (2024) 210-225.
[117] G. Alloisio, D.B. Rodriguez, M. Luce, C. Ciaccio, S. Marini, A. Cricenti, M. Gioia, Cyclic Stretch-Induced Mechanical Stress Applied at 1 Hz Frequency Can Alter the Metastatic Potential Properties of SAOS-2 Osteosarcoma Cells, Int J Mol Sci 24(9) (2023).
[118] L. Qin, W. Liu, H. Cao, G. Xiao, Molecular mechanosensors in osteocytes, Bone Res 8 (2020) 23.
[119] B. Zhang, X. Li, X. Zhou, C. Lou, S. Wang, H. Lv, G. Zhang, Y. Fang, D. Yin, P. Shang, Magneto-mechanical stimulation modulates osteocyte fate via the ECM-integrin-CSK axis and wnt pathway, iScience 26(8) (2023) 107365.
[120] O. Jeon, T.H. Kim, E. Alsberg, Reversible dynamic mechanics of hydrogels for regulation of cellular behavior, Acta Biomater 136 (2021) 88-98.
[121] I. Dasgupta, D. McCollum, Control of cellular responses to mechanical cues through YAP/TAZ regulation, J Biol Chem 294(46) (2019) 17693-17706.

[122] H. Atcha, A. Jairaman, J.R. Holt, V.S. Meli, R.R. Nagalla, P.K. Veerasubramanian, K.T. Brumm, H.E. Lim, S. Othy, M.D. Cahalan, M.M. Pathak, W.F. Liu, Mechanically activated ion channel Piezo1 modulates macrophage polarization and stiffness sensing, Nat Commun 12(1) (2021) 3256.
[123] H. Yoon, J.P. Dehart, J.M. Murphy, S.T. Lim, Understanding the roles of FAK in cancer: inhibitors, genetic models, and new insights, J Histochem Cytochem 63(2) (2015) 114-28.
[124] L. Ding, X. Sun, Y. You, N. Liu, Z. Fu, Expression of focal adhesion kinase and phosphorylated focal adhesion kinase in human gliomas is associated with unfavorable overall survival, Transl Res 156(1) (2010) 45-52.
[125] D.J. Sieg, C.R. Hauck, D. Ilic, C.K. Klingbeil, E. Schaefer, C.H. Damsky, D.D. Schlaepfer, FAK integrates growth-factor and integrin signals to promote cell migration, Nat Cell Biol 2(5) (2000) 249-56.
[126] K. Ren, X. Lu, N. Yao, Y. Chen, A. Yang, H. Chen, J. Zhang, S. Wu, X. Shi, C. Wang, X. Sun, Focal adhesion kinase overexpression and its impact on human osteosarcoma, Oncotarget 6(31) (2015) 31085-103.
[127] M. Yao, A. Tijore, D. Cheng, J.V. Li, A. Hariharan, B. Martinac, G. Tran Van Nhieu, C.D. Cox, M. Sheetz, Force- and cell state-dependent recruitment of Piezo1 drives focal adhesion dynamics and calcium entry, Sci Adv 8(45) (2022) eabo1461.
[128] G. Du, W. Chen, L. Li, Q. Zhang, The potential role of mechanosensitive ion channels in substrate stiffness-regulated Ca(2+) response in chondrocytes, Connect Tissue Res 63(5) (2022) 453-462.
[129] H.J. Wang, Y. Wang, S.S. Mirjavadi, T. Andersen, L. Moldovan, P. Vatankhah, B. Russell, J. Jin, Z. Zhou, Q. Li, C.D. Cox, Q.P. Su, L.A. Ju, Microscale geometrical modulation of PIEZO1 mediated mechanosensing through cytoskeletal redistribution, Nat Commun 15(1) (2024) 5521.
[130] G. Du, L. Li, X. Zhang, J. Liu, J. Hao, J. Zhu, H. Wu, W. Chen, Q. Zhang, Roles of TRPV4 and piezo channels in stretch-evoked Ca(2+) response in chondrocytes, Exp Biol Med (Maywood) 245(3) (2020) 180-189.
[131] A. Mussell, C. Frangou, J. Zhang, Regulation of the Hippo signaling pathway by deubiquitinating enzymes in cancer, Genes Dis 6(4) (2019) 335-341.
[132] T.R. Coughlin, A. Sana, K. Voss, A. Gadi, U. Basu-Roy, C.M. Curtin, A. Mansukhani, O.D. Kennedy, The Effect of Fluid Flow Shear Stress and Substrate Stiffness on Yes-Associated Protein (YAP) Activity and Osteogenesis in Murine Osteosarcoma Cells, Cancers (Basel) 13(13) (2021).
[133] Z. Xiang, P. Zhang, C. Jia, R. Xu, D. Cao, Z. Xu, T. Lu, J. Liu, X. Wang, C. Qiu, W. Fu, W. Li, L. Cheng, Q. Yang, S. Feng, L. Wang, Y. Zhao, X. Liu, Piezo1 channel exaggerates ferroptosis of nucleus pulposus cells by mediating mechanical stress-induced iron influx, Bone Res 12(1) (2024) 20.
[134] Y. Peng, R. Qu, Y. Yang, T. Fan, B. Sun, A.U. Khan, S. Wu, W. Liu, J. Zhu, J. Chen, X. Li, J. Dai, J. Ouyang, Regulation of the integrin alphaVbeta3- actin filaments axis in early osteogenic differentiation of human mesenchymal stem cells under cyclic tensile stress, Cell Commun Signal 21(1) (2023) 308.
[135] M.F. Hansen, M. Seton, A. Merchant, Osteosarcoma in Paget's disease of bone, J Bone Miner Res 21 Suppl 2 (2006) P58-63.
[136] H. Kovar, L. Bierbaumer, B. Radic-Sarikas, The YAP/TAZ Pathway in Osteogenesis and Bone Sarcoma Pathogenesis, Cells 9(4) (2020).
[137] A. Totaro, T. Panciera, S. Piccolo, YAP/TAZ upstream signals and downstream responses, Nat Cell Biol 20(8) (2018) 888-899.
[138] Y. Zhang, R.A. Brekken, Direct and indirect regulation of the tumor immune microenvironment by VEGF, J Leukoc Biol 111(6) (2022) 1269-1286.
[139] K. Mori, B. Le Goff, M. Berreur, A. Riet, A. Moreau, F. Blanchard, C. Chevalier, I. Guisle-Marsollier, J. Leger, J. Guicheux, M. Masson, F. Gouin, F. Redini, D. Heymann, Human osteosarcoma cells express functional receptor activator of nuclear factor-kappa B, J Pathol 211(5) (2007) 555-562.
[140] Z. Zhang, J. Du, S. Wang, L. Shao, K. Jin, F. Li, B. Wei, W. Ding, P. Fu, H. van Dam, A. Wang, J. Jin, C. Ding, B. Yang, M. Zheng, X.H. Feng, K.L. Guan, L. Zhang, OTUB2 Promotes Cancer Metastasis via Hippo-Independent Activation of YAP and TAZ, Mol Cell 73(1) (2019) 7-21 e7.

[141] Y. Liu, P. Lei, R.Z. Samuel, A.M. Kashyap, T. Groth, W. Bshara, S. Neelamegham, S.T. Andreadis, Cadherin-11 increases tumor cell proliferation and metastatic potential via Wnt pathway activation, Mol Oncol 17(10) (2023) 2056-2073.
[142] F. Lamoureux, P. Richard, Y. Wittrant, S. Battaglia, P. Pilet, V. Trichet, F. Blanchard, F. Gouin, B. Pitard, D. Heymann, F. Redini, Therapeutic relevance of osteoprotegerin gene therapy in osteosarcoma: blockade of the vicious cycle between tumor cell proliferation and bone resorption, Cancer Res 67(15) (2007) 7308-18.
[143] D. Xie, C. Hu, Y. Zhu, J. Yao, J. Li, J. Xia, L. Ye, Y. Jin, S. Jiang, T. Hu, J. Lu, H. Song, P. Tang, J. Dai, Y. Xi, Z. Hu, Sequential Therapy for Osteosarcoma and Bone Regeneration via Chemodynamic Effect and Cuproptosis Using a 3D-Printed Scaffold with TME-Responsive Hydrogel, Small 21(5) (2025) e2406639.
[144] X. Wang, X. Guo, H. Ren, X. Song, L. Chen, L. Yu, J. Ren, Y. Chen, An "Outer Piezoelectric and Inner Epigenetic" Logic-Gated PANoptosis for Osteosarcoma Sono-Immunotherapy and Bone Regeneration, Adv Mater 37(7) (2025) e2415814.
[145] Y. Li, S. Yang, S. Yang, Verteporfin Inhibits the Progression of Spontaneous Osteosarcoma Caused by Trp53 and Rb1 Deficiency in Ctsk-Expressing Cells via Impeding Hippo Pathway, Cells 11(8) (2022).
[146] S. Morice, M. Mullard, R. Brion, M. Dupuy, S. Renault, R. Tesfaye, B. Brounais-Le Royer, B. Ory, F. Redini, F. Verrecchia, The YAP/TEAD Axis as a New Therapeutic Target in Osteosarcoma: Effect of Verteporfin and CA3 on Primary Tumor Growth, Cancers (Basel) 12(12) (2020).
[147] F. Punzo, C. Tortora, M. Argenziano, D.D. Pinto, E. Pota, M.D. Martino, A.D. Paola, F. Rossi, Can Denosumab be used in combination with Doxorubicin in Osteosarcoma?, Oncotarget 11(28) (2020) 2763-2773.
[148] F. van Zijl, G. Krupitza, W. Mikulits, Initial steps of metastasis: cell invasion and endothelial transmigration, Mutat Res 728(1-2) (2011) 23-34.
[149] N.V. Krakhmal, M.V. Zavyalova, E.V. Denisov, S.V. Vtorushin, V.M. Perelmuter, Cancer Invasion: Patterns and Mechanisms, Acta Naturae 7(2) (2015) 17-28.
[150] G.W. Pearson, Control of Invasion by Epithelial-to-Mesenchymal Transition Programs during Metastasis, J Clin Med 8(5) (2019).
[151] A. Lorentzen, J. Bamber, A. Sadok, I. Elson-Schwab, C.J. Marshall, An ezrin-rich, rigid uropod-like structure directs movement of amoeboid blebbing cells, J Cell Sci 124(Pt 8) (2011) 1256-67.
[152] A. Haeger, K. Wolf, M.M. Zegers, P. Friedl, Collective cell migration: guidance principles and hierarchies, Trends Cell Biol 25(9) (2015) 556-66.
[153] R. Torka, F. Thuma, V. Herzog, G. Kirfel, ROCK signaling mediates the adoption of different modes of migration and invasion in human mammary epithelial tumor cells, Exp Cell Res 312(19) (2006) 3857-71.
[154] A.W. Holle, N. Govindan Kutty Devi, K. Clar, A. Fan, T. Saif, R. Kemkemer, J.P. Spatz, Cancer Cells Invade Confined Microchannels via a Self-Directed Mesenchymal-to-Amoeboid Transition, Nano Lett 19(4) (2019) 2280-2290.
[155] E. Paluch, M. Piel, J. Prost, M. Bornens, C. Sykes, Cortical actomyosin breakage triggers shape oscillations in cells and cell fragments, Biophys J 89(1) (2005) 724-33.
[156] E.K. Paluch, E. Raz, The role and regulation of blebs in cell migration, Curr Opin Cell Biol 25(5) (2013) 582-90.
[157] N.O. Carragher, S.M. Walker, L.A. Scott Carragher, F. Harris, T.K. Sawyer, V.G. Brunton, B.W. Ozanne, M.C. Frame, Calpain 2 and Src dependence distinguishes mesenchymal and amoeboid modes of tumour cell invasion: a link to integrin function, Oncogene 25(42) (2006) 5726-40.
[158] S. Yan, H. Xue, P. Zhang, X. Han, X. Guo, G. Yuan, L. Deng, G. Li, MMP inhibitor Ilomastat induced amoeboid-like motility via activation of the Rho signaling pathway in glioblastoma cells, Tumour Biol 37 (2016) 16177-16186.
[159] Y. Hegerfeldt, M. Tusch, E.B. Brocker, P. Friedl, Collective cell movement in primary melanoma explants: plasticity of cell-cell interaction, beta1-integrin function, and migration strategies, Cancer Res 62(7) (2002) 2125-30.

[160] V. Sanz-Moreno, G. Gadea, J. Ahn, H. Paterson, P. Marra, S. Pinner, E. Sahai, C.J. Marshall, Rac activation and inactivation control plasticity of tumor cell movement, Cell 135(3) (2008) 510-23.
[161] N.M. Aiello, R. Maddipati, R.J. Norgard, D. Balli, J. Li, S. Yuan, T. Yamazoe, T. Black, A. Sahmoud, E.E. Furth, D. Bar-Sagi, B.Z. Stanger, EMT Subtype Influences Epithelial Plasticity and Mode of Cell Migration, Dev Cell 45(6) (2018) 681-695 e4.
[162] A. Sadok, C.J. Marshall, Rho GTPases: masters of cell migration, Small GTPases 5 (2014) e29710.
[163] B. Serrels, M.C. Frame, FAK and talin: who is taking whom to the integrin engagement party?, J Cell Biol 196(2) (2012) 185-7.
[164] H.E. Balcioglu, H. van Hoorn, D.M. Donato, T. Schmidt, E.H. Danen, The integrin expression profile modulates orientation and dynamics of force transmission at cell-matrix adhesions, J Cell Sci 128(7) (2015) 1316-26.
[165] P. Gui, M. Ben-Neji, E. Belozertseva, F. Dalenc, C. Franchet, J. Gilhodes, A. Labrousse, E. Bellard, M. Golzio, R. Poincloux, I. Maridonneau-Parini, V. Le Cabec, The Protease-Dependent Mesenchymal Migration of Tumor-Associated Macrophages as a Target in Cancer Immunotherapy, Cancer Immunol Res 6(11) (2018) 1337-1351.
[166] A. Hallou, J. Jennings, A.J. Kabla, Tumour heterogeneity promotes collective invasion and cancer metastatic dissemination, R Soc Open Sci 4(8) (2017) 161007.
[167] P.W. Choi, J. Yang, S.K. Ng, C. Feltmate, M.G. Muto, K. Hasselblatt, K. Lafferty-Whyte, L. JeBailey, L. MacConaill, W.R. Welch, W.P. Fong, R.S. Berkowitz, S.W. Ng, Loss of E-cadherin disrupts ovarian epithelial inclusion cyst formation and collective cell movement in ovarian cancer cells, Oncotarget 7(4) (2016) 4110-21.
[168] R. Mayor, S. Etienne-Manneville, The front and rear of collective cell migration, Nat Rev Mol Cell Biol 17(2) (2016) 97-109.
[169] A. Haeger, S. Alexander, M. Vullings, F.M.P. Kaiser, C. Veelken, U. Flucke, G.E. Koehl, M. Hirschberg, M. Flentje, R.M. Hoffman, E.K. Geissler, S. Kissler, P. Friedl, Collective cancer invasion forms an integrin-dependent radioresistant niche, J Exp Med 217(1) (2020).
[170] L.L. Yin, C.M. Chung, J. Chen, K.L. Fok, C.P. Ng, R.R. Jia, X. Ren, J. Zhou, T. Zhang, X.H. Zhao, M. Lin, H. Zhu, X.H. Zhang, L.L. Tsang, Y. Bi, Z. Zhou, F. Mo, N. Wong, Y.W. Chung, J. Sha, H.C. Chan, A suppressor of multiple extracellular matrix-degrading proteases and cancer metastasis, J Cell Mol Med 13(9B) (2009) 4034-41.
[171] C. Gaggioli, S. Hooper, C. Hidalgo-Carcedo, R. Grosse, J.F. Marshall, K. Harrington, E. Sahai, Fibroblast-led collective invasion of carcinoma cells with differing roles for RhoGTPases in leading and following cells, Nat Cell Biol 9(12) (2007) 1392-400.
[172] E.N. Arwert, A.S. Harney, D. Entenberg, Y. Wang, E. Sahai, J.W. Pollard, J.S. Condeelis, A Unidirectional Transition from Migratory to Perivascular Macrophage Is Required for Tumor Cell Intravasation, Cell Rep 23(5) (2018) 1239-1248.
[173] J.S. Wu, J. Jiang, B.J. Chen, K. Wang, Y.L. Tang, X.H. Liang, Plasticity of cancer cell invasion: Patterns and mechanisms, Transl Oncol 14(1) (2021) 100899.
[174] A. Diz-Munoz, K. Thurley, S. Chintamen, S.J. Altschuler, L.F. Wu, D.A. Fletcher, O.D. Weiner, Membrane Tension Acts Through PLD2 and mTORC2 to Limit Actin Network Assembly During Neutrophil Migration, PLoS Biol 14(6) (2016) e1002474.
[175] Y. Huang, L. Tong, L. Yi, C. Zhang, L. Hai, T. Li, S. Yu, W. Wang, Z. Tao, H. Ma, P. Liu, Y. Xie, X. Yang, Three-dimensional hydrogel is suitable for targeted investigation of amoeboid migration of glioma cells, Mol Med Rep 17(1) (2018) 250-256.
[176] J. Shi, X. Wu, M. Surma, S. Vemula, L. Zhang, Y. Yang, R. Kapur, L. Wei, Distinct roles for ROCK1 and ROCK2 in the regulation of cell detachment, Cell Death Dis 4(2) (2013) e483.
[177] P. Tan, Y. Ye, L. He, J. Xie, J. Jing, G. Ma, H. Pan, L. Han, W. Han, Y. Zhou, TRIM59 promotes breast cancer motility by suppressing p62-selective autophagic degradation of PDCD10, PLoS Biol 16(11) (2018) e3000051.
[178] H.J. Seol, J.H. Chang, J. Yamamoto, R. Romagnuolo, Y. Suh, A. Weeks, S. Agnihotri, C.A. Smith, J.T. Rutka, Overexpression of CD99 Increases the Migration and Invasiveness of Human Malignant Glioma Cells, Genes Cancer 3(9-10) (2012) 535-49.

[179] A.E. Sedgwick, J.W. Clancy, M. Olivia Balmert, C. D'Souza-Schorey, Extracellular microvesicles and invadopodia mediate non-overlapping modes of tumor cell invasion, Sci Rep 5 (2015) 14748.
[180] E. Giannoni, M.L. Taddei, M. Parri, F. Bianchini, M. Santosuosso, R. Grifantini, G. Fibbi, B. Mazzanti, L. Calorini, P. Chiarugi, EphA2-mediated mesenchymal-amoeboid transition induced by endothelial progenitor cells enhances metastatic spread due to cancer-associated fibroblasts, J Mol Med (Berl) 91(1) (2013) 103-15.
[181] A. Cartier-Michaud, M. Malo, C. Charriere-Bertrand, G. Gadea, C. Anguille, A. Supiramaniam, A. Lesne, F. Delaplace, G. Hutzler, P. Roux, D.A. Lawrence, G. Barlovatz-Meimon, Matrix-bound PAI-1 supports cell blebbing via RhoA/ROCK1 signaling, PLoS One 7(2) (2012) e32204.
[182] L. Pietrovito, A. Leo, V. Gori, M. Lulli, M. Parri, V. Becherucci, L. Piccini, F. Bambi, M.L. Taddei, P. Chiarugi, Bone marrow-derived mesenchymal stem cells promote invasiveness and transendothelial migration of osteosarcoma cells via a mesenchymal to amoeboid transition, Mol Oncol 12(5) (2018) 659-676.
[183] A.D. Grigore, M.K. Jolly, D. Jia, M.C. Farach-Carson, H. Levine, Tumor Budding: The Name is EMT. Partial EMT, J Clin Med 5(5) (2016).
[184] L. Kager, A. Zoubek, U. Potschger, U. Kastner, S. Flege, B. Kempf-Bielack, D. Branscheid, R. Kotz, M. Salzer-Kuntschik, W. Winkelmann, G. Jundt, H. Kabisch, P. Reichardt, H. Jurgens, H. Gadner, S.S. Bielack, G. Cooperative German-Austrian-Swiss Osteosarcoma Study, Primary metastatic osteosarcoma: presentation and outcome of patients treated on neoadjuvant Cooperative Osteosarcoma Study Group protocols, J Clin Oncol 21(10) (2003) 2011-8.
[185] J. PosthumaDeBoer, M.A. Witlox, G.J. Kaspers, B.J. van Royen, Molecular alterations as target for therapy in metastatic osteosarcoma: a review of literature, Clin Exp Metastasis 28(5) (2011) 493-503.
[186] C. Zucchini, A. Rocchi, M.C. Manara, P. De Sanctis, C. Capanni, M. Bianchini, P. Carinci, K. Scotlandi, L. Valvassori, Apoptotic genes as potential markers of metastatic phenotype in human osteosarcoma cell lines, Int J Oncol 32(1) (2008) 17-31.
[187] M.D. Cameron, E.E. Schmidt, N. Kerkvliet, K.V. Nadkarni, V.L. Morris, A.C. Groom, A.F. Chambers, I.C. MacDonald, Temporal progression of metastasis in lung: cell survival, dormancy, and location dependence of metastatic inefficiency, Cancer Res 60(9) (2000) 2541-6.
[188] T. Matsubara, G.R. Diresta, S. Kakunaga, D. Li, J.H. Healey, Additive Influence of Extracellular pH, Oxygen Tension, and Pressure on Invasiveness and Survival of Human Osteosarcoma Cells, Front Oncol 3 (2013) 199.
[189] M.M. Lizardo, J.J. Morrow, T.E. Miller, E.S. Hong, L. Ren, A. Mendoza, C.H. Halsey, P.C. Scacheri, L.J. Helman, C. Khanna, Upregulation of Glucose-Regulated Protein 78 in Metastatic Cancer Cells Is Necessary for Lung Metastasis Progression, Neoplasia 18(11) (2016) 699-710.
[190] P. Chaiyawat, P. Sungngam, P. Teeyakasem, N. Sirikaew, J. Klangjorhor, J. Settakorn, P. Diskul-Na-Ayudthaya, D. Chokchaichamnankit, C. Srisomsap, J. Svasti, D. Pruksakorn, Protein profiling of osteosarcoma tissue and soft callus unveils activation of the unfolded protein response pathway, Int J Oncol 54(5) (2019) 1704-1718.
[191] Y. Guo, X. Ji, J. Liu, D. Fan, Q. Zhou, C. Chen, W. Wang, G. Wang, H. Wang, W. Yuan, Z. Ji, Z. Sun, Effects of exosomes on pre-metastatic niche formation in tumors, Mol Cancer 18(1) (2019) 39.
[192] G. Sheng, Y. Gao, Y. Yang, H. Wu, Osteosarcoma and Metastasis, Front Oncol 11 (2021) 780264.
[193] L. Rodriguez Calleja, C. Jacques, F. Lamoureux, M. Baud'huin, M. Tellez Gabriel, T. Quillard, D. Sahay, P. Perrot, J. Amiaud, C. Charrier, R. Brion, F. Lecanda, F. Verrecchia, D. Heymann, L.W. Ellisen, B. Ory, DeltaNp63alpha Silences a miRNA Program to Aberrantly Initiate a Wound-Healing Program That Promotes TGFbeta-Induced Metastasis, Cancer Res 76(11) (2016) 3236-51.
[194] H.K. Bid, R.D. Roberts, M. Cam, A. Audino, R.T. Kurmasheva, J. Lin, P.J. Houghton, H. Cam, DeltaNp63 promotes pediatric neuroblastoma and osteosarcoma by regulating tumor angiogenesis, Cancer Res 74(1) (2014) 320-9.
[195] A.C. Gross, H. Cam, D.A. Phelps, A.J. Saraf, H.K. Bid, M. Cam, C.A. London, S.A. Winget, M.A. Arnold, L. Brandolini, X. Mo, J.M. Hinckley, P.J. Houghton, R.D. Roberts, IL-6 and CXCL8 mediate osteosarcoma-lung interactions critical to metastasis, JCI Insight 3(16) (2018).

[196] W. Zhang, J.M. Zhao, J. Lin, C.Z. Hu, W.B. Zhang, W.L. Yang, J. Zhang, J.W. Zhang, J. Zhu, Adaptive Fibrogenic Reprogramming of Osteosarcoma Stem Cells Promotes Metastatic Growth, Cell Rep 24(5) (2018) 1266-1277 e5.
[197] N.V. Koshkina, C. Khanna, A. Mendoza, H. Guan, L. DeLauter, E.S. Kleinerman, Fas-negative osteosarcoma tumor cells are selected during metastasis to the lungs: the role of the Fas pathway in the metastatic process of osteosarcoma, Mol Cancer Res 5(10) (2007) 991-9.
[198] Y. Araki, H. Aiba, T. Yoshida, N. Yamamoto, K. Hayashi, A. Takeuchi, S. Miwa, K. Igarashi, T.D. Nguyen, K.A. Ishii, T. Nojima, S. Takahashi, H. Murakami, H. Tsuchiya, R. Hanayama, Osteosarcoma-Derived Small Extracellular Vesicles Enhance Tumor Metastasis and Suppress Osteoclastogenesis by miR-146a-5p, Front Oncol 11 (2021) 667109.
[199] J. Wang, H. Zhang, X. Sun, X. Wang, T. Ren, Y. Huang, R. Zhang, B. Zheng, W. Guo, Exosomal PD-L1 and N-cadherin predict pulmonary metastasis progression for osteosarcoma patients, J Nanobiotechnology 18(1) (2020) 151.
[200] R. Macklin, H. Wang, D. Loo, S. Martin, A. Cumming, N. Cai, R. Lane, N.S. Ponce, E. Topkas, K. Inder, N.A. Saunders, L. Endo-Munoz, Extracellular vesicles secreted by highly metastatic clonal variants of osteosarcoma preferentially localize to the lungs and induce metastatic behaviour in poorly metastatic clones, Oncotarget 7(28) (2016) 43570-43587.
[201] W. Zhao, P. Qin, D. Zhang, X. Cui, J. Gao, Z. Yu, Y. Chai, J. Wang, J. Li, Long non-coding RNA PVT1 encapsulated in bone marrow mesenchymal stem cell-derived exosomes promotes osteosarcoma growth and metastasis by stabilizing ERG and sponging miR-183-5p, Aging (Albany NY) 11(21) (2019) 9581-9596.
[202] O. Neklyudova, M.J. Arlt, P. Brennecke, M. Thelen, A. Gvozdenovic, A. Kuzmanov, B. Robl, S.M. Botter, W. Born, B. Fuchs, Altered CXCL12 expression reveals a dual role of CXCR4 in osteosarcoma primary tumor growth and metastasis, J Cancer Res Clin Oncol 142(8) (2016) 1739-50.
[203] E. Goguet-Surmenian, P. Richard-Fiardo, E. Guillemot, M. Benchetrit, A. Gomez-Brouchet, P. Buzzo, B. Karimdjee-Soilihi, P. Alemanno, J.F. Michiels, A. Schmid-Alliana, H. Schmid-Antomarchi, CXCR7-mediated progression of osteosarcoma in the lungs, Br J Cancer 109(6) (2013) 1579-85.
[204] L. Du, X.G. Han, B. Tu, M.Q. Wang, H. Qiao, S.H. Zhang, Q.M. Fan, T.T. Tang, CXCR1/Akt signaling activation induced by mesenchymal stem cell-derived IL-8 promotes osteosarcoma cell anoikis resistance and pulmonary metastasis, Cell Death Dis 9(7) (2018) 714.
[205] Y.X. Liao, Z.Z. Fu, C.H. Zhou, L.C. Shan, Z.Y. Wang, F. Yin, L.P. Zheng, Y.Q. Hua, Z.D. Cai, AMD3100 reduces CXCR4-mediated survival and metastasis of osteosarcoma by inhibiting JNK and Akt, but not p38 or Erk1/2, pathways in in vitro and mouse experiments, Oncol Rep 34(1) (2015) 33-42.
[206] S. Georges, J. Chesneau, S. Hervouet, J. Taurelle, F. Gouin, F. Redini, M. Padrines, D. Heymann, Y. Fortun, F. Verrecchia, A Disintegrin And Metalloproteinase 12 produced by tumour cells accelerates osteosarcoma tumour progression and associated osteolysis, Eur J Cancer 49(9) (2013) 2253-63.
[207] T. Akiyama, P.F. Choong, C.R. Dass, RANK-Fc inhibits malignancy via inhibiting ERK activation and evoking caspase-3-mediated anoikis in human osteosarcoma cells, Clin Exp Metastasis 27(4) (2010) 207-15.
[208] T. Akiyama, C.R. Dass, Y. Shinoda, H. Kawano, S. Tanaka, P.F. Choong, Systemic RANK-Fc protein therapy is efficacious against primary osteosarcoma growth in a murine model via activity against osteoclasts, J Pharm Pharmacol 62(4) (2010) 470-6.
[209] T. Akiyama, C.R. Dass, P.F. Choong, Novel therapeutic strategy for osteosarcoma targeting osteoclast differentiation, bone-resorbing activity, and apoptosis pathway, Mol Cancer Ther 7(11) (2008) 3461-9.
[210] L. Endo-Munoz, A. Cumming, D. Rickwood, D. Wilson, C. Cueva, C. Ng, G. Strutton, A.I. Cassady, A. Evdokiou, S. Sommerville, I. Dickinson, A. Guminski, N.A. Saunders, Loss of osteoclasts contributes to development of osteosarcoma pulmonary metastases, Cancer Res 70(18) (2010) 7063-72.
[211] P. Saharinen, L. Eklund, K. Pulkki, P. Bono, K. Alitalo, VEGF and angiopoietin signaling in tumor angiogenesis and metastasis, Trends Mol Med 17(7) (2011) 347-62.

[212] G. Han, Y. Wang, W. Bi, J. Jia, W. Wang, M. Xu, Effects of vascular endothelial growth factor expression on pathological characteristics and prognosis of osteosarcoma, Clin Exp Med 16(4) (2016) 577-584.
[213] G. Wang, M. Sun, Y. Jiang, T. Zhang, W. Sun, H. Wang, F. Yin, Z. Wang, W. Sang, J. Xu, M. Mao, D. Zuo, Z. Zhou, C. Wang, Z. Fu, Z. Wang, Z. Duan, Y. Hua, Z. Cai, Anlotinib, a novel small molecular tyrosine kinase inhibitor, suppresses growth and metastasis via dual blockade of VEGFR2 and MET in osteosarcoma, Int J Cancer 145(4) (2019) 979-993.
[214] Y. Liu, N. Huang, S. Liao, E. Rothzerg, F. Yao, Y. Li, D. Wood, J. Xu, Current research progress in targeted anti-angiogenesis therapy for osteosarcoma, Cell Prolif 54(9) (2021) e13102.
[215] C. Lehuede, F. Dupuy, R. Rabinovitch, R.G. Jones, P.M. Siegel, Metabolic Plasticity as a Determinant of Tumor Growth and Metastasis, Cancer Res 76(18) (2016) 5201-8.
[216] J. Roy, P. Dibaeinia, T.M. Fan, S. Sinha, A. Das, Global analysis of osteosarcoma lipidomes reveal altered lipid profiles in metastatic versus nonmetastatic cells, J Lipid Res 60(2) (2019) 375-387.
[217] W.J. Kort, W.C. Hulsmann, T.E. Stehman, Modulation of metastatic ability by inhibition of cholesterol synthesis, Clin Exp Metastasis 7(5) (1989) 517-23.
[218] L. Ren, E.S. Hong, A. Mendoza, S. Issaq, C. Tran Hoang, M. Lizardo, A. LeBlanc, C. Khanna, Metabolomics uncovers a link between inositol metabolism and osteosarcoma metastasis, Oncotarget 8(24) (2017) 38541-38553.
[219] H. Zhao, Y. Wu, Y. Chen, H. Liu, Clinical significance of hypoxia-inducible factor 1 and VEGF-A in osteosarcoma, Int J Clin Oncol 20(6) (2015) 1233-43.
[220] A.A. Sabile, M.J. Arlt, R. Muff, B. Bode, B. Langsam, J. Bertz, T. Jentzsch, G.J. Puskas, W. Born, B. Fuchs, Cyr61 expression in osteosarcoma indicates poor prognosis and promotes intratibial growth and lung metastasis in mice, J Bone Miner Res 27(1) (2012) 58-67.
[221] N. Habel, M. Vilalta, O. Bawa, P. Opolon, J. Blanco, O. Fromigue, Cyr61 silencing reduces vascularization and dissemination of osteosarcoma tumors, Oncogene 34(24) (2015) 3207-13.
[222] E. Gaudio, A. Palamarchuk, T. Palumbo, F. Trapasso, Y. Pekarsky, C.M. Croce, R.I. Aqeilan, Physical association with WWOX suppresses c-Jun transcriptional activity, Cancer Res 66(24) (2006) 11585-9.
[223] S. Del Mare, R.I. Aqeilan, Tumor Suppressor WWOX inhibits osteosarcoma metastasis by modulating RUNX2 function, Sci Rep 5 (2015) 12959.
[224] B.W. Ozanne, H.J. Spence, L.C. McGarry, R.F. Hennigan, Transcription factors control invasion: AP-1 the first among equals, Oncogene 26(1) (2007) 1-10.
[225] D. Weekes, T.G. Kashima, C. Zandueta, N. Perurena, D.P. Thomas, A. Sunters, C. Vuillier, A. Bozec, E. El-Emir, I. Miletich, A. Patino-Garcia, F. Lecanda, A.E. Grigoriadis, Regulation of osteosarcoma cell lung metastasis by the c-Fos/AP-1 target FGFR1, Oncogene 35(22) (2016) 2852-61.
[226] S. Avnet, T. Chano, A. Massa, G. Bonuccelli, S. Lemma, L. Falzetti, G. Grisendi, M. Dominici, N. Baldini, Acid microenvironment promotes cell survival of human bone sarcoma through the activation of cIAP proteins and NF-kappaB pathway, Am J Cancer Res 9(6) (2019) 1127-1144.
[227] E.P. Buddingh, M.L. Kuijjer, R.A. Duim, H. Burger, K. Agelopoulos, O. Myklebost, M. Serra, F. Mertens, P.C. Hogendoorn, A.C. Lankester, A.M. Cleton-Jansen, Tumor-infiltrating macrophages are associated with metastasis suppression in high-grade osteosarcoma: a rationale for treatment with macrophage activating agents, Clin Cancer Res 17(8) (2011) 2110-9.
[228] A. Gomez-Brouchet, C. Illac, J. Gilhodes, C. Bouvier, S. Aubert, J.M. Guinebretiere, B. Marie, F. Larousserie, N. Entz-Werle, G. de Pinieux, T. Filleron, V. Minard, V. Minville, E. Mascard, F. Gouin, M. Jimenez, M.C. Ledeley, S. Piperno-Neumann, L. Brugieres, F. Redini, CD163-positive tumor-associated macrophages and CD8-positive cytotoxic lymphocytes are powerful diagnostic markers for the therapeutic stratification of osteosarcoma patients: An immunohistochemical analysis of the biopsies fromthe French OS2006 phase 3 trial, Oncoimmunology 6(9) (2017) e1331193.
[229] X.J. Shao, S.F. Xiang, Y.Q. Chen, N. Zhang, J. Cao, H. Zhu, B. Yang, Q. Zhou, M.D. Ying, Q.J. He, Inhibition of M2-like macrophages by all-trans retinoic acid prevents cancer initiation and stemness in osteosarcoma cells, Acta Pharmacol Sin 40(10) (2019) 1343-1350.

[230] B. Fritzsching, J. Fellenberg, L. Moskovszky, Z. Sapi, T. Krenacs, I. Machado, J. Poeschl, B. Lehner, M. Szendroi, A.L. Bosch, L. Bernd, M. Csoka, G. Mechtersheimer, V. Ewerbeck, R. Kinscherf, P. Kunz, CD8(+)/FOXP3(+)-ratio in osteosarcoma microenvironment separates survivors from non-survivors: a multicenter validated retrospective study, Oncoimmunology 4(3) (2015) e990800.
[231] C. Chen, L. Xie, T. Ren, Y. Huang, J. Xu, W. Guo, Immunotherapy for osteosarcoma: Fundamental mechanism, rationale, and recent breakthroughs, Cancer Lett 500 (2021) 1-10.
[232] D.P. Bartel, MicroRNAs: genomics, biogenesis, mechanism, and function, Cell 116(2) (2004) 281-97.
[233] J.H. Mao, R.P. Zhou, A.F. Peng, Z.L. Liu, S.H. Huang, X.H. Long, Y. Shu, microRNA-195 suppresses osteosarcoma cell invasion and migration in vitro by targeting FASN, Oncol Lett 4(5) (2012) 1125-1129.
[234] F. Lian, Y. Cui, C. Zhou, K. Gao, L. Wu, Identification of a plasma four-microRNA panel as potential noninvasive biomarker for osteosarcoma, PLoS One 10(3) (2015) e0121499.
[235] Z. Salah, R. Arafeh, V. Maximov, M. Galasso, S. Khawaled, S. Abou-Sharieha, S. Volinia, K.B. Jones, C.M. Croce, R.I. Aqeilan, miR-27a and miR-27a* contribute to metastatic properties of osteosarcoma cells, Oncotarget 6(7) (2015) 4920-35.
[236] N. Dai, Z.Y. Zhong, Y.P. Cun, Y. Qing, C. Chen, P. Jiang, M.X. Li, D. Wang, Alteration of the microRNA expression profile in human osteosarcoma cells transfected with APE1 siRNA, Neoplasma 60(4) (2013) 384-94.
[237] Y. Zhang, H. Hu, L. Song, L. Cai, R. Wei, W. Jin, Epirubicin-mediated expression of miR-302b is involved in osteosarcoma apoptosis and cell cycle regulation, Toxicol Lett 222(1) (2013) 1-9.
[238] Y. Li, J. Zhang, L. Zhang, M. Si, H. Yin, J. Li, Diallyl trisulfide inhibits proliferation, invasion and angiogenesis of osteosarcoma cells by switching on suppressor microRNAs and inactivating of Notch-1 signaling, Carcinogenesis 34(7) (2013) 1601-10.
[239] G. Ramazzotti, R. Fiume, F. Chiarini, G. Campana, S. Ratti, A.M. Billi, L. Manzoli, M.Y. Follo, P.G. Suh, J. McCubrey, L. Cocco, I. Faenza, Phospholipase C-beta1 interacts with cyclin E in adipose-derived stem cells osteogenic differentiation, Adv Biol Regul 71 (2019) 1-9.
[240] V.Z. Valeria Marigo, Cellule e Segnali, 2012.
[241] V.R. Lo Vasco, C. Fabrizi, L. Fumagalli, L. Cocco, Expression of phosphoinositide-specific phospholipase C isoenzymes in cultured astrocytes activated after stimulation with lipopolysaccharide, J Cell Biochem 109(5) (2010) 1006-12.
[242] P.G. Suh, J.I. Park, L. Manzoli, L. Cocco, J.C. Peak, M. Katan, K. Fukami, T. Kataoka, S. Yun, S.H. Ryu, Multiple roles of phosphoinositide-specific phospholipase C isozymes, BMB Rep 41(6) (2008) 415-34.
[243] A.R. Abdul Wasai, Phospholipases in Physiology and Pathology, 2023.
[244] A. Gresset, J. Sondek, T.K. Harden, The phospholipase C isozymes and their regulation, Subcell Biochem 58 (2012) 61-94.
[245] V.R. Lo Vasco, M. Leopizzi, C. Della Rocca, Ezrin-related Phosphoinositide pathway modifies RhoA and Rac1 in human osteosarcoma cell lines, J Cell Commun Signal 9(1) (2015) 55-62.
[246] C. Molinari, L. Medri, M.Y. Follo, M. Piazzi, G.A. Mariani, D. Calistri, L. Cocco, PI-PLCbeta1 gene copy number alterations in breast cancer, Oncol Rep 27(2) (2012) 403-8.
[247] C.A. Sengelaub, K. Navrazhina, J.B. Ross, N. Halberg, S.F. Tavazoie, PTPRN2 and PLCbeta1 promote metastatic breast cancer cell migration through PI(4,5)P2-dependent actin remodeling, EMBO J 35(1) (2016) 62-76.
[248] J.T. Snyder, A.U. Singer, M.R. Wing, T.K. Harden, J. Sondek, The pleckstrin homology domain of phospholipase C-beta2 as an effector site for Rac, J Biol Chem 278(23) (2003) 21099-104.
[249] G. Mao, J. Jin, S.P. Kunapuli, A.K. Rao, Nuclear factor-kappaB regulates expression of platelet phospholipase C-beta2 (PLCB2), Thromb Haemost 116(5) (2016) 931-940.
[250] H. Zhang, T. Xie, Y. Shui, Y. Qi, Knockdown of PLCB2 expression reduces melanoma cell viability and promotes melanoma cell apoptosis by altering Ras/Raf/MAPK signals, Mol Med Rep 21(1) (2020) 420-428.

[251] V. Bertagnolo, M. Benedusi, F. Brugnoli, P. Lanuti, M. Marchisio, P. Querzoli, S. Capitani, Phospholipase C-beta 2 promotes mitosis and migration of human breast cancer-derived cells, Carcinogenesis 28(8) (2007) 1638-45.
[252] K.N. Phoenix, Z. Yue, L. Yue, C.G. Cronin, B.T. Liang, L.H. Hoeppner, K.P. Claffey, PLCbeta2 Promotes VEGF-Induced Vascular Permeability, Arterioscler Thromb Vasc Biol 42(10) (2022) 1229-1241.
[253] S. Wang, D. Xie, H. Yue, G. Li, B. Jiang, Y. Gao, Z. Zheng, X. Zheng, G. Wu, Phospholipase C Beta 2 as a Key Regulator of Tumor Progression and Epithelial-Mesenchymal Transition via PI3K/AKT Signaling in Renal Cell Carcinoma, Biomedicines 13(2) (2025).
[254] M. Hoberg, H.H. Gratz, M. Noll, D.B. Jones, Mechanosensitivity of human osteosarcoma cells and phospholipase C beta2 expression, Biochem Biophys Res Commun 333(1) (2005) 142-9.
[255] E. Siraliev-Perez, J.T.B. Stariha, R.M. Hoffmann, B.R.S. Temple, Q. Zhang, N. Hajicek, M.L. Jenkins, J.E. Burke, J. Sondek, Dynamics of allosteric regulation of the phospholipase C-gamma isozymes upon recruitment to membranes, Elife 11 (2022).
[256] Y.S. Bae, L.G. Cantley, C.S. Chen, S.R. Kim, K.S. Kwon, S.G. Rhee, Activation of phospholipase C-gamma by phosphatidylinositol 3,4,5-trisphosphate, J Biol Chem 273(8) (1998) 4465-9.
[257] C. Raimondi, M. Falasca, Phosphoinositides signalling in cancer: focus on PI3K and PLC, Adv Biol Regul 52(1) (2012) 166-82.
[258] S. Mandal, S. Bandyopadhyay, K. Tyagi, A. Roy, Recent advances in understanding the molecular role of phosphoinositide-specific phospholipase C gamma 1 as an emerging onco-driver and novel therapeutic target in human carcinogenesis, Biochim Biophys Acta Rev Cancer 1876(2) (2021) 188619.
[259] Q.S. Ji, G.E. Winnier, K.D. Niswender, D. Horstman, R. Wisdom, M.A. Magnuson, G. Carpenter, Essential role of the tyrosine kinase substrate phospholipase C-gamma1 in mammalian growth and development, Proc Natl Acad Sci U S A 94(7) (1997) 2999-3003.
[260] G.A. Gonzalez-Conchas, L. Rodriguez-Romo, D. Hernandez-Barajas, J.F. Gonzalez-Guerrero, I.A. Rodriguez-Fernandez, A. Verdines-Perez, A.J. Templeton, A. Ocana, B. Seruga, I.F. Tannock, E. Amir, F.E. Vera-Badillo, Epidermal growth factor receptor overexpression and outcomes in early breast cancer: A systematic review and a meta-analysis, Cancer Treat Rev 62 (2018) 1-8.
[261] B. Jiang, J. Chen, W. Yuan, J. Ji, Z. Liu, L. Wu, Q. Tang, X. Shu, Platelet-derived growth factor-D promotes colorectal cancer cell migration, invasion and proliferation by regulating Notch1 and matrix metalloproteinase-9, Oncol Lett 15(2) (2018) 1573-1579.
[262] J.B. Park, C.S. Lee, J.H. Jang, J. Ghim, Y.J. Kim, S. You, D. Hwang, P.G. Suh, S.H. Ryu, Phospholipase signalling networks in cancer, Nat Rev Cancer 12(11) (2012) 782-92.
[263] G. Mouneimne, L. Soon, V. DesMarais, M. Sidani, X. Song, S.C. Yip, M. Ghosh, R. Eddy, J.M. Backer, J. Condeelis, Phospholipase C and cofilin are required for carcinoma cell directionality in response to EGF stimulation, J Cell Biol 166(5) (2004) 697-708.
[264] J.C. Peak, N.P. Jones, S. Hobbs, M. Katan, S.A. Eccles, Phospholipase C gamma 1 regulates the Rap GEF1-Rap1 signalling axis in the control of human prostate carcinoma cell adhesion, Oncogene 27(20) (2008) 2823-32.
[265] H. Nozawa, G. Howell, S. Suzuki, Q. Zhang, Y. Qi, J. Klein-Seetharaman, A. Wells, J.R. Grandis, S.M. Thomas, Combined inhibition of PLCgamma-1 and c-Src abrogates epidermal growth factor receptor-mediated head and neck squamous cell carcinoma invasion, Clin Cancer Res 14(13) (2008) 4336-44.
[266] Y. Ou, L. Ma, L. Dong, L. Ma, Z. Zhao, L. Ma, W. Zhou, J. Fan, C. Wu, C. Yu, Q. Zhan, Y. Song, Migfilin protein promotes migration and invasion in human glioma through epidermal growth factor receptor-mediated phospholipase C-gamma and STAT3 protein signaling pathways, J Biol Chem 287(39) (2012) 32394-405.
[267] L.M. Balz, K. Bartkowiak, A. Andreas, K. Pantel, B. Niggemann, K.S. Zanker, B.H. Brandt, T. Dittmar, The interplay of HER2/HER3/PI3K and EGFR/HER2/PLC-gamma1 signalling in breast cancer cell migration and dissemination, J Pathol 227(2) (2012) 234-44.

[268] S.Y. Park, X. Shi, J. Pang, C. Yan, B.C. Berk, Thioredoxin-interacting protein mediates sustained VEGFR2 signaling in endothelial cells required for angiogenesis, Arterioscler Thromb Vasc Biol 33(4) (2013) 737-43.
[269] M. Kostas, E.M. Haugsten, Y. Zhen, V. Sorensen, P. Szybowska, E. Fiorito, S. Lorenz, N. Jones, G.A. de Souza, A. Wiedlocha, J. Wesche, Protein Tyrosine Phosphatase Receptor Type G (PTPRG) Controls Fibroblast Growth Factor Receptor (FGFR) 1 Activity and Influences Sensitivity to FGFR Kinase Inhibitors, Mol Cell Proteomics 17(5) (2018) 850-870.
[270] J.T. Jackson, E. Mulazzani, S.L. Nutt, S.L. Masters, The role of PLCgamma2 in immunological disorders, cancer, and neurodegeneration, J Biol Chem 297(2) (2021) 100905.
[271] M. Katan, R. Rodriguez, M. Matsuda, Y.M. Newbatt, G.W. Aherne, Structural and mechanistic aspects of phospholipase Cgamma regulation, Adv Enzyme Regul 43 (2003) 77-85.
[272] R. Lattanzio, M. Piantelli, M. Falasca, Role of phospholipase C in cell invasion and metastasis, Adv Biol Regul 53(3) (2013) 309-18.
[273] R. Faccio, V. Cremasco, PLCgamma2: where bone and immune cells find their common ground, Ann N Y Acad Sci 1192 (2010) 124-30.
[274] H. Epple, V. Cremasco, K. Zhang, D. Mao, G.D. Longmore, R. Faccio, Phospholipase Cgamma2 modulates integrin signaling in the osteoclast by affecting the localization and activation of Src kinase, Mol Cell Biol 28(11) (2008) 3610-22.
[275] W.J. Smith, N. Nassar, A. Bretscher, R.A. Cerione, P.A. Karplus, Structure of the active N-terminal domain of Ezrin. Conformational and mobility changes identify keystone interactions, J Biol Chem 278(7) (2003) 4949-56.
[276] L. Heiska, K. Alfthan, M. Gronholm, P. Vilja, A. Vaheri, O. Carpen, Association of ezrin with intercellular adhesion molecule-1 and -2 (ICAM-1 and ICAM-2). Regulation by phosphatidylinositol 4, 5-bisphosphate, J Biol Chem 273(34) (1998) 21893-900.
[277] Y. Song, X. Ma, M. Zhang, M. Wang, G. Wang, Y. Ye, W. Xia, Ezrin Mediates Invasion and Metastasis in Tumorigenesis: A Review, Front Cell Dev Biol 8 (2020) 588801.
[278] C. Khanna, X. Wan, S. Bose, R. Cassaday, O. Olomu, A. Mendoza, C. Yeung, R. Gorlick, S.M. Hewitt, L.J. Helman, The membrane-cytoskeleton linker ezrin is necessary for osteosarcoma metastasis, Nat Med 10(2) (2004) 182-6.
[279] T.S. Yeh, J.H. Tseng, N.J. Liu, T.C. Chen, Y.Y. Jan, M.F. Chen, Significance of cellular distribution of ezrin in pancreatic cystic neoplasms and ductal adenocarcinoma, Arch Surg 140(12) (2005) 1184-90.
[280] N. Akisawa, I. Nishimori, T. Iwamura, S. Onishi, M.A. Hollingsworth, High levels of ezrin expressed by human pancreatic adenocarcinoma cell lines with high metastatic potential, Biochem Biophys Res Commun 258(2) (1999) 395-400.
[281] G. Bulut, S.H. Hong, K. Chen, E.M. Beauchamp, S. Rahim, G.W. Kosturko, E. Glasgow, S. Dakshanamurthy, H.S. Lee, I. Daar, J.A. Toretsky, C. Khanna, A. Uren, Small molecule inhibitors of ezrin inhibit the invasive phenotype of osteosarcoma cells, Oncogene 31(3) (2012) 269-81.
[282] K.F. Tolias, J.H. Hartwig, H. Ishihara, Y. Shibasaki, L.C. Cantley, C.L. Carpenter, Type Ialpha phosphatidylinositol-4-phosphate 5-kinase mediates Rac-dependent actin assembly, Curr Biol 10(3) (2000) 153-6.
[283] C. Barret, C. Roy, P. Montcourrier, P. Mangeat, V. Niggli, Mutagenesis of the phosphatidylinositol 4,5-bisphosphate (PIP(2)) binding site in the NH(2)-terminal domain of ezrin correlates with its altered cellular distribution, J Cell Biol 151(5) (2000) 1067-80.
[284] J.J. Hao, Y. Liu, M. Kruhlak, K.E. Debell, B.L. Rellahan, S. Shaw, Phospholipase C-mediated hydrolysis of PIP2 releases ERM proteins from lymphocyte membrane, J Cell Biol 184(3) (2009) 451-62.
[285] A. Gautreau, P. Poullet, D. Louvard, M. Arpin, Ezrin, a plasma membrane-microfilament linker, signals cell survival through the phosphatidylinositol 3-kinase/Akt pathway, Proc Natl Acad Sci U S A 96(13) (1999) 7300-5.
[286] V.L. Bonilha, S.C. Finnemann, E. Rodriguez-Boulan, Ezrin promotes morphogenesis of apical microvilli and basal infoldings in retinal pigment epithelium, J Cell Biol 147(7) (1999) 1533-48.

[287] P. Pujuguet, L. Del Maestro, A. Gautreau, D. Louvard, M. Arpin, Ezrin regulates E-cadherin-dependent adherens junction assembly through Rac1 activation, Mol Biol Cell 14(5) (2003) 2181-91.
[288] H. Zhao, H. Shiue, S. Palkon, Y. Wang, P. Cullinan, J.K. Burkhardt, M.W. Musch, E.B. Chang, J.R. Turner, Ezrin regulates NHE3 translocation and activation after Na+-glucose cotransport, Proc Natl Acad Sci U S A 101(25) (2004) 9485-90.
[289] T. Grune, T. Reinheckel, J.A. North, R. Li, P.B. Bescos, R. Shringarpure, K.J. Davies, Ezrin turnover and cell shape changes catalyzed by proteasome in oxidatively stressed cells, FASEB J 16(12) (2002) 1602-10.
[290] Y. Yu, J. Khan, C. Khanna, L. Helman, P.S. Meltzer, G. Merlino, Expression profiling identifies the cytoskeletal organizer ezrin and the developmental homeoprotein Six-1 as key metastatic regulators, Nat Med 10(2) (2004) 175-81.
[291] X. Wan, A. Mendoza, C. Khanna, L.J. Helman, Rapamycin inhibits ezrin-mediated metastatic behavior in a murine model of osteosarcoma, Cancer Res 65(6) (2005) 2406-11.
[292] V.R. Lo Vasco, M. Leopizzi, D. Stoppoloni, C. Della Rocca, Silencing of phosphoinositide-specific phospholipase C epsilon remodulates the expression of the phosphoinositide signal transduction pathway in human osteosarcoma cell lines, Anticancer Res 34(8) (2014) 4069-75.
[293] V.R. Lo Vasco, M. Leopizzi, C. Puggioni, C. Della Rocca, Ezrin silencing remodulates the expression of Phosphoinositide-specific Phospholipase C enzymes in human osteosarcoma cell lines, J Cell Commun Signal 8(3) (2014) 219-29.
[294] E. Auvinen, N. Kivi, A. Vaheri, Regulation of ezrin localization by Rac1 and PIPK in human epithelial cells, Exp Cell Res 313(4) (2007) 824-33.
[295] J.E. Bleasdale, N.R. Thakur, R.S. Gremban, G.L. Bundy, F.A. Fitzpatrick, R.J. Smith, S. Bunting, Selective inhibition of receptor-coupled phospholipase C-dependent processes in human platelets and polymorphonuclear neutrophils, J Pharmacol Exp Ther 255(2) (1990) 756-68.
[296] R.R. Klein, D.M. Bourdon, C.L. Costales, C.D. Wagner, W.L. White, J.D. Williams, S.N. Hicks, J. Sondek, D.R. Thakker, Direct activation of human phospholipase C by its well known inhibitor u73122, J Biol Chem 286(14) (2011) 12407-16.
[297] N.E. Wilsher, W.J. Court, R. Ruddle, Y.M. Newbatt, W. Aherne, P.W. Sheldrake, N.P. Jones, M. Katan, S.A. Eccles, F.I. Raynaud, The phosphoinositide-specific phospholipase C inhibitor U73122 (1-(6-((17beta-3-methoxyestra-1,3,5(10)-trien-17-yl)amino)hexyl)-1H-pyrrole-2,5-dione) spontaneously forms conjugates with common components of cell culture medium, Drug Metab Dispos 35(7) (2007) 1017-22.
[298] B. Cenni, D. Picard, Two compounds commonly used for phospholipase C inhibition activate the nuclear estrogen receptors, Biochem Biophys Res Commun 261(2) (1999) 340-4.
[299] C. Hellberg, L. Molony, L. Zheng, T. Andersson, Ca2+ signalling mechanisms of the beta 2 integrin on neutrophils: involvement of phospholipase C gamma 2 and Ins(1,4,5)P3, Biochem J 317 (Pt 2)(Pt 2) (1996) 403-9.
[300] S.A. Hughes, W.J. Gibson, J.M. Young, The interaction of U-73122 with the histamine H1 receptor: implications for the use of U-73122 in defining H1 receptor-coupled signalling pathways, Naunyn Schmiedebergs Arch Pharmacol 362(6) (2000) 555-8.
[301] V.R. Lo Vasco, M. Leopizzi, V. Di Maio, C. Della Rocca, U-73122 reduces the cell growth in cultured MG-63 ostesarcoma cell line involving Phosphoinositide-specific Phospholipases C, Springerplus 5 (2016) 156.

[1] L. Mirabello, R.J. Troisi, S.A. Savage, International osteosarcoma incidence patterns in children and adolescents, middle ages and elderly persons, Int J Cancer 125(1) (2009) 229-34.
[2] D.S. Geller, R. Gorlick, Osteosarcoma: a review of diagnosis, management, and treatment strategies, Clin Adv Hematol Oncol 8(10) (2010) 705-18.
[3] A. Misaghi, A. Goldin, M. Awad, A.A. Kulidjian, Osteosarcoma: a comprehensive review, SICOT J 4 (2018) 12.
[4] Z.S. Kundu, Classification, imaging, biopsy and staging of osteosarcoma, Indian J Orthop 48(3) (2014) 238-46.
[5] G. Ottaviani, N. Jaffe, The epidemiology of osteosarcoma, Cancer Treat Res 152 (2009) 3-13.

[6] J. Gill, R. Gorlick, Advancing therapy for osteosarcoma, Nat Rev Clin Oncol 18(10) (2021) 609-624.
[7] S.M. Botter, D. Neri, B. Fuchs, Recent advances in osteosarcoma, Curr Opin Pharmacol 16 (2014) 15-23.
[8] L. Marchandet, M. Lallier, C. Charrier, M. Baud'huin, B. Ory, F. Lamoureux, Mechanisms of Resistance to Conventional Therapies for Osteosarcoma, Cancers (Basel) 13(4) (2021).
[9] W.F. Flintoff, H. Sadlish, R. Gorlick, R. Yang, F.M. Williams, Functional analysis of altered reduced folate carrier sequence changes identified in osteosarcomas, Biochim Biophys Acta 1690(2) (2004) 110-7.
[10] R. Gorlick, P. Anderson, I. Andrulis, C. Arndt, G.P. Beardsley, M. Bernstein, J. Bridge, N.K. Cheung, J.S. Dome, D. Ebb, T. Gardner, M. Gebhardt, H. Grier, M. Hansen, J. Healey, L. Helman, J. Hock, J. Houghton, P. Houghton, A. Huvos, C. Khanna, M. Kieran, E. Kleinerman, M. Ladanyi, C. Lau, D. Malkin, N. Marina, P. Meltzer, P. Meyers, D. Schofield, C. Schwartz, M.A. Smith, J. Toretsky, M. Tsokos, L. Wexler, J. Wigginton, S. Withrow, M. Schoenfeldt, B. Anderson, Biology of childhood osteogenic sarcoma and potential targets for therapeutic development: meeting summary, Clin Cancer Res 9(15) (2003) 5442-53.
[11] C.M. Gomes, H. van Paassen, S. Romeo, M.M. Welling, R.I. Feitsma, A.J. Abrunhosa, M.F. Botelho, P.C. Hogendoorn, E. Pauwels, A.M. Cleton-Jansen, Multidrug resistance mediated by ABC transporters in osteosarcoma cell lines: mRNA analysis and functional radiotracer studies, Nucl Med Biol 33(7) (2006) 831-40.
[12] M. D'Incalci, N. Badri, C.M. Galmarini, P. Allavena, Trabectedin, a drug acting on both cancer cells and the tumour microenvironment, Br J Cancer 111(4) (2014) 646-50.
[13] A.J. Chou, R. Gorlick, Chemotherapy resistance in osteosarcoma: current challenges and future directions, Expert Rev Anticancer Ther 6(7) (2006) 1075-85.
[14] T. Rajkumar, M. Yamuna, Multiple pathways are involved in drug resistance to doxorubicin in an osteosarcoma cell line, Anticancer Drugs 19(3) (2008) 257-65.
[15] A. Nguyen, C. Lasthaus, E. Guerin, L. Marcellin, E. Pencreach, M.P. Gaub, D. Guenot, N. Entz-Werle, Role of Topoisomerases in Pediatric High Grade Osteosarcomas: TOP2A Gene Is One of the Unique Molecular Biomarkers of Chemoresponse, Cancers (Basel) 5(2) (2013) 662-75.
[16] M. Fanelli, E. Tavanti, M.P. Patrizio, S. Vella, A. Fernandez-Ramos, F. Magagnoli, S. Luppi, C.M. Hattinger, M. Serra, Cisplatin Resistance in Osteosarcoma: In vitro Validation of Candidate DNA Repair-Related Therapeutic Targets and Drugs for Tailored Treatments, Front Oncol 10 (2020) 331.
[17] C.M. Hattinger, M.P. Patrizio, L. Fantoni, C. Casotti, C. Riganti, M. Serra, Drug Resistance in Osteosarcoma: Emerging Biomarkers, Therapeutic Targets and Treatment Strategies, Cancers (Basel) 13(12) (2021).
[18] M. Kovac, C. Blattmann, S. Ribi, J. Smida, N.S. Mueller, F. Engert, F. Castro-Giner, J. Weischenfeldt, M. Kovacova, A. Krieg, D. Andreou, P.U. Tunn, H.R. Durr, H. Rechl, K.D. Schaser, I. Melcher, S. Burdach, A. Kulozik, K. Specht, K. Heinimann, S. Fulda, S. Bielack, G. Jundt, I. Tomlinson, J.O. Korbel, M. Nathrath, D. Baumhoer, Exome sequencing of osteosarcoma reveals mutation signatures reminiscent of BRCA deficiency, Nat Commun 6 (2015) 8940.
[19] H.J. Park, J.S. Bae, K.M. Kim, Y.J. Moon, S.H. Park, S.H. Ha, U.K. Hussein, Z. Zhang, H.S. Park, B.H. Park, W.S. Moon, J.R. Kim, K.Y. Jang, The PARP inhibitor olaparib potentiates the effect of the DNA damaging agent doxorubicin in osteosarcoma, J Exp Clin Cancer Res 37(1) (2018) 107.
[20] J. Fellenberg, M.J. Dechant, V. Ewerbeck, H. Mau, Identification of drug-regulated genes in osteosarcoma cells, Int J Cancer 105(5) (2003) 636-43.
[21] Y. Suehara, D. Alex, A. Bowman, S. Middha, A. Zehir, D. Chakravarty, L. Wang, G. Jour, K. Nafa, T. Hayashi, A.A. Jungbluth, D. Frosina, E. Slotkin, N. Shukla, P. Meyers, J.H. Healey, M. Hameed, M. Ladanyi, Clinical Genomic Sequencing of Pediatric and Adult Osteosarcoma Reveals Distinct Molecular Subsets with Potentially Targetable Alterations, Clin Cancer Res 25(21) (2019) 6346-6356.
[22] S. Iwata, Y. Tatsumi, T. Yonemoto, A. Araki, M. Itami, H. Kamoda, T. Tsukanishi, Y. Hagiwara, H. Kinoshita, T. Ishii, H. Nagase, M. Ohira, CDK4 overexpression is a predictive biomarker for resistance to conventional chemotherapy in patients with osteosarcoma, Oncol Rep 46(1) (2021).

[23] Y. Zhou, J.K. Shen, Z. Yu, F.J. Hornicek, Q. Kan, Z. Duan, Expression and therapeutic implications of cyclin-dependent kinase 4 (CDK4) in osteosarcoma, Biochim Biophys Acta Mol Basis Dis 1864(5 Pt A) (2018) 1573-1582.
[24] T. Higuchi, N. Sugisawa, K. Miyake, H. Oshiro, N. Yamamoto, K. Hayashi, H. Kimura, S. Miwa, K. Igarashi, S.P. Chawla, M. Bouvet, S.R. Singh, H. Tsuchiya, R.M. Hoffman, Sorafenib and Palbociclib Combination Regresses a Cisplatinum-resistant Osteosarcoma in a PDOX Mouse Model, Anticancer Res 39(8) (2019) 4079-4084.
[25] W. Xu, Z. Li, X. Zhu, R. Xu, Y. Xu, miR-29 Family Inhibits Resistance to Methotrexate and Promotes Cell Apoptosis by Targeting COL3A1 and MCL1 in Osteosarcoma, Med Sci Monit 24 (2018) 8812-8821.
[26] E.C. Watson, L. Whitehead, R.H. Adams, G. Dewson, L. Coultas, Endothelial cell survival during angiogenesis requires the pro-survival protein MCL1, Cell Death Differ 23(8) (2016) 1371-9.
[27] B.S. Moriarity, G.M. Otto, E.P. Rahrmann, S.K. Rathe, N.K. Wolf, M.T. Weg, L.A. Manlove, R.S. LaRue, N.A. Temiz, S.D. Molyneux, K. Choi, K.J. Holly, A.L. Sarver, M.C. Scott, C.L. Forster, J.F. Modiano, C. Khanna, S.M. Hewitt, R. Khokha, Y. Yang, R. Gorlick, M.A. Dyer, D.A. Largaespada, A Sleeping Beauty forward genetic screen identifies new genes and pathways driving osteosarcoma development and metastasis, Nat Genet 47(6) (2015) 615-24.
[28] M. Kansara, M.W. Teng, M.J. Smyth, D.M. Thomas, Translational biology of osteosarcoma, Nat Rev Cancer 14(11) (2014) 722-35.
[29] Y.H. Lin, B.E. Jewell, J. Gingold, L. Lu, R. Zhao, L.L. Wang, D.F. Lee, Osteosarcoma: Molecular Pathogenesis and iPSC Modeling, Trends Mol Med 23(8) (2017) 737-755.
[30] X. Chen, A. Bahrami, A. Pappo, J. Easton, J. Dalton, E. Hedlund, D. Ellison, S. Shurtleff, G. Wu, L. Wei, M. Parker, M. Rusch, P. Nagahawatte, J. Wu, S. Mao, K. Boggs, H. Mulder, D. Yergeau, C. Lu, L. Ding, M. Edmonson, C. Qu, J. Wang, Y. Li, F. Navid, N.C. Daw, E.R. Mardis, R.K. Wilson, J.R. Downing, J. Zhang, M.A. Dyer, P. St. Jude Children's Research Hospital-Washington University Pediatric Cancer Genome, Recurrent somatic structural variations contribute to tumorigenesis in pediatric osteosarcoma, Cell Rep 7(1) (2014) 104-12.
[31] S. Lorenz, T. Baroy, J. Sun, T. Nome, D. Vodak, J.C. Bryne, A.M. Hakelien, L. Fernandez-Cuesta, B. Mohlendick, H. Rieder, K. Szuhai, O. Zaikova, T.C. Ahlquist, G.O. Thomassen, R.I. Skotheim, R.A. Lothe, P.S. Tarpey, P. Campbell, A. Flanagan, O. Myklebost, L.A. Meza-Zepeda, Unscrambling the genomic chaos of osteosarcoma reveals extensive transcript fusion, recurrent rearrangements and frequent novel TP53 aberrations, Oncotarget 7(5) (2016) 5273-88.
[32] M.P. Yavropoulou, J.G. Yovos, The role of the Wnt signaling pathway in osteoblast commitment and differentiation, Hormones (Athens) 6(4) (2007) 279-94.
[33] C.H. Lin, Y. Guo, S. Ghaffar, P. McQueen, J. Pourmorady, A. Christ, K. Rooney, T. Ji, R. Eskander, X. Zi, B.H. Hoang, Dkk-3, a secreted wnt antagonist, suppresses tumorigenic potential and pulmonary metastasis in osteosarcoma, Sarcoma 2013 (2013) 147541.
[34] M. Kansara, M. Tsang, L. Kodjabachian, N.A. Sims, M.K. Trivett, M. Ehrich, A. Dobrovic, J. Slavin, P.F. Choong, P.J. Simmons, I.B. Dawid, D.M. Thomas, Wnt inhibitory factor 1 is epigenetically silenced in human osteosarcoma, and targeted disruption accelerates osteosarcomagenesis in mice, J Clin Invest 119(4) (2009) 837-51.
[35] J. Yang, M. Kitami, H. Pan, M.T. Nakamura, H. Zhang, F. Liu, L. Zhu, Y. Komatsu, Y. Mishina, Augmented BMP signaling commits cranial neural crest cells to a chondrogenic fate by suppressing autophagic beta-catenin degradation, Sci Signal 14(665) (2021).
[36] H. Lin, T. Wu, L. Peng, W. Su, Y. Wang, X. Li, Q. Liu, C. Zhong, J. Huang, B. Wei, Lnc-MAP6-1:3 knockdown inhibits osteosarcoma progression by modulating Bax/Bcl-2 and Wnt/beta-catenin pathways, Int J Med Sci 17(15) (2020) 2248-2256.
[37] M. Enomoto, S. Hayakawa, S. Itsukushima, D.Y. Ren, M. Matsuo, K. Tamada, C. Oneyama, M. Okada, T. Takumi, M. Nishita, Y. Minami, Autonomous regulation of osteosarcoma cell invasiveness by Wnt5a/Ror2 signaling, Oncogene 28(36) (2009) 3197-208.
[38] K. van Loon, E.J.M. Huijbers, A.W. Griffioen, Secreted frizzled-related protein 2: a key player in noncanonical Wnt signaling and tumor angiogenesis, Cancer Metastasis Rev 40(1) (2021) 191-203.

[39] L. Li, L. Hobson, L. Perry, B. Clark, S. Heavey, A. Haider, A. Sridhar, G. Shaw, J. Kelly, A. Freeman, I. Wilson, H. Whitaker, E. Nurmemmedov, S. Oltean, S. Porazinski, M. Ladomery, Targeting the ERG oncogene with splice-switching oligonucleotides as a novel therapeutic strategy in prostate cancer, Br J Cancer 123(6) (2020) 1024-1032.
[40] E. Peixoto, S. Richard, K. Pant, A. Biswas, S.A. Gradilone, The primary cilium: Its role as a tumor suppressor organelle, Biochem Pharmacol 175 (2020) 113906.
[41] W. Yang, X. Liu, E. Choy, H. Mankin, F.J. Hornicek, Z. Duan, Targeting hedgehog-GLI-2 pathway in osteosarcoma, J Orthop Res 31(3) (2013) 502-9.
[42] F.C. Kelleher, J.E. Cain, J.M. Healy, D.N. Watkins, D.M. Thomas, Prevailing importance of the hedgehog signaling pathway and the potential for treatment advancement in sarcoma, Pharmacol Ther 136(2) (2012) 153-68.
[43] J. Reichrath, S. Reichrath, Notch Signaling in Prevention And Therapy: Fighting Cancer with a Two-Sided Sword, Adv Exp Med Biol 1287 (2021) 1-7.
[44] E.A. Kolb, R. Gorlick, S.T. Keir, J.M. Maris, R. Lock, H. Carol, R.T. Kurmasheva, C.P. Reynolds, M.H. Kang, J. Wu, P.J. Houghton, M.A. Smith, Initial testing (stage 1) by the pediatric preclinical testing program of RO4929097, a gamma-secretase inhibitor targeting notch signaling, Pediatr Blood Cancer 58(5) (2012) 815-8.
[45] G. Grignani, E. Palmerini, V. Ferraresi, L. D'Ambrosio, R. Bertulli, S.D. Asaftei, A. Tamburini, Y. Pignochino, D. Sangiolo, E. Marchesi, F. Capozzi, R. Biagini, M. Gambarotti, F. Fagioli, P.G. Casali, P. Picci, S. Ferrari, M. Aglietta, G. Italian Sarcoma, Sorafenib and everolimus for patients with unresectable high-grade osteosarcoma progressing after standard treatment: a non-randomised phase 2 clinical trial, Lancet Oncol 16(1) (2015) 98-107.
[46] P. Frankel, C. Ruel, A. Uche, E. Choy, S. Okuno, N. Somiah, W.A. Chow, Pazopanib in Patients with Osteosarcoma Metastatic to the Lung: Phase 2 Study Results and the Lessons for Tumor Measurement, J Oncol 2022 (2022) 3691025.
[47] Y. Liu, Y.H. Ma, Z.Z. Sun, Y.J. Rui, Q.D. Yin, S. Song, X.M. Wei, J. Liu, X.G. Liu, K.J. Hu, Effect of c-erbB2 overexpression on prognosis in osteosarcoma: evidence from eight studies, Tumour Biol 35(9) (2014) 8939-43.
[48] D. Ebb, P. Meyers, H. Grier, M. Bernstein, R. Gorlick, S.E. Lipshultz, M. Krailo, M. Devidas, D.A. Barkauskas, G.P. Siegal, W.S. Ferguson, G.D. Letson, K. Marcus, A. Goorin, P. Beardsley, N. Marina, Phase II trial of trastuzumab in combination with cytotoxic chemotherapy for treatment of metastatic osteosarcoma with human epidermal growth factor receptor 2 overexpression: a report from the children's oncology group, J Clin Oncol 30(20) (2012) 2545-51.
[49] N. Hay, N. Sonenberg, Upstream and downstream of mTOR, Genes Dev 18(16) (2004) 1926-45.
[50] C. Porta, C. Paglino, A. Mosca, Targeting PI3K/Akt/mTOR Signaling in Cancer, Front Oncol 4 (2014) 64.
[51] Z. Ji, J. Shen, Y. Lan, Q. Yi, H. Liu, Targeting signaling pathways in osteosarcoma: Mechanisms and clinical studies, MedComm (2020) 4(4) (2023) e308.
[52] L. Ding, L. Congwei, Q. Bei, Y. Tao, W. Ruiguo, Y. Heze, D. Bo, L. Zhihong, mTOR: An attractive therapeutic target for osteosarcoma?, Oncotarget 7(31) (2016) 50805-50813.
[53] L. Liu, C.A. Parent, Review series: TOR kinase complexes and cell migration, J Cell Biol 194(6) (2011) 815-24.
[54] D. Tewari, P. Patni, A. Bishayee, A.N. Sah, A. Bishayee, Natural products targeting the PI3K-Akt-mTOR signaling pathway in cancer: A novel therapeutic strategy, Semin Cancer Biol 80 (2022) 1-17.
[55] W. Yu, P.B. Chen, F.C. Chen, S.L. Ding, X.Y. Pan, MicroRNA-744 promotes proliferation of osteosarcoma cells by targeting PTEN, Mol Med Rep 21(5) (2020) 2276-2282.
[56] Y. Sukawa, H. Yamamoto, K. Nosho, H. Kunimoto, H. Suzuki, Y. Adachi, M. Nakazawa, T. Nobuoka, M. Kawayama, M. Mikami, T. Matsuno, T. Hasegawa, K. Hirata, K. Imai, Y. Shinomura, Alterations in the human epidermal growth factor receptor 2-phosphatidylinositol 3-kinase-v-Akt pathway in gastric cancer, World J Gastroenterol 18(45) (2012) 6577-86.
[57] M. Zhuang, X. Qiu, D. Cheng, C. Zhu, L. Chen, MicroRNA-524 promotes cell proliferation by down-regulating PTEN expression in osteosarcoma, Cancer Cell Int 18 (2018) 114.

[58] G.D. Demetri, S.P. Chawla, I. Ray-Coquard, A. Le Cesne, A.P. Staddon, M.M. Milhem, N. Penel, R.F. Riedel, B. Bui-Nguyen, L.D. Cranmer, P. Reichardt, E. Bompas, T. Alcindor, D. Rushing, Y. Song, R.M. Lee, S. Ebbinghaus, J.E. Eid, J.W. Loewy, F.G. Haluska, P.F. Dodion, J.Y. Blay, Results of an international randomized phase III trial of the mammalian target of rapamycin inhibitor ridaforolimus versus placebo to control metastatic sarcomas in patients after benefit from prior chemotherapy, J Clin Oncol 31(19) (2013) 2485-92.
[59] S.P. Chawla, A.P. Staddon, L.H. Baker, S.M. Schuetze, A.W. Tolcher, G.Z. D'Amato, J.Y. Blay, M.M. Mita, K.K. Sankhala, L. Berk, V.M. Rivera, T. Clackson, J.W. Loewy, F.G. Haluska, G.D. Demetri, Phase II study of the mammalian target of rapamycin inhibitor ridaforolimus in patients with advanced bone and soft tissue sarcomas, J Clin Oncol 30(1) (2012) 78-84.
[60] Y. Pignochino, C. Dell'Aglio, M. Basirico, F. Capozzi, M. Soster, S. Marchio, S. Bruno, L. Gammaitoni, D. Sangiolo, E. Torchiaro, L. D'Ambrosio, F. Fagioli, S. Ferrari, M. Alberghini, P. Picci, M. Aglietta, G. Grignani, The Combination of Sorafenib and Everolimus Abrogates mTORC1 and mTORC2 upregulation in osteosarcoma preclinical models, Clin Cancer Res 19(8) (2013) 2117-31.
[61] T. Saeki, M. Ouchi, T. Ouchi, Physiological and oncogenic Aurora-A pathway, Int J Biol Sci 5(7) (2009) 758-62.
[62] M. Martini, E. Ciraolo, F. Gulluni, E. Hirsch, Targeting PI3K in Cancer: Any Good News?, Front Oncol 3 (2013) 108.
[63] A.M. Martelli, F. Chiarini, C. Evangelisti, A. Cappellini, F. Buontempo, D. Bressanin, M. Fini, J.A. McCubrey, Two hits are better than one: targeting both phosphatidylinositol 3-kinase and mammalian target of rapamycin as a therapeutic strategy for acute leukemia treatment, Oncotarget 3(4) (2012) 371-94.
[64] K.E. O'Reilly, F. Rojo, Q.B. She, D. Solit, G.B. Mills, D. Smith, H. Lane, F. Hofmann, D.J. Hicklin, D.L. Ludwig, J. Baselga, N. Rosen, mTOR inhibition induces upstream receptor tyrosine kinase signaling and activates Akt, Cancer Res 66(3) (2006) 1500-8.
[65] A. Carracedo, L. Ma, J. Teruya-Feldstein, F. Rojo, L. Salmena, A. Alimonti, A. Egia, A.T. Sasaki, G. Thomas, S.C. Kozma, A. Papa, C. Nardella, L.C. Cantley, J. Baselga, P.P. Pandolfi, Inhibition of mTORC1 leads to MAPK pathway activation through a PI3K-dependent feedback loop in human cancer, J Clin Invest 118(9) (2008) 3065-74.
[66] E.M. Sommer, H. Dry, D. Cross, S. Guichard, B.R. Davies, D.R. Alessi, Elevated SGK1 predicts resistance of breast cancer cells to Akt inhibitors, Biochem J 452(3) (2013) 499-508.
[67] L. Rosich, D. Colomer, G. Roue, Autophagy controls everolimus (RAD001) activity in mantle cell lymphoma, Autophagy 9(1) (2013) 115-7.
[68] Y. Zhou, Y. Wei, X. Tian, X. Wei, Cancer vaccines: current status and future directions, J Hematol Oncol 18(1) (2025) 18.
[69] Y. Zhou, N. Slone, T.T. Chrisikos, O. Kyrysyuk, R.L. Babcock, Y.B. Medik, H.S. Li, E.S. Kleinerman, S.S. Watowich, Vaccine efficacy against primary and metastatic cancer with in vitro-generated CD103(+) conventional dendritic cells, J Immunother Cancer 8(1) (2020).
[70] Y. Inagaki, E. Hookway, K.A. Williams, A.B. Hassan, U. Oppermann, Y. Tanaka, E. Soilleux, N.A. Athanasou, Dendritic and mast cell involvement in the inflammatory response to primary malignant bone tumours, Clin Sarcoma Res 6 (2016) 13.
[71] G.Z. Zhang, Z.L. Wu, C.Y. Li, E.H. Ren, W.H. Yuan, Y.J. Deng, Q.Q. Xie, Development of a Machine Learning-Based Autophagy-Related lncRNA Signature to Improve Prognosis Prediction in Osteosarcoma Patients, Front Mol Biosci 8 (2021) 615084.
[72] M. Kansara, K. Thomson, P. Pang, A. Dutour, L. Mirabello, F. Acher, J.P. Pin, E.G. Demicco, J. Yan, M.W.L. Teng, M.J. Smyth, D.M. Thomas, Infiltrating Myeloid Cells Drive Osteosarcoma Progression via GRM4 Regulation of IL23, Cancer Discov 9(11) (2019) 1511-1519.
[73] M. Kawano, I. Itonaga, T. Iwasaki, H. Tsumura, Enhancement of antitumor immunity by combining anti-cytotoxic T lymphocyte antigen-4 antibodies and cryotreated tumor lysate-pulsed dendritic cells in murine osteosarcoma, Oncol Rep 29(3) (2013) 1001-6.

[74] P. Koirala, M.E. Roth, J. Gill, S. Piperdi, J.M. Chinai, D.S. Geller, B.H. Hoang, A. Park, M.A. Fremed, X. Zang, R. Gorlick, Immune infiltration and PD-L1 expression in the tumor microenvironment are prognostic in osteosarcoma, Sci Rep 6 (2016) 30093.
[75] T. Le, S. Su, L. Shahriyari, Immune classification of osteosarcoma, Math Biosci Eng 18(2) (2021) 1879-1897.
[76] H. Yabe, T. Tsukahara, S. Kawaguchi, T. Wada, T. Torigoe, N. Sato, C. Terai, M. Aoki, S. Hirose, H. Morioka, H. Yabe, Prognostic significance of HLA class I expression in Ewing's sarcoma family of tumors, J Surg Oncol 103(5) (2011) 380-5.
[77] Y.T. Sundara, M. Kostine, A.H. Cleven, J.V. Bovee, M.W. Schilham, A.M. Cleton-Jansen, Increased PD-L1 and T-cell infiltration in the presence of HLA class I expression in metastatic high-grade osteosarcoma: a rationale for T-cell-based immunotherapy, Cancer Immunol Immunother 66(1) (2017) 119-128.
[78] J.A. Ligon, W. Choi, G. Cojocaru, W. Fu, E.H. Hsiue, T.F. Oke, N. Siegel, M.H. Fong, B. Ladle, C.A. Pratilas, C.D. Morris, A. Levin, D.S. Rhee, C.F. Meyer, A.J. Tam, R. Blosser, E.D. Thompson, A. Suru, D. McConkey, F. Housseau, R. Anders, D.M. Pardoll, N. Llosa, Pathways of immune exclusion in metastatic osteosarcoma are associated with inferior patient outcomes, J Immunother Cancer 9(5) (2021).
[79] Q. Han, H. Shi, F. Liu, CD163(+) M2-type tumor-associated macrophage support the suppression of tumor-infiltrating T cells in osteosarcoma, Int Immunopharmacol 34 (2016) 101-106.
[80] T. Matsuo, S. Shimose, T. Kubo, Y. Mikami, K. Arihiro, Y. Yasunaga, M. Ochi, Extraskeletal osteosarcoma with partial spontaneous regression, Anticancer Res 29(12) (2009) 5197-201.
[81] D. Pende, M. Falco, M. Vitale, C. Cantoni, C. Vitale, E. Munari, A. Bertaina, F. Moretta, G. Del Zotto, G. Pietra, M.C. Mingari, F. Locatelli, L. Moretta, Killer Ig-Like Receptors (KIRs): Their Role in NK Cell Modulation and Developments Leading to Their Clinical Exploitation, Front Immunol 10 (2019) 1179.
[82] A.D. Barrow, C.J. Martin, M. Colonna, The Natural Cytotoxicity Receptors in Health and Disease, Front Immunol 10 (2019) 909.
[83] F. Souza-Fonseca-Guimaraes, J. Cursons, N.D. Huntington, The Emergence of Natural Killer Cells as a Major Target in Cancer Immunotherapy, Trends Immunol 40(2) (2019) 142-158.
[84] H.J. Baek, J.S. Kim, M. Yoon, J.J. Lee, M.G. Shin, D.W. Ryang, H. Kook, S.K. Kim, D. Cho, Ex vivo expansion of natural killer cells using cryopreserved irradiated feeder cells, Anticancer Res 33(5) (2013) 2011-9.
[85] L. Fernandez, J. Valentin, M. Zalacain, W. Leung, A. Patino-Garcia, A. Perez-Martinez, Activated and expanded natural killer cells target osteosarcoma tumor initiating cells in an NKG2D-NKG2DL dependent manner, Cancer Lett 368(1) (2015) 54-63.
[86] F. Otegbeye, M.A.F. Vina, T. Wang, Y.T. Bolon, A. Lazaryan, A. Beitinjaneh, V.R. Bhatt, P. Castillo, S.G.E. Marsh, G.C. Hildebrandt, A. Assal, V.I. Brown, J. Hsu, S. Spellman, M. de Lima, S.J. Lee, Natural Killer Cell Alloreactivity Predicted By Killer Cell Immunoglobulin-Like Receptor Ligand Mismatch Does Not Impact Engraftment in Umbilical Cord Blood and Haploidentical Stem Cell Transplantation, Transplant Cell Ther 28(8) (2022) 483 e1-483 e7.
[87] Q. Huang, X. Liang, T. Ren, Y. Huang, H. Zhang, Y. Yu, C. Chen, W. Wang, J. Niu, J. Lou, W. Guo, The role of tumor-associated macrophages in osteosarcoma progression - therapeutic implications, Cell Oncol (Dordr) 44(3) (2021) 525-539.
[88] K. Kielbassa, S. Vegna, C. Ramirez, L. Akkari, Understanding the Origin and Diversity of Macrophages to Tailor Their Targeting in Solid Cancers, Front Immunol 10 (2019) 2215.
[89] S.O. Dudzinski, J.E. Bader, K.E. Beckermann, K.L. Young, R. Hongo, M.Z. Madden, A. Abraham, B.I. Reinfeld, X. Ye, N.J. MacIver, T.D. Giorgio, J.C. Rathmell, Leptin Augments Antitumor Immunity in Obesity by Repolarizing Tumor-Associated Macrophages, J Immunol 207(12) (2021) 3122-3130.
[90] C. Deng, Y. Xu, J. Fu, X. Zhu, H. Chen, H. Xu, G. Wang, Y. Song, G. Song, J. Lu, R. Liu, Q. Tang, W. Huang, J. Wang, Reprograming the tumor immunologic microenvironment using neoadjuvant chemotherapy in osteosarcoma, Cancer Sci 111(6) (2020) 1899-1909.

[91] L. Cassetta, J.W. Pollard, Targeting macrophages: therapeutic approaches in cancer, Nat Rev Drug Discov 17(12) (2018) 887-904.
[92] B.Z. Qian, J.W. Pollard, Macrophage diversity enhances tumor progression and metastasis, Cell 141(1) (2010) 39-51.
[93] P. Zhang, Y.F. Jin, Q. Zhang, Y.M. Wu, W.D. Wu, W. Yao, Y.J. Wu, Z.T. Li, Y. Zhao, Y. Liu, F.F. Feng, Macrophages promote coal tar pitch extract-induced tumorigenesis of BEAS-2B cells and tumor metastasis in nude mice mediated by AP-1, Asian Pac J Cancer Prev 15(12) (2014) 4871-6.
[94] Y. Han, W. Guo, T. Ren, Y. Huang, S. Wang, K. Liu, B. Zheng, K. Yang, H. Zhang, X. Liang, Tumor-associated macrophages promote lung metastasis and induce epithelial-mesenchymal transition in osteosarcoma by activating the COX-2/STAT3 axis, Cancer Lett 440-441 (2019) 116-125.
[95] A. Etzerodt, K. Tsalkitzi, M. Maniecki, W. Damsky, M. Delfini, E. Baudoin, M. Moulin, M. Bosenberg, J.H. Graversen, N. Auphan-Anezin, S.K. Moestrup, T. Lawrence, Specific targeting of CD163(+) TAMs mobilizes inflammatory monocytes and promotes T cell-mediated tumor regression, J Exp Med 216(10) (2019) 2394-2411.
[96] L. Wu, S. Saxena, M. Awaji, R.K. Singh, Tumor-Associated Neutrophils in Cancer: Going Pro, Cancers (Basel) 11(4) (2019).
[97] J. Pillay, I. den Braber, N. Vrisekoop, L.M. Kwast, R.J. de Boer, J.A. Borghans, K. Tesselaar, L. Koenderman, In vivo labeling with 2H2O reveals a human neutrophil lifespan of 5.4 days, Blood 116(4) (2010) 625-7.
[98] Z.G. Fridlender, J. Sun, S. Kim, V. Kapoor, G. Cheng, L. Ling, G.S. Worthen, S.M. Albelda, Polarization of tumor-associated neutrophil phenotype by TGF-beta: "N1" versus "N2" TAN, Cancer Cell 16(3) (2009) 183-94.
[99] Z.J. Wu, J.C. Tan, X. Qin, B. Liu, Z.C. Yuan, Significance of circulating tumor cells in osteosarcoma patients treated by neoadjuvant chemotherapy and surgery, Cancer Manag Res 10 (2018) 3333-3339.
[100] M. Cortini, A. Armirotti, M. Columbaro, D.L. Longo, G. Di Pompo, E. Cannas, A. Maresca, C. Errani, A. Longhi, A. Righi, V. Carelli, N. Baldini, S. Avnet, Exploring Metabolic Adaptations to the Acidic Microenvironment of Osteosarcoma Cells Unveils Sphingosine 1-Phosphate as a Valuable Therapeutic Target, Cancers (Basel) 13(2) (2021).
[101] Y. Zhang, Q. Ma, T. Liu, G. Guan, K. Zhang, J. Chen, N. Jia, S. Yan, G. Chen, S. Liu, K. Jiang, Y. Lu, Y. Wen, H. Zhao, Y. Zhou, Q. Fan, X. Qiu, Interleukin-6 suppression reduces tumour self-seeding by circulating tumour cells in a human osteosarcoma nude mouse model, Oncotarget 7(1) (2016) 446-58.
[102] T. Liu, Q. Ma, Y. Zhang, X. Wang, K. Xu, K. Yan, W. Dong, Q. Fan, Y. Zhang, X. Qiu, Self-seeding circulating tumor cells promote the proliferation and metastasis of human osteosarcoma by upregulating interleukin-8, Cell Death Dis 10(8) (2019) 575.
[103] J. Karbach, A. Neumann, K. Brand, C. Wahle, E. Siegel, M. Maeurer, E. Ritter, T. Tsuji, S. Gnjatic, L.J. Old, G. Ritter, E. Jager, Phase I clinical trial of mixed bacterial vaccine (Coley's toxins) in patients with NY-ESO-1 expressing cancers: immunological effects and clinical activity, Clin Cancer Res 18(19) (2012) 5449-59.
[104] C. Moore, D. Eslin, A. Levy, J. Roberson, V. Giusti, R. Sutphin, Prognostic significance of early lymphocyte recovery in pediatric osteosarcoma, Pediatr Blood Cancer 55(6) (2010) 1096-102.
[105] L.M. Jeys, R.J. Grimer, S.R. Carter, R.M. Tillman, A. Abudu, Post operative infection and increased survival in osteosarcoma patients: are they associated?, Ann Surg Oncol 14(10) (2007) 2887-95.
[106] A. Le Cesne, P. Marec-Berard, J.Y. Blay, N. Gaspar, F. Bertucci, N. Penel, E. Bompas, S. Cousin, M. Toulmonde, A. Bessede, W.H. Fridman, C. Sautes-Fridman, M. Kind, F. Le Loarer, M. Pulido, A. Italiano, Programmed cell death 1 (PD-1) targeting in patients with advanced osteosarcomas: results from the PEMBROSARC study, Eur J Cancer 119 (2019) 151-157.
[107] Y. Zhou, Q. Yang, Y. Dong, T. Ji, B. Zhang, C. Yang, S. Zheng, L. Tang, C. Zhou, G. Qian, Y. Huang, W. Yu, H. Li, Y. Wang, A. He, Z. Shen, Q. Bao, Y. Hua, H. Bai, J. Zhao, X. Li, X. Dai, J. Zhang, H. Hu, Y. Yao, First-in-Maintenance Therapy for Localized High-Grade Osteosarcoma: An Open-Label Phase I/II Trial of the Anti-PD-L1 Antibody ZKAB001, Clin Cancer Res 29(4) (2023) 764-774.

[108] N. Himoudi, R. Wallace, K.L. Parsley, K. Gilmour, A.U. Barrie, K. Howe, R. Dong, N.J. Sebire, A. Michalski, A.J. Thrasher, J. Anderson, Lack of T-cell responses following autologous tumour lysate pulsed dendritic cell vaccination, in patients with relapsed osteosarcoma, Clin Transl Oncol 14(4) (2012) 271-9.
[109] C. Zhang, L.M. Morimoto, A.J. de Smith, H.M. Hansen, J. Gonzalez-Maya, A.A. Endicott, I.V. Smirnov, C. Metayer, Q. Wei, W.C. Eward, J.L. Wiemels, K.M. Walsh, Genetic determinants of childhood and adult height associated with osteosarcoma risk, Cancer 124(18) (2018) 3742-3752.
[110] S. Chen, L. Yang, F. Pu, H. Lin, B. Wang, J. Liu, Z. Shao, High Birth Weight Increases the Risk for Bone Tumor: A Systematic Review and Meta-Analysis, Int J Environ Res Public Health 12(9) (2015) 11178-95.
[111] A.K. Luu, A.M. Viloria-Petit, Targeting Mechanotransduction in Osteosarcoma: A Comparative Oncology Perspective, Int J Mol Sci 21(20) (2020).
[112] R. Ayyasamy, S. Fan, P. Czernik, B. Lecka-Czernik, S. Chattopadhyay, R. Chakravarti, 14-3-3zeta suppresses RANKL signaling by destabilizing TRAF6, J Biol Chem 300(7) (2024) 107487.
[113] C.Y. Lin, A. Sassi, Y. Wu, K. Seaman, W. Tang, X. Song, R. Bienenstock, H. Yokota, Y. Sun, F. Geng, L. Wang, L. You, Mechanotransduction pathways regulating YAP nuclear translocation under Yoda1 and vibration in osteocytes, Bone 190 (2025) 117283.
[114] S. Lu, T. Lu, J. Zhang, L. Gan, X. Wu, D. Han, K. Zhang, C. Xu, S. Liu, W. Qin, F. Yang, W. Wen, CD248 promotes migration and metastasis of osteosarcoma through ITGB1-mediated FAK-paxillin pathway activation, BMC Cancer 23(1) (2023) 290.
[115] M. Cortini, F. Macchi, F. Reggiani, E. Vitale, M.V. Lipreri, F. Perut, A. Ciarrocchi, N. Baldini, S. Avnet, Endogenous Extracellular Matrix Regulates the Response of Osteosarcoma 3D Spheroids to Doxorubicin, Cancers (Basel) 15(4) (2023).
[116] W.D. Rindt, M. Krug, S. Yamada, F. Sennefelder, L. Belz, W.H. Cheng, M. Azeem, M. Kuric, M. Evers, E. Leich, T.N. Hartmann, A.R. Pereira, M. Hermann, J. Hansmann, C. Mussoni, P. Stahlhut, T. Ahmad, M.A. Yassin, K. Mustafa, R. Ebert, F. Jundt, A 3D bioreactor model to study osteocyte differentiation and mechanobiology under perfusion and compressive mechanical loading, Acta Biomater 184 (2024) 210-225.
[117] G. Alloisio, D.B. Rodriguez, M. Luce, C. Ciaccio, S. Marini, A. Cricenti, M. Gioia, Cyclic Stretch-Induced Mechanical Stress Applied at 1 Hz Frequency Can Alter the Metastatic Potential Properties of SAOS-2 Osteosarcoma Cells, Int J Mol Sci 24(9) (2023).
[118] L. Qin, W. Liu, H. Cao, G. Xiao, Molecular mechanosensors in osteocytes, Bone Res 8 (2020) 23.
[119] B. Zhang, X. Li, X. Zhou, C. Lou, S. Wang, H. Lv, G. Zhang, Y. Fang, D. Yin, P. Shang, Magneto-mechanical stimulation modulates osteocyte fate via the ECM-integrin-CSK axis and wnt pathway, iScience 26(8) (2023) 107365.
[120] O. Jeon, T.H. Kim, E. Alsberg, Reversible dynamic mechanics of hydrogels for regulation of cellular behavior, Acta Biomater 136 (2021) 88-98.
[121] I. Dasgupta, D. McCollum, Control of cellular responses to mechanical cues through YAP/TAZ regulation, J Biol Chem 294(46) (2019) 17693-17706.
[122] H. Atcha, A. Jairaman, J.R. Holt, V.S. Meli, R.R. Nagalla, P.K. Veerasubramanian, K.T. Brumm, H.E. Lim, S. Othy, M.D. Cahalan, M.M. Pathak, W.F. Liu, Mechanically activated ion channel Piezo1 modulates macrophage polarization and stiffness sensing, Nat Commun 12(1) (2021) 3256.
[123] H. Yoon, J.P. Dehart, J.M. Murphy, S.T. Lim, Understanding the roles of FAK in cancer: inhibitors, genetic models, and new insights, J Histochem Cytochem 63(2) (2015) 114-28.
[124] L. Ding, X. Sun, Y. You, N. Liu, Z. Fu, Expression of focal adhesion kinase and phosphorylated focal adhesion kinase in human gliomas is associated with unfavorable overall survival, Transl Res 156(1) (2010) 45-52.
[125] D.J. Sieg, C.R. Hauck, D. Ilic, C.K. Klingbeil, E. Schaefer, C.H. Damsky, D.D. Schlaepfer, FAK integrates growth-factor and integrin signals to promote cell migration, Nat Cell Biol 2(5) (2000) 249-56.

[126] K. Ren, X. Lu, N. Yao, Y. Chen, A. Yang, H. Chen, J. Zhang, S. Wu, X. Shi, C. Wang, X. Sun, Focal adhesion kinase overexpression and its impact on human osteosarcoma, Oncotarget 6(31) (2015) 31085-103.
[127] M. Yao, A. Tijore, D. Cheng, J.V. Li, A. Hariharan, B. Martinac, G. Tran Van Nhieu, C.D. Cox, M. Sheetz, Force- and cell state-dependent recruitment of Piezo1 drives focal adhesion dynamics and calcium entry, Sci Adv 8(45) (2022) eabo1461.
[128] G. Du, W. Chen, L. Li, Q. Zhang, The potential role of mechanosensitive ion channels in substrate stiffness-regulated Ca(2+) response in chondrocytes, Connect Tissue Res 63(5) (2022) 453-462.
[129] H.J. Wang, Y. Wang, S.S. Mirjavadi, T. Andersen, L. Moldovan, P. Vatankhah, B. Russell, J. Jin, Z. Zhou, Q. Li, C.D. Cox, Q.P. Su, L.A. Ju, Microscale geometrical modulation of PIEZO1 mediated mechanosensing through cytoskeletal redistribution, Nat Commun 15(1) (2024) 5521.
[130] G. Du, L. Li, X. Zhang, J. Liu, J. Hao, J. Zhu, H. Wu, W. Chen, Q. Zhang, Roles of TRPV4 and piezo channels in stretch-evoked Ca(2+) response in chondrocytes, Exp Biol Med (Maywood) 245(3) (2020) 180-189.
[131] A. Mussell, C. Frangou, J. Zhang, Regulation of the Hippo signaling pathway by deubiquitinating enzymes in cancer, Genes Dis 6(4) (2019) 335-341.
[132] T.R. Coughlin, A. Sana, K. Voss, A. Gadi, U. Basu-Roy, C.M. Curtin, A. Mansukhani, O.D. Kennedy, The Effect of Fluid Flow Shear Stress and Substrate Stiffness on Yes-Associated Protein (YAP) Activity and Osteogenesis in Murine Osteosarcoma Cells, Cancers (Basel) 13(13) (2021).
[133] Z. Xiang, P. Zhang, C. Jia, R. Xu, D. Cao, Z. Xu, T. Lu, J. Liu, X. Wang, C. Qiu, W. Fu, W. Li, L. Cheng, Q. Yang, S. Feng, L. Wang, Y. Zhao, X. Liu, Piezo1 channel exaggerates ferroptosis of nucleus pulposus cells by mediating mechanical stress-induced iron influx, Bone Res 12(1) (2024) 20.
[134] Y. Peng, R. Qu, Y. Yang, T. Fan, B. Sun, A.U. Khan, S. Wu, W. Liu, J. Zhu, J. Chen, X. Li, J. Dai, J. Ouyang, Regulation of the integrin alphaVbeta3- actin filaments axis in early osteogenic differentiation of human mesenchymal stem cells under cyclic tensile stress, Cell Commun Signal 21(1) (2023) 308.
[135] M.F. Hansen, M. Seton, A. Merchant, Osteosarcoma in Paget's disease of bone, J Bone Miner Res 21 Suppl 2 (2006) P58-63.
[136] H. Kovar, L. Bierbaumer, B. Radic-Sarikas, The YAP/TAZ Pathway in Osteogenesis and Bone Sarcoma Pathogenesis, Cells 9(4) (2020).
[137] A. Totaro, T. Panciera, S. Piccolo, YAP/TAZ upstream signals and downstream responses, Nat Cell Biol 20(8) (2018) 888-899.
[138] Y. Zhang, R.A. Brekken, Direct and indirect regulation of the tumor immune microenvironment by VEGF, J Leukoc Biol 111(6) (2022) 1269-1286.
[139] K. Mori, B. Le Goff, M. Berreur, A. Riet, A. Moreau, F. Blanchard, C. Chevalier, I. Guisle-Marsollier, J. Leger, J. Guicheux, M. Masson, F. Gouin, F. Redini, D. Heymann, Human osteosarcoma cells express functional receptor activator of nuclear factor-kappa B, J Pathol 211(5) (2007) 555-562.
[140] Z. Zhang, J. Du, S. Wang, L. Shao, K. Jin, F. Li, B. Wei, W. Ding, P. Fu, H. van Dam, A. Wang, J. Jin, C. Ding, B. Yang, M. Zheng, X.H. Feng, K.L. Guan, L. Zhang, OTUB2 Promotes Cancer Metastasis via Hippo-Independent Activation of YAP and TAZ, Mol Cell 73(1) (2019) 7-21 e7.
[141] Y. Liu, P. Lei, R.Z. Samuel, A.M. Kashyap, T. Groth, W. Bshara, S. Neelamegham, S.T. Andreadis, Cadherin-11 increases tumor cell proliferation and metastatic potential via Wnt pathway activation, Mol Oncol 17(10) (2023) 2056-2073.
[142] F. Lamoureux, P. Richard, Y. Wittrant, S. Battaglia, P. Pilet, V. Trichet, F. Blanchard, F. Gouin, B. Pitard, D. Heymann, F. Redini, Therapeutic relevance of osteoprotegerin gene therapy in osteosarcoma: blockade of the vicious cycle between tumor cell proliferation and bone resorption, Cancer Res 67(15) (2007) 7308-18.
[143] D. Xie, C. Hu, Y. Zhu, J. Yao, J. Li, J. Xia, L. Ye, Y. Jin, S. Jiang, T. Hu, J. Lu, H. Song, P. Tang, J. Dai, Y. Xi, Z. Hu, Sequential Therapy for Osteosarcoma and Bone Regeneration via Chemodynamic Effect and Cuproptosis Using a 3D-Printed Scaffold with TME-Responsive Hydrogel, Small 21(5) (2025) e2406639.

[144] X. Wang, X. Guo, H. Ren, X. Song, L. Chen, L. Yu, J. Ren, Y. Chen, An "Outer Piezoelectric and Inner Epigenetic" Logic-Gated PANoptosis for Osteosarcoma Sono-Immunotherapy and Bone Regeneration, Adv Mater 37(7) (2025) e2415814.
[145] Y. Li, S. Yang, S. Yang, Verteporfin Inhibits the Progression of Spontaneous Osteosarcoma Caused by Trp53 and Rb1 Deficiency in Ctsk-Expressing Cells via Impeding Hippo Pathway, Cells 11(8) (2022).
[146] S. Morice, M. Mullard, R. Brion, M. Dupuy, S. Renault, R. Tesfaye, B. Brounais-Le Royer, B. Ory, F. Redini, F. Verrecchia, The YAP/TEAD Axis as a New Therapeutic Target in Osteosarcoma: Effect of Verteporfin and CA3 on Primary Tumor Growth, Cancers (Basel) 12(12) (2020).
[147] F. Punzo, C. Tortora, M. Argenziano, D.D. Pinto, E. Pota, M.D. Martino, A.D. Paola, F. Rossi, Can Denosumab be used in combination with Doxorubicin in Osteosarcoma?, Oncotarget 11(28) (2020) 2763-2773.
[148] F. van Zijl, G. Krupitza, W. Mikulits, Initial steps of metastasis: cell invasion and endothelial transmigration, Mutat Res 728(1-2) (2011) 23-34.
[149] N.V. Krakhmal, M.V. Zavyalova, E.V. Denisov, S.V. Vtorushin, V.M. Perelmuter, Cancer Invasion: Patterns and Mechanisms, Acta Naturae 7(2) (2015) 17-28.
[150] G.W. Pearson, Control of Invasion by Epithelial-to-Mesenchymal Transition Programs during Metastasis, J Clin Med 8(5) (2019).
[151] A. Lorentzen, J. Bamber, A. Sadok, I. Elson-Schwab, C.J. Marshall, An ezrin-rich, rigid uropod-like structure directs movement of amoeboid blebbing cells, J Cell Sci 124(Pt 8) (2011) 1256-67.
[152] A. Haeger, K. Wolf, M.M. Zegers, P. Friedl, Collective cell migration: guidance principles and hierarchies, Trends Cell Biol 25(9) (2015) 556-66.
[153] R. Torka, F. Thuma, V. Herzog, G. Kirfel, ROCK signaling mediates the adoption of different modes of migration and invasion in human mammary epithelial tumor cells, Exp Cell Res 312(19) (2006) 3857-71.
[154] A.W. Holle, N. Govindan Kutty Devi, K. Clar, A. Fan, T. Saif, R. Kemkemer, J.P. Spatz, Cancer Cells Invade Confined Microchannels via a Self-Directed Mesenchymal-to-Amoeboid Transition, Nano Lett 19(4) (2019) 2280-2290.
[155] E. Paluch, M. Piel, J. Prost, M. Bornens, C. Sykes, Cortical actomyosin breakage triggers shape oscillations in cells and cell fragments, Biophys J 89(1) (2005) 724-33.
[156] E.K. Paluch, E. Raz, The role and regulation of blebs in cell migration, Curr Opin Cell Biol 25(5) (2013) 582-90.
[157] N.O. Carragher, S.M. Walker, L.A. Scott Carragher, F. Harris, T.K. Sawyer, V.G. Brunton, B.W. Ozanne, M.C. Frame, Calpain 2 and Src dependence distinguishes mesenchymal and amoeboid modes of tumour cell invasion: a link to integrin function, Oncogene 25(42) (2006) 5726-40.
[158] S. Yan, H. Xue, P. Zhang, X. Han, X. Guo, G. Yuan, L. Deng, G. Li, MMP inhibitor Ilomastat induced amoeboid-like motility via activation of the Rho signaling pathway in glioblastoma cells, Tumour Biol 37 (2016) 16177-16186.
[159] Y. Hegerfeldt, M. Tusch, E.B. Brocker, P. Friedl, Collective cell movement in primary melanoma explants: plasticity of cell-cell interaction, beta1-integrin function, and migration strategies, Cancer Res 62(7) (2002) 2125-30.
[160] V. Sanz-Moreno, G. Gadea, J. Ahn, H. Paterson, P. Marra, S. Pinner, E. Sahai, C.J. Marshall, Rac activation and inactivation control plasticity of tumor cell movement, Cell 135(3) (2008) 510-23.
[161] N.M. Aiello, R. Maddipati, R.J. Norgard, D. Balli, J. Li, S. Yuan, T. Yamazoe, T. Black, A. Sahmoud, E.E. Furth, D. Bar-Sagi, B.Z. Stanger, EMT Subtype Influences Epithelial Plasticity and Mode of Cell Migration, Dev Cell 45(6) (2018) 681-695 e4.
[162] A. Sadok, C.J. Marshall, Rho GTPases: masters of cell migration, Small GTPases 5 (2014) e29710.
[163] B. Serrels, M.C. Frame, FAK and talin: who is taking whom to the integrin engagement party?, J Cell Biol 196(2) (2012) 185-7.
[164] H.E. Balcioglu, H. van Hoorn, D.M. Donato, T. Schmidt, E.H. Danen, The integrin expression profile modulates orientation and dynamics of force transmission at cell-matrix adhesions, J Cell Sci 128(7) (2015) 1316-26.

[165] P. Gui, M. Ben-Neji, E. Belozertseva, F. Dalenc, C. Franchet, J. Gilhodes, A. Labrousse, E. Bellard, M. Golzio, R. Poincloux, I. Maridonneau-Parini, V. Le Cabec, The Protease-Dependent Mesenchymal Migration of Tumor-Associated Macrophages as a Target in Cancer Immunotherapy, Cancer Immunol Res 6(11) (2018) 1337-1351.
[166] A. Hallou, J. Jennings, A.J. Kabla, Tumour heterogeneity promotes collective invasion and cancer metastatic dissemination, R Soc Open Sci 4(8) (2017) 161007.
[167] P.W. Choi, J. Yang, S.K. Ng, C. Feltmate, M.G. Muto, K. Hasselblatt, K. Lafferty-Whyte, L. JeBailey, L. MacConaill, W.R. Welch, W.P. Fong, R.S. Berkowitz, S.W. Ng, Loss of E-cadherin disrupts ovarian epithelial inclusion cyst formation and collective cell movement in ovarian cancer cells, Oncotarget 7(4) (2016) 4110-21.
[168] R. Mayor, S. Etienne-Manneville, The front and rear of collective cell migration, Nat Rev Mol Cell Biol 17(2) (2016) 97-109.
[169] A. Haeger, S. Alexander, M. Vullings, F.M.P. Kaiser, C. Veelken, U. Flucke, G.E. Koehl, M. Hirschberg, M. Flentje, R.M. Hoffman, E.K. Geissler, S. Kissler, P. Friedl, Collective cancer invasion forms an integrin-dependent radioresistant niche, J Exp Med 217(1) (2020).
[170] L.L. Yin, C.M. Chung, J. Chen, K.L. Fok, C.P. Ng, R.R. Jia, X. Ren, J. Zhou, T. Zhang, X.H. Zhao, M. Lin, H. Zhu, X.H. Zhang, L.L. Tsang, Y. Bi, Z. Zhou, F. Mo, N. Wong, Y.W. Chung, J. Sha, H.C. Chan, A suppressor of multiple extracellular matrix-degrading proteases and cancer metastasis, J Cell Mol Med 13(9B) (2009) 4034-41.
[171] C. Gaggioli, S. Hooper, C. Hidalgo-Carcedo, R. Grosse, J.F. Marshall, K. Harrington, E. Sahai, Fibroblast-led collective invasion of carcinoma cells with differing roles for RhoGTPases in leading and following cells, Nat Cell Biol 9(12) (2007) 1392-400.
[172] E.N. Arwert, A.S. Harney, D. Entenberg, Y. Wang, E. Sahai, J.W. Pollard, J.S. Condeelis, A Unidirectional Transition from Migratory to Perivascular Macrophage Is Required for Tumor Cell Intravasation, Cell Rep 23(5) (2018) 1239-1248.
[173] J.S. Wu, J. Jiang, B.J. Chen, K. Wang, Y.L. Tang, X.H. Liang, Plasticity of cancer cell invasion: Patterns and mechanisms, Transl Oncol 14(1) (2021) 100899.
[174] A. Diz-Munoz, K. Thurley, S. Chintamen, S.J. Altschuler, L.F. Wu, D.A. Fletcher, O.D. Weiner, Membrane Tension Acts Through PLD2 and mTORC2 to Limit Actin Network Assembly During Neutrophil Migration, PLoS Biol 14(6) (2016) e1002474.
[175] Y. Huang, L. Tong, L. Yi, C. Zhang, L. Hai, T. Li, S. Yu, W. Wang, Z. Tao, H. Ma, P. Liu, Y. Xie, X. Yang, Three-dimensional hydrogel is suitable for targeted investigation of amoeboid migration of glioma cells, Mol Med Rep 17(1) (2018) 250-256.
[176] J. Shi, X. Wu, M. Surma, S. Vemula, L. Zhang, Y. Yang, R. Kapur, L. Wei, Distinct roles for ROCK1 and ROCK2 in the regulation of cell detachment, Cell Death Dis 4(2) (2013) e483.
[177] P. Tan, Y. Ye, L. He, J. Xie, J. Jing, G. Ma, H. Pan, L. Han, W. Han, Y. Zhou, TRIM59 promotes breast cancer motility by suppressing p62-selective autophagic degradation of PDCD10, PLoS Biol 16(11) (2018) e3000051.
[178] H.J. Seol, J.H. Chang, J. Yamamoto, R. Romagnuolo, Y. Suh, A. Weeks, S. Agnihotri, C.A. Smith, J.T. Rutka, Overexpression of CD99 Increases the Migration and Invasiveness of Human Malignant Glioma Cells, Genes Cancer 3(9-10) (2012) 535-49.
[179] A.E. Sedgwick, J.W. Clancy, M. Olivia Balmert, C. D'Souza-Schorey, Extracellular microvesicles and invadopodia mediate non-overlapping modes of tumor cell invasion, Sci Rep 5 (2015) 14748.
[180] E. Giannoni, M.L. Taddei, M. Parri, F. Bianchini, M. Santosuosso, R. Grifantini, G. Fibbi, B. Mazzanti, L. Calorini, P. Chiarugi, EphA2-mediated mesenchymal-amoeboid transition induced by endothelial progenitor cells enhances metastatic spread due to cancer-associated fibroblasts, J Mol Med (Berl) 91(1) (2013) 103-15.
[181] A. Cartier-Michaud, M. Malo, C. Charriere-Bertrand, G. Gadea, C. Anguille, A. Supiramaniam, A. Lesne, F. Delaplace, G. Hutzler, P. Roux, D.A. Lawrence, G. Barlovatz-Meimon, Matrix-bound PAI-1 supports cell blebbing via RhoA/ROCK1 signaling, PLoS One 7(2) (2012) e32204.
[182] L. Pietrovito, A. Leo, V. Gori, M. Lulli, M. Parri, V. Becherucci, L. Piccini, F. Bambi, M.L. Taddei, P. Chiarugi, Bone marrow-derived mesenchymal stem cells promote invasiveness and transendothelial

migration of osteosarcoma cells via a mesenchymal to amoeboid transition, Mol Oncol 12(5) (2018) 659-676.
[183] A.D. Grigore, M.K. Jolly, D. Jia, M.C. Farach-Carson, H. Levine, Tumor Budding: The Name is EMT. Partial EMT, J Clin Med 5(5) (2016).
[184] L. Kager, A. Zoubek, U. Potschger, U. Kastner, S. Flege, B. Kempf-Bielack, D. Branscheid, R. Kotz, M. Salzer-Kuntschik, W. Winkelmann, G. Jundt, H. Kabisch, P. Reichardt, H. Jurgens, H. Gadner, S.S. Bielack, G. Cooperative German-Austrian-Swiss Osteosarcoma Study, Primary metastatic osteosarcoma: presentation and outcome of patients treated on neoadjuvant Cooperative Osteosarcoma Study Group protocols, J Clin Oncol 21(10) (2003) 2011-8.
[185] J. PosthumaDeBoer, M.A. Witlox, G.J. Kaspers, B.J. van Royen, Molecular alterations as target for therapy in metastatic osteosarcoma: a review of literature, Clin Exp Metastasis 28(5) (2011) 493-503.
[186] C. Zucchini, A. Rocchi, M.C. Manara, P. De Sanctis, C. Capanni, M. Bianchini, P. Carinci, K. Scotlandi, L. Valvassori, Apoptotic genes as potential markers of metastatic phenotype in human osteosarcoma cell lines, Int J Oncol 32(1) (2008) 17-31.
[187] M.D. Cameron, E.E. Schmidt, N. Kerkvliet, K.V. Nadkarni, V.L. Morris, A.C. Groom, A.F. Chambers, I.C. MacDonald, Temporal progression of metastasis in lung: cell survival, dormancy, and location dependence of metastatic inefficiency, Cancer Res 60(9) (2000) 2541-6.
[188] T. Matsubara, G.R. Diresta, S. Kakunaga, D. Li, J.H. Healey, Additive Influence of Extracellular pH, Oxygen Tension, and Pressure on Invasiveness and Survival of Human Osteosarcoma Cells, Front Oncol 3 (2013) 199.
[189] M.M. Lizardo, J.J. Morrow, T.E. Miller, E.S. Hong, L. Ren, A. Mendoza, C.H. Halsey, P.C. Scacheri, L.J. Helman, C. Khanna, Upregulation of Glucose-Regulated Protein 78 in Metastatic Cancer Cells Is Necessary for Lung Metastasis Progression, Neoplasia 18(11) (2016) 699-710.
[190] P. Chaiyawat, P. Sungngam, P. Teeyakasem, N. Sirikaew, J. Klangjorhor, J. Settakorn, P. Diskul-Na-Ayudthaya, D. Chokchaichamnankit, C. Srisomsap, J. Svasti, D. Pruksakorn, Protein profiling of osteosarcoma tissue and soft callus unveils activation of the unfolded protein response pathway, Int J Oncol 54(5) (2019) 1704-1718.
[191] Y. Guo, X. Ji, J. Liu, D. Fan, Q. Zhou, C. Chen, W. Wang, G. Wang, H. Wang, W. Yuan, Z. Ji, Z. Sun, Effects of exosomes on pre-metastatic niche formation in tumors, Mol Cancer 18(1) (2019) 39.
[192] G. Sheng, Y. Gao, Y. Yang, H. Wu, Osteosarcoma and Metastasis, Front Oncol 11 (2021) 780264.
[193] L. Rodriguez Calleja, C. Jacques, F. Lamoureux, M. Baud'huin, M. Tellez Gabriel, T. Quillard, D. Sahay, P. Perrot, J. Amiaud, C. Charrier, R. Brion, F. Lecanda, F. Verrecchia, D. Heymann, L.W. Ellisen, B. Ory, DeltaNp63alpha Silences a miRNA Program to Aberrantly Initiate a Wound-Healing Program That Promotes TGFbeta-Induced Metastasis, Cancer Res 76(11) (2016) 3236-51.
[194] H.K. Bid, R.D. Roberts, M. Cam, A. Audino, R.T. Kurmasheva, J. Lin, P.J. Houghton, H. Cam, DeltaNp63 promotes pediatric neuroblastoma and osteosarcoma by regulating tumor angiogenesis, Cancer Res 74(1) (2014) 320-9.
[195] A.C. Gross, H. Cam, D.A. Phelps, A.J. Saraf, H.K. Bid, M. Cam, C.A. London, S.A. Winget, M.A. Arnold, L. Brandolini, X. Mo, J.M. Hinckley, P.J. Houghton, R.D. Roberts, IL-6 and CXCL8 mediate osteosarcoma-lung interactions critical to metastasis, JCI Insight 3(16) (2018).
[196] W. Zhang, J.M. Zhao, J. Lin, C.Z. Hu, W.B. Zhang, W.L. Yang, J. Zhang, J.W. Zhang, J. Zhu, Adaptive Fibrogenic Reprogramming of Osteosarcoma Stem Cells Promotes Metastatic Growth, Cell Rep 24(5) (2018) 1266-1277 e5.
[197] N.V. Koshkina, C. Khanna, A. Mendoza, H. Guan, L. DeLauter, E.S. Kleinerman, Fas-negative osteosarcoma tumor cells are selected during metastasis to the lungs: the role of the Fas pathway in the metastatic process of osteosarcoma, Mol Cancer Res 5(10) (2007) 991-9.
[198] Y. Araki, H. Aiba, T. Yoshida, N. Yamamoto, K. Hayashi, A. Takeuchi, S. Miwa, K. Igarashi, T.D. Nguyen, K.A. Ishii, T. Nojima, S. Takahashi, H. Murakami, H. Tsuchiya, R. Hanayama, Osteosarcoma-Derived Small Extracellular Vesicles Enhance Tumor Metastasis and Suppress Osteoclastogenesis by miR-146a-5p, Front Oncol 11 (2021) 667109.

[199] J. Wang, H. Zhang, X. Sun, X. Wang, T. Ren, Y. Huang, R. Zhang, B. Zheng, W. Guo, Exosomal PD-L1 and N-cadherin predict pulmonary metastasis progression for osteosarcoma patients, J Nanobiotechnology 18(1) (2020) 151.
[200] R. Macklin, H. Wang, D. Loo, S. Martin, A. Cumming, N. Cai, R. Lane, N.S. Ponce, E. Topkas, K. Inder, N.A. Saunders, L. Endo-Munoz, Extracellular vesicles secreted by highly metastatic clonal variants of osteosarcoma preferentially localize to the lungs and induce metastatic behaviour in poorly metastatic clones, Oncotarget 7(28) (2016) 43570-43587.
[201] W. Zhao, P. Qin, D. Zhang, X. Cui, J. Gao, Z. Yu, Y. Chai, J. Wang, J. Li, Long non-coding RNA PVT1 encapsulated in bone marrow mesenchymal stem cell-derived exosomes promotes osteosarcoma growth and metastasis by stabilizing ERG and sponging miR-183-5p, Aging (Albany NY) 11(21) (2019) 9581-9596.
[202] O. Neklyudova, M.J. Arlt, P. Brennecke, M. Thelen, A. Gvozdenovic, A. Kuzmanov, B. Robl, S.M. Botter, W. Born, B. Fuchs, Altered CXCL12 expression reveals a dual role of CXCR4 in osteosarcoma primary tumor growth and metastasis, J Cancer Res Clin Oncol 142(8) (2016) 1739-50.
[203] E. Goguet-Surmenian, P. Richard-Fiardo, E. Guillemot, M. Benchetrit, A. Gomez-Brouchet, P. Buzzo, B. Karimdjee-Soilihi, P. Alemanno, J.F. Michiels, A. Schmid-Alliana, H. Schmid-Antomarchi, CXCR7-mediated progression of osteosarcoma in the lungs, Br J Cancer 109(6) (2013) 1579-85.
[204] L. Du, X.G. Han, B. Tu, M.Q. Wang, H. Qiao, S.H. Zhang, Q.M. Fan, T.T. Tang, CXCR1/Akt signaling activation induced by mesenchymal stem cell-derived IL-8 promotes osteosarcoma cell anoikis resistance and pulmonary metastasis, Cell Death Dis 9(7) (2018) 714.
[205] Y.X. Liao, Z.Z. Fu, C.H. Zhou, L.C. Shan, Z.Y. Wang, F. Yin, L.P. Zheng, Y.Q. Hua, Z.D. Cai, AMD3100 reduces CXCR4-mediated survival and metastasis of osteosarcoma by inhibiting JNK and Akt, but not p38 or Erk1/2, pathways in in vitro and mouse experiments, Oncol Rep 34(1) (2015) 33-42.
[206] S. Georges, J. Chesneau, S. Hervouet, J. Taurelle, F. Gouin, F. Redini, M. Padrines, D. Heymann, Y. Fortun, F. Verrecchia, A Disintegrin And Metalloproteinase 12 produced by tumour cells accelerates osteosarcoma tumour progression and associated osteolysis, Eur J Cancer 49(9) (2013) 2253-63.
[207] T. Akiyama, P.F. Choong, C.R. Dass, RANK-Fc inhibits malignancy via inhibiting ERK activation and evoking caspase-3-mediated anoikis in human osteosarcoma cells, Clin Exp Metastasis 27(4) (2010) 207-15.
[208] T. Akiyama, C.R. Dass, Y. Shinoda, H. Kawano, S. Tanaka, P.F. Choong, Systemic RANK-Fc protein therapy is efficacious against primary osteosarcoma growth in a murine model via activity against osteoclasts, J Pharm Pharmacol 62(4) (2010) 470-6.
[209] T. Akiyama, C.R. Dass, P.F. Choong, Novel therapeutic strategy for osteosarcoma targeting osteoclast differentiation, bone-resorbing activity, and apoptosis pathway, Mol Cancer Ther 7(11) (2008) 3461-9.
[210] L. Endo-Munoz, A. Cumming, D. Rickwood, D. Wilson, C. Cueva, C. Ng, G. Strutton, A.I. Cassady, A. Evdokiou, S. Sommerville, I. Dickinson, A. Guminski, N.A. Saunders, Loss of osteoclasts contributes to development of osteosarcoma pulmonary metastases, Cancer Res 70(18) (2010) 7063-72.
[211] P. Saharinen, L. Eklund, K. Pulkki, P. Bono, K. Alitalo, VEGF and angiopoietin signaling in tumor angiogenesis and metastasis, Trends Mol Med 17(7) (2011) 347-62.
[212] G. Han, Y. Wang, W. Bi, J. Jia, W. Wang, M. Xu, Effects of vascular endothelial growth factor expression on pathological characteristics and prognosis of osteosarcoma, Clin Exp Med 16(4) (2016) 577-584.
[213] G. Wang, M. Sun, Y. Jiang, T. Zhang, W. Sun, H. Wang, F. Yin, Z. Wang, W. Sang, J. Xu, M. Mao, D. Zuo, Z. Zhou, C. Wang, Z. Fu, Z. Wang, Z. Duan, Y. Hua, Z. Cai, Anlotinib, a novel small molecular tyrosine kinase inhibitor, suppresses growth and metastasis via dual blockade of VEGFR2 and MET in osteosarcoma, Int J Cancer 145(4) (2019) 979-993.
[214] Y. Liu, N. Huang, S. Liao, E. Rothzerg, F. Yao, Y. Li, D. Wood, J. Xu, Current research progress in targeted anti-angiogenesis therapy for osteosarcoma, Cell Prolif 54(9) (2021) e13102.

[215] C. Lehuede, F. Dupuy, R. Rabinovitch, R.G. Jones, P.M. Siegel, Metabolic Plasticity as a Determinant of Tumor Growth and Metastasis, Cancer Res 76(18) (2016) 5201-8.
[216] J. Roy, P. Dibaeinia, T.M. Fan, S. Sinha, A. Das, Global analysis of osteosarcoma lipidomes reveal altered lipid profiles in metastatic versus nonmetastatic cells, J Lipid Res 60(2) (2019) 375-387.
[217] W.J. Kort, W.C. Hulsmann, T.E. Stehman, Modulation of metastatic ability by inhibition of cholesterol synthesis, Clin Exp Metastasis 7(5) (1989) 517-23.
[218] L. Ren, E.S. Hong, A. Mendoza, S. Issaq, C. Tran Hoang, M. Lizardo, A. LeBlanc, C. Khanna, Metabolomics uncovers a link between inositol metabolism and osteosarcoma metastasis, Oncotarget 8(24) (2017) 38541-38553.
[219] H. Zhao, Y. Wu, Y. Chen, H. Liu, Clinical significance of hypoxia-inducible factor 1 and VEGF-A in osteosarcoma, Int J Clin Oncol 20(6) (2015) 1233-43.
[220] A.A. Sabile, M.J. Arlt, R. Muff, B. Bode, B. Langsam, J. Bertz, T. Jentzsch, G.J. Puskas, W. Born, B. Fuchs, Cyr61 expression in osteosarcoma indicates poor prognosis and promotes intratibial growth and lung metastasis in mice, J Bone Miner Res 27(1) (2012) 58-67.
[221] N. Habel, M. Vilalta, O. Bawa, P. Opolon, J. Blanco, O. Fromigue, Cyr61 silencing reduces vascularization and dissemination of osteosarcoma tumors, Oncogene 34(24) (2015) 3207-13.
[222] E. Gaudio, A. Palamarchuk, T. Palumbo, F. Trapasso, Y. Pekarsky, C.M. Croce, R.I. Aqeilan, Physical association with WWOX suppresses c-Jun transcriptional activity, Cancer Res 66(24) (2006) 11585-9.
[223] S. Del Mare, R.I. Aqeilan, Tumor Suppressor WWOX inhibits osteosarcoma metastasis by modulating RUNX2 function, Sci Rep 5 (2015) 12959.
[224] B.W. Ozanne, H.J. Spence, L.C. McGarry, R.F. Hennigan, Transcription factors control invasion: AP-1 the first among equals, Oncogene 26(1) (2007) 1-10.
[225] D. Weekes, T.G. Kashima, C. Zandueta, N. Perurena, D.P. Thomas, A. Sunters, C. Vuillier, A. Bozec, E. El-Emir, I. Miletich, A. Patino-Garcia, F. Lecanda, A.E. Grigoriadis, Regulation of osteosarcoma cell lung metastasis by the c-Fos/AP-1 target FGFR1, Oncogene 35(22) (2016) 2852-61.
[226] S. Avnet, T. Chano, A. Massa, G. Bonuccelli, S. Lemma, L. Falzetti, G. Grisendi, M. Dominici, N. Baldini, Acid microenvironment promotes cell survival of human bone sarcoma through the activation of cIAP proteins and NF-kappaB pathway, Am J Cancer Res 9(6) (2019) 1127-1144.
[227] E.P. Buddingh, M.L. Kuijjer, R.A. Duim, H. Burger, K. Agelopoulos, O. Myklebost, M. Serra, F. Mertens, P.C. Hogendoorn, A.C. Lankester, A.M. Cleton-Jansen, Tumor-infiltrating macrophages are associated with metastasis suppression in high-grade osteosarcoma: a rationale for treatment with macrophage activating agents, Clin Cancer Res 17(8) (2011) 2110-9.
[228] A. Gomez-Brouchet, C. Illac, J. Gilhodes, C. Bouvier, S. Aubert, J.M. Guinebretiere, B. Marie, F. Larousserie, N. Entz-Werle, G. de Pinieux, T. Filleron, V. Minard, V. Minville, E. Mascard, F. Gouin, M. Jimenez, M.C. Ledeley, S. Piperno-Neumann, L. Brugieres, F. Redini, CD163-positive tumor-associated macrophages and CD8-positive cytotoxic lymphocytes are powerful diagnostic markers for the therapeutic stratification of osteosarcoma patients: An immunohistochemical analysis of the biopsies fromthe French OS2006 phase 3 trial, Oncoimmunology 6(9) (2017) e1331193.
[229] X.J. Shao, S.F. Xiang, Y.Q. Chen, N. Zhang, J. Cao, H. Zhu, B. Yang, Q. Zhou, M.D. Ying, Q.J. He, Inhibition of M2-like macrophages by all-trans retinoic acid prevents cancer initiation and stemness in osteosarcoma cells, Acta Pharmacol Sin 40(10) (2019) 1343-1350.
[230] B. Fritzsching, J. Fellenberg, L. Moskovszky, Z. Sapi, T. Krenacs, I. Machado, J. Poeschl, B. Lehner, M. Szendroi, A.L. Bosch, L. Bernd, M. Csoka, G. Mechtersheimer, V. Ewerbeck, R. Kinscherf, P. Kunz, CD8(+)/FOXP3(+)-ratio in osteosarcoma microenvironment separates survivors from non-survivors: a multicenter validated retrospective study, Oncoimmunology 4(3) (2015) e990800.
[231] C. Chen, L. Xie, T. Ren, Y. Huang, J. Xu, W. Guo, Immunotherapy for osteosarcoma: Fundamental mechanism, rationale, and recent breakthroughs, Cancer Lett 500 (2021) 1-10.
[232] D.P. Bartel, MicroRNAs: genomics, biogenesis, mechanism, and function, Cell 116(2) (2004) 281-97.

[233] J.H. Mao, R.P. Zhou, A.F. Peng, Z.L. Liu, S.H. Huang, X.H. Long, Y. Shu, microRNA-195 suppresses osteosarcoma cell invasion and migration in vitro by targeting FASN, Oncol Lett 4(5) (2012) 1125-1129.
[234] F. Lian, Y. Cui, C. Zhou, K. Gao, L. Wu, Identification of a plasma four-microRNA panel as potential noninvasive biomarker for osteosarcoma, PLoS One 10(3) (2015) e0121499.
[235] Z. Salah, R. Arafeh, V. Maximov, M. Galasso, S. Khawaled, S. Abou-Sharieha, S. Volinia, K.B. Jones, C.M. Croce, R.I. Aqeilan, miR-27a and miR-27a* contribute to metastatic properties of osteosarcoma cells, Oncotarget 6(7) (2015) 4920-35.
[236] N. Dai, Z.Y. Zhong, Y.P. Cun, Y. Qing, C. Chen, P. Jiang, M.X. Li, D. Wang, Alteration of the microRNA expression profile in human osteosarcoma cells transfected with APE1 siRNA, Neoplasma 60(4) (2013) 384-94.
[237] Y. Zhang, H. Hu, L. Song, L. Cai, R. Wei, W. Jin, Epirubicin-mediated expression of miR-302b is involved in osteosarcoma apoptosis and cell cycle regulation, Toxicol Lett 222(1) (2013) 1-9.
[238] Y. Li, J. Zhang, L. Zhang, M. Si, H. Yin, J. Li, Diallyl trisulfide inhibits proliferation, invasion and angiogenesis of osteosarcoma cells by switching on suppressor microRNAs and inactivating of Notch-1 signaling, Carcinogenesis 34(7) (2013) 1601-10.
[239] G. Ramazzotti, R. Fiume, F. Chiarini, G. Campana, S. Ratti, A.M. Billi, L. Manzoli, M.Y. Follo, P.G. Suh, J. McCubrey, L. Cocco, I. Faenza, Phospholipase C-beta1 interacts with cyclin E in adipose-derived stem cells osteogenic differentiation, Adv Biol Regul 71 (2019) 1-9.
[240] V.Z. Valeria Marigo, Cellule e Segnali, 2012.
[241] V.R. Lo Vasco, C. Fabrizi, L. Fumagalli, L. Cocco, Expression of phosphoinositide-specific phospholipase C isoenzymes in cultured astrocytes activated after stimulation with lipopolysaccharide, J Cell Biochem 109(5) (2010) 1006-12.
[242] P.G. Suh, J.I. Park, L. Manzoli, L. Cocco, J.C. Peak, M. Katan, K. Fukami, T. Kataoka, S. Yun, S.H. Ryu, Multiple roles of phosphoinositide-specific phospholipase C isozymes, BMB Rep 41(6) (2008) 415-34.
[243] A.R. Abdul Wasai, Phospholipases in Physiology and Pathology, 2023.
[244] A. Gresset, J. Sondek, T.K. Harden, The phospholipase C isozymes and their regulation, Subcell Biochem 58 (2012) 61-94.
[245] V.R. Lo Vasco, M. Leopizzi, C. Della Rocca, Ezrin-related Phosphoinositide pathway modifies RhoA and Rac1 in human osteosarcoma cell lines, J Cell Commun Signal 9(1) (2015) 55-62.
[246] C. Molinari, L. Medri, M.Y. Follo, M. Piazzi, G.A. Mariani, D. Calistri, L. Cocco, PI-PLCbeta1 gene copy number alterations in breast cancer, Oncol Rep 27(2) (2012) 403-8.
[247] C.A. Sengelaub, K. Navrazhina, J.B. Ross, N. Halberg, S.F. Tavazoie, PTPRN2 and PLCbeta1 promote metastatic breast cancer cell migration through PI(4,5)P2-dependent actin remodeling, EMBO J 35(1) (2016) 62-76.
[248] J.T. Snyder, A.U. Singer, M.R. Wing, T.K. Harden, J. Sondek, The pleckstrin homology domain of phospholipase C-beta2 as an effector site for Rac, J Biol Chem 278(23) (2003) 21099-104.
[249] G. Mao, J. Jin, S.P. Kunapuli, A.K. Rao, Nuclear factor-kappaB regulates expression of platelet phospholipase C-beta2 (PLCB2), Thromb Haemost 116(5) (2016) 931-940.
[250] H. Zhang, T. Xie, Y. Shui, Y. Qi, Knockdown of PLCB2 expression reduces melanoma cell viability and promotes melanoma cell apoptosis by altering Ras/Raf/MAPK signals, Mol Med Rep 21(1) (2020) 420-428.
[251] V. Bertagnolo, M. Benedusi, F. Brugnoli, P. Lanuti, M. Marchisio, P. Querzoli, S. Capitani, Phospholipase C-beta 2 promotes mitosis and migration of human breast cancer-derived cells, Carcinogenesis 28(8) (2007) 1638-45.
[252] K.N. Phoenix, Z. Yue, L. Yue, C.G. Cronin, B.T. Liang, L.H. Hoeppner, K.P. Claffey, PLCbeta2 Promotes VEGF-Induced Vascular Permeability, Arterioscler Thromb Vasc Biol 42(10) (2022) 1229-1241.
[253] S. Wang, D. Xie, H. Yue, G. Li, B. Jiang, Y. Gao, Z. Zheng, X. Zheng, G. Wu, Phospholipase C Beta 2 as a Key Regulator of Tumor Progression and Epithelial-Mesenchymal Transition via PI3K/AKT Signaling in Renal Cell Carcinoma, Biomedicines 13(2) (2025).

[254] M. Hoberg, H.H. Gratz, M. Noll, D.B. Jones, Mechanosensitivity of human osteosarcoma cells and phospholipase C beta2 expression, Biochem Biophys Res Commun 333(1) (2005) 142-9.
[255] E. Siraliev-Perez, J.T.B. Stariha, R.M. Hoffmann, B.R.S. Temple, Q. Zhang, N. Hajicek, M.L. Jenkins, J.E. Burke, J. Sondek, Dynamics of allosteric regulation of the phospholipase C-gamma isozymes upon recruitment to membranes, Elife 11 (2022).
[256] Y.S. Bae, L.G. Cantley, C.S. Chen, S.R. Kim, K.S. Kwon, S.G. Rhee, Activation of phospholipase C-gamma by phosphatidylinositol 3,4,5-trisphosphate, J Biol Chem 273(8) (1998) 4465-9.
[257] C. Raimondi, M. Falasca, Phosphoinositides signalling in cancer: focus on PI3K and PLC, Adv Biol Regul 52(1) (2012) 166-82.
[258] S. Mandal, S. Bandyopadhyay, K. Tyagi, A. Roy, Recent advances in understanding the molecular role of phosphoinositide-specific phospholipase C gamma 1 as an emerging onco-driver and novel therapeutic target in human carcinogenesis, Biochim Biophys Acta Rev Cancer 1876(2) (2021) 188619.
[259] Q.S. Ji, G.E. Winnier, K.D. Niswender, D. Horstman, R. Wisdom, M.A. Magnuson, G. Carpenter, Essential role of the tyrosine kinase substrate phospholipase C-gamma1 in mammalian growth and development, Proc Natl Acad Sci U S A 94(7) (1997) 2999-3003.
[260] G.A. Gonzalez-Conchas, L. Rodriguez-Romo, D. Hernandez-Barajas, J.F. Gonzalez-Guerrero, I.A. Rodriguez-Fernandez, A. Verdines-Perez, A.J. Templeton, A. Ocana, B. Seruga, I.F. Tannock, E. Amir, F.E. Vera-Badillo, Epidermal growth factor receptor overexpression and outcomes in early breast cancer: A systematic review and a meta-analysis, Cancer Treat Rev 62 (2018) 1-8.
[261] B. Jiang, J. Chen, W. Yuan, J. Ji, Z. Liu, L. Wu, Q. Tang, X. Shu, Platelet-derived growth factor-D promotes colorectal cancer cell migration, invasion and proliferation by regulating Notch1 and matrix metalloproteinase-9, Oncol Lett 15(2) (2018) 1573-1579.
[262] J.B. Park, C.S. Lee, J.H. Jang, J. Ghim, Y.J. Kim, S. You, D. Hwang, P.G. Suh, S.H. Ryu, Phospholipase signalling networks in cancer, Nat Rev Cancer 12(11) (2012) 782-92.
[263] G. Mouneimne, L. Soon, V. DesMarais, M. Sidani, X. Song, S.C. Yip, M. Ghosh, R. Eddy, J.M. Backer, J. Condeelis, Phospholipase C and cofilin are required for carcinoma cell directionality in response to EGF stimulation, J Cell Biol 166(5) (2004) 697-708.
[264] J.C. Peak, N.P. Jones, S. Hobbs, M. Katan, S.A. Eccles, Phospholipase C gamma 1 regulates the Rap GEF1-Rap1 signalling axis in the control of human prostate carcinoma cell adhesion, Oncogene 27(20) (2008) 2823-32.
[265] H. Nozawa, G. Howell, S. Suzuki, Q. Zhang, Y. Qi, J. Klein-Seetharaman, A. Wells, J.R. Grandis, S.M. Thomas, Combined inhibition of PLCgamma-1 and c-Src abrogates epidermal growth factor receptor-mediated head and neck squamous cell carcinoma invasion, Clin Cancer Res 14(13) (2008) 4336-44.
[266] Y. Ou, L. Ma, L. Dong, L. Ma, Z. Zhao, L. Ma, W. Zhou, J. Fan, C. Wu, C. Yu, Q. Zhan, Y. Song, Migfilin protein promotes migration and invasion in human glioma through epidermal growth factor receptor-mediated phospholipase C-gamma and STAT3 protein signaling pathways, J Biol Chem 287(39) (2012) 32394-405.
[267] L.M. Balz, K. Bartkowiak, A. Andreas, K. Pantel, B. Niggemann, K.S. Zanker, B.H. Brandt, T. Dittmar, The interplay of HER2/HER3/PI3K and EGFR/HER2/PLC-gamma1 signalling in breast cancer cell migration and dissemination, J Pathol 227(2) (2012) 234-44.
[268] S.Y. Park, X. Shi, J. Pang, C. Yan, B.C. Berk, Thioredoxin-interacting protein mediates sustained VEGFR2 signaling in endothelial cells required for angiogenesis, Arterioscler Thromb Vasc Biol 33(4) (2013) 737-43.
[269] M. Kostas, E.M. Haugsten, Y. Zhen, V. Sorensen, P. Szybowska, E. Fiorito, S. Lorenz, N. Jones, G.A. de Souza, A. Wiedlocha, J. Wesche, Protein Tyrosine Phosphatase Receptor Type G (PTPRG) Controls Fibroblast Growth Factor Receptor (FGFR) 1 Activity and Influences Sensitivity to FGFR Kinase Inhibitors, Mol Cell Proteomics 17(5) (2018) 850-870.
[270] J.T. Jackson, E. Mulazzani, S.L. Nutt, S.L. Masters, The role of PLCgamma2 in immunological disorders, cancer, and neurodegeneration, J Biol Chem 297(2) (2021) 100905.

[271] M. Katan, R. Rodriguez, M. Matsuda, Y.M. Newbatt, G.W. Aherne, Structural and mechanistic aspects of phospholipase Cgamma regulation, Adv Enzyme Regul 43 (2003) 77-85.
[272] R. Lattanzio, M. Piantelli, M. Falasca, Role of phospholipase C in cell invasion and metastasis, Adv Biol Regul 53(3) (2013) 309-18.
[273] R. Faccio, V. Cremasco, PLCgamma2: where bone and immune cells find their common ground, Ann N Y Acad Sci 1192 (2010) 124-30.
[274] H. Epple, V. Cremasco, K. Zhang, D. Mao, G.D. Longmore, R. Faccio, Phospholipase Cgamma2 modulates integrin signaling in the osteoclast by affecting the localization and activation of Src kinase, Mol Cell Biol 28(11) (2008) 3610-22.
[275] W.J. Smith, N. Nassar, A. Bretscher, R.A. Cerione, P.A. Karplus, Structure of the active N-terminal domain of Ezrin. Conformational and mobility changes identify keystone interactions, J Biol Chem 278(7) (2003) 4949-56.
[276] L. Heiska, K. Alfthan, M. Gronholm, P. Vilja, A. Vaheri, O. Carpen, Association of ezrin with intercellular adhesion molecule-1 and -2 (ICAM-1 and ICAM-2). Regulation by phosphatidylinositol 4, 5-bisphosphate, J Biol Chem 273(34) (1998) 21893-900.
[277] Y. Song, X. Ma, M. Zhang, M. Wang, G. Wang, Y. Ye, W. Xia, Ezrin Mediates Invasion and Metastasis in Tumorigenesis: A Review, Front Cell Dev Biol 8 (2020) 588801.
[278] C. Khanna, X. Wan, S. Bose, R. Cassaday, O. Olomu, A. Mendoza, C. Yeung, R. Gorlick, S.M. Hewitt, L.J. Helman, The membrane-cytoskeleton linker ezrin is necessary for osteosarcoma metastasis, Nat Med 10(2) (2004) 182-6.
[279] T.S. Yeh, J.H. Tseng, N.J. Liu, T.C. Chen, Y.Y. Jan, M.F. Chen, Significance of cellular distribution of ezrin in pancreatic cystic neoplasms and ductal adenocarcinoma, Arch Surg 140(12) (2005) 1184-90.
[280] N. Akisawa, I. Nishimori, T. Iwamura, S. Onishi, M.A. Hollingsworth, High levels of ezrin expressed by human pancreatic adenocarcinoma cell lines with high metastatic potential, Biochem Biophys Res Commun 258(2) (1999) 395-400.
[281] G. Bulut, S.H. Hong, K. Chen, E.M. Beauchamp, S. Rahim, G.W. Kosturko, E. Glasgow, S. Dakshanamurthy, H.S. Lee, I. Daar, J.A. Toretsky, C. Khanna, A. Uren, Small molecule inhibitors of ezrin inhibit the invasive phenotype of osteosarcoma cells, Oncogene 31(3) (2012) 269-81.
[282] K.F. Tolias, J.H. Hartwig, H. Ishihara, Y. Shibasaki, L.C. Cantley, C.L. Carpenter, Type Ialpha phosphatidylinositol-4-phosphate 5-kinase mediates Rac-dependent actin assembly, Curr Biol 10(3) (2000) 153-6.
[283] C. Barret, C. Roy, P. Montcourrier, P. Mangeat, V. Niggli, Mutagenesis of the phosphatidylinositol 4,5-bisphosphate (PIP(2)) binding site in the NH(2)-terminal domain of ezrin correlates with its altered cellular distribution, J Cell Biol 151(5) (2000) 1067-80.
[284] J.J. Hao, Y. Liu, M. Kruhlak, K.E. Debell, B.L. Rellahan, S. Shaw, Phospholipase C-mediated hydrolysis of PIP2 releases ERM proteins from lymphocyte membrane, J Cell Biol 184(3) (2009) 451-62.
[285] A. Gautreau, P. Poullet, D. Louvard, M. Arpin, Ezrin, a plasma membrane-microfilament linker, signals cell survival through the phosphatidylinositol 3-kinase/Akt pathway, Proc Natl Acad Sci U S A 96(13) (1999) 7300-5.
[286] V.L. Bonilha, S.C. Finnemann, E. Rodriguez-Boulan, Ezrin promotes morphogenesis of apical microvilli and basal infoldings in retinal pigment epithelium, J Cell Biol 147(7) (1999) 1533-48.
[287] P. Pujuguet, L. Del Maestro, A. Gautreau, D. Louvard, M. Arpin, Ezrin regulates E-cadherin-dependent adherens junction assembly through Rac1 activation, Mol Biol Cell 14(5) (2003) 2181-91.
[288] H. Zhao, H. Shiue, S. Palkon, Y. Wang, P. Cullinan, J.K. Burkhardt, M.W. Musch, E.B. Chang, J.R. Turner, Ezrin regulates NHE3 translocation and activation after Na+-glucose cotransport, Proc Natl Acad Sci U S A 101(25) (2004) 9485-90.
[289] T. Grune, T. Reinheckel, J.A. North, R. Li, P.B. Bescos, R. Shringarpure, K.J. Davies, Ezrin turnover and cell shape changes catalyzed by proteasome in oxidatively stressed cells, FASEB J 16(12) (2002) 1602-10.

[290] Y. Yu, J. Khan, C. Khanna, L. Helman, P.S. Meltzer, G. Merlino, Expression profiling identifies the cytoskeletal organizer ezrin and the developmental homeoprotein Six-1 as key metastatic regulators, Nat Med 10(2) (2004) 175-81.
[291] X. Wan, A. Mendoza, C. Khanna, L.J. Helman, Rapamycin inhibits ezrin-mediated metastatic behavior in a murine model of osteosarcoma, Cancer Res 65(6) (2005) 2406-11.
[292] V.R. Lo Vasco, M. Leopizzi, D. Stoppoloni, C. Della Rocca, Silencing of phosphoinositide-specific phospholipase C epsilon remodulates the expression of the phosphoinositide signal transduction pathway in human osteosarcoma cell lines, Anticancer Res 34(8) (2014) 4069-75.
[293] V.R. Lo Vasco, M. Leopizzi, C. Puggioni, C. Della Rocca, Ezrin silencing remodulates the expression of Phosphoinositide-specific Phospholipase C enzymes in human osteosarcoma cell lines, J Cell Commun Signal 8(3) (2014) 219-29.
[294] E. Auvinen, N. Kivi, A. Vaheri, Regulation of ezrin localization by Rac1 and PIPK in human epithelial cells, Exp Cell Res 313(4) (2007) 824-33.
[295] J.E. Bleasdale, N.R. Thakur, R.S. Gremban, G.L. Bundy, F.A. Fitzpatrick, R.J. Smith, S. Bunting, Selective inhibition of receptor-coupled phospholipase C-dependent processes in human platelets and polymorphonuclear neutrophils, J Pharmacol Exp Ther 255(2) (1990) 756-68.
[296] R.R. Klein, D.M. Bourdon, C.L. Costales, C.D. Wagner, W.L. White, J.D. Williams, S.N. Hicks, J. Sondek, D.R. Thakker, Direct activation of human phospholipase C by its well known inhibitor u73122, J Biol Chem 286(14) (2011) 12407-16.
[297] N.E. Wilsher, W.J. Court, R. Ruddle, Y.M. Newbatt, W. Aherne, P.W. Sheldrake, N.P. Jones, M. Katan, S.A. Eccles, F.I. Raynaud, The phosphoinositide-specific phospholipase C inhibitor U73122 (1-(6-((17beta-3-methoxyestra-1,3,5(10)-trien-17-yl)amino)hexyl)-1H-pyrrole-2,5-dione) spontaneously forms conjugates with common components of cell culture medium, Drug Metab Dispos 35(7) (2007) 1017-22.
[298] B. Cenni, D. Picard, Two compounds commonly used for phospholipase C inhibition activate the nuclear estrogen receptors, Biochem Biophys Res Commun 261(2) (1999) 340-4.
[299] C. Hellberg, L. Molony, L. Zheng, T. Andersson, Ca2+ signalling mechanisms of the beta 2 integrin on neutrophils: involvement of phospholipase C gamma 2 and Ins(1,4,5)P3, Biochem J 317 (Pt 2)(Pt 2) (1996) 403-9.
[300] S.A. Hughes, W.J. Gibson, J.M. Young, The interaction of U-73122 with the histamine H1 receptor: implications for the use of U-73122 in defining H1 receptor-coupled signalling pathways, Naunyn Schmiedebergs Arch Pharmacol 362(6) (2000) 555-8.
[301] V.R. Lo Vasco, M. Leopizzi, V. Di Maio, C. Della Rocca, U-73122 reduces the cell growth in cultured MG-63 ostesarcoma cell line involving Phosphoinositide-specific Phospholipases C, Springerplus 5 (2016) 156.
[302] F. Paganelli, A. Poli, S. Truocchio, A.M. Martelli, C. Palumbo, G. Lattanzi, F. Chiarini, At the nucleus of cancer: how the nuclear envelope controls tumor progression, MedComm (2020) 6(2) (2025) e70073.